Functional role of a histone deacetylase encoded by Legionella pneumophila

Daniel Schator

Sorbonne Université

ED515 : Complexité du vivant

Biologie des bactéries intracellulaires/Institut Pasteur

Rôle fonctionnel d'une histone désacétylase codée par *Legionella pneumophila*

Par **Daniel Schator**

Thèse de doctorat de Microbiologie

Dirigée par Carmen Buchrieser et Monica Rolando

Présentée et soutenue publiquement le 15 Décembre 2021

Devant un jury composé de :

M. Guennadi Sezonov	Professeur, Sorbonne Université	Président
Mme. Antje Flieger	Professeur, Robert Koch Institut	Rapporteur
M. Jonathan Weitzman	Professeur, Université de Paris	Rapporteur
Mme. Hélène Bierne	Directrice de Recherche, Université Paris Saclay	Examinateur
M. Hubert Hilbi	Professeur, Université de Zurich	Examinateur
Mme. Carmen Buchrieser	Professeur, Institut Pasteur	Directrice de thèse

Sorbonne University

ED515: Complexité du vivant

Biology of intracellular bacteria/Institut Pasteur

Functional role of a histone deacetylase encoded by *Legionella pneumophila*

by **Daniel Schator**

Doctoral thesis in Microbiology

Supervised by Carmen Buchrieser and Monica Rolando

Publicly presented and defended on December 15, 2021

Before a jury composed of:

Guennadi Sezonov	Professor, Sorbonne University	President
Antje Flieger	Professor, Robert Koch Institut	Reviewer
Jonathan Weitzman	Professor, Université de Paris	Reviewer
Hélène Bierne	Associate Professor, Université Paris Saclay	Examiner
Hubert Hilbi	Professor, University of Zurich	Examiner
Carmen Buchrieser	Professor, Institut Pasteur	Supervisor

Acknowledgment

First and foremost, I want to thank my supervisors Monica and Carmen. They gave me the opportunity to work on this project and I could not have asked for better guidance during this time. I would also like to acknowledge all the people who helped me with this project, from my collaborators – Jérémy, Fernando, Mathilde, and Anne Marie – to my colleagues, especially Sonia, without whom this thesis would not have been possible. A big *merci* also to every member of the lab, past and present, who I had the pleasure of working with during my time in Paris. Last but not least, I want to thank my family and friends for their continuous support throughout these past years.

Also, I would like to thank Bob Dylan,
whose song "Legionnaire's disease" is the inspiration for the titles in the chapter "Legionellosis".

Table of contents

Legionella: an introduction

The genus *Legionella*

Is it a toxin? Is it a virus? It's *Legionella*! – discovery of a new bacterial genus

In July of 1976, the American Legion, the U.S. military veterans' organization, hosted its annual three-day convention at the Bellevue-Stratford Hotel in Philadelphia, Pennsylvania in the Unites States. A few days to weeks after the convention was over, 182 attendees fell ill with a mysterious disease. This disease manifested as a severe pneumonia, which was fatal in 29 cases (Fraser et al., 1977). The source of this disease was not identified right away, so many theories were circling, ranging from an infectious agent like bacteria or viruses, to chemical intoxications, which maybe even were caused on purpose by an unknown culprit (1977a). One early stage theory was nickel carbonyl poisoning, because high amounts of nickel were detected in the lung tissue of 9 fatal cases (Chen et al., 1977). Finally, on January 18, 1977 the mystery was solved and the Center for Disease Control (CDC) announced that they identified the causative agent of this severe illness: a small rod-shaped bacterium, similar to members of the genus *Rickettsia* (1977b). In December of 1977, Joseph E. McDade and Charles C. Shepard published their results about this newly discovered bacterium that was isolated from patients that fell ill with this pneumonia. They used antigens of the gram-negative, acid-fast bacillus that they had isolated from lungs of Legionnaires' disease patients, that were produced by yolk sac culture, to screen the serum of patients – suspected to have this disease – for the presence of specific antibodies. This allowed them to confirm this bacterium as the causative agent of the mysterious Legionnaires' disease (McDade et al., 1977). Later, this bacterium was described as *Legionella pneumophila* strain Philadelphia, the first member of the new bacterial genus *Legionella* (Brenner et al., 1979).

Soon after its identification it became clear that the American Legion convention in 1976 was not the first time a widespread infection with this bacterium has been recorded. It was not even the first time a widespread infection with this bacterium was recorded in the same location. In 1974, several attendees of the convention of the Independent Order of Odd Fellows – held in the same hotel as the American Legion convention described above – suffered from an unknown pneumonia-like disease, which was later attributed to *L. pneumophila*. In retrospect, several outbreaks before 1976 could be identified. An outbreak in St. Elizabeth's Hospital (Washington, D.C.) in 1965, where 81 patients fell sick, 17 of whom succumbed to the disease, was attributed to *Legionella pneumophila* (Thacker et al., 1978). In addition, in 1968 at least 144 people in Pontiac, Michigan, suffered from an unknown disease, which also

was later proven to be caused by the same bacteria (Glick et al., 1978). The name for this disease, Pontiac Fever, is nowadays mostly used for a milder progression of the infection with members of the genus *Legionella*, since no deaths occurred during this outbreak in 1968. The earliest case of Legionnaires' disease was identified in frozen sera samples from 1947 (McDade et al., 1979).

Soon after its discovery, the members of the genus *Legionella* started to grow rapidly, as more and more species were identified.

From lakes to lungs – Characteristics of the genus *Legionella*

All members of the genus *Legionella* are aerobic, rod-shaped, Gram-negative bacteria. *L. pneumophila* expresses a polar flagellum, enabling bacterial motility (**Figure 1A**). It is a facultative intracellular bacterium that can grow in a planktonic form but is most frequently found parasitizing different free-living protozoa in aquatic environments (Anand et al., 1983; Rowbotham, 1980). In the laboratory, *L. pneumophila* is grown under strictly aerobic conditions on specific medium called buffered charcoal yeast extract (BCYE), a nutrient rich medium supplemented with iron and L-cystein (Fields, 1996). On the black BCYE plates, the bacteria appear as opaque, round, white/gray colonies, with clear edges and a smooth shine

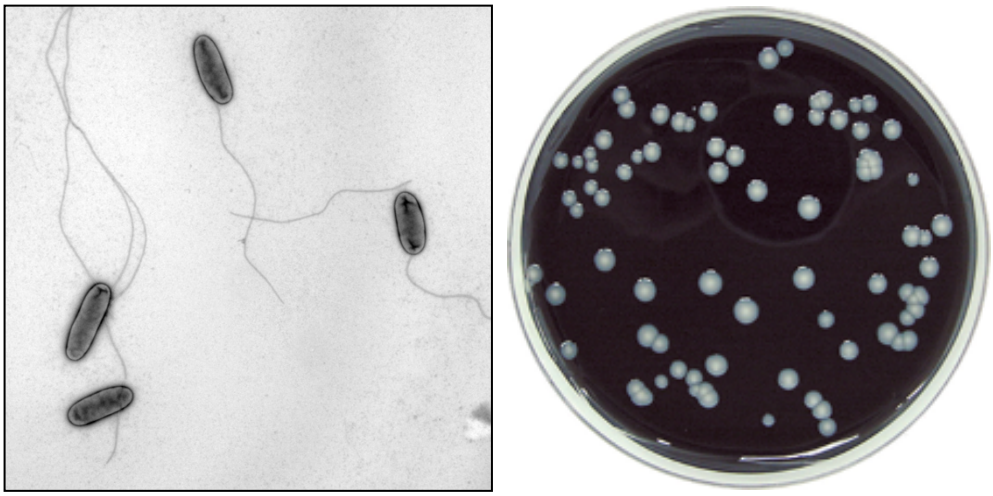

Figure 1: *L. pneumophila* in electron microscopy (A) and on a BCYE plate (B). (A) Electron microscopy picture of *L. pneumophila* growing in liquid culture with its polar flagellum. (B) *L. pneumophila* growing on BCYE agar. (A) Pictures taken by the group Biology of Intracellular Bacteria, Institut Pasteur, Paris. (B) Adapted from http://www.biomerieux-culturemedia.com/product/95-legionella-agar-with-l-cysteine--bcye--and-without-l-cysteine--bcy- .

(**Figure 1B**). The main energy and carbon source for the bacteria are amino acids and other organic acids (George et al., 1980; Sauer et al., 2005; Tesh et al., 1983). However, carbohydrates also play a role in in the bacterial metabolism (Eylert et al., 2010; Gillmaier et al., 2016; Herrmann et al., 2011).

The genus *Legionella* comprises 65 species to date, which are mostly found in natural aquatic environments such as lakes, rivers, and ponds, but also human-made environments such as cooling towers, showers, and air conditioning systems (Gomez-Valero et al., 2019; Mondino et al., 2020a). Out of the 65 species known today, at least 20 have been connected to human disease, in particular pneumonia (Muder and Yu, 2002). In human-made environments *Legionella* spp. are mainly present in biofilms, however, their replication within these biofilms seems dependent on the presence of a protozoan host (Murga et al., 2001; Rogers et al., 1994). Many protozoa have been identified to enable replication of *Legionella* spp, including amoebae such as *Acanthamoeba*, *Neaglaria*, *Dictyostelium, Balamuthia* and *Hartmannella* as well as ciliates like *Tetrahymena* and *Paramecium* (Barbaree et al., 1986; Fields et al., 1984; Hägele et al., 2000; Kuiper et al., 2004; Newsome et al., 1985; Shadrach et al., 2005; Steinert et al., 1997; Watanabe et al., 2016). Biofilms and the association with protozoa seem to be the main reservoirs of *Legionella* spp. in natural as well as human-made aquatic environments. In natural aquatic environments, the bacterial burden with *Legionella* spp. is generally very low due to non-optimal growth conditions (low temperatures and limited nutrients). Yet, in human-made environments such as air conditioning systems, the elevated water temperature can promote bacterial growth, especially if the system has longer periods of water flow stagnation. Indeed, many outbreaks of Legionnaires' disease have been linked to the dissemination of *Legionella*-contaminated aerosols by human-made aquatic systems (García-Fulgueiras et al., 2003; Nhu Nguyen et al., 2006; Shivaji et al., 2014; Weiss et al., 2017). Also the outbreak at the American Legion convention in 1976 was later linked to the hotel's air conditioning system (Fraser et al., 1977; Terranova et al., 1978).

Thus, the emergence of Legionnaires' disease in the past decades is thought to be caused by the progressive industrialization as well as the ubiquity of artificial aquatic environments.

Legionellosis

"But whatever it was, it came out of the trees" – Epidemiology of legionellosis

As mentioned before, the case numbers of legionellosis, the umbrella term for infections by *Legionella* spp., are steadily increasing over the past decades. There are large outbreaks occurring worldwide, with the biggest cluster reported to date being an outbreak in a hospital in Murcia, Spain with more than 800 suspected cases (García-Fulgueiras et al., 2003). However, the precise incidence rate of Legionnaires' disease worldwide is not known, due to vastly different surveillance methods, diagnostics and generally different awareness levels around the globe. This can lead to a strong discrepancy between diagnosed and undiagnosed cases.

Legionellosis is one of the most common causes of community-acquired pneumonia (von Baum et al., 2008; Muder et al., 1989). In the United Stated in 2018, around 10.000 cases of legionellosis were reported, which corresponds to an increase of almost nine times since the year 2000. The possible explanations for this steep rise in cases are manifold: increased presence of *Legionella* in the environment, increased susceptibility of the population to the infection, increased awareness and therefore, increased diagnosis, or a combination of factors. In addition, seasonal variations in case numbers can be seen, with most cases occurring in summer and early fall (https://www.cdc.gov/legionella/about/history.html). Moreover, the 2016-2017 Legionnaires' disease Surveillance Summary Report revealed that the two most prevalent exposure categories for Legionnaires' disease in the United States are healthcare and travel, with 21.3% and 15.8% of cases being traced back to these settings, respectively (https://www.cdc.gov/legionella/health-depts/surv-reporting/2016-17-surv-report-508.pdf). In a recent study from January 2021, it is estimated that the true burden of Legionnaires' disease in the United States is still vastly under-reported and that the true case number might be more than two times higher (Collier et al., 2021).

In Europe, the European Center for Disease Prevention and Control (ECDC) coordinates the European Legionnaires' Disease Surveillance Network (ELDSNet), which traces and records legionellosis cases in the 27 member states of the European Union, as well as Norway and Iceland (EEA). The ELDSNet reported more than 11.000 cases of Legionnaires' disease in 2019, an increase of almost 100% since 2009. In France, the case numbers rose by around 50% in the same time frame, from 1206 in 2009 to 1816 in 2019 (**Figure 2**).

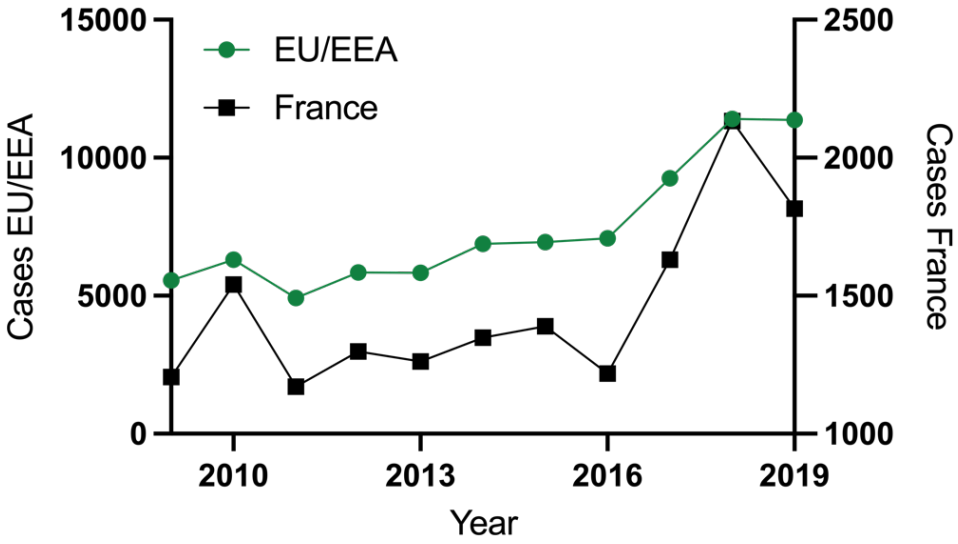

Figure 2: Number of reported Legionnaires' disease cases in Europe and France. Graph comparing case numbers of Legionnaires' disease in Europe (left axis, green circles) and France (right axis, black squares). Data obtained from https://www.ecdc.europa.eu/en/legionnaires-disease/surveillance/atlas.

As previously stated, at least 20 of the 65 *Legionella* species known to date have been linked to disease (Muder and Yu, 2002). Yet, if we look at the distribution of the different *Legionella* species among legionellosis cases in Europe and the United States, we see that the vast majority (91,5%) can be attributed to one species, *L. pneumophila*. Within this species, members of the serogroup 1 (Sg1) are responsible for around 84% of infections (Yu et al., 2002). Furthermore, it should be noted that five sequence types of Sg1 – out of a total of over 2000 sequence types – have emerged and are responsible for over 50% of legionellosis cases in northwest Europe today (David et al., 2016). The most common causes of non-*pneumophila* legionellosis are *Legionella longbeachae, Legionella bozemanii*, and *Legionella micdadei* (Yu et al., 2002). Interestingly, *Legionella longbeachae* only accounts for a small percentage of infections worldwide, however, this changes if we look at Australia and New Zealand. In Australia for example, *L. longbeachae* was responsible for 40% of legionellosis cases in 2016 (2021).

It should be noted that the human infection is usually a dead end for the bacteria. All infections – where the source has been identified – could be traced back to direct exposure to contaminated aerosols and there has been only one recorded case of putative person-to-person transmission (Correia et al., 2016).

"But whatever it was, it drove them to their knees" – Risk factors for legionellosis

Legionella spp. are opportunistic pathogens, meaning that individuals with specific risk factors are more prone to develop disease after exposure to the bacteria.

Interestingly, legionellosis has a higher prevalence in men than in women. In 2017 in the United States and Europe, men accounted for around 62% and 70% of infections, respectively. The reason for this phenomenon is yet to be discovered. Another risk factor is age (**Figure 3**). In 2020, around 50% of reported legionellosis cases in Europe were observed in people over the age of 65, but the same group accounts for almost 80% of all fatalities (https://www.ecdc.europa.eu/en/legionnaires-disease/surveillance/atlas). Yet, it should be noted that in recent years several cases of fatal neonatal pneumonia were connected to Legionnaires' disease, in particular in the context of birthing pools (Barton et al., 2017; Collins et al., 2016; Vanderlaan and Hall, 2020).

Other risk factors include chronic lung disease, immunosuppression, and smoking (Cameron et al., 2016; Carratala et al., 1994). In addition, many cases of legionellosis occur as nosocomial infections, with transplant patients being a high risk group (Bangsborg et al., 1995; Fraser et al., 2004; Wilmes et al., 2018).

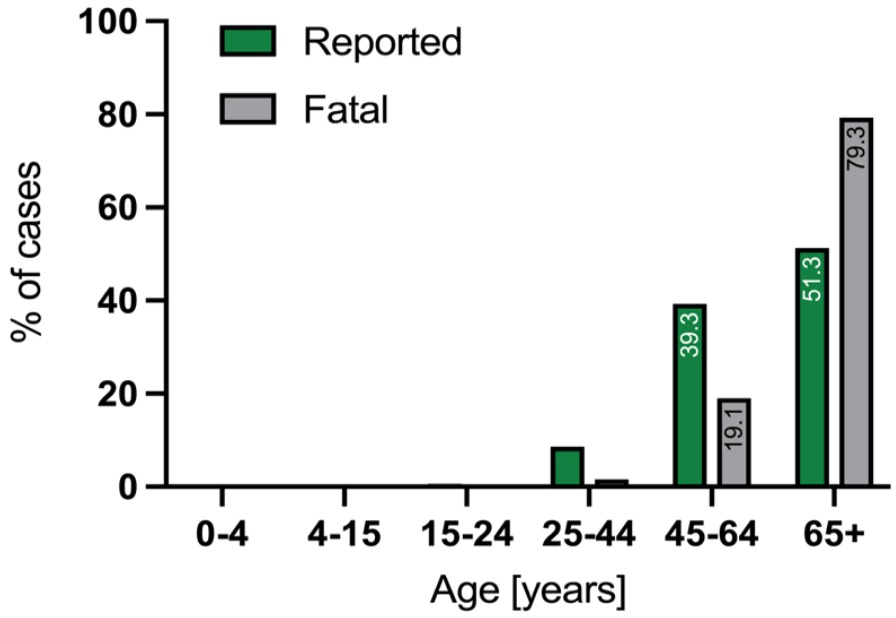

Figure 3: Comparison of reported cases and fatal cases of Legionnaires' disease over different age groups in Europe in 2020. Graph represents the percentage of cases (reported and fatal) (Y axis) and the different age groups (X axis) in Europe in 2020. Data obtained from https://www.ecdc.europa.eu/en/legionnaires-disease/surveillance/atlas .

"Now within my heart, it sure put on a squeeze" – Clinical manifestations of legionellosis

As mentioned before, legionellosis is the umbrella term for illnesses caused by different *Legionella* species. Besides Legionnaires' disease, this term comprises the non-pneumonic Pontiac fever, as well as other rare infections, such as wound infections and arthritis.

- Legionnaires' disease

Legionnaires' disease is an atypical pneumonia and the most severe form of legionellosis. The average incubation time from exposure to onset of the first symptoms is 2-10 days. However, incubation times of up to 24 days have been recorded (Bargellini et al., 2013). The first symptoms to occur are usually non-productive cough, shortness of breath, and fever. This clinical presentation is similar to many other bacterial pneumonias, for example infections caused by *Streptococcus pneumoniae* (Bradley and Bryan, 2019). However, one feature that helps to distinguish Legionnaires' disease from more common bacterial pneumonias is the frequent manifestation of extrapulmonary symptoms. These symptoms include gastrointestinal and renal symptoms as well as neurological abnormalities, such as mental confusion (Cunha and Cunha, 2017; Kao et al., 2019). A rare but severe complication of Legionnaires' disease is the formation of cavitary lesions. The formation of these cavities has been most prevalent in immunocompromised individuals or patients with other underlying conditions (Fraser et al., 2004; Guy et al., 2011; Khokher et al., 2021; Morales et al., 2018). The overall fatality rate of Legionnaires' disease is highly variable depending on the outbreak setting and other factors, but can reach from 5-40% (Bradley and Bryan, 2019).

- Pontiac fever

Pontiac fever is a non-pneumonic disease caused by the infection with different *Legionella* spp. It is a self-limited febrile illness without pneumonia. The most common symptoms include cough, fever, myalgia, headaches and malaise. Interestingly, the incubation period for Pontiac fever is with 1-2 days much shorter than the one of Legionnaires' disease. No fatalities for Pontiac fever have been reported yet (Kaufmann et al., 1981; Marrie and Hoffman, 2011).

- Other types of extrapulmonary legionellosis

Even though infections with *Legionella* spp. are usually connected to pulmonary infections, there have been reported cases of extrapulmonary infections with different members of this genus. Several reports of wound infections caused by different *Legionella* spp. (*L. pneumophila*, *L.micdadei*, *L. dumoffii*, *L. longbeachae*) have been reported (Ampel et al., 1985; Brabender et al., 1983; Lowry et al., 1991; Mentula et al., 2014). Another possible manifestation of extrapulmonary legionellosis is arthritis. This can mostly be seen in patients with underlying conditions or the elderly (Flendrie et al., 2011; Ibranosyan et al., 2019; Naito et al., 2007; Thurneysen and Boggian, 2014). Other rare infections include sinusitis and peritonitis (Dournon et al., 1982; Schlanger et al., 1984).

"Oh, that Legionnaire's disease" – diagnosis and treatment of legionellosis

The discovery and first description of *L. pneumophila* was performed by isolating the bacteria from lung tissue of four patients who have succumbed to the disease. This was a complicated and tedious process. First, guinea pigs were intraperitoneally inoculated with these samples. Afterwards, during the necropsy of these animals, tissue samples were taken and used to inoculate embryonated hen's eggs. However, to avoid contamination, antibiotics were added, thus no bacteria could be isolated. Later, the bacteria could be isolated from the yolk sac of the egg inoculated without antibiotics. This procedure was also applied for production of antigens, which subsequently were used to screen patient samples for the presence of *Legionella*-specific antibodies (McDade et al., 1977). Another common method was culturing the bacteria on a, at that time, recently developed medium, buffered-charcoal yeast extract (BCYE) (Edelstein, 1984). The serological tests and the culture-based identification were common practice for several years for the diagnosis of Legionnaires' disease and are still used today to investigate possible outbreaks in retrospect or to diagnose infections with less frequent species of *Legionella*. However, these tests are very time consuming and tedious, which makes them less than ideal for a rapid diagnosis of suspected cases of Legionnaires' disease. Within a few years after the initial discovery of *L. pneumophila* several new tests have been developed to diagnose a possible infection.

One of the first ones were urinary antigen tests, which took advantage of the fact that bacterial LPS is present in the patient's urine. First, a radioimmunoassay was developed, shortly followed by an enzyme-linked immunosorbent assay (ELISA)-based test to detect these urinary antigens (Kohler et al., 1981; Sathapatayavongs et al., 1982). Today, lateral flow tests are

widely used for the detection of soluble *Legionella* antigens in urine samples. However, these tests are only able to detect infection with *L. pneumophila* serogroup 1 (Domínguez et al., 1999). In parallel to the development of urinary antigen tests, new methods were developed based on a now very frequently used technique, polymerase chain reaction (PCR). First only used for the detection of *Legionella* spp. in environmental samples (Starnbach et al., 1989), this technique was quickly refined to detect and differentiate between several pathogenic *Legionella* species in patients samples (Jaulhac et al., 1992). In recent years, these PCR tests have been improved more and more to enable not only the differentiation between specific emerging *L. pneumophila* sequence types, but also to detect several non-pneumophila *Legionella* species in a multiplex approach (Benitez and Winchell, 2016; Cross et al., 2016; Mentasti et al., 2017; Mérault et al., 2011). Yet, the "gold standard" for the identification of a specific *Legionella* strain and serogroup remains culture and isolation, which are widely used in outbreak investigation (Mercante and Winchell, 2015; Mondino et al., 2020a). All these techniques enable a rapid diagnosis of Legionnaires' disease, which subsequently allows physicians to decide on effective treatment plans.

To this date, antibiotic resistance is a very rare occurrence in *L. pneumophila* infection. It should be noted that *Legionella* spp. are naturally resistant to β-lactam antibiotics (Fu and Neu, 1979), thus highlighting the importance of rapid diagnosis, since β-lactam antibiotics are a common first-line treatment for other bacterial pneumonias (Ceccato et al., 2021; Garau, 2005). However, in recent years there have been several reports of antibiotic resistances in *L. pneumophila* (Bruin et al., 2014; Jia et al., 2019; Shadoud et al., 2015). To stay one step ahead of the possible emergence of antibiotic resistant *L. pneumophila* the Study Group for Legionella Infection (ESGLI) of the European Society of Clinical Microbiology and Infectious Diseases (ESCMID) endorsed the routine use of antimicrobial susceptibility testing of *Legionella* isolated from patients (Portal et al., 2021). Today, the recommended treatment for *Legionella* infections are fluoroquinolones (e.g. levofloxacin or ciprofloxacin) and macrolides (e.g. azithromycin) (Pedro-Botet and Yu, 2006). Over the past few years, new approaches for the treatment of Legionnaires' disease are being developed. These new approaches include drugs like lefamulin, a novel pleuromutilin antibiotic, or the usage of gene therapy to target and inhibit specific bacterial genes (Mercuro and Veve, 2020; Pashaei-Asl et al., 2017; Veve and Wagner, 2018). These techniques could be on the forefront of Legionnaires' disease treatment in the near future.

Hijacking of the host by *Legionella*

As mentioned before, *L. pneumophila* can infect a wide range of protozoan hosts but also alveolar macrophages. The basic process is the same, independent of the host. After the entry of the bacteria into the host cell, the bacteria establish a protective vacuole, the so-called Legionella-containing vacuole (LCV), which allows the bacteria to replicate in a safe niche within this otherwise hostile environment. The LCV is remodeled during the infection by recruiting endoplasmic reticulum (ER) vesicles and ribosomes (Isberg et al., 2009). The similarities between the two host types underline the high adaptability of the bacteria. However, due to the lack of transmission between humans it was hypothesized that the co-evolution of *L. pneumophila* with its protozoan hosts has led to their capability to use these very same strategies to infect and replicate within mammalian macrophages (Al-Quadan et al., 2012; Cianciotto and Fields, 1992; Escoll et al., 2013; Molmeret et al., 2005). One indispensable factor for the infection is the bacterial type IV secretion system, Dot/Icm (Berger and Isberg, 1993; Marra et al., 1992). Through this system, more than 330 bacterial effectors are secreted into the host cell, manipulating countless signaling and metabolic pathways to the advantage of the microbial invaders (**Figure 4**) (Burstein et al., 2009; Campodonico et al., 2005; Heidtman

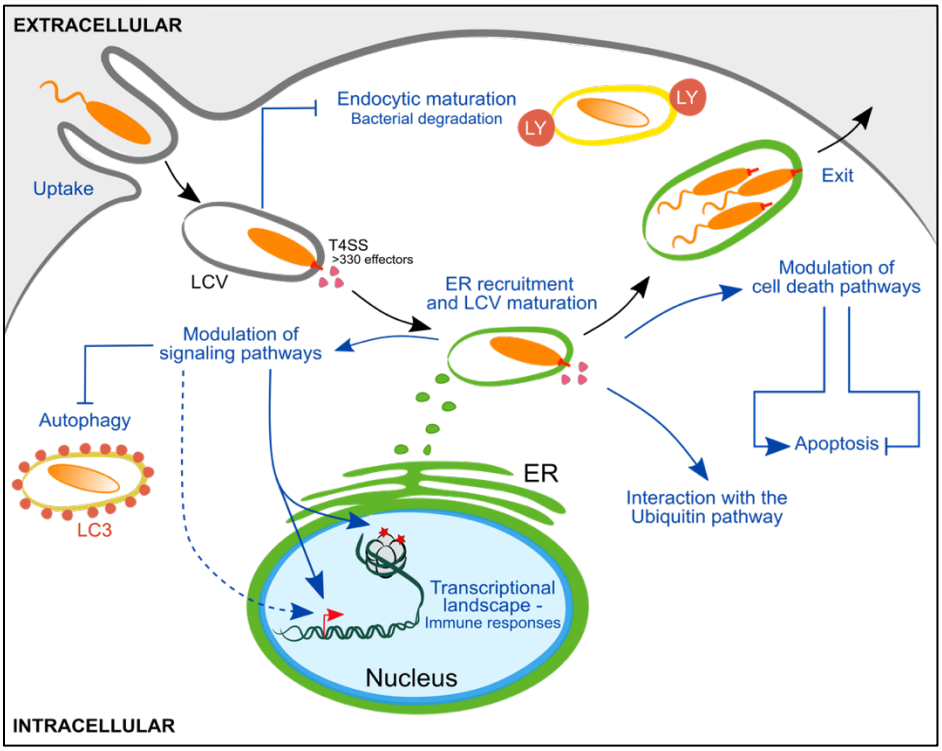

Figure 4: Schematic representation of the intracellular life cycle of *L. pneumophila* in phagocytic cells and the cellular pathways targeted by the bacteria. After uptake of the bacteria, they establish the Legionella-containing vacuole (LCV). Through secretion of a wide variety of effectors, the bacteria promote the recruitment of mitochondria and ER-derived vesicles to the LCV. Within the LCV, the bacteria replicate and switch again to their more virulent, flagellated form, until they egress from the host cell. Adapted from Mondino et al. (2020).

et al., 2009; Lifshitz et al., 2013; Zhu et al., 2011). The focus of this chapter will be the different strategies *L. pneumophila* deploys to replicate within a host cell. The general intracellular life cycle of *L. pneumophila* will be discussed, as well as its usage of the Dot/Icm secretion system and its effectors to manipulate the host.

It's the inner values that count – the intracellular life cycle of *L. pneumophila*

The first step of the infection is the attachment of the bacteria to the host cell. For macrophages, this process seems to be dependent on the complement receptors CR1 (CD35) and CR3 (CD18/CD11b). By blocking these receptors via monoclonal antibodies, bacterial uptake is strongly reduced (Payne and Horwitz, 1987). However, this CR1/CR3-dependent attachment seems also to rely on the presence of specific antibodies, produced in response to the infection (Husmann and Johnson, 1992). There have also been several reports of non-complement mediated adherence of *L. pneumophila*, which might play a role during the early stages of infection, when no specific antibody response has been mounted yet (Elliott and Winn, 1986; Gibson et al., 1994; Rodgers and Gibson, 1993). The bacterial factors that have been described so far to be involved in the attachment to the host are the two proteins MOMP and Lcl. MOMP, an outer membrane porin, was shown to bind complement components C3b and C3bi (Bellinger-Kawahara and Horwitz, 1990). In addition, it was reported to regulate bacterial attachment in a complement-independent manner (Krinos et al., 1999). Lcl binds a complement receptor, C1qR (CD93), to mediate attachment to the host (Vandersmissen et al., 2010). Another bacterial protein shown to influence bacterial entry is LpnE. It has been shown that an *lpnE* knock out leads to a decrease in bacterial entry in several different cell types (Newton et al., 2006). In addition, LpnE interacts with the eukaryotic polyphosphate-5 phosphatase, OCRL (oculocerebrorenal syndrome of Lowe), leading to its recruitment to the LCV(Voth et al., 2019; Weber et al., 2009).

The exact mode of bacterial entry into the host cell is still a strongly discussed topic. A mechanism called coiled phagocytosis was described in several hosts, but only seems to represent a small portion of bacterial uptake (**Figure 5**) (Bozue and Johnson, 1996; Horwitz, 1984).

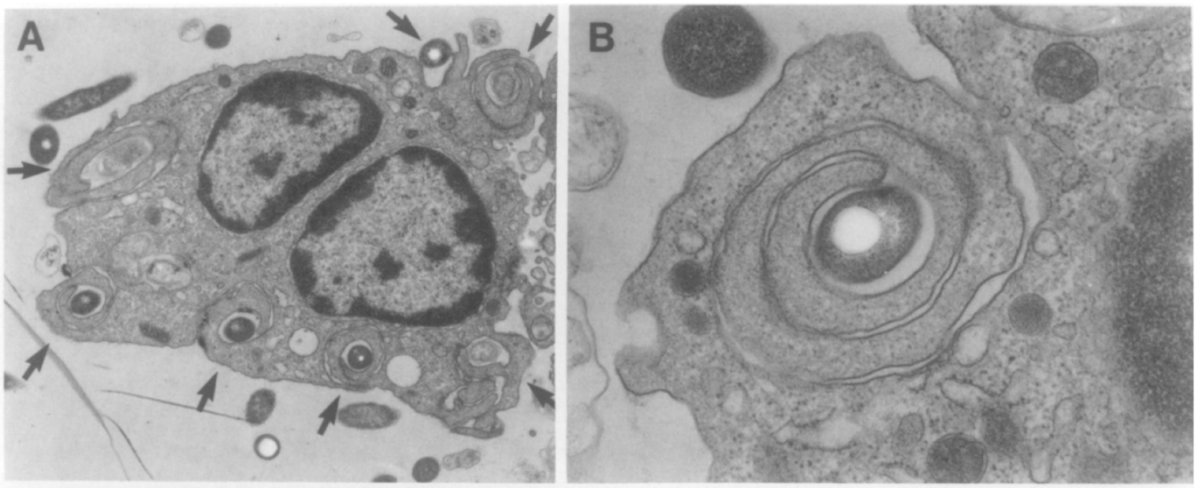

Figure 5: Electron microscopy of coiled phagocytosis of *L. pneumophila* by human monocytes. Human monocytes were incubated with *L. pneumophila* at 37˚C for 3.5 min to allow phagocytosis to begin. Then cells were fixed and analyzed by electron microscopy. Adapted from Horwitz (1984).

The conventional internalization of the bacteria is mediated by the MOMP-C3b interaction, mentioned before (Bellinger-Kawahara and Horwitz, 1990). Even though, many questions remain about the exact mechanisms of uptake, it is well-known that the uptake and the following internalization in mammalian cells is dependent on actin polymerization. By using cytochalasin-D – a known inhibitor of actin polymerization – the uptake of *L. pneumophila* in macrophages as well as lung epithelial cells is inhibited (Elliott and Winn, 1986; King et al., 1991; Prashar et al., 2012).

Once the bacteria enter the host cell, they start to establish the LCV. Under normal conditions, after the cell engulfs different microbes in a phagosome, the phagosome matures by different fusion/fission steps with parts of the endosomal network, leading to the formation of the phagolysosome. Subsequently, this leads to the acidification of the phagolysosome triggering the degradation of its contents (Vieira et al., 2002). However, *Legionella* is able to inhibit the fusion with the lysosome, thus manipulating the host cell and enabling the formation of a replicative vacuole where the bacteria can grow to high numbers (Isberg et al., 2009; Mondino et al., 2020a; Newton et al., 2010). Interestingly, the process of acidification is delayed in the LCV but not completely inhibited. In the first few hours of infection, the pH within the phagosome stays neutral. This changes at later infection stages, when the LCV acquires more endosomal markers and the LCV acidifies. Moreover, the bacteria obtained from cell culture, but not the ones from broth, have a higher tolerance to low pH, indicating that maintaining the neutral pH within the LCV is only necessary at the beginning of the infection (Sturgill-Koszycki and Swanson, 2000). So far, one secreted effector protein of *L. pneumophila*, SidK, has been reported to inhibit vacuole acidification by interacting with the proton pump

VatA (L et al., 2010; Zhao et al., 2017). However, many questions remain about the exact regulation of LCV acidification.

The remodeling of the LCV membrane during infection is an intricate and finely regulated process. Within the first few minutes, ER-derived vesicles are recruited to the LCV. By intercepting secretory vesicles of the ER and Golgi, the bacteria transform the LCV into an ER-like organelle that permits their replication (Derré and Isberg, 2004; Kagan et al., 2004; Weber et al., 2018). Two of the earliest and most prominently recruited proteins are the small GTPase Rab1 and the soluble N-ethylmaleimide-sensitive factor attachment protein receptors (SNARE) Sec22b (Kagan et al., 2004). Rab1 usually regulates the fusion of ER-derived vesicles with the Golgi and Sec22b is responsible for vesicle tethering and fusion between said vesicles and the Golgi (Moyer et al., 2001; Xu et al., 2000). Moreover, the inhibition of Rab1 activity in infected cells can drastically reduce *L. pneumophila* replication, highlighting its importance in the process of establishing a functional LCV (Kagan et al., 2004). The fusion of the ER-derived vesicles also releases their contests into the LCV, functioning as a nutrient delivery system for the bacteria (Robinson and Roy, 2006). At late infection times, the LVC associates with late-endosome markers, like LAMP-1 (lysosome-associated membrane protein 1), suggesting that the lysosomal compartments provide a nutrient-rich environment for bacterial replication (Sturgill-Koszycki and Swanson, 2000). After 18-24 hours post-infection, the cells are filling with bacteria, ready to be released and infect new cells (**Figure 6**).

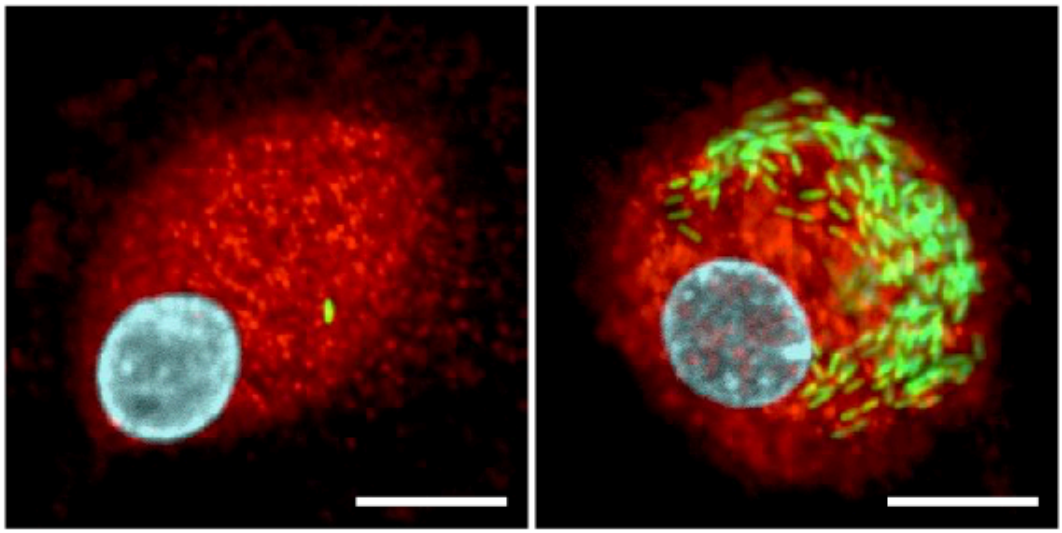

Figure 6: Intracellular replication of *L. pneumophila* in macrophages. Confocal microscopy images of human monocyte-derived macrophages (hMDM), infected with *L. pneumophila* constitutively expressing GFP for 2 (left) and 20 (right) hours. DAPI (cyan), *L. pneumophila* (green), cytoplasm (red). (Pictures kindly provided by Pedro Escoll, Institut Pasteur)

The depletion of nutrients in the host cell triggers a transformation within the bacteria. Under these conditions, the bacteria change from their replicative form – characterized by low cytotoxicity and low motility – to their transmissive form, where the bacteria produce their flagellum, causing high motility, and strongly increase the expression of other virulence associated genes (Molofsky and Swanson, 2004; Oliva et al., 2018). Following this phenotypic switch is the bacterial egress. At late infection stages the bacteria seem to disrupt the LCV and are freely present in the host cell cytoplasm. There is evidence that this disruption of the LCV membrane is caused by the ability of the bacteria to form pores, which consequently cause membrane lysis (Alli et al., 2000). The bacterial egress from the cell itself also seems to be pore-related. However, it is suggested that this process is dependent on the host response to the cytoplasmic bacteria. The activation of the NLRC4 inflammasome by the cytoplasmic bacterial flagellin induces this pore formation. This phenotype can neither be seen when cells are infected with an *L. pneumophila* flagellin knockout strain nor when cells lacking caspase 1 – a crucial component for the activation of the inflammasome – are infected (Silveira and Zamboni, 2010). Moreover, several studies have demonstrated that *L. pneumophila* actively inhibits host cell apoptosis during the early stages of infection (Abu-Zant et al., 2007; Arasaki and Tagaya, 2017; Losick and Isberg, 2006). It is only at late stages that macrophages exhibit increasingly apoptotic phenotypes. This regulation of apoptosis by the bacteria represents another possible strategy to control the bacterial egress (Speir et al., 2014).

Weapon of choice – *Legionella*'s Dot/Icm secretion system

In *L. pneumophila*, four secretion systems have been characterized: a type I secretion system (T1SS), a T2SS and two T4SS (T4ASS, T4BSS) (De Buck et al., 2007). In addition, the presence of a T5SS and a TAT secretion system has been predicted through genome sequence analysis in certain *L. pneumophila* strains (Cazalet et al., 2004). The knowledge about the T1SS and the T4ASS are quite limited, but both have been implicated in bacterial replication and virulence (Fuche et al., 2015; Ridenour et al., 2003). The T2SS has been shown to translocate about 25 effectors into the host cell and its activity has been linked to bacterial virulence (Cianciotto, 2009, 2014; Hiller et al., 2018; Lang et al., 2017). However, the main virulence factor of *L. pneumophila* and the majority of other *Legionella* spp. is a type IVB secretion system (T4BSS), the so-called Dot/Icm (defective organelle trafficking/intra cellular multiplication) secretion system. The Dot/Icm system is essential for intracellular replication of the bacteria (Berger and Isberg, 1993; Marra et al., 1992). There are many other pathogens

that possess a T4SS, yet what makes the Dot/Icm of *Legionella* exceptional is the large number of proteins that are translocated through this system. To this date, more than 330 Dot/Icm effector proteins have been shown to be translocated in *L. pneumophila*, which represents around 10% of the bacterial genome. Surprisingly, these effectors are highly variable between different *Legionella* species, with only 8 being conserved between 58 analyzed species (Gomez-Valero et al., 2019). However, if we look at the conservation level of the Dot/Icm system between species, we can see that all components except one (IcmR) are present in all *Legionella* species (Burstein et al., 2016; Feldman et al., 2005; Gomez-Valero et al., 2019). In addition to its protein secretion function, the Dot/Icm system has also been described to transfer DNA, the main function of the first described T4SS, the VirB/D4 system in *Agrobacterium tumefaciens* (Bundock et al., 1995; Vogel et al., 1998).

The Dot/Icm system is a big complex, with around 27 proteins predicted to be involved in its assembly and function. The main components are an inner membrane complex and a core complex, spanning the periplasmic space. In addition, the Dot/Icm system shows polar localization, which is crucial for bacterial virulence, as well as tethering the bacteria to the LCV, facilitating protein translocation (Böck et al., 2021; Jeong et al., 2017). The core complex structure has been described as a "Wi-Fi symbol"-like particle, due to its distinct curved layers (**Figure 7**) (Ghosal et al., 2017).

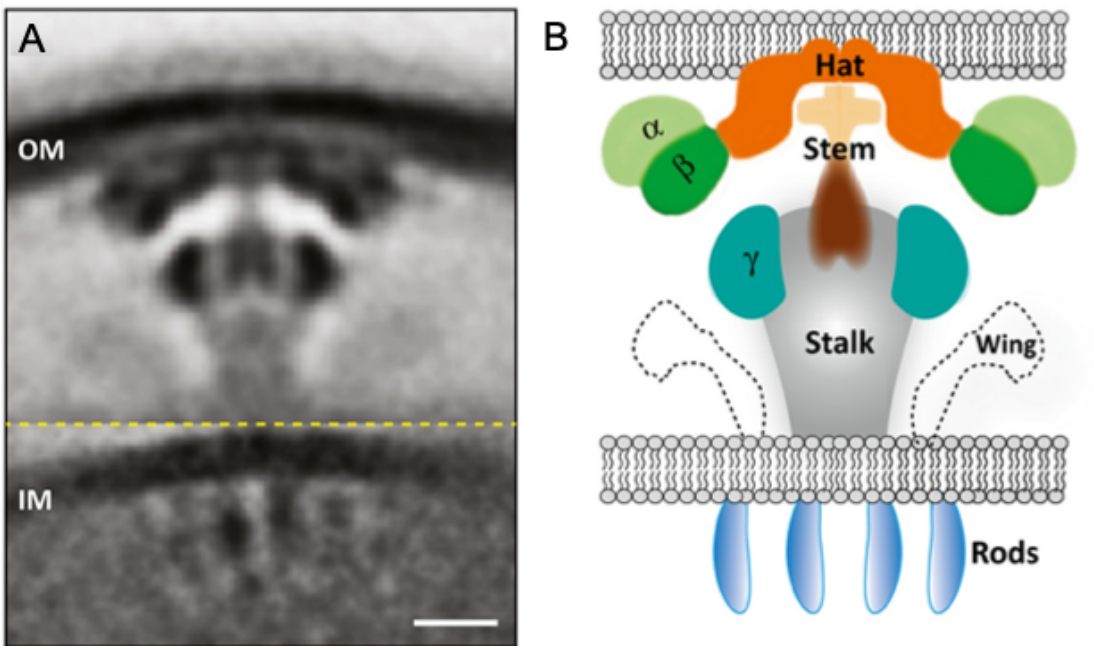

Figure 7: Dot/Icm secretion system of *L. pneumophila*. (A) Subtomogram of the Dot/Icm system of *L. pneumophila* depicting its connection between inner membrane (IM) and outer membrane (OM). Scale bar, 10 nm. (B) Schematic representation of the subtomogram, showing the known structures of the Dot/Icm system. Adapted from Ghosal et al. (2017).

Recently, new structural components of the Dot/Icm system have been described. A protein, previously not connected to the secretion complex, has been detected by isolating the complex directly from *L. pneumophila* and analyzing it by mass spectrometry (Durie et al., 2020). For more in-depth information about the Dot/Icm structure and T4SS in general, please refer to the review by Costa et al. (Costa et al., 2021).

Another vast field of study connected to the Dot/Icm system is effector recognition and their translocation signals. One of the earliest discoveries was that many translocated effectors contain short C-terminal translocation signals consisting of polar and negatively charged amino acids (Burstein et al., 2009; Nagai et al., 2005). A big step forward was the discovery of the so-called E block motif, a cluster of glutamine residues within 20 amino acids from the C-terminus present in more than 100 Dot/Icm effectors (Huang et al., 2011). However, it was also seen that adaptor proteins, such as IcmS and IcmW can modulate the translocation of proteins with and without E block motifs, indicating that other mechanisms of translocation recognition are also involved in this process (Lifshitz et al., 2013). Indeed, it was described that DotL, a known type IV coupling protein, together with the adaptor proteins IcmS and IcmW, as well as other components, forms a complex that can regulate effector translocation (Sutherland et al., 2012). Moreover, recent studies revealed that the composition of this complex seems to be variable and that this variability can determine which effectors are recognized. In addition, the interaction with the effectors seems more dependent on structural features, than exact amino acid motifs (Kim et al., 2020; Meir et al., 2020). Moreover, the expression of these Dot/Icm effectors is regulated in a life-cycle dependent manner, adding another layer of secretion regulation (Aurass et al., 2016). Taken together, these examples show that effector recognition and translocation are a highly complex processes that enable the bacteria to manipulate the host in specific ways at specific times of the infection.

Legionella: a jack of many (eukaryotic-like) traits

The ability of *Legionella* species to invade amoebae and macrophages, to manipulate numerous host pathways, and to create an environment enabling bacterial replication, is key to its survival. One notch of this key is the fact that members of this genus, probably due to their close co-evolution with their protozoan hosts, have acquired numerous protein-coding genes from said hosts (Cazalet et al., 2004; Corpas-López et al., 2019; de Felipe et al., 2005; Gomez-Valero et al., 2011; Lurie-Weinberger et al., 2010; Mondino et al., 2020b). The high number of secreted eukaryotic-like proteins – even though their mode of acquisition is still unknown –

represent a unique feature of this bacterial genus. As mentioned before, more than 18,000 effectors have recently been predicted in the genus *Legionella*, comprising 137 different eukaryotic domains and more than 250 eukaryotic-like proteins (Gomez-Valero et al., 2019). In *L. pneumophila*, these eukaryotic-like proteins influence countless pathways in the host, from intracellular trafficking and signal transduction, to metabolism and gene transcription, just to name a few (**Figure 8**). Here we will discuss some examples of bacterial effectors targeting these pathways.

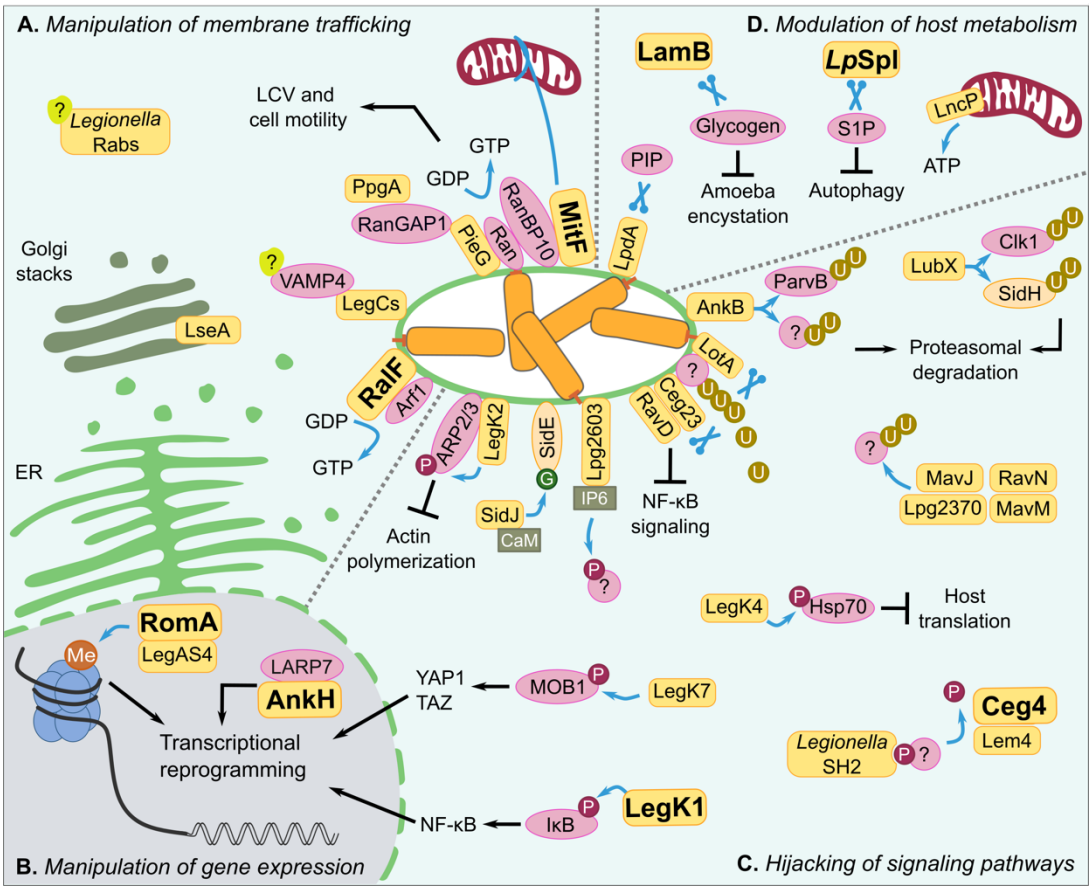

Figure 8: Schematic representation of selected *Legionella* effectors. Effectors are T4SS-dependently secreted into the host and target several different cellular pathways by either containing eukaryotic-domains or by mimicking eukaryotic proteins as a whole. Orange box, *Legionella* effector; pink oval, host target protein/molecule; orange oval, *Legionella* target protein; Me, methylation; U, ubiquitination; P, phosphorylation; G, glutamylation, CaM, calmodulin; IP6, inositol hexakisphosphate; ER, endoplasmic reticulum. Effectors highlighted in bold are discussed in this chapter. Adapted from Mondino et al. (2020).

Influencing intracellular trafficking pathways is essential for *L. pneumophila* to establish and maintain the LCV. One class of key regulators of membrane trafficking are small GTPases, such as the Arf, Rho, Ras, and Rab families. Small GTPases can be found in an active GTP-bound state and an inactive, GDP-bound state. Switching between these two states is regulated by two classes of proteins, guanine nucleotide exchange factors (GEFs) and GTPase-activating proteins (GAPs) (Cherfils and Zeghouf, 2013). *L. pneumophila* secrets several effectors directly influencing small GTPases, one of which is RalF, the first *L. pneumophila*

Dot/Icm secreted effector characterized. RalF acts as a GEF for Arf 1, leading to its recruitment to the LCV (Nagai et al., 2002). It was shown that RalF indeed contains a Sec7 domain, a feature usually found in Arf GEFs and that this domain is highly conserved in the bacterial protein (Amor et al., 2005). Another *L. pneumophila* effector imitating eukaryotic GEFs is MitF (LegG1). This effector causes activation of Ran proteins, thereby stimulating microtubule stabilization, cell migration, and LCV motility (Rothmeier et al., 2013; Simon et al., 2014). Moreover, MitF (LegG1) was shown to promote mitochondrial fragmentation, consequently leading to a Warburg-like metabolism in the host cell, thus promoting bacterial replication (Escoll et al., 2017). The example of MitF (LegG1) also shows that the same effector can be involved in manipulating several different pathways in the host.

Signal transduction is another potent target for pathogens. Protein kinases and phosphatases are crucial components of many signaling pathways in eukaryotic cells (Graves and Krebs, 1999). The *L. pneumophila* LegK1, a eukaryotic-like serine/threonine protein kinase, can activate the transcription factor NF-κB. NF-κB is a key regulator of innate and adaptive immunity, inflammation, and cell death (Perkins, 2007). The activation of NF-κB is achieved by LegK1 mimicking the activity of the IκB kinase (IKK), a protein promoting the degradation of the NF-κB inhibitor IκB. The activity of LegK1 is independent of the known upstream pathways of IKK, suggesting that it is a constitutively active kinase or that it is activated through an unknown mechanism (Ge et al., 2009). Furthermore, *L. pneumophila* not only secrets its own protein kinases, but also phosphatases. The recently discovered Ceg4, with its haloacid dehalogenase (HAD)-like domain, is a phosphotyrosine phosphatase. *In vitro*, Ceg4 attenuates the activation of mitogen-activated protein kinases (MAPK) (Quaile et al., 2018). MAPKs are key regulators of countless cellular processes such as gene expression, cell differentiation, and apoptosis, just to name a few (Pearson et al., 2001). However, the exact consequence of this MAPK inhibition during infection is yet to be determined.

Another process targeted by *L. pneumophila* is host cell metabolism. There are several effectors connected to the manipulation of metabolic pathways, whether it is to scavenge nutrients and promote bacterial replication or to manipulate host cell pathways that are dependent on different metabolic products. In eukaryotes, amylases are responsible for the hydrolysis of starch and glycogen into glucose, a process usually not occurring in bacteria, since they do not synthesize these products. LamB, an amylase-like protein encoded by *L. pneumophila*, exhibits strong amylase activity *in vitro* and its loss severely impairs bacterial growth in human monocyte-derived macrophages and decreases pathogenicity in a mouse

model (Best et al., 2018). However, *L. pneumophila* not only targets carbohydrates but also lipids, and in particular sphingolipids. One of the main enzymes regulating the intracellular concentration and degradation of sphingolipids, especially sphingosine-1 phosphate (S1P), is the sphingosine-1 phosphate lyase (SPL) (Bourquin et al., 2010). *L. pneumophila* encodes its own SPL-like protein called *Lp*Spl (LegS2). During infection *Lp*Spl promotes the degradation of host sphingolipids. This decrease in sphingolipid levels subsequently impairs the autophagic response of the cell, thus promoting the intracellular survival of the bacteria (Rolando et al., 2016).

Last, but certainly not least, is the manipulation of the host cell on the transcriptional level. Many pathogenic bacteria encode so-called nucleomodulins: bacterial effectors that specifically target the host cell nucleus to hijack the transcriptional machinery (Bierne and Cossart, 2012; Escoll et al., 2016). One of the 8 core effectors conserved between all sequenced *Legionella* species in AnkH (Gomez-Valero et al., 2019). AnkH contains four ankyrin repeats, which in eukaryotic proteins mediate protein-protein interaction. During infection, AnkH binds to the 7SK small nuclear ribonucleoprotein (snRNP) complex, specifically the La-related protein 7 (LARP7). The interaction of AnkH with LARP7 interferes with its binding to the 7SK snRNP complex, ultimately impeding the transcriptional elongation by RNA polymerase II. In addition, by mutating the ankyrin domains, the interaction of AnkH with LARP7 can be abolished, leading to an intracellular growth defect of *L. pneumophila* (Von Dwingelo et al., 2019). One of the best described nucleomodulins in *L. pneumophila* strain Paris is the SET (su[var]3-9, enhancer-of-zeste and trithorax)-domain containing eukaryotic-like protein RomA. In eukaryotes, SET-domain proteins function as lysine methyltransferases, that can target and modify histones, thus influencing chromatin condensation and transcriptional activity (Dillon et al., 2005). RomA is a Dot/Icm secreted effector that targets the host cell nucleus and specifically methylates lysine 14 of histone H3 (H3K14). The methylation of H3K14 – a residue that is usually acetylated – causes a transcriptional repression of specific host genes involved in the innate immune response of the cell (Rolando et al., 2013). Moreover, RomA was also shown to target non-histone proteins. AROS, a regulator of histone deacetylase SIRT1, is also methylated by RomA. However, the exact effect of this methylation is yet to be discovered (Schuhmacher et al., 2018). In addition to its SET-domain, RomA also contains several ankyrin repeats, but their role during infection remains to be investigated. In *L. pneumophila* strain Philadelphia-1 a homologue of RomA, LegAS4, was reported methylate lysine 4 on histone H3 (H3K4). It is proposed that this methylation promotes the transcription of host cell ribosomal DNA, which boosts bacterial replication (Li et al., 2013). However, strain Philademphia-1 also

methylates H3K14, thus LegsA4/RomA might fulfill both functions (Rolando and Buchrieser, 2014).

In conclusion, these examples demonstrate that the acquisition of eukaryotic-like proteins has enabled *Legionella* spp. to manipulate a wide variety of host cell pathways, ensuring the bacterial survival and replication by molecular mimicry of eukaryotic proteins (Gomez-Valero et al., 2011). Moreover, many of the 250+ predicted eukaryotic-like proteins are yet to be investigated and the number of possible strategies employed by the bacteria to subvert the host response seem sheer endless.

Chromatin and infection

Chromatin and Epigenetics

A string of information – Chromatin and its structure

Each eukaryotic cell contains an enormous amount of genomic DNA. This DNA – around 2 m from end to end – has to be organized in a meticulously planned manner, to fit into the cell nucleus, with its size of 2-10 µm. To achieve that, genomic DNA interacts with small basic proteins, called histones. Histones form octamers that the DNA is wrapped around. This DNA-histone complex is called a nucleosome (**Figure 9**). With the help of so-called linker histones, nucleosomes can interact with each other and form chromatin fibers, which lastly, can be organized in higher structures, such as chromosomes (Alberts et al., 2002). Each of these organization steps regulates DNA-accessibility and thereby all DNA-related processes, such as transcription and replication. The regulation of chromatin organization is highly dynamic and flexible, to enable a rapid response of the cell to numerous internal and external stimuli. The histone octamer consists of the highly conserved core histones: H2A, H2B, H3, and H4. However, several different variants/isoforms of these core histones are known to date,

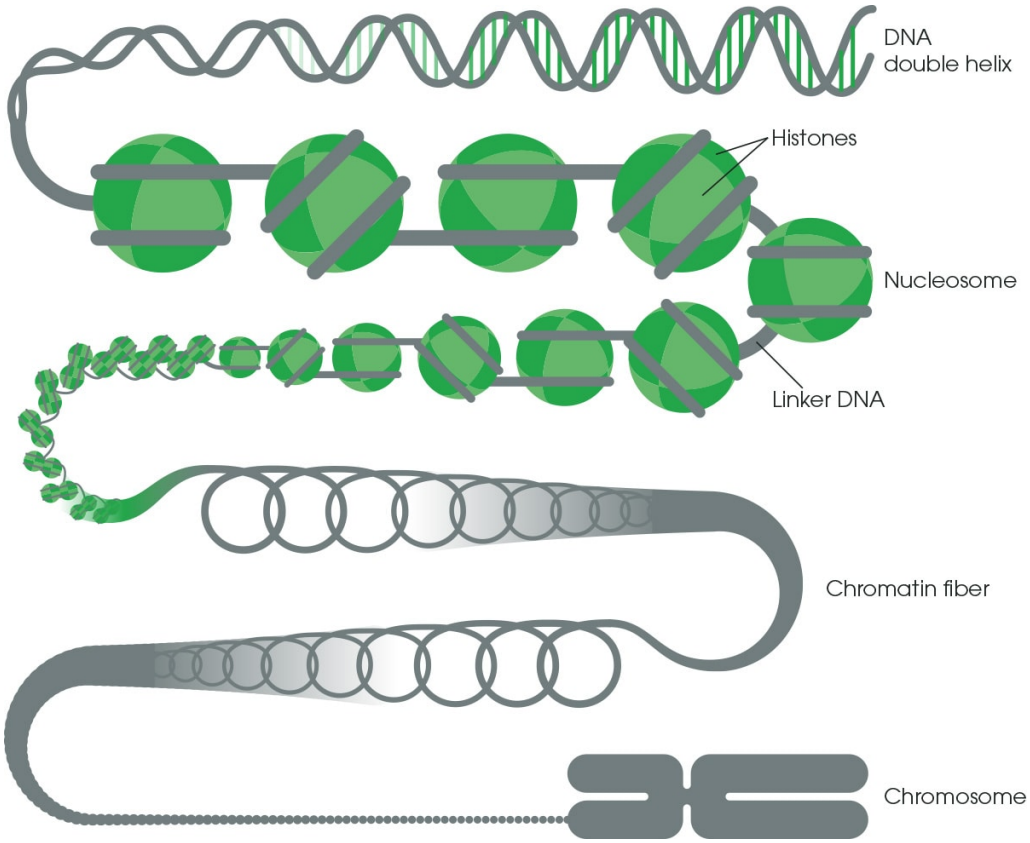

Figure 9: Schematic representation of chromatin organization in eukaryotic cells. DNA wraps around histone octamers, forming nucleosomes. Nucleosomes are connected by linker DNA and form chromatin fibers, which subsequently are organized into chromosomes. Adapted from https://www.abcam.com/epigenetics/chromatin-accessibility-and-architecture.

representing another level of chromatin structure regulation (Singh et al., 2018). All of these core histones contain a so-called histone fold region as well as flexible N-terminal tails. The octamer is formed by the interaction of two H2A/H2B dimers with one H3/H4 tetramer. In addition, the linker histone, H1, acts as a clamp, tethering the DNA to the core histones (Arents and Moudrianakis, 1993). This interaction is stabilized by several binding sites, such as a four-helix bundle and the H2A docking domain. The DNA is wrapped around this histone core around 1.7 times, – which equals to 147 base pairs – in a left-handed manner (**Figure 10**) (Luger et al., 1997). These nucleosome core particles (NCPs) are connected via 15-50 base pair long linker DNA, which, at low salt concentrations, adopts characteristic "beads on a string" appearance (Baldi et al., 2020; Olins and Olins, 1978). At higher salt concentrations, chromatin compacts into fibers with a diameter of ~30-nm (Wedemann and Langowski, 2002).

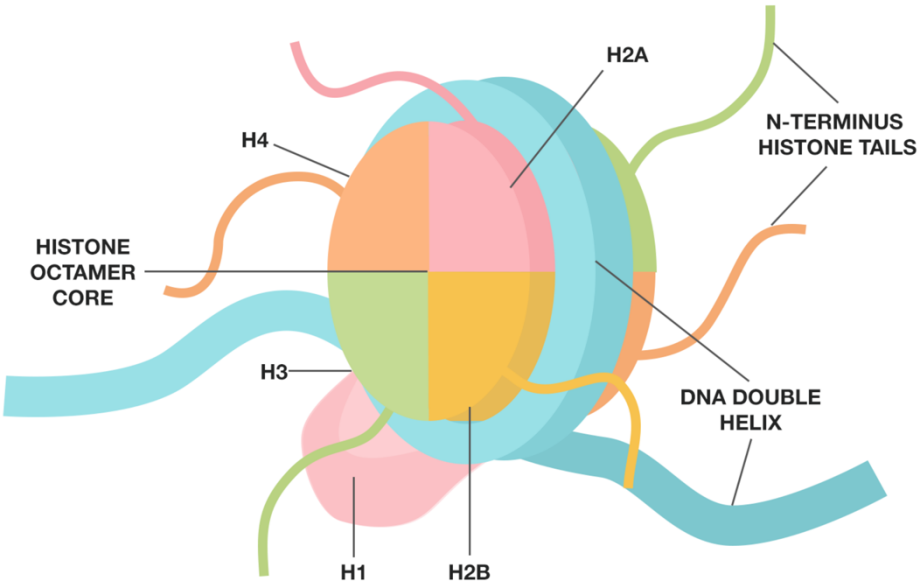

Figure 10: Schematic representation of a nucleosome. DNA is wrapped around the core histone octamer, consisting of two copies of each H2A, H2B, H3 and H4. H1 acts as a clamp on the outside of the complex and stabilizes the protein/DNA interaction. Adapted from https://www.behance.net/gallery/83812381/How-DNA-is-Organised-Nucleosome-Structure?tracking_source=search_projects_recommended%7Cnucleosome.

The exact structural mechanism of chromatin fiber formation is still an open question. There are two models that have been proposed: the zigzag model and the solenoid model (Chen et al., 2021). In the first one, as the name suggests, the nucleosomes are connected by straight linkers, leading to a ladder-like structure, where the nucleosomes zigzag back and forth, leading to a "two start model" (Staynov et al., 1983). In the solenoid model, the nucleosomes are stacked on top of each other connected by bend linkers, forming a "one start" helix-like structure (**Figure 11**) (McGhee et al., 1983). The type of structure is determined by a variety of factors. One factor it the average nucleosome repeat length (NRL). The NRL is the average distance between two nucleosomes. Shorter NRLs promote the formation of the zigzag topology,

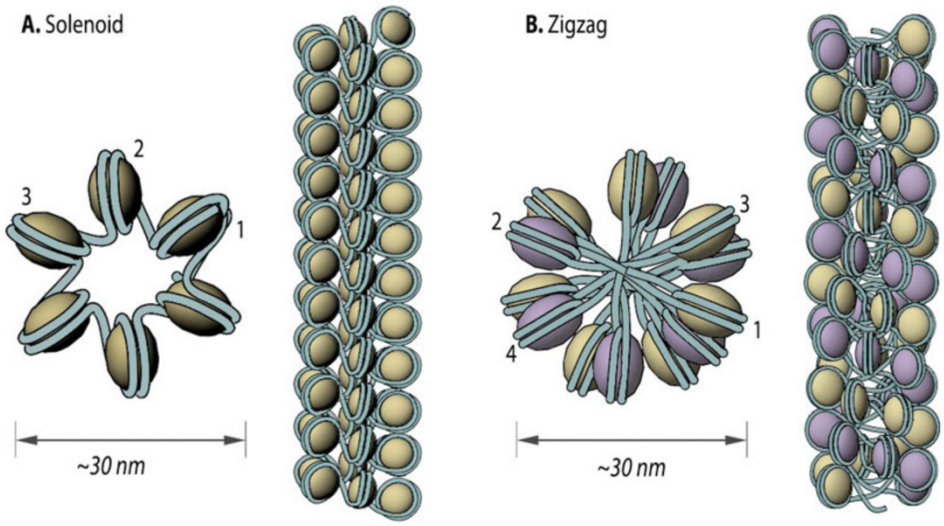

Figure 11: Schematic representation of the solenoid and zigzag model of nucleosome organization. (A) In the solenoid model interactions between the histone cores occur sequentially (1, 2, 3, 4, etc.). (B) In the zigzag model, the alternate octamers become interacting partners (1 and 3, 2 and 4, etc.), which is represented by two different colors of histone octamers. Adapted from https://www.mechanobio.info/genome-regulation/what-are-nucleosomes/.

whereas longer NRLs lead to the formation of the more compact solenoid structure (Robinson et al., 2006). Another factor is the binding of the linker histones, H1. Interestingly, H1 is not has highly conserved as the other histone proteins. In humans 11 different H1 variants have been identified (Izzo et al., 2008). The different H1 variants bind to the NCPs slightly differently, subsequently promoting the formation of one chromatin configuration over the other (Song et al., 2014; Zhou et al., 2015).

Besides the histones, there are also several non-histone proteins that are involved in chromatin architecture. One of these non-histone proteins is the FACT (facilitates chromatin transcription) complex. This complex acts as a chaperone for H2A/H2B dimers, and is crucial for nucleosome destabilization during transcription, enabling RNA polymerase II progression (Belotserkovskaya et al., 2003). Other examples of chromatin decondensation by non-histone proteins are the high mobility group (HMG) proteins. HMG proteins regulate chromatin decompaction, which consequently enables the targeting of the chromatin by different regulatory factors. Their binding sites compete with the ones of linker histone H1, attenuating the H1-dependent compaction of chromatin (Postnikov and Bustin, 2010). Another protein competing with H1 for its binding site is the methyl CpG binding protein 2 (MeCP2). However, it has the opposite effect of the HMG proteins. Through its binding, MeCP2 drastically reduces the angles though which DNA enters and exits the nucleosomes, causing a dramatic increase in chromatin condensation (Ghosh et al., 2010).

The level of chromatin condensation can influence which genes are accessible for transcription and which genes are silenced. Less condensed chromatin with higher accessibility

for the transcription machinery is called euchromatin. In euchromatin, the nucleosomes are wider spaced and are exactly positioned at promoters due to specific DNA sequence guided DNA-protein interactions. The counterpart of euchromatin, heterochromatin, lacks nucleosome positioning and is characterized by high levels of condensation and less transcriptional activity, which includes tissue-specific and developmental genes (the facultative heterochromatin) or gene-poor regions (the constitutive heterochromatin) (Morrison and Thakur, 2021).

As mentioned above, the condensation is dependent on a variety of different factors, including DNA-histone interaction, histone variants, and the binding of non-histone proteins. All of these factors together represent transcriptional information on chromatin that is independent of the DNA sequence. This sequence-independent information is summarized under the term epigenetics (Radford, 2018).

Change without change – the principle of epigenetics

The definition of epigenetics has changed over the past decades to reflect the newest advances in this ever-growing field of research. One of the best-known definitions is from Russo et al., stating epigenetics is "the study of mitotically and/or meiotically heritable changes in gene function that cannot be explained by changes in DNA sequence" (Russo et al., 1996). Under this definition, epigenetics only encompasses phenomena that are stringently heritable from one cell to its daughters. However, the latest research in this field suggests that, yes, in some cases these changes can indeed be inherited by the progeny, but this is not always the case. Epigenetic changes are more and more seen as dynamic changes that can appear and disappear within the life time of a single cell. Therefore, newer and updated definitions are becoming more popular. One definition, by Adrian Bird, summarizes epigenetics as follows: "the structural adaptation of chromosomal regions so as to register, signal or perpetuate altered activity states" (Bird, 2007). This definition does not limit epigenetics to changes stably maintained over several cell generations, but also includes transient modifications, which can still affect cells greatly.

There are several possibilities how epigenetic information can be classified: covalent modifications of the DNA (e.g. DNA- methylation) (Jones, 2012), activity of long non-coding RNAs (Mercer and Mattick, 2013), as well as covalent modifications of the histones (Kimura, 2013).

Epigenetic changes and infection

Reading between the genetic lines – classes of epigenetic information

As mentioned before, there are different classes of epigenetic information: activity of long non-coding RNAs, DNA methylation, and post-translational modification of histones.

Long non-coding RNAs (lncRNAs), as the name suggests, have a length of more than 200 base pairs and show no apparent potential to encode proteins. After their transcription, this type of RNA is similarly processed to mRNAs, which includes splicing, 5' capping, and 3' polyadenylation. However, these processes seem to be less efficient for lncRNAs (Melé et al., 2017). Another difference between the two types of RNA is their localization: mRNAs are almost exclusively found in the cytoplasm, whereas lncRNAs are mainly found in the nucleus, where they are involved in a wide variety of processes, such as chromatin architecture and remodeling, transcriptional regulation, and formation of nuclear bodies (Yao et al., 2019). In fact, lncRNAs contain structural domains can sense or bind RNAs, via complementary base pair interactions, proteins, and possibly DNA that can induce allosteric conformational changes due to the other structures in the lncRNA (Mercer and Mattick, 2013). The probably most studied lncRNA is the X-inactive-specific transcript (Xist), which controls the X-chromosome inactivation in female mammals (Hall and Lawrence, 2010). After transcription, Xist accumulates at many sites across the X chromosome, where it can recruit heterochromatin protein HP1 to satellite repeats. The continued local accumulation of HP1 results in the spreading of facultative heterochromatin to demarcate broad repressive chromosomal domains (Wutz, 2011). LncRNAs can also directly influence transcription. This can be achieved by, for example, recruiting transcription factors and other chromatin remodelers to specific chromatin regions, or by directly interfering with the activity of RNA polymerase II (Mariner et al., 2008; Postepska-Igielska et al., 2015). Moreover, lncRNAs are involved in immune and inflammatory processes, which are crucial during viral and bacterial infections (Prasad and Prasad, 2021; Schmerer and Schulte, 2021).

Covalent modification of the DNA, by methylation, and post-translational modifications (PTMs) of the histone tails can be attributed to specific protein complexes that regulate their generation, interpretation, as well as removal. Depending on which step of this process the complexes regulate, they can be classified in three different groups: writers, reader, and erasers.

In eukaryotes, the two main enzyme classes involved in the process of DNA methylation are DNA methyltransferases (DNMTs) – which promote methylation – and proteins of the ten-

eleven translocation (TET) methylcytosine dioxygenases family, which actively remove the methyl moieties through a complex cycle of oxidation (Wu and Zhang, 2017). In addition, DNA methylation can also be passively reduced through cell division (Lyko, 2018; Rasmussen and Helin, 2016). DNA can be methylated at the C5 position of cytosine and occurs mainly in a context of CpG dinucleotides. CpG dinucleotides are symmetrically methylated on both strands, enabling the faithful inheritance of pre-existing CpG methylation marks on new daughter strands during semiconservative DNA replication (Ming et al., 2021). In general, DNA methylation is thought to contribute to the formation of heterochromatic regions on the genome and connected to transcriptional silencing. In contrast, regions of the genome that are enriched for non-methylated CpGs are associated with gene promoters and contribute to transcriptionally permissive environments. However, this notion gets more and more challenged by new research showing that DNA methylation can inhibit but also promote transcription, depending on its position (Lyko, 2018). DNA methylation is an intricately balanced process, whose deregulation has been linked to several diseases, e.g. Alzheimer's disease and epilepsy (Mastroeni et al., 2010; Zhang et al., 2021). In recent years however, the role of DNA methylation during infection has moved more and more into the limelight. For more detailed information on this topic, we refer the reader to the recent review by Qin et al., in which the involvement of DNA methylation in infection as well as its potential as a target for pathogens is explained (Qin et al., 2021).

Histone modifications represent the third group of epigenetic information. The modifications mainly target the histone tails, short peptide sequences reaching out of the core histone structure. The histone tails are prone to a wide variety of modifications: methylation, phosphorylation, ubiquitination, SUMOylation, and acetylation, the latter being the most common one (du Preez and Patterton, 2013). PTMs on histone proteins function in elaborate combinations to regulate the many activities associated with chromatin. Many of the enzymes that are responsible for the placement (writers) or the removal (erasers) of these modifications, as well as the multi-protein complexes they participate in, have been extensively characterized. While the functional significance of some of these modifications remains to be determined, it is clear that they, whether at the single amino acid level or in combinatorial ways, can disturb contacts between neighboring histones as well as histones and DNA (Lawrence et al., 2016). Acetylation of lysine residues, for example, neutralizes the basic charge of the residue on which it occurs, thereby disrupting electrostatic interactions between the histones and the phosphate group in the DNA, leading to a loser configuration and, in turn, to an open chromatin fiber (Shahbazian and Grunstein, 2007).

Intercepted at the source – how pathogens manipulate epigenetic information

Epigenetic information is crucial for every cell and is not only deciding its function and fate, but also its response to numerous stimuli. This omnipresence of epigenetic information also makes it an excellent target for a range of pathogens, which can manipulate this information to their own advantage. In fact, one of the strategies employed by them is to hijack and alter the host's epigenetic information. The research in this field has been growing rapidly in recent years, highlighting the importance of epigenetic information, not only for the host, but also the pathogens. Both bacterial and viral pathogens have been shown to directly interfere with the different classes of epigenetic information listed before.

The Hepatitis C virus (HCV) is an RNA virus causing chronic hepatitis, which frequently can lead to hepatocellular carcinoma (hepatoma) (Westbrook and Dusheiko, 2014). Moreover, the virus can manipulate lncRNA transcription. In hepatoma patients, an lncRNA called HULC was identified to be involved in cancer progression and its levels in the blood are also used as a post-treatment prognostic tool (Panzitt et al., 2007). It was recently demonstrated that an increase in HULC levels promotes HCV replication and conversely, HULC suppression impedes viral replication. Moreover, the viral non-structural protein NS5A was shown to promote HULC transcription by directly increasing promotor activity, thus increasing viral replication (Kitabayashi et al., 2020).

One example of a pathogen directly targeting DNA methylation is *Pseudomonas aeruginosa*. *P. aeruginosa* is one of the most common sources for chronical airway infections in patients with cystic fibrosis and, in addition, one of the most common causes for nosocomial pneumonia (Fujitani et al., 2011). It was demonstrated that an infection with *P. aeruginosa* in bronchial epithelial cells (BECs) inhibits the expression of NODAL by manipulating the methylation levels of its promotor region. NODAL is a key regulator of BEC proliferation as well as BEC-induced T helper cell differentiation(Wang et al., 2015). In addition, lung macrophages exposed to extracellular vesicles of *P. aeruginosa* show a loss of DNA methylation in specific genetic regions, including a downregulation in immune response gene expression (Kyung Lee et al., 2020). However, the probably best-known pathogen for modulation of host DNA methylation is *Helicobacter pylori*. *H. pylori* is a Gram-negative extracellular bacterium that infects the stomach, where it induces excessive acid production, leading to severe inflammation, including ulcers, then chronic inflammation, and finally gastric cancers (Touati, 2010). The vast majority of gastric cancers are commonly associated with *H. pylori* infections, due to aberrant DNA methylation in gastric mucosae, in particular in promoter regions of genes encoding tumor-suppressor proteins and oncogenes (Alvarez et al., 2013).

The wide variety of histone modifications, as well as the army of proteins responsible for their regulation, makes this type of epigenetic information a cornucopia of possible manipulations by pathogens. Secreted bacterial proteins targeting the nucleus to hijack cellular pathways by manipulating gene transcription and other nuclear processes are collectively termed *nucleomodulins* (**Figure 12**) (Bierne and Cossart, 2012) and their number, as well the histone proteins they target, are continuously increasing. For a recent review extensively describing nucleomodulins and their roles during infection, please refer to (Bierne and Pourpre, 2020).

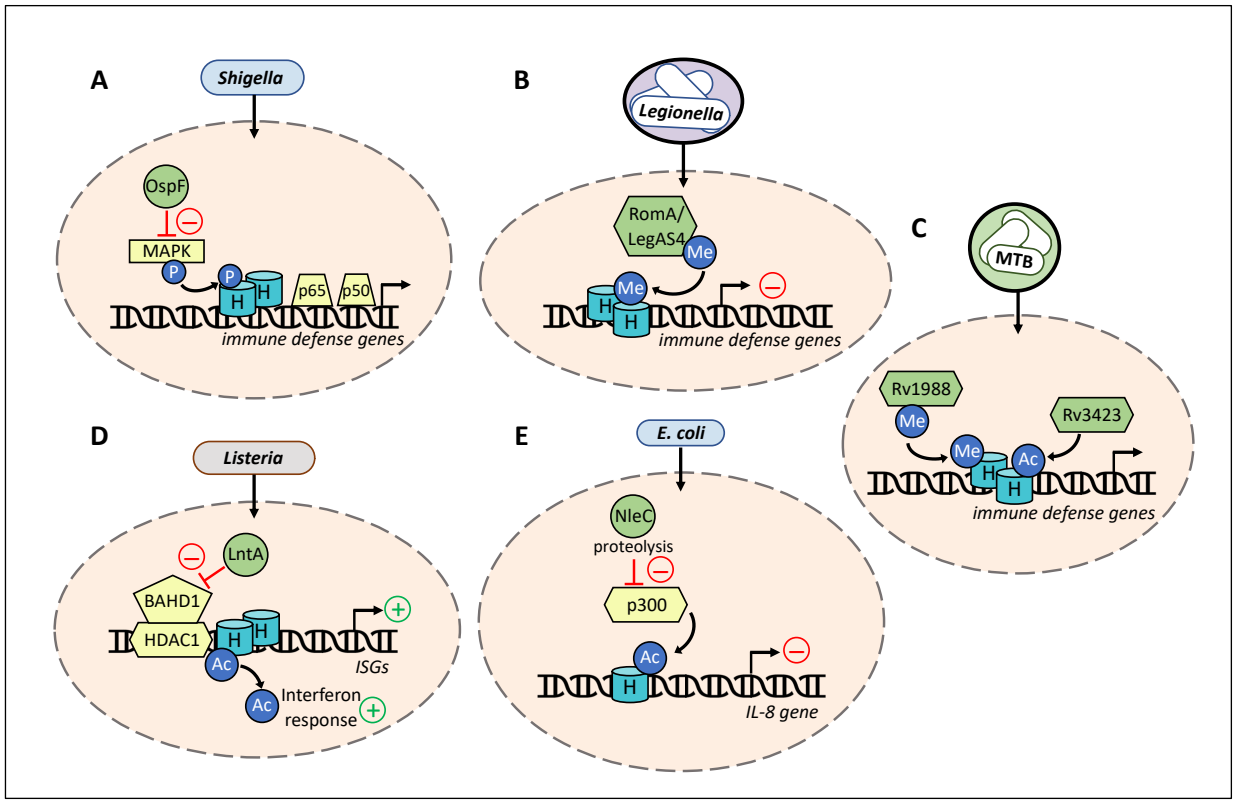

Figure 12: Selected nucleomodulins of *S. flexneri, L. pneumophila, M. tuberculosis* (MTB), *L. monocytogenes* and *E. coli*. Secreted nucleomodulins (in green) that enter the nucleus (represented by an orange oval; blue cylinders labeled "H" represent histones; host nuclear factors are in yellow). Post-translational modifications (PTMs): acetylation (Ac), methylation (Me), phosphorylation (P). Adapted from Bierne and Pourpre (2020).

One example for a bacterium targeting histone proteins with a secreted effector is *Shigella flexneri*. OspF, a secreted phosphothreonine lyase, modifies MAPK, rendering it permanently inactive in the host cell nucleus. This inactivation consequently inhibits H3S10 phosphorylation by MAPK and impedes the expression of NF-κB regulated proinflammatory genes (Arbibe et al., 2007) (**Figure 12A**).

Histone methylation is another known target for pathogens. As mentioned before, *L. pneumophila* secrets a SET-domain methyltransferase into the host cell, targeting H3K14 (Rolando et al., 2013) (**Figure 12B**). For more information about this effector, please refer to the chapter "*Legionella* – a jack of many (eukaryotic-like) traits". But not only *L. pneumophila*

encodes its own methyltransferases, also *Mycobacterium tuberculosis* secrets similar proteins. The Rv1988 protein of *M. tuberculosis* is a methyltransferase targeting a non-canonical histone residue, arginine 42 on histone H3 (H3R42). This methylation, comparable to the methylation of H3K14 by RomA, causes a decrease in gene expression connected to the cell's response to the bacteria. In addition, the deletion of Rv1988 leads to a decrease of bacterial survival in the host (Yaseen et al., 2015) (**Figure 12C**). *Chlamydia trachomatis* is another bacterium possessing its own histone methyltransferase, named NUE. This T3SS-dependent effector was shown to methylate histones H2B, H3, and H4 *in vitro*, however its specific target and function *in vivo* remains to be determined (Pennini et al., 2010). *Bacillus anthracis*, the causative agent of anthrax, has a rather uncommon target for histone methylation, namely histone H1. The bacterial *Ba*SET protein is secreted through an unknown mechanism and localizes to the eukaryotic nucleus, where it methylates histone H1. This methylation seems to specifically target the promotor regions of NF-κB regulated genes, causing a decrease in the transcription of pro-inflammatory genes. Moreover, the deletion of *Ba*SET renders the bacteria unable to cause disease in a mouse model (Mujtaba et al., 2013).

Histone acetylation, the most common modification of histones, is also subject to manipulation by a variety of pathogens, due to its importance in many immune and inflammatory processes. *Listeria monocytogenes*, a foodborne pathogen, targets histone acetylation during infection by secreting an effector called LntA into the host cell. LntA translocates to the nucleus where it interacts with BAHD1, a promotor of chromatin compaction and histone deacetylation (Lebreton et al., 2011). BAHD1 is part of a chromatin remodeling-complex which includes histone methyltransferases, histone deacetylases, and heterochromatin proteins, that promotes heterochromatin formation and gene silencing (Bierne et al., 2009). The interaction of LntA with BAHD1 impedes its recruitment to the promotor regions of interferon stimulated genes (ISGs), subsequently enhancing acetylation and activating ISGs, a process crucial for infection in a mouse model (Lebreton et al., 2011) (**Figure 12D**). Another example of manipulation of histone acetylation by a pathogen is the secreted metalloprotease NleC of enteropathogenic and enterohaemorrhagic *E. coli* (EPEC and EHEC, respectively). NleC degrades histone acetyltransferase p300 in the host cell nucleus, causing a decrease in histone acetylation, followed by a decrease in the expression of pro-inflammatory IL-8 (Shames et al., 2011) (**Figure 12E**). *Mycobacterium tuberculosis* goes one step further by expressing its own histone acetyltransferase, Rv3423.1. This protein was shown to directly interact with histone H3 and acetylating K9/14. In addition, the recombinant expression of Rv3424.1 in *Mycobacterium smegmatis* increased intracellular replication of the bacteria. However, the

exact consequence of this hyperacetylation remains an open question (Jose et al., 2016) (**Figure 12C**). These examples show that the balance between histone acetylation and deacetylation is a finely tuned process crucial for cellular processes and thus, presents a potent target for pathogens to promote their own survival. This topic, with a strong focus on histone deacetylases, will be discussed in more detail in the next chapter.

Nuclear nodes – histone deacetylases and their implication in infection

Bibliographic publication

Accepted at microLife

PATHO-EPIGENETICS: HISTONE DEACETYLASES AS TARGETS OF PATHOGENS AND THERAPEUTICS

Daniel Schator[1,2], Laura Gomez-Valero[1] Carmen Buchrieser[1*] and Monica Rolando[1*]

[1]Institut Pasteur, Université de Paris, CNRS UMR 3525, Unité Biologie des Bactéries Intracellulaires, F-75015 Paris, France, [2]Sorbonne Université, Collège doctoral, F-75005 Paris, France

One-sentence summary: HDACs play important roles in gene regulation and the immune response, thus they are targeted by pathogens to manipulate the host cell and their inhibition may allow to fight infections.

Key words: Histone deacetylases (HDAC), histone modifications, infection, Legionella, HDAC inhibitors

[*]For correspondence:

Carmen Buchrieser and Monica Rolando

Institut Pasteur

Biologie des Bactéries Intracellulaires

28, rue du Dr. Roux, 75724 Paris Cedex 15, France

Tel: +33.1.45.68.83.72

E-mail: cbuch@pasteur.fr, mrolando@pasteur.fr

Manuscripts submitted to microLife

OXFORD UNIVERSITY PRESS | microLife

Epigenetic reprogramming: histone deacetylases as targets of pathogens and therapeutics

Journal:	*microLife*
Manuscript ID	MICRO-2021-016.R1
Manuscript Type:	Short review
Date Submitted by the Author:	12-Nov-2021
Complete List of Authors:	Schator, Daniel; Institut Pasteur, Biology of Intracellular Bacteria CNRS URA 2171 Gomez-Valero, Laura; Institut Pasteur, Biology of Intracellular Bacteria CNRS URA 2171 Buchrieser, Carmen; Institut Pasteur, Biology of Intracellular Bacteria CNRS URA 2171 Roando, Monica; Institut Pasteur, Biology of Intracellular Bacteria CNRS URA 2171
Keywords:	Histone deacetylases (HDAC), histone modifications, infection, Legionella, HDAC inhibitors, epigenetics

ABSTRACT

In recent years the interplay of epigenetics and infection moved into the limelight. Epigenetic regulation describes modifications in gene expression without alterations of the DNA sequence. In eukaryotes, this mechanism is central for fundamental cellular processes such as cell development and differentiation, but it is also involved in more specific tasks such as the response to infection by a pathogen. One of the most common types of epigenetic changes is the modification of histones. Histones, the small protein building blocks that are wrapped with DNA are the fundamental packaging unit of chromatin. Histones can be modified by linking different moieties to them – one of the most abundant ones is acetylation. Histone acetylation is regulated by two main classes of enzymes, histone acetyl transferases (HAT) and their counterparts, histone deacetylases (HDAC). Given the high abundance and importance in regulating gene expression, histone acetylation is an excellent target for pathogens to manipulate the host cell to their advantage. Targeting HDACs gained particular interest in recent years, due to the increased use of HDAC inhibitors in clinical practice. Recently, the possibility to fight an infection with HDAC inhibitors was suggested as an alternative to overcome the ever-growing problem of antibiotic resistance. In this review we focus on the regulation of HDACs and their involvement in immune cell function. We then highlight different mechanisms employed by pathogens to manipulate histone deacetylases and we discuss the possibility of HDAC inhibitors as therapeutics to fight infections.

INTRODUCTION

Epigenetics and the histone code

The study of epigenetic regulation, defined as "structural adaptation of chromosomal regions to register, signal or perpetuate altered activity states", has become an emerging topic in life sciences over the past decades (Bird, 2007). Such expression changes can be substantial in a cell and are crucial for its function. Three main mechanisms causing these changes in gene expression are known: DNA methylation, regulation by non-coding RNAs, and histone modifications (Goldberg, Allis, & Bernstein, 2007).

DNA methylation, especially when found at promotors, is a repressive modification of DNA transcription caused by enzymes called DNA methyltransferases (DNMTs). In mammals, cytosine residues in CpG dinucleotides are the main target of this modification. Areas of the chromatin where these modifications accumulate are known as CpG islands, which are connected to transcriptional repression (Goll & Bestor, 2005). This repressive effect is mostly connected to promotor methylation (Jones, 2012) while methylation of gene body regions has been connected to active gene transcription, highlighting a core principle of epigenetic regulation, which is context-dependency (Arechederra et al., 2018; Maunakea et al., 2010). Moreover, methylated cytosines can be oxidized by TET (ten-eleven translocation) proteins, giving rise to several new modification types such as hydroxymethyl-, formyl-, and carboxylcytosine, each of which has distinct effects. For detailed descriptions of these modifications and their effects on transcription, we refer the reader to one of the following reviews (Hardwick, Lane, & Brown, 2018; Richa & Sinha, 2014; Wu & Zhang, 2017; Yingqian Zhang & Zhou, 2019).

The role of non-coding RNAs in epigenetics is not completely understood yet (Knowling & Morris, 2011). However, more and more experimental evidence pushes some types of non-coding RNAs, namely long non-coding RNAs (lncRNA), in the realm of epigenetics. The functions of lncRNAs are manifold as they can repress gene expression, interfere with RNA polymerases, impede mRNA processing, and change the cellular localization of proteins by binding to them (Jiao Chen, Ao, & Yang, 2019). Furthermore, lncRNAs and miRNAs seem to impact the epigenetic machinery at two levels: *i)* their expression can be regulated by epigenetic mechanisms and *ii)* they have been shown to repress key enzymes that drive epigenetic remodeling (epi-miRNAs) (Moutinho & Esteller, 2017). In addition, miRNAs can be involved in establishing DNA methylation (Bao, Lye, & Barton, 2004).

The third mechanism is the post-translational modification (PTM) of histones. Histones are small highly basic proteins that are crucial for chromatin formation and DNA packaging. The DNA is wrapped around a core octamer complex consisting of two copies of histones H2A, H2B, H3, and H4. H1, the linker histone, sits on top of this complex like a clamp, to maintain the structural integrity. This complex of DNA and histone proteins is called the nucleosome, which then forms the chromatin fiber (Kornberg, 1974). Each histone protein can be the target of numerous post-translational modifications, especially the histone tails, the N- or C-terminal parts of the core histone that stick out from the complex, are prone to modifications which include phosphorylation, ubiquitination, SUMOylation, methylation, and acetylation (du Preez & Patterton, 2013). Recently, novel histone modifications have been identified, for instance propionylation, crotonylation, succinylation, and benzoylation (Barnes, English, & Cowley, 2019). Specific modifications on certain amino acids can drastically influence the transcription of genes associated with the respective histones (Berger, 2007; Lawrence, Daujat, & Schneider, 2016). First, the modifications can directly interfere with the interaction between the different histones, as well as neighboring nucleosomes. Second, proteins and protein complexes – such as nucleosome remodelers – recruited to these modifications can further modify the chromatin structure or influence the activity of transcription factors by condensing the chromatin. However, the effects of a single modification cannot be seen in isolation, but rather in synergy between different modifications within the histone tails (Kouzarides, 2007).

A key concept of epigenetics is the highly regulated balance between the addition and the removal of modifications by specific enzymes, so-called *writers* and *erasers*, as well as recognition proteins, the so-called *readers*. The *writers*, enzymes that add for example methyl or acetyl groups, include histone methyltransferases, histone acetyltransferases, and many others. The *readers* recognize these modifications and mediate their downstream effects. Numerous protein domains have evolved to detect these modifications, such as chromodomains and ankyrin domains for histone methylation, or bromodomains and double PHD finger domains for histone acetylation. The third group of enzymes, the *erasers*, are responsible for removing histone modifications, thus reversing their effect on gene expression. The most common examples of *erasers* are histone demethylases and histone deacetylases. Additionally, it should be noted that many proteins involved in epigenetic regulation can comprise more than one of these properties. The protein p300/CBP, for example, encodes a histone acetyltransferase domain (*writer*) as well as a bromodomain

(*reader*) (Breen & Mapp, 2018). The balanced interplay between *writers*, *readers*, and *erasers* is paramount to a variety of cellular processes (Biswas & Rao, 2018).

One of the most abundant histone modifications is the reversible acetylation of lysine residues on histone tails. Histone acetylation is mostly connected to a transcriptional activation (Barnes et al., 2019; Hebbes, Thorne, & Crane-Robinson, 1988). The *writers* and *erasers* controlling the acetylation status of histones are histone acetyltransferases (HAT) and histone deacetylases (HDAC), respectively. In recent years, the role of HDACs in the immune response and their manipulation by certain pathogens became evident. In addition, the therapeutic use of HDAC inhibitors might open a new window to bypass the prominent problem of antibiotic resistance. These topics will be the main focus of this review.

HDACs and their regulation

Five classes of HDAC proteins that are split up in two groups are known to date. The first group, formed by Zn^{2+}-dependent histone deacetylases, comprises class I (HDAC1, HDAC2, HDAC3, and HDAC8), class IIa (HDAC4, HDAC5, HDAC7, and HDAC9), class IIb (HDAC6 and HDAC10), and class IV (HDAC11). The second group, NAD^{+}-dependent histone deacetylases, contains class III, the so-called Sirtuins (SIRT1-7). This classification is based on the homology of the enzymes to specific yeast proteins: Rpd3 for class I, Hda1 for class II and Sir2 for class III. Class IV shares sequence similarity with both class I and class II (H. P. Chen, Zhao, & Zhao, 2015).

However, despite their name, HDACs can also deacetylate non-histone proteins. The tumor suppressor p53 and the adaptor protein MyD88 are two of the most prominent non-histone targets of HDAC enzymes (A Ito et al., 2001; Akihiro Ito et al., 2002; Menden et al., 2019). MyD88 is a crucial component of toll-like-receptor (TLR) signaling, leading to the activation of NF-κB, consequently promoting the production of pro-inflammatory cytokines (New et al., 2016). MyD88 is deacetylated by HDAC6, thereby increasing both its activity and half-life time (Menden et al., 2019). Thus, acetylation of MyD88 is paramount in the TLR signaling cascade because it supports the interaction of MyD88 with downstream effectors such as TNF receptor associated factor-6 (TRAF6)(Kawai et al., 2004).

The regulation of HDAC activity is a complex and multilayered process with four main regulation mechanisms: gene expression, subcellular localization, protein complex formation, and post-translational modifications (PTMs). The expression of histone deacetylase-coding genes has been studied in detail, but exceeds the scope of this review

(Sengupta & Seto, 2004). However, an interesting characteristic of HDACs is that some can regulate their own expression by interacting with their own promoter regions. For example in mice, HDAC1 autoregulates its own expression by deacetylating the promoter region and, thereby, repressing its own gene expression (Schuettengruber, Simboeck, Khier, & Seiser, 2003). In addition, HDAC1 seems to be involved in regulating the gene expression of HDAC2 and HDAC3 (Lagger et al., 2002).

The regulation dependent on the subcellular localization is seen mostly with class IIa HDACs since these proteins shuttle between the nucleus and the cytoplasm. A striking example for the regulation by subcellular localization is the interaction of HDAC4 and HDAC5 with the 14-3-3 family adaptor proteins. In mammals, the seven different isoforms of 14-3-3 proteins are highly conserved and they assist in various processes such as protein-protein interactions, protein folding, and protein localization (Stevers et al., 2018). HDAC4 and HDAC5 enzymes directly interact with 14-3-3 proteins, leading to an accumulation of these HDACs in the cytoplasm. This cytoplasmic retention of HDAC4 and HDAC5 dampens the transcriptional repression of a subset of genes (Grozinger & Schreiber, 2000). For HDAC7, a similar mechanism of regulation is known (Kao et al., 2001). A different regulation mechanism, which is best studied in class I HDACs, is the control of HDAC activity through protein complex formation. HDAC1 and HDAC2 are crucial components of at least five different protein complexes: Mi-2/NuRD (nuclear remodeling deacetylase), Sin3 (switch intensive 3), CoREST (corepressor of REST), MiDAC (mitotic deacetylase), and the recently discovered BAHD1 (Bromo adjacent homology domain protein 1) (Kelly & Cowley, 2013; Lakisic et al., 2016; Millard, Watson, Fairall, & Schwabe, 2017). As part of these complexes, the HDACs become maximally activated and are targeted to specific regions of chromatin. Moreover, through scaffolding proteins, HDACs are connected with other important epigenetic regulators (Lakisic et al., 2016; Millard et al., 2017). The NuRD complex is an excellent example to illustrate such a combinatorial assembly. The core MTA scaffolding proteins (MTA1, MTA2, MTA3) bridge HDAC1 and HDAC2 with subunits involved in nucleosome remodeling (CHD3, CHD4), histone demethylation (LSD1), binding to other subunits and histones (RBBP4, RBBP7, GATAD2A, GATAD2B), and binding to methylated DNA (MBD2). The combinatorial assembly of these subunits determines the function of NuRD in genomic targeting and association with specific transcription factors, in the mediation of cell type- specific transcriptional regulations, such as the repression of tumor suppressor genes (Lai & Wade, 2011).

The recruitment of these complexes to specific chromatin regions is mediated by their interaction with different transcription factors or directly by histone-recognition motifs present in subunits of these complexes (Adams, Chandru, & Cowley, 2018; Kelly & Cowley, 2013; Millard et al., 2017). Another example is the interaction of HDAC3 with NCoR (nuclear receptor corepressor) and SMRT (silencing mediator for retinoid and thyroid receptor) (J. Li et al., 2000). These HDAC3-containing complexes act as ligand-dependent transcription factors and are involved in the transcriptional repression of a specific subset of genes (J. Li et al., 2000). Interestingly, this complex is not only crucial for the activity of HDAC3, but also for the activity of class IIa HDACs, like HDAC4 and HDAC5 (Fischle et al., 2002). In addition, the NCoR/SMRT complex seems to be in competition with 14-3-3 proteins in the binding of HDAC3. 14-3-3 proteins promote the cytoplasmic localization of HDAC3, hence interfering with its repressive activity, demonstrating an elaborate interplay between the different types of HDAC regulation (Rajendran et al., 2011).

Another major regulatory mechanism of HDAC activity are post-translational modifications (PTM). There are numerous PTMs that regulate HDAC function, such as acetylation, SUMOylation, ubiquitination, and phosphorylation (Eom & Kook, 2014). Furthermore, the regulation via PTMs is tightly connected to other regulatory mechanisms such as subcellular localization and protein complex formation. A well described example is the phosphorylation of specific residues in HDAC4 that enables the binding of 14-3-3 proteins. Without this interaction, HDAC4 accumulates in the nucleus, leading to a decrease in gene expression (Grozinger & Schreiber, 2000). PTMs can, in addition, influence HDAC protein complex formation. Casein kinase 2 (CK2) phosphorylates two serine residues of HDAC1 that mediate its interaction with Sin3, Mi-2/NuRD, and CoREST (Pflum, Tong, Lane, & Schreiber, 2001). As mentioned before, the interplay of HDAC1 with these complexes is essential for its histone deacetylase activity (Kelly & Cowley, 2013).

These examples highlight the multiple levels of regulation that ensure the correct function of histone deacetylases, important for fundamental cellular processes such as cell division, metabolism, and others, but also complex intercellular processes like regulating the immune response.

HDACs and the immune response

The function of histone deacetylases in regulating immune cells is manifold (Busslinger & Tarakhovsky, 2014). Here we focus on the involvement of HDACs in the development of different cell types of the innate and adaptive immune system as well as the regulation of cytokine signaling.

Innate immunity and cytokine signaling

The regulation of immune cells by HDACs starts during myeloid development. During this process hematopoietic stem cells differentiate into either myeloid cells—which are precursor cells of the innate immune system, such as macrophages and neutrophils—or into lymphoid cells, which later differentiate into B cells and T cells (Weiskopf et al., 2016).

HDAC5 and HDAC9, both members of class II, are involved in the differentiation of progenitor cells into macrophages. Especially HDAC5 seems to be a negative regulator of differentiation, since its expression is upregulated in non-differentiated cells (Baek et al., 2009). Also, HDAC3 plays a role in the differentiation process as it is recruited to promoter regions that are normally occupied by the transcription factor PU.1 – a key player in the differentiation process of hematopoietic cells (Oikawa et al., 1999) – where it impedes its activity (Ueki, Zhang, & Haymann, 2008).

The function of another subgroup of macrophages, microglia cells, is also regulated by HDACs. The treatment of mouse microglia cells with HDAC inhibitors reduced the production of cytokines, such as IL-6, TNF-α, and IL-10. Furthermore, this treatment impedes the expression of markers associated with anti-inflammatory M2 macrophages (Kannan et al., 2013). Sirtuins are also implicated in macrophage function: a deficiency of SIRT2, which is highly expressed in myeloid cells, promotes phagocytosis in macrophages, probably through metabolic changes, without interfering with their development or their cytokine production (Ciarlo et al., 2017). In neutrophils, HDAC11 seems to be a key regulator of their activity, as neutrophils lacking HDAC11 show a stronger migratory phenotype and higher phagocytic capacity (Sahakian et al., 2017).

These examples illustrate that the regulation of immune cells is closely tied to the repression or activation of cytokine production and other immune signals. Indeed, broad range HDAC inhibitors can impair the expression of TLR-dependent pro-inflammatory cytokines such as IL-6 and TNF-α in primary mouse macrophages (Roger et al., 2011). Similar results can be seen in dendritic cells, where HDAC inhibition interferes with the expression and

secretion of IL-12p40, a potent chemoattractant for macrophages and dendritic cells (Cooper & Khader, 2007), and interferon-β (Bode et al., 2007), a cytokine central to the activity of dendritic cells (Barchet, Cella, & Colonna, 2005). A more specific example for the involvement of HDACs in pro-inflammatory signaling is HDAC4. A knock-out of HDAC4 reduces the expression of interferon stimulated genes (ISG), a phenotype rescued by reintroducing HDAC4 but not by any other HDAC (Lu et al., 2019). Sirtuins have also been recently described to act in the process of ISG expression. SIRT2 is activated in a type-I IFN-dependent manner, leading to a downstream activation of the transcription factor STAT1, promoting the expression of ISG (Kosciuczuk et al., 2019).

Interestingly, HDACs not only promote inflammatory responses but can also inhibit them. In endothelial cells, HDAC6 is a key player in TLR-signaling. HDAC6 deacetylates MyD88, thereby impeding its interaction with TNF receptor associated factor-6 (TRAF6) and the subsequent expression of pro-inflammatory genes (Menden et al., 2019). However, HDACs also contribute to dampen the immune response as in activated macrophages HDAC1 is recruited to the IL-6 promoter by death domain-associated protein-6 (Daxx), leading to histone deacetylation and prevention of IL-6 overproduction (Yao et al., 2014). Furthermore, in macrophages, the retinoblastoma protein (Rb) can recruit HDAC1 and HDAC8 to the promoter region of Interferon-β and selectively inhibit its expression(Meng et al., 2016).

The role of HDACs in adaptive immunity

HDACs also regulate differentiation and function of adaptive immune cells. In T cells, HDAC3 plays an important role in the CD4-CD8 lineage commitment in the thymus. Indeed, Philips and colleagues have shown that HDAC3 expression maintains bipotency of thymocytes and that a knockout of HDAC3 redirects the cells towards CD8 lineage commitment (Philips et al., 2019). In T-regulatory (Treg) cells, a deficiency of HDAC5 reduces protein levels of Foxp3, a characteristic transcription factor of these cells. Furthermore, in CD8 cytotoxic T cells, a lack of HDAC5 impairs the production of Interferon-γ, a central pro-inflammatory cytokine for CD8 cytotoxic activity (Xiao et al., 2016). In addition, the production of the pro-inflammatory cytokine IL-17 is regulated by HDAC6 in CD4 helper T cells (Yan et al., 2017). The process of T cell differentiation in the thymus ends by generating terminally differentiated cells. This terminal differentiation goes hand in hand with specific metabolic changes within the cell. Recently, it was shown that these changes are dependent on the expression of FoxO1, a transcription factor regulated by SIRT1 (Jeng et al., 2018).

In B cells, a SIRT1 knockout shows a decrease in viability and IgM production (Han et al., 2019). Another histone deacetylase, HDAC3, is involved in regulating B cell maturation and function. The loss of HDAC3 impairs B cell maturation and changes the expression of numerous B cell genes. In addition, the absence of HDAC3 reduces productive VDJ rearrangement, a process essential for generating suitable B cell antigen receptors (Stengel et al., 2017).

These examples summarize a small fraction of what is known about the involvement of HDACs in the activation and regulation of immune cells. However, they underline the abundance of HDACs in these processes. For a more detailed discussion on this specific topic we refer the readers to excellent reviews about this topic (Busslinger & Tarakhovsky, 2014; Shakespear, Halili, Irvine, Fairlie, & Sweet, 2011). In the following sections of this review, we will focus on examples of how HDACs may be manipulated by pathogens and discuss the possibility to use HDAC inhibitors as treatment options against infectious diseases.

HDACs as targets during infection

Given the major role of histone deacetylases in numerous cell types and signaling pathways, changes in histone acetylation in the context of infection have been reported (Aung et al., 2006; Hamon et al., 2007; Hamon & Cossart, 2008).

Bacterial compounds, such as LPS, change the histone acetylation pattern by inducing an immune response, consequently leading to changes in the expression of specific genes. More specifically, cells challenged with LPS modify their histone H3 acetylation profile, which is mediated by the activation of TLR-4, subsequently promoting the production of IL-8 (Angrisano et al., 2010). But, as mentioned before, histone deacetylases also represent excellent targets for pathogens to actively manipulate the host. First, we discuss three different mechanisms how pathogens can exploit histone deacetylases (**Table 1**): *(i)* alter HDAC activity, *(ii)* change the intracellular localization (often leading to HDAC degradation), or *(iii)* modify their expression at the gene level. Secondly, we discuss the potential of pathogens to directly target the acetylation of histones by encoding enzymes mimicking host HDACs.

Pathogens alter HDAC activity

Pathogens known to impact HDAC functions either target macromolecular complexes containing HDACs or alter HDAC activity directly. The first pathogen reported to target HDAC-containing macromolecular complexes is the intracellular bacterium *Mycobacterium tuberculosis*, the cause of severe pulmonary infections and *Mycobacterium avium* a human pathogen in immune compromised patients (Pai et al., 2016; Wassilew, Hoffmann, Andrejak, & Lange, 2016). Infections with these bacteria lead to a repression of HLA-DR expression, a class II Major Histocompatibility Complex and a key player in cellular antigen presentation. HLA-DR repression is caused by an overexpression of mSin3A, a core component of the HDAC1/2-containing Sin3 complex (Adams et al., 2018), which leads to an enhanced deacetylation of the HLA-DRα promoter (Y. Wang, Curry, Zwilling, & Lafuse, 2005). This inhibition of class-II MHC expression is thought to impair antigen presentation, thereby promoting the survival of intracellular bacteria, as similar effects can be seen with the intracellular pathogen *Toxoplasma gondii* (Lüder, Walter, Beuerle, Maeurer, & Gross, 2001). Another bacteria shown to interact with HDAC complexes is *Listeria monocytogenes*, a food-borne pathogen that may cause infections with symptoms ranging from fever and diarrhea to sepsis and meningitis (Schlech, 2019). During infection, *L. monocytogenes* secretes a small

basic protein called LntA (*Listeria*-nuclear-targeted protein A), which translocates into the host cell nucleus, where interacts with BAHD1, a core component of the BAHD1 chromatin repressive complex (Lebreton et al., 2011). This interaction alleviates the binding of the BAHD1 complex to the promotor regions of Interferon-stimulated-genes (ISGs), which subsequently promotes the transcription of these genes. In addition, the deletion of LntA leads to drastic changes in the infection process as seen in a murine model (Lebreton et al., 2014, 2011).

The beta-herpesviruses, in particular the human cytomegalovirus, a virus linked to infections of fetuses, AIDS patients, and allograft transplant recipients (Griffiths, Baraniak, & Reeves, 2015), manipulates cellular HDACs in a similar way. The viral proteins UL38 and UL29/28 can interact with the HDAC1/2-containing nucleosome remodeling and deacetylase complex (NuRD). The viral proteins recruit the complex to the viral major immediate-early promoter, leading to an accumulation of viral RNA in the host cell. A deficiency of either protein, UL38 or 29/28, leads to a decrease in viral replication (Terhune et al., 2010).

Also, eukaryotic pathogens exploit host HDAC complexes. An example is the protozoan parasite *Toxoplasma gondii,* the causative agent of toxoplasmosis. In healthy adults, toxoplasmosis is often asymptomatic or causes mild flu-like symptoms, however, children and immune compromised individuals can develop a severe form that can be fatal. Recently, two secreted effectors have been described in this pathogen that target the expression of IFN-γ stimulated genes through different mechanisms. The first one, TgIST (*Toxoplasma* inhibitor of STAT1-dependent transcription), recruits the repressive Mi-2/NuRD complex to STAT1 (signal transducer and activator of transcription 1), thereby inhibiting its activation by IFN-γ and the expression of ISGs (Olias, Etheridge, Zhang, Holtzman, & Sibley, 2016). The second effector, TgNSM (*Toxoplasma* NCoR/SMRT modulator), also targets the nucleus of the host cell, where it interacts with the NCoR/SMRT complex. The recruitment of NCoR/SMRT by TgNSM impedes the expression of interferon-regulated necroptotic genes, such as PRK (protein kinase K) and MLKL (mixed-lineage-kinase-domain-like pseudokinase). By blocking necroptosis, the parasite protects its intracellular replication niche. Moreover, TgIST is also involved in this process of inhibition, highlighting its importance for the survival of the parasite (Rosenberg & Sibley, 2021).

One of the pathogens that were shown to alter HDAC activity directly is *Helicobacter pylori,* a leading cause of gastric diseases worldwide, from gastritis to ulcers and malignancies (Schulz, Schütte, Mayerle, & Malfertheiner, 2019). During *H. pylori* infection, lysine 23 of

histone H3 (H3K23) is genome-wide deacetylated. This deacetylation is dependent on the presence of the *cag* pathogenicity island (*cag*PAI) encoded by many *H. pylori* strains; but interestingly, deacetylation is not dependent on CagA, the only known translocated effector encoded in the *cag*PAI (Ding et al., 2010). Thus, the exact mechanism and consequence of this deacetylation remains to be explored.

Another well-studied example is the type IV secreted effector AnkA of *Anaplasma phagocytophilium*. *A. phagocytophilium* is an obligate intracellular bacterium that is transmitted by ticks and can cause granulocytic anaplasmosis in humans (Atif, 2015). AnkA contains several ankyrin repeats, which are commonly found in eukaryotic proteins, but are also present in some bacterial and archaeal proteins. Their main function is the mediation of protein-protein interactions (Mosavi, Cammett, Desrosiers, & Peng, 2004). AnkA recruits HDAC1 in the host cell, promoting the deacetylation of specific promotors. This deacetylation leads to a repression of host defense genes, one of which is *CYBB*. This gene encodes the beta subunit of the NADPH oxidase 2, an enzyme crucial for the production of reactive oxygen species, which are paramount for the cellular defense against intracellular pathogens (Rennoll-Bankert, Garcia-Garcia, Sinclair, & Dumler, 2015).

Members of the *Herpesviridae* family encode protein kinases that can influence HDAC activity. Herpes simplex virus 1, the causative agent of oral herpes, and other members of the alpha-herpesviruses, encode the US3 kinase that can hyperphosphorylate HDAC2 on a conserved serine residue in the C-terminus of the protein. Mutants lacking the US3 kinase exhibit an impaired growth in different cell lines, but this growth defect can partially be rescued by the addition of HDAC inhibitors. This suggests that hyperphosphorylation impedes the activity of HDAC2, thereby promoting viral replication. However, the exact mechanism is not known (Walters, Kinchington, Banfield, & Silverstein, 2010). Another subfamily of the *Herpesviridae*, the gamma-herpesviruses, with its well-known representatives the Epstein-Barr virus, the causative agent of infectious mononucleosis (Nowalk & Green, 2016), also encode for a conserved protein kinase, which is involved in the process of HDAC inhibition. This kinase, named orf36 in the mouse gamma herpesvirus 68 and its EBV homologue BGLF4, were shown to directly interact with HDAC1 and HDAC2. Moreover, the interaction orf36 with these HDACs impedes their binding to the promoter region of RTA, a crucial viral transcriptional activator. The deletion of orf36 disrupts viral replication and DNA synthesis. However, this phenotype can be rescued by knockdown of HDAC1 and HDAC2, meaning both of these HDACs seem to be involved in repressing viral DNA synthesis (Mounce, Mboko, Bigley, Terhune, & Tarakanova, 2013).

In *T. gondii*, the secreted serine-threonine kinase ROP18 was identified as a major virulence factor (Taylor et al., 2006). Recently, it was shown that ROP18 targets the host protein RTN1-C, a key regulator of the stress response of the endoplasmic reticulum. Subsequently, this ER-stress response induces apoptosis, a common consequence of *T. gondii* infection. The phosphorylation of RTN1-C leads to a downregulation of HDAC3 activity, causing the accumulation of acetylated GRP78, a chaperone present in the ER (An et al., 2018). GRP78 is one of the main regulators of the unfolded-protein response in the ER, which can, under prolonged conditions, induce apoptosis (Madeo & Kroemer, 2009).

Interfering with histone deacetylase activity or recruiting these enzymes to specific proteins or genetic regions is only one way, pathogens can manipulate host HDACs. Another possibility to influence the activity of HDACs is to change their intracellular localization (**Figure 1**).

Pathogens change the localization of HDACs

As mentioned before, the activity of many histone deacetylases is tightly linked to their subcellular localization. Hence, this represents a major target for pathogens to manipulate cellular functions.

The histone deacetylase SIRT1 shuttles between the nucleus and the cytoplasm, a process regulated by the PI3K-AKT signaling pathway (Tanno, Sakamoto, Miura, Shimamoto, & Horio, 2007). Infection with *Salmonella typhimurium*, which causes nontyphoidal salmonellosis, a severe enteritis leading to diarrhea and fever, induces the activations of mTOR and AKT. This activation leads to the accumulation of SIRT1 in the cytoplasm, where it is degraded in a lysosome-dependent manner. This relocalization of SIRT1 allows the bacteria to evade the host autophagy response and it promotes their intracellular survival. The type III-secretion system is crucial for this process, however no specific effector connected to this mechanism has been identified (Ganesan et al., 2017). Another bacterium, *L. monocytogenes* has its own method to manipulate the PI3K-AKT signaling pathway. One of its surface proteins, InlB, interacts with the host c-Met receptor, which subsequently leads to the uptake of the bacteria by non-phagocytic cells. In addition, binding of InlB to c-Met activates the PI3-kinase, causing the translocation of SIRT2 from the cytoplasm to the nucleus. Here, SIRT2 deacetylates lysine 18 of histone 3 (H3K18) at the transcriptional start sites of SIRT2-regulated genes, altering the host gene expression to the pathogen's advantage. Indeed, a lack of SIRT2, or its inhibition, impairs *L. monocytogenes*

infection, demonstrating the importance of HDAC manipulation for this pathogen (Eskandarian et al., 2013).

In HIV-1, Vpr is an important virulence factor that was shown to interact with E3 ubiquitin ligases, promoting the degradation of specific proteins by the proteasome (Romani & Engelbrecht, 2009). One class of proteins targeted for degradation are class I HDACs, in particular HDAC1 and HDAC3. In HIV-infected macrophages, the depletion of HDACs leads to a hyperacetylation of the viral LTR regions. The hyperacetylation promotes the expression of viral genes and helps the virus to infect more cells by overcoming latent infections (Romani, Baygloo, Hamidi-Fard, Aghasadeghi, & Allahbakhshi, 2016). During vaccinia virus infection, HDAC4 is involved in regulating the interferon-α response of the cell to infection; furthermore, an overexpression of HDAC4 interferes with viral replication and spreading. To counteract the activity of HDAC4, the vaccinia virus encodes for protein C6, which was shown to interact with HDAC4 and to promote its degradation by the proteasome. However, the exact mechanism is yet to be understood (Lu et al., 2019).

The manipulation of histone deacetylases by obstructing their intracellular localization or promoting their degradation is a sophisticated mechanism that pathogens can employ to boost their own survival and replication. Yet, this process has its limits, since, like the changes in HDAC activity, it is restricted by the intrinsic protein levels in the host cell.

Pathogens induce changes in HDAC expression

Influencing the expression levels of histone deacetylases may affect the entire cell, however, pathogens targeting this process, seem to be able to exactly regulate and fine-tune the changes they cause.

As mentioned before, IL-10 is an important anti-inflammatory cytokine produced by immune cells. During *M. tuberculosis* infection, the production of IL-10 is highly increased in macrophages. This is caused by changes in the levels of HDAC6 and HDAC11. *M. tuberculosis* promotes, through an unknown process, an increase in HDAC6 gene expression and protein level as well as a decrease in HDAC11 protein levels. HDAC6 is subsequently recruited to the promoter regions of IL-10, inducing its overexpression, which subsequently supports the intracellular survival of the bacteria by dampening the immune response (X. Wang, Wu, Jiao, & Huang, 2018). *M. tuberculosis* infection also leads to a downregulation of SIRT1. Under normal conditions, SIRT1 promotes autophagy and phagosome-lysosome fusion, furthermore, its activation leads to a decrease in *M. tuberculosis* growth in a mouse model. Both processes are detrimental to the bacteria but by inhibiting SIRT1 expression

during infection, the bacteria can evade the host response and facilitate their intracellular growth (Cheng et al., 2017).

Changes in HDAC expression have also been observed during viral infections. The hepatitis C virus (HCV), causing chronic hepatitis, upregulates HDAC9 expression, which linked to metabolic changes, that can lead to hyperglycemia and type 2 diabetes mellitus. HDAC9 was shown to play a major role in regulating hepatic gluconeogenesis by deacetylating Forkhead box O1 (FoxO1), a transcription factor central to the regulation of gluconeogenic genes in hepatocytes. These results suggest that HDAC9 is a key regulator in gluconeogenesis connected to type 2 diabetes (Jizheng Chen et al., 2015).

Influenza A virus (IAV) infection decreases the protein levels of HDAC4, a histone deacetylase known to regulate antiviral responses (Q. Yang et al., 2019). HDAC4 downregulation is caused both, at the gene expression level, where the viral RNA-endonuclease PA-X strongly interferes with HDAC4 mRNA levels, and at the protein level, due to the proteolytic activity of caspase 3. However, the exact mechanism of caspase 3 activation by IAV remains to be elucidated. Furthermore, this decrease cannot be rescued by adding caspase inhibitors. This demonstrates that the virus employs two independent mechanisms to impede HDAC4 and its antiviral activity (Galvin & Husain, 2019).

The hepatitis B virus (HBV) induces autophagy in infected hepatocytes, a step critical to promote its own DNA replication (Sir et al., 2010). One of the key activators of autophagy is the viral protein X (HBx), which was shown to inhibit binding of transcription factor SP1 to the promoter region of HDAC1, hence repressing HDAC1 expression. The lack of HDAC1 subsequently causes the accumulation of acetylated high mobility group box 1 (HMGB1), causing its translocation from the nucleus to the cytoplasm, where it acts as an enhancer of autophagy by directly binding Beclin1, a major regulator of autophagy. In addition, HBx is directly involved in the regulation of autophagy, by binding HMGB1 and promoting the complex formation with Beclin1 (Fu et al., 2018). This shows that a single viral protein not only changes expression levels of a specific HDAC, but it can also influence processes downstream of this histone deacetylase.

Pathogens may mimic HDAC enzymes

Pathogens can influence many steps in the regulation of HDAC activity, but some go even a step further by encoding HDAC-like proteins to manipulate the host cell.

HDAC-like proteins have been structurally described in different bacterial species, but were never assessed for their possible involvement in virulence (Finnin et al., 1999; Hildmann

et al., 2004). However, this changed very recently as an HDAC-like protein, named Gc-HDAC, was described to play a role in the pathogenesis of *Neisseria gonorrhoeae.* Gc-HDAC seems to directly influence H3K9ac and thereby causes a down-regulation in the expression of specific genes like beta-defensin 1 and cathelicidin (Zughaier, Rouquette-Loughlin, & Shafer, 2020). Interestingly, homologues of this gene have been found in many commensal and pathogenic *Neisseria* species (Zughaier et al., 2020). However, *Neisseria* is probably not the only bacterial genus encoding HDAC homologues. For example, *Legionella pneumophila* is known to encode many eukaryotic-like proteins and proteins containing eukaryotic-like domains, acquired during their co-evolution with aquatic protozoa (Cazalet et al., 2010, 2004; de Felipe et al., 2005; Lurie-Weinberger et al., 2010). Indeed, *Legionella* is known to mimic a vast variety of eukaryotic protein that allow this pathogen to subvert many signaling pathways in the host (Mondino, Schmidt, & Buchrieser, 2020). Recently the genome sequences of the entire genus *Legionella* were analyzed, which revealed many new eukaryotic domains encoded in these bacteria, including known chromatin remodeling domains like SET or DOT1 (Gomez-Valero et al., 2019). Furthermore, it has been shown previously that *L. pneumophila* encodes a SET-domain containing protein that confers methyltransferase activity. In *L. pneumophila* strain Paris this protein was named RomA and was shown to methylate H3K14 during infection (Rolando et al., 2013). Thus, it was tempting to assume that *Legionella* might also mimic HDAC proteins.

To investigate if HDAC-like proteins are present in the genus *Legionella*, we searched for proteins containing a histone deacetylase domain in 80 *Legionella* genomes belonging to 58 different *Legionella* species(Gomez-Valero et al., 2019). Excitingly, when using the pfam database (Mistry et al., 2021) we identified in 51 of the 58 analyzed species, proteins predicted to encode a HDAC domain. The majority encode only one HDAC domain, whereas five species contain two and one species (*L. gresilensis*) contains as many as three HDAC domain encoding proteins. These *Legionella* HDAC proteins can be classified in two different orthologous groups according to OrthoMCL results (L. Li, Stoeckert, & Roos, 2003) (**Figure 2**). Only in *L. gresiliensis* two inparalogs were found in the same orthologous group, which suggests a gene duplication event after the speciation. The proteins in group 1 are with an average length of 447 amino acids bigger than those of group 2, which are on average 309 amino acids long. Moreover, group 1 proteins also possess a longer HDAC domain than group 2 proteins. The HDAC domain in group 1 is on average 350 amino acids long,

compared to 283 amino acids for group 2. Interestingly, although the second group contains smaller proteins with smaller HDAC domains, the domain covers almost the whole protein length (92%), in contrast, in the first group the HDAC domain represents on average 79% of the amino acid sequence of the protein.

Interestingly, the two HDAC domains are matching differently with the HMM profile as the match of the group 2 HDAC domain against the HMM profile is complete, whereas the match of the group 1 HDAC domain is only partial. To understand their evolution within the genus *Legionella*, we mapped their distribution on the phylogenetic tree of the genus that we had constructed previously (Gomez-Valero et al., 2019). We found that the distribution of the two HDAC groups followed the phylogeny of the species. Their distribution on the *Legionella* phylogeny suggests that both HDAC types have followed an independent vertical evolution for a long time, with several loss events in specific strains/clusters. According to the most parsimonic scenario, proteins of group 1 were probably present in the ancestor of *Legionella*, as they are also present in the outgroup species *L. geestiana* and *L. osnabrueckensis*. The second group might have been acquired at the same time but was lost in the outgroup species or it was acquired in a more recent ancestor. However, additional analyses are necessary to determine the exact evolution of the two different HDAC domains. It will be particularly exciting to functionally analyze whether these HDAC domains confer histone deacetylase activity in the host cell and help *Legionella* to establish their intracellular infection cycle.

The examples discussed above further show that histone deacetylases are auspicious targets for pathogens, whether it is by using their activity for their own advantage, obstructing their intracellular localization or directly interfering with their expression on the genetic level. As promising as HDACs are for pathogens, the same can be said about their potential as therapeutic targets during infection.

HDAC inhibitors as promising therapeutics for infections

In recent years, it became clear that HDAC functions are not only exploited, or inhibited by pathogens, but may also be used as novel targets to fight infectious diseases (**Table 2**). Their influence on immune cells and the host immune response is multifaceted, underlining the importance they might have as therapeutic targets.

The pre-treatment of macrophages with broad spectrum histone deacetylase inhibitors (HDACi), such as suberanilohydroxamic acid (SAHA, also known as vorinostat) and trichostatin A (TSA) decreases bacterial phagocytosis in cells challenged with either *S. typhimurium* or *Escherichia coli*. In addition, co-treatment with these inhibitors on cells already infected by the bacteria leads to an increase of bacterial clearance. This observation could be explained by the enhanced production of reactive oxygen species from the mitochondria caused by the HDACi treatment (Ariffin et al., 2015). Especially tubastatin A, a specific HDAC6 inhibitor, seems to be very potent in reducing the intracellular survival of *S. typhimurium* and *L. pneumophila* (Ariffin et al., 2015; X. Yang, Cao, Sheng, & Yang, 2021). Another example of the possible usage of HDACi during infections are chronic lung infections, called non-resolving pneumonia. One of the most prevalent pathogens to cause this type of infection is *Klebsiella pneumoniae*. During this infection cell death induces a release of cardiolipin, the main lipid component of the inner mitochondrial membrane and a mitochondrial damage-associated molecular pattern. Amid the lung infection, the released cardiolipin causes the SUMOylation of nuclear receptor PPARγ, which consequently leads to the recruitment of a protein complex containing HDAC3 to the promoter region of IL-10, repressing its expression. This repression promotes a persistent inflammation in the lung. Inhibiting HDAC3 restores the IL-10 production and increases the survival in an *in vivo* mouse model (Chakraborty et al., 2017).

HDAC inhibition is not only a therapeutic option in fighting bacterial infections but can also be used in viral infections. Lately, several studies assessed if HDACi could be used to treat viral infections: *e.g.* SAHA drastically decreases human adenovirus replication by interfering with viral gene expression, protein production, and DNA replication (Saha & Parks, 2019).

Also, Sirtuin-specific inhibitors show promising antiviral properties. One example is Tenovin-1 that displays antiviral activity against different members of the Arbovirus family(Hackett et al., 2019). Arboviruses include major human pathogens such as West Nile virus, Chikungunya virus, and Zika virus (Barzon, 2018). The treatment of infected cell cultures with Tenovin-1 reduces the viral load of these three viruses. In addition, sirtinol, a

SIRT1 and SIRT2 inhibitor, interferes with the formation of West Nile virus replication foci, a process where viral dsRNA accumulates in the host cell (Hackett et al., 2019). These results support the potential of HDACi as therapeutic options for the treatment of viral infections in the near future.

Pan HDAC inhibitors, such as vorinostat, not only show antiviral properties (Banerjee, Moore, Broker, & Chow, 2018), but also can be used to treat protozoan infections. However, the success of HDAC inhibition to alleviate protozoal infections is often not based on the inhibition of the host HDAC, but rather on the inhibition of the parasite's HDACs. An example is the use of HDACi as treatment of *Cryptosporidium* infections, a genus closely related to *Plasmodium* and *Toxoplasma*. In a mouse model, treatment with low concentrations of vorinostat led to a decrease of *Cryptosporidium parvum* oocysts. Oocysts are formed during the life cycle of the parasite and are crucial for the spreading of the parasite from one host to another. In addition, low concentrations of vorinostat killed the majority of *C. parvum* parasites in a cell culture model (Guo, Zhang, McNair, Mead, & Zhu, 2018).

The efficacy of a vorinostat derivative was also tested using a mouse model of visceral leishmaniasis, a severe infection with members of the genus *Leishmania*. Visceral leishmaniasis is characterized by a dissemination of the parasites to internal organs such as the liver, the spleen, and the bone marrow. The study demonstrates that the vorinostat derivative shows a high efficacy against the parasite *in vivo* at very low doses. This corroborates the potency of vorinostat, and its derivatives, as a possible treatment option for parasitic infections (Corpas-López et al., 2019). Very recently, HDACi have also been described to alleviate infections caused by multicellular pathogens such as nematodes and fungi. Trichostatin A contributes to the alleviation of eosinophilic meningitis caused by the nematode *Angiostrongylus cantonensis* in a mouse model. The main cause for this might be the reduction of the inflammatory response in the animals (Yanhua Zhang et al., 2019). Another mouse model, one for fungal keratitis caused by *Fusarium solani*, illustrated that HDAC1 is upregulated during infection, causing an overexpression of proinflammatory cytokines. This overexpression and the resulting keratitis can be counteracted using vorinostat (X. Li et al., 2019).

Taken together, the studies presented here show that the inhibition of histone deacetylases may be a potent mean to fight infectious diseases. However, further research is required to elucidate the mechanism of action of these inhibitors. Moreover, clinical studies in this field are scarce and many questions are yet to be answered. Additionally, the development of new HDACi derivatives might help to minimize negative side effects as well

as potentiate their antimicrobial properties, so that these molecules might become novel options to treat infectious diseases.

CONCLUSIONS

The examples discussed in this review show the importance of histone deacetylases in the immune response, as targets of pathogens and as possible treatment options. However, there are still many unanswered questions surrounding HDACs and their function. For example, how bacterial, viral or protozoan pathogens exploit or mimic eukaryotic HDACs is a wide-open field of investigation and only little is known to date. Excitingly, as shown here, *Legionella* and probably also other bacterial pathogens encode HDAC mimics in their genome and might secrete them into the host cell to manipulate it to their advantage. Further analyses will elucidate in which ways these HDAC mimics function. This knowledge might lead to the discovery of new targets to fight bacterial infections. However, as already shown in cellular and animal models, inhibition of HDACs might also be a promising alterative to fight infections caused by antibiotic resistant bacteria. Future research will proof if this approach is applicable. We are convinced that the research on the function of eukaryotic and bacterial HDACs, as well as on the mechanisms employed by bacterial, viral or protozoan pathogens to subvert HDAC function will lead to a wealth of new knowledge. This will ultimately lead to a better understanding of many fundamental processes but may also lead to the development of new therapeutics.

ACKNOWLEDGEMENTS

Work in the CB laboratory is financed by the Institut Pasteur and funding has been received from the Agence National de recherche grants ANR-10-LABX-62-IBEID and ANR-15-CE17-0014-03 to CB and ANR-18-CE15-0005-01 to MR, and the “Fondation de la Recherche Médicale” grant EQU201903007847 to CB. DS was supported by the École Doctorale “ED515: Complexité du vivant”.

REFERENCES

Adams, G. E., Chandru, A., & Cowley, S. M. (2018). Co-repressor, co-activator and general transcription factor: the many faces of the Sin3 histone deacetylase (HDAC) complex. *The Biochemical Journal*, *475*(24), 3921–3932. https://doi.org/10.1042/BCJ20170314

An, R., Tang, Y., Chen, L., Cai, H., Lai, D.-H., Liu, K., … Du, J. (2018). Encephalitis is mediated by ROP18 of *Toxoplasma gondii* , a severe pathogen in AIDS patients. *Proceedings of the National Academy of Sciences*, *115*(23), E5344–E5352. https://doi.org/10.1073/pnas.1801118115

Angrisano, T., Pero, R., Peluso, S., Keller, S., Sacchetti, S., Bruni, C. B., … Lembo, F. (2010). LPS-induced IL-8 activation in human intestinal epithelial cells is accompanied by specific histone H3 acetylation and methylation changes. *BMC Microbiology*, *10*, 172. https://doi.org/10.1186/1471-2180-10-172

Arechederra, M., Daian, F., Yim, A., Bazai, S. K., Richelme, S., Dono, R., … Maina, F. (2018). Hypermethylation of gene body CpG islands predicts high dosage of functional oncogenes in liver cancer. *Nature Communications*, *9*(1), 3164. https://doi.org/10.1038/s41467-018-05550-5

Ariffin, J. K., das Gupta, K., Kapetanovic, R., Iyer, A., Reid, R. C., Fairlie, D. P., & Sweet, M. J. (2015). Histone Deacetylase Inhibitors Promote Mitochondrial Reactive Oxygen Species Production and Bacterial Clearance by Human Macrophages. *Antimicrobial Agents and Chemotherapy*, *60*(3), 1521–1529. https://doi.org/10.1128/AAC.01876-15

Atif, F. A. (2015). Anaplasma marginale and Anaplasma phagocytophilum: Rickettsiales pathogens of veterinary and public health significance. *Parasitology Research*, *114*(11), 3941–3957. https://doi.org/10.1007/s00436-015-4698-2

Aung, H. T., Schroder, K., Himes, S. R., Brion, K., van Zuylen, W., Trieu, A., … Ravasi, T. (2006). LPS regulates proinflammatory gene expression in macrophages by altering histone deacetylase expression. *The FASEB Journal*, *20*(9), 1315–1327. https://doi.org/10.1096/fj.05-5360com

Baek, Y.-S., Haas, S., Hackstein, H., Bein, G., Santana, M. H., Lehrach, H., … Seitz, H. (2009). Identification of novel transcriptional regulators involved in macrophage differentiation and activation in U937 cells. *BMC Immunology*, *10*(1), 18. https://doi.org/10.1186/1471-2172-10-18

Banerjee, N. S., Moore, D. W., Broker, T. R., & Chow, L. T. (2018). Vorinostat, a pan-HDAC inhibitor, abrogates productive HPV-18 DNA amplification. *Proceedings of the National Academy of Sciences of the United States of America*, *115*(47), E11138–E11147. https://doi.org/10.1073/pnas.1801156115

Bao, N., Lye, K.-W., & Barton, M. K. (2004). MicroRNA binding sites in Arabidopsis class III HD-ZIP mRNAs are required for methylation of the template chromosome. *Developmental Cell*, *7*(5), 653–662. https://doi.org/10.1016/j.devcel.2004.10.003

Barchet, W., Cella, M., & Colonna, M. (2005). Plasmacytoid dendritic cells—virus experts of innate

immunity. *Seminars in Immunology*, *17*(4), 253–261. https://doi.org/https://doi.org/10.1016/j.smim.2005.05.008

Barnes, C. E., English, D. M., & Cowley, S. M. (2019). Acetylation & Co: an expanding repertoire of histone acylations regulates chromatin and transcription. *Essays in Biochemistry*, *63*(1), 97–107. https://doi.org/10.1042/EBC20180061

Barzon, L. (2018). Ongoing and emerging arbovirus threats in Europe. *Journal of Clinical Virology*, *107*, 38–47. https://doi.org/https://doi.org/10.1016/j.jcv.2018.08.007

Berger, S. L. (2007). The complex language of chromatin regulation during transcription. *Nature*, *447*(7143), 407–412. https://doi.org/10.1038/nature05915

Bird, A. (2007). Perceptions of epigenetics. *Nature*, *447*(7143), 396–398. https://doi.org/10.1038/nature05913

Biswas, S., & Rao, C. M. (2018). Epigenetic tools (The Writers, The Readers and The Erasers) and their implications in cancer therapy. *European Journal of Pharmacology*, *837*, 8–24. https://doi.org/10.1016/j.ejphar.2018.08.021

Bode, K. A., Schroder, K., Hume, D. A., Ravasi, T., Heeg, K., Sweet, M. J., & Dalpke, A. H. (2007). Histone deacetylase inhibitors decrease Toll-like receptor-mediated activation of proinflammatory gene expression by impairing transcription factor recruitment. *Immunology*, *122*(4), 596–606. https://doi.org/10.1111/j.1365-2567.2007.02678.x

Breen, M. E., & Mapp, A. K. (2018). Modulating the masters: chemical tools to dissect CBP and p300 function. *Current Opinion in Chemical Biology*, *45*, 195–203. https://doi.org/10.1016/J.CBPA.2018.06.005

Busslinger, M., & Tarakhovsky, A. (2014). Epigenetic control of immunity. *Cold Spring Harbor Perspectives in Biology*, *6*(6), a019307. https://doi.org/10.1101/cshperspect.a019307

Cazalet, C., Gomez-Valero, L., Rusniok, C., Lomma, M., Dervins-Ravault, D., Newton, H. J., … Buchrieser, C. (2010). Analysis of the Legionella longbeachae genome and transcriptome uncovers unique strategies to cause Legionnaires' disease. *PLoS Genetics*, *6*(2), e1000851. https://doi.org/10.1371/journal.pgen.1000851

Cazalet, C., Rusniok, C., Brüggemann, H., Zidane, N., Magnier, A., Ma, L., … Buchrieser, C. (2004). Evidence in the Legionella pneumophila genome for exploitation of host cell functions and high genome plasticity. *Nature Genetics*, *36*(11), 1165–1173. https://doi.org/10.1038/ng1447

Chakraborty, K., Raundhal, M., Chen, B. B., Morse, C., Tyurina, Y. Y., Khare, A., … Ray, P. (2017). The mito-DAMP cardiolipin blocks IL-10 production causing persistent inflammation during bacterial pneumonia. *Nature Communications*, *8*, 13944. https://doi.org/10.1038/ncomms13944

Chen, H. P., Zhao, Y. T., & Zhao, T. C. (2015). Histone deacetylases and mechanisms of regulation of gene expression. *Critical Reviews in Oncogenesis*, *20*(1–2), 35–47. https://doi.org/10.1615/critrevoncog.2015012997

Chen, Jiao, Ao, L., & Yang, J. (2019). Long non-coding RNAs in diseases related to inflammation and

immunity. *Annals of Translational Medicine*, *7*(18), 494. https://doi.org/10.21037/atm.2019.08.37

Chen, Jizheng, Wang, N., Dong, M., Guo, M., Zhao, Y., Zhuo, Z., … Chen, X. (2015). The Metabolic Regulator Histone Deacetylase 9 Contributes to Glucose Homeostasis Abnormality Induced by Hepatitis C Virus Infection. *Diabetes*, *64*(12), 4088–4098. https://doi.org/10.2337/db15-0197

Cheng, C. Y., Gutierrez, N. M., Marzuki, M. B., Lu, X., Foreman, T. W., Paleja, B., … Singhal, A. (2017). Host sirtuin 1 regulates mycobacterial immunopathogenesis and represents a therapeutic target against tuberculosis. *Science Immunology*, *2*(9). https://doi.org/10.1126/sciimmunol.aaj1789

Ciarlo, E., Heinonen, T., Théroude, C., Herderschee, J., Mombelli, M., Lugrin, J., … Roger, T. (2017). Sirtuin 2 Deficiency Increases Bacterial Phagocytosis by Macrophages and Protects from Chronic Staphylococcal Infection. *Frontiers in Immunology*, *8*, 1037. https://doi.org/10.3389/fimmu.2017.01037

Cooper, A. M., & Khader, S. A. (2007). IL-12p40: an inherently agonistic cytokine. *Trends in Immunology*, *28*(1), 33–38. https://doi.org/10.1016/J.IT.2006.11.002

Corpas-López, V., Díaz-Gavilán, M., Franco-Montalbán, F., Merino-Espinosa, G., López-Viota, M., López-Viota, J., … Martín-Sánchez, J. (2019). A nanodelivered Vorinostat derivative is a promising oral compound for the treatment of visceral leishmaniasis. *Pharmacological Research*, *139*, 375–383. https://doi.org/10.1016/J.PHRS.2018.11.039

de Felipe, K. S., Pampou, S., Jovanovic, O. S., Pericone, C. D., Ye, S. F., Kalachikov, S., & Shuman, H. A. (2005). Evidence for Acquisition of Legionella Type IV Secretion Substrates via Interdomain Horizontal Gene Transfer. *Journal of Bacteriology*, *187*(22), 7716–7726. https://doi.org/10.1128/JB.187.22.7716-7726.2005

Ding, S.-Z., Fischer, W., Kaparakis-Liaskos, M., Liechti, G., Merrell, D. S., Grant, P. A., … Goldberg, J. B. (2010). Helicobacter pylori-induced histone modification, associated gene expression in gastric epithelial cells, and its implication in pathogenesis. *PloS One*, *5*(4), e9875. https://doi.org/10.1371/journal.pone.0009875

du Preez, L. L., & Patterton, H.-G. (2013). Secondary Structures of the Core Histone N-terminal Tails: Their Role in Regulating Chromatin Structure (pp. 37–55). Springer, Dordrecht. https://doi.org/10.1007/978-94-007-4525-4_2

Eom, G. H., & Kook, H. (2014). Posttranslational modifications of histone deacetylases: Implications for cardiovascular diseases. *Pharmacology & Therapeutics*, *143*(2), 168–180. https://doi.org/https://doi.org/10.1016/j.pharmthera.2014.02.012

Eskandarian, H. A., Impens, F., Nahori, M.-A., Soubigou, G., Coppee, J.-Y., Cossart, P., & Hamon, M. A. (2013). A Role for SIRT2-Dependent Histone H3K18 Deacetylation in Bacterial Infection. *Science*, *341*(6145), 1238858–1238858. https://doi.org/10.1126/science.1238858

Finnin, M. S., Donigian, J. R., Cohen, A., Richon, V. M., Rifkind, R. A., Marks, P. A., … Pavletich,

N. P. (1999). Structures of a histone deacetylase homologue bound to the TSA and SAHA inhibitors. *Nature*, *401*(6749), 188–193. https://doi.org/10.1038/43710

Fischle, W., Dequiedt, F., Hendzel, M. J., Guenther, M. G., Lazar, M. A., Voelter, W., & Verdin, E. (2002). Enzymatic Activity Associated with Class II HDACs Is Dependent on a Multiprotein Complex Containing HDAC3 and SMRT/N-CoR. *Molecular Cell*, *9*(1), 45–57. https://doi.org/https://doi.org/10.1016/S1097-2765(01)00429-4

Fu, S., Wang, J., Hu, X., Zhou, R.-R., Fu, Y., Tang, D., … Fan, X.-G. (2018). Crosstalk between hepatitis B virus X and high-mobility group box 1 facilitates autophagy in hepatocytes. *Molecular Oncology*, *12*(3), 322–338. https://doi.org/10.1002/1878-0261.12165

Galvin, H. D., & Husain, M. (2019). Influenza A virus-induced host caspase and viral PA-X antagonise the antiviral host factor, histone deacetylase 4. *The Journal of Biological Chemistry*. https://doi.org/10.1074/jbc.RA119.010650

Ganesan, R., Hos, N. J., Gutierrez, S., Fischer, J., Stepek, J. M., Daglidu, E., … Robinson, N. (2017). Salmonella Typhimurium disrupts Sirt1/AMPK checkpoint control of mTOR to impair autophagy. *PLoS Pathogens*, *13*(2), e1006227. https://doi.org/10.1371/journal.ppat.1006227

Goldberg, A. D., Allis, C. D., & Bernstein, E. (2007). Epigenetics: A Landscape Takes Shape. *Cell*, *128*(4), 635–638. https://doi.org/10.1016/J.CELL.2007.02.006

Goll, M. G., & Bestor, T. H. (2005). Eukaryotic cytosine methyltransferases. *Annual Review of Biochemistry*, *74*(1), 481–514. https://doi.org/10.1146/annurev.biochem.74.010904.153721

Gomez-Valero, L., Rusniok, C., Carson, D., Mondino, S., Pérez-Cobas, A. E., Rolando, M., … Buchrieser, C. (2019). More than 18,000 effectors in the Legionella genus genome provide multiple, independent combinations for replication in human cells. *Proceedings of the National Academy of Sciences of the United States of America*, *116*(6), 2265–2273. https://doi.org/10.1073/pnas.1808016116

Griffiths, P., Baraniak, I., & Reeves, M. (2015). The pathogenesis of human cytomegalovirus. *The Journal of Pathology*, *235*(2), 288–297. https://doi.org/10.1002/path.4437

Grozinger, C. M., & Schreiber, S. L. (2000). Regulation of histone deacetylase 4 and 5 and transcriptional activity by 14-3-3-dependent cellular localization. *Proceedings of the National Academy of Sciences of the United States of America*, *97*(14), 7835–7840. https://doi.org/10.1073/pnas.140199597

Guo, F., Zhang, H., McNair, N. N., Mead, J. R., & Zhu, G. (2018). The Existing Drug Vorinostat as a New Lead Against Cryptosporidiosis by Targeting the Parasite Histone Deacetylases. *The Journal of Infectious Diseases*, *217*(7), 1110–1117. https://doi.org/10.1093/infdis/jix689

Hackett, B. A., Dittmar, M., Segrist, E., Pittenger, N., To, J., Griesman, T., … Cherry, S. (2019). Sirtuin Inhibitors Are Broadly Antiviral against Arboviruses. *MBio*, *10*(4). https://doi.org/10.1128/mBio.01446-19

Hamon, M. A., Batsché, E., Régnault, B., Tham, T. N., Seveau, S., Muchardt, C., & Cossart, P.

(2007). Histone modifications induced by a family of bacterial toxins. *Proceedings of the National Academy of Sciences of the United States of America*, *104*(33), 13467–13472. https://doi.org/10.1073/pnas.0702729104

Hamon, M. A., & Cossart, P. (2008). Histone Modifications and Chromatin Remodeling during Bacterial Infections. *Cell Host & Microbe*, *4*(2), 100–109. https://doi.org/10.1016/J.CHOM.2008.07.009

Han, Y., Kang, Y., Yu, J., Yu, S.-L., Park, H.-W., Shin, J., … Kang, J. (2019). Increase of Hspa1a and Hspa1b genes in the resting B cells of Sirt1 knockout mice. *Molecular Biology Reports*, *46*(4), 4225–4234. https://doi.org/10.1007/s11033-019-04876-7

Hardwick, J. S., Lane, A. N., & Brown, T. (2018). Epigenetic Modifications of Cytosine: Biophysical Properties, Regulation, and Function in Mammalian DNA. *BioEssays : News and Reviews in Molecular, Cellular and Developmental Biology*, *40*(3). https://doi.org/10.1002/bies.201700199

Hebbes, T. R., Thorne, A. W., & Crane-Robinson, C. (1988). A direct link between core histone acetylation and transcriptionally active chromatin. *The EMBO Journal*, *7*(5), 1395–1402. https://doi.org/10.1002/j.1460-2075.1988.tb02956.x

Hildmann, C., Ninkovic, M., Dietrich, R., Wegener, D., Riester, D., Zimmermann, T., … Schwienhorst, A. (2004). A new amidohydrolase from Bordetella or Alcaligenes strain FB188 with similarities to histone deacetylases. *Journal of Bacteriology*, *186*(8), 2328–2339. https://doi.org/10.1128/JB.186.8.2328-2339.2004

Ito, A, Lai, C. H., Zhao, X., Saito, S., Hamilton, M. H., Appella, E., & Yao, T. P. (2001). p300/CBP-mediated p53 acetylation is commonly induced by p53-activating agents and inhibited by MDM2. *The EMBO Journal*, *20*(6), 1331–1340. https://doi.org/10.1093/emboj/20.6.1331

Ito, Akihiro, Kawaguchi, Y., Lai, C.-H., Kovacs, J. J., Higashimoto, Y., Appella, E., & Yao, T.-P. (2002). MDM2-HDAC1-mediated deacetylation of p53 is required for its degradation. *The EMBO Journal*, *21*(22), 6236–6245. https://doi.org/10.1093/emboj/cdf616

Jeng, M. Y., Hull, P. A., Fei, M., Kwon, H.-S., Tsou, C.-L., Kasler, H., … Ott, M. (2018). Metabolic reprogramming of human CD8+ memory T cells through loss of SIRT1. *The Journal of Experimental Medicine*, *215*(1), 51–62. https://doi.org/10.1084/jem.20161066

Jones, P. A. (2012). Functions of DNA methylation: islands, start sites, gene bodies and beyond. *Nature Reviews Genetics*, *13*(7), 484–492. https://doi.org/10.1038/nrg3230

Kannan, V., Brouwer, N., Hanisch, U.-K., Regen, T., Eggen, B. J. L., & Boddeke, H. W. G. M. (2013). Histone deacetylase inhibitors suppress immune activation in primary mouse microglia. *Journal of Neuroscience Research*, *91*(9), 1133–1142. https://doi.org/10.1002/jnr.23221

Kao, H. Y., Verdel, A., Tsai, C. C., Simon, C., Juguilon, H., & Khochbin, S. (2001). Mechanism for nucleocytoplasmic shuttling of histone deacetylase 7. *The Journal of Biological Chemistry*, *276*(50), 47496–47507. https://doi.org/10.1074/jbc.M107631200

Kawai, T., Sato, S., Ishii, K. J., Coban, C., Hemmi, H., Yamamoto, M., … Akira, S. (2004).

Interferon-alpha induction through Toll-like receptors involves a direct interaction of IRF7 with MyD88 and TRAF6. *Nature Immunology*, *5*(10), 1061–1068. https://doi.org/10.1038/ni1118

Kelly, R. D. W., & Cowley, S. M. (2013). The physiological roles of histone deacetylase (HDAC) 1 and 2: complex co-stars with multiple leading parts. *Biochemical Society Transactions*, *41*(3), 741–749. https://doi.org/10.1042/BST20130010

Knowling, S., & Morris, K. V. (2011). Non-coding RNA and antisense RNA. Nature's trash or treasure? *Biochimie*, *93*(11), 1922–1927. https://doi.org/10.1016/J.BIOCHI.2011.07.031

Kornberg, R. D. (1974). Chromatin structure: a repeating unit of histones and DNA. *Science (New York, N.Y.)*, *184*(4139), 868–871. https://doi.org/10.1126/science.184.4139.868

Kosciuczuk, E. M., Mehrotra, S., Saleiro, D., Kroczynska, B., Majchrzak-Kita, B., Lisowski, P., … Platanias, L. C. (2019). Sirtuin 2-mediated deacetylation of cyclin-dependent kinase 9 promotes STAT1 signaling in type I interferon responses. *The Journal of Biological Chemistry*, *294*(3), 827–837. https://doi.org/10.1074/jbc.RA118.005956

Kouzarides, T. (2007). Chromatin Modifications and Their Function. *Cell*, *128*(4), 693–705. https://doi.org/https://doi.org/10.1016/j.cell.2007.02.005

Lagger, G., O'Carroll, D., Rembold, M., Khier, H., Tischler, J., Weitzer, G., … Seiser, C. (2002). Essential function of histone deacetylase 1 in proliferation control and CDK inhibitor repression. *The EMBO Journal*, *21*(11), 2672–2681. https://doi.org/10.1093/emboj/21.11.2672

Lai, A. Y., & Wade, P. A. (2011). Cancer biology and NuRD: a multifaceted chromatin remodelling complex. *Nature Reviews Cancer*, *11*(8), 588–596. https://doi.org/10.1038/nrc3091

Lakisic, G., Lebreton, A., Pourpre, R., Wendling, O., Libertini, E., Radford, E. J., … Bierne, H. (2016). Role of the BAHD1 Chromatin-Repressive Complex in Placental Development and Regulation of Steroid Metabolism. *PLoS Genetics*, *12*(3), e1005898. https://doi.org/10.1371/journal.pgen.1005898

Lawrence, M., Daujat, S., & Schneider, R. (2016). Lateral Thinking: How Histone Modifications Regulate Gene Expression. *Trends in Genetics*, *32*(1), 42–56. https://doi.org/10.1016/J.TIG.2015.10.007

Lebreton, A., Job, V., Ragon, M., Le Monnier, A., Dessen, A., Cossart, P., & Bierne, H. (2014). Structural Basis for the Inhibition of the Chromatin Repressor BAHD1 by the Bacterial Nucleomodulin LntA. *MBio*, *5*(1). https://doi.org/10.1128/mBio.00775-13

Lebreton, A., Lakisic, G., Job, V., Fritsch, L., Tham, T. N., Camejo, A., … Bierne, H. (2011). A Bacterial Protein Targets the BAHD1 Chromatin Complex to Stimulate Type III Interferon Response. *Science*, *331*(6022), 1319–1321. https://doi.org/10.1126/science.1200120

Li, J., Wang, J., Wang, J., Nawaz, Z., Liu, J. M., Qin, J., & Wong, J. (2000). Both corepressor proteins SMRT and N-CoR exist in large protein complexes containing HDAC3. *The EMBO Journal*, *19*(16), 4342–4350. https://doi.org/10.1093/emboj/19.16.4342

Li, L., Stoeckert, C. J., & Roos, D. S. (2003). OrthoMCL: identification of ortholog groups for

eukaryotic genomes. *Genome Research*, *13*(9), 2178–2189. https://doi.org/10.1101/gr.1224503

Li, X., Yuan, M., Yin, R., Liu, X., Zhang, Y., Sun, S., … He, S. (2019). Histone deacetylase inhibitor attenuates experimental fungal keratitis in mice. *Scientific Reports*, *9*(1), 9859. https://doi.org/10.1038/s41598-019-46361-y

Lu, Y., Stuart, J. H., Talbot-Cooper, C., Agrawal-Singh, S., Huntly, B., Smid, A. I., … Smith, G. L. (2019). Histone deacetylase 4 promotes type I interferon signaling, restricts DNA viruses, and is degraded via vaccinia virus protein C6. *Proceedings of the National Academy of Sciences of the United States of America*, *116*(24), 11997–12006. https://doi.org/10.1073/pnas.1816399116

Lüder, C. G. K., Walter, W., Beuerle, B., Maeurer, M. J., & Gross, U. (2001). Toxoplasma gondii down-regulates MHC class II gene expression and antigen presentation by murine macrophages via interference with nuclear translocation of STAT1α . *European Journal of Immunology*, *31*(5), 1475–1484. https://doi.org/10.1002/1521-4141(200105)31:5<1475::AID-IMMU1475>3.0.CO;2-C

Lurie-Weinberger, M. N., Gomez-Valero, L., Merault, N., Glöckner, G., Buchrieser, C., & Gophna, U. (2010). The origins of eukaryotic-like proteins in Legionella pneumophila. *International Journal of Medical Microbiology : IJMM*, *300*(7), 470–481. https://doi.org/10.1016/j.ijmm.2010.04.016

Madeo, F., & Kroemer, G. (2009). Intricate Links between ER Stress and Apoptosis. *Molecular Cell*, *33*(6), 669–670. https://doi.org/10.1016/J.MOLCEL.2009.03.002

Maunakea, A. K., Nagarajan, R. P., Bilenky, M., Ballinger, T. J., D'Souza, C., Fouse, S. D., … Costello, J. F. (2010). Conserved role of intragenic DNA methylation in regulating alternative promoters. *Nature*, *466*(7303), 253–257. https://doi.org/10.1038/nature09165

Menden, H., Xia, S., Mabry, S. M., Noel-MacDonnell, J., Rajasingh, J., Ye, S. Q., & Sampath, V. (2019). Histone deacetylase 6 regulates endothelial MyD88-dependent canonical TLR signaling, lung inflammation, and alveolar remodeling in the developing lung. *American Journal of Physiology-Lung Cellular and Molecular Physiology*, *317*(3), L332–L346. https://doi.org/10.1152/ajplung.00247.2018

Meng, J., Liu, X., Zhang, P., Li, D., Xu, S., Zhou, Q., … Cao, X. (2016). Rb selectively inhibits innate IFN-β production by enhancing deacetylation of IFN-β promoter through HDAC1 and HDAC8. *Journal of Autoimmunity*, *73*, 42–53. https://doi.org/10.1016/j.jaut.2016.05.012

Millard, C. J., Watson, P. J., Fairall, L., & Schwabe, J. W. R. (2017). Targeting Class I Histone Deacetylases in a "Complex" Environment. *Trends in Pharmacological Sciences*, *38*(4), 363–377. https://doi.org/10.1016/j.tips.2016.12.006

Mistry, J., Chuguransky, S., Williams, L., Qureshi, M., Salazar, G. A., Sonnhammer, E. L. L., … Bateman, A. (2021). Pfam: The protein families database in 2021. *Nucleic Acids Research*, *49*(D1), D412–D419. https://doi.org/10.1093/nar/gkaa913

Mondino, S., Schmidt, S., & Buchrieser, C. (2020). Molecular Mimicry: a Paradigm of Host-Microbe Coevolution Illustrated by Legionella. *MBio*, *11*(5). https://doi.org/10.1128/mBio.01201-20

Mosavi, L. K., Cammett, T. J., Desrosiers, D. C., & Peng, Z.-Y. (2004). The ankyrin repeat as molecular architecture for protein recognition. *Protein Science : A Publication of the Protein Society*, *13*(6), 1435–1448. https://doi.org/10.1110/ps.03554604

Mounce, B. C., Mboko, W. P., Bigley, T. M., Terhune, S. S., & Tarakanova, V. L. (2013). A Conserved Gammaherpesvirus Protein Kinase Targets Histone Deacetylases 1 and 2 To Facilitate Viral Replication in Primary Macrophages. *Journal of Virology*, *87*(13), 7314–7325. https://doi.org/10.1128/JVI.02713-12

Moutinho, C., & Esteller, M. (2017). MicroRNAs and Epigenetics. *Advances in Cancer Research*, *135*, 189–220. https://doi.org/10.1016/BS.ACR.2017.06.003

New, M., Sheikh, S., Bekheet, M., Olzscha, H., Thezenas, M.-L., Care, M. A., … La Thangue, N. B. (2016). TLR Adaptor Protein MYD88 Mediates Sensitivity to HDAC Inhibitors via a Cytokine-Dependent Mechanism. *Cancer Research*, *76*(23), 6975 LP – 6987. https://doi.org/10.1158/0008-5472.CAN-16-0504

Nowalk, A., & Green, M. (2016). Epstein-Barr Virus. *Microbiology Spectrum*, *4*(3). https://doi.org/10.1128/microbiolspec.DMIH2-0011-2015

Oikawa, T., Yamada, T., Kihara-Negishi, F., Yamamoto, H., Kondoh, N., Hitomi, Y., & Hashimoto, Y. (1999). The role of Ets family transcription factor PU.1 in hematopoietic cell differentiation, proliferation and apoptosis. *Cell Death & Differentiation*, *6*(7), 599–608. https://doi.org/10.1038/sj.cdd.4400534

Olias, P., Etheridge, R. D., Zhang, Y., Holtzman, M. J., & Sibley, L. D. (2016). Toxoplasma Effector Recruits the Mi-2/NuRD Complex to Repress STAT1 Transcription and Block IFN-γ-Dependent Gene Expression. *Cell Host & Microbe*, *20*(1), 72–82. https://doi.org/10.1016/J.CHOM.2016.06.006

Pai, M., Behr, M. A., Dowdy, D., Dheda, K., Divangahi, M., Boehme, C. C., … Raviglione, M. (2016). Tuberculosis. *Nature Reviews Disease Primers*, *2*(1), 16076. https://doi.org/10.1038/nrdp.2016.76

Pflum, M. K., Tong, J. K., Lane, W. S., & Schreiber, S. L. (2001). Histone deacetylase 1 phosphorylation promotes enzymatic activity and complex formation. *The Journal of Biological Chemistry*, *276*(50), 47733–47741. https://doi.org/10.1074/jbc.M105590200

Philips, R. L., Lee, J.-H., Gaonkar, K., Chanana, P., Chung, J. Y., Romero Arocha, S. R., … Shapiro, V. S. (2019). HDAC3 restrains CD8-lineage genes to maintain a bi-potential state in CD4+CD8+ thymocytes for CD4-lineage commitment. *ELife*, *8*. https://doi.org/10.7554/eLife.43821

Rajendran, P., Delage, B., Dashwood, W. M., Yu, T.-W., Wuth, B., Williams, D. E., … Dashwood, R. H. (2011). Histone deacetylase turnover and recovery in sulforaphane-treated colon cancer cells: competing actions of 14-3-3 and Pin1 in HDAC3/SMRT corepressor complex dissociation/reassembly. *Molecular Cancer*, *10*, 68. https://doi.org/10.1186/1476-4598-10-68

Rennoll-Bankert, K. E., Garcia-Garcia, J. C., Sinclair, S. H., & Dumler, J. S. (2015). Chromatin-bound

bacterial effector ankyrin A recruits histone deacetylase 1 and modifies host gene expression. *Cellular Microbiology*, *17*(11), 1640–1652. https://doi.org/10.1111/cmi.12461

Richa, R., & Sinha, R. P. (2014). Hydroxymethylation of DNA: an epigenetic marker. *EXCLI Journal*, *13*, 592–610. Retrieved from http://www.ncbi.nlm.nih.gov/pubmed/26417286

Roger, T., Lugrin, J., Le Roy, D., Goy, G., Mombelli, M., Koessler, T., … Calandra, T. (2011). Histone deacetylase inhibitors impair innate immune responses to Toll-like receptor agonists and to infection. *Blood*, *117*(4), 1205–1217. https://doi.org/10.1182/blood-2010-05-284711

Rolando, M., Sanulli, S., Rusniok, C., Gomez-Valero, L., Bertholet, C., Sahr, T., … Buchrieser, C. (2013). Legionella pneumophila effector RomA uniquely modifies host chromatin to repress gene expression and promote intracellular bacterial replication. *Cell Host & Microbe*, *13*(4), 395–405. https://doi.org/10.1016/j.chom.2013.03.004

Romani, B., Baygloo, N. S., Hamidi-Fard, M., Aghasadeghi, M. R., & Allahbakhshi, E. (2016). HIV-1 Vpr Protein Induces Proteasomal Degradation of Chromatin-associated Class I HDACs to Overcome Latent Infection of Macrophages. *The Journal of Biological Chemistry*, *291*(6), 2696–2711. https://doi.org/10.1074/jbc.M115.689018

Romani, B., & Engelbrecht, S. (2009). Human immunodeficiency virus type 1 Vpr: functions and molecular interactions. *The Journal of General Virology*, *90*(Pt 8), 1795–1805. https://doi.org/10.1099/vir.0.011726-0

Rosenberg, A., & Sibley, L. D. (2021). Toxoplasma gondii secreted effectors co-opt host repressor complexes to inhibit necroptosis. *Cell Host & Microbe*, *29*(7), 1186-1198.e8. https://doi.org/10.1016/J.CHOM.2021.04.016

Saha, B., & Parks, R. J. (2019). Histone Deacetylase Inhibitor Suberoylanilide Hydroxamic Acid Suppresses Human Adenovirus Gene Expression and Replication. *Journal of Virology*, *93*(12). https://doi.org/10.1128/JVI.00088-19

Sahakian, E., Chen, J., Powers, J. J., Chen, X., Maharaj, K., Deng, S. L., … Pinilla-Ibarz, J. (2017). Essential role for histone deacetylase 11 (HDAC11) in neutrophil biology. *Journal of Leukocyte Biology*, *102*(2), 475–486. https://doi.org/10.1189/jlb.1A0415-176RRR

Schlech, W. F. (2019). Epidemiology and Clinical Manifestations of Listeria monocytogenes Infection. *Microbiology Spectrum*, *7*(3). https://doi.org/10.1128/microbiolspec.GPP3-0014-2018

Schuettengruber, B., Simboeck, E., Khier, H., & Seiser, C. (2003). Autoregulation of mouse histone deacetylase 1 expression. *Molecular and Cellular Biology*, *23*(19), 6993–7004. https://doi.org/10.1128/mcb.23.19.6993-7004.2003

Schulz, C., Schütte, K., Mayerle, J., & Malfertheiner, P. (2019). The role of the gastric bacterial microbiome in gastric cancer: Helicobacter pylori and beyond. *Therapeutic Advances in Gastroenterology*, *12*, 1756284819894062–1756284819894062. https://doi.org/10.1177/1756284819894062

Sengupta, N., & Seto, E. (2004). Regulation of histone deacetylase activities. *Journal of Cellular*

Biochemistry, *93*(1), 57–67. https://doi.org/10.1002/jcb.20179

Shakespear, M. R., Halili, M. A., Irvine, K. M., Fairlie, D. P., & Sweet, M. J. (2011). Histone deacetylases as regulators of inflammation and immunity. *Trends in Immunology*, *32*(7), 335–343. https://doi.org/10.1016/J.IT.2011.04.001

Sir, D., Tian, Y., Chen, W., Ann, D. K., Yen, T.-S. B., & Ou, J. J. (2010). The early autophagic pathway is activated by hepatitis B virus and required for viral DNA replication. *Proceedings of the National Academy of Sciences*, *107*(9), 4383 LP – 4388. https://doi.org/10.1073/pnas.0911373107

Stengel, K. R., Barnett, K. R., Wang, J., Liu, Q., Hodges, E., Hiebert, S. W., & Bhaskara, S. (2017). Deacetylase activity of histone deacetylase 3 is required for productive VDJ recombination and B-cell development. *Proceedings of the National Academy of Sciences of the United States of America*, *114*(32), 8608–8613. https://doi.org/10.1073/pnas.1701610114

Stevers, L. M., Sijbesma, E., Botta, M., MacKintosh, C., Obsil, T., Landrieu, I., … Ottmann, C. (2018). Modulators of 14-3-3 Protein-Protein Interactions. *Journal of Medicinal Chemistry*, *61*(9), 3755–3778. https://doi.org/10.1021/acs.jmedchem.7b00574

Tanno, M., Sakamoto, J., Miura, T., Shimamoto, K., & Horio, Y. (2007). Nucleocytoplasmic shuttling of the NAD+-dependent histone deacetylase SIRT1. *The Journal of Biological Chemistry*, *282*(9), 6823–6832. https://doi.org/10.1074/jbc.M609554200

Taylor, S., Barragan, A., Su, C., Fux, B., Fentress, S. J., Tang, K., … Sibley, L. D. (2006). A secreted serine-threonine kinase determines virulence in the eukaryotic pathogen Toxoplasma gondii. *Science (New York, N.Y.)*, *314*(5806), 1776–1780. https://doi.org/10.1126/science.1133643

Terhune, S. S., Moorman, N. J., Cristea, I. M., Savaryn, J. P., Cuevas-Bennett, C., Rout, M. P., … Shenk, T. (2010). Human cytomegalovirus UL29/28 protein interacts with components of the NuRD complex which promote accumulation of immediate-early RNA. *PLoS Pathogens*, *6*(6), e1000965–e1000965. https://doi.org/10.1371/journal.ppat.1000965

Ueki, N., Zhang, L., & Haymann, M. J. (2008). Ski can negatively regulates macrophage differentiation through its interaction with PU.1. *Oncogene*, *27*(3), 300–307. https://doi.org/10.1038/sj.onc.1210654

Walters, M. S., Kinchington, P. R., Banfield, B. W., & Silverstein, S. (2010). Hyperphosphorylation of histone deacetylase 2 by alphaherpesvirus US3 kinases. *Journal of Virology*, *84*(19), 9666–9676. https://doi.org/10.1128/JVI.00981-10

Wang, X., Wu, Y., Jiao, J., & Huang, Q. (2018). Mycobacterium tuberculosis infection induces IL-10 gene expression by disturbing histone deacetylase 6 and histonedeacetylase 11 equilibrium in macrophages. *Tuberculosis*, *108*, 118–123. https://doi.org/10.1016/J.TUBE.2017.11.008

Wang, Y., Curry, H. M., Zwilling, B. S., & Lafuse, W. P. (2005). Mycobacteria inhibition of IFN-gamma induced HLA-DR gene expression by up-regulating histone deacetylation at the promoter region in human THP-1 monocytic cells. *Journal of Immunology (Baltimore, Md. : 1950)*,

174(9), 5687–5694. Retrieved from http://www.ncbi.nlm.nih.gov/pubmed/15843570

Wassilew, N., Hoffmann, H., Andrejak, C., & Lange, C. (2016). Pulmonary Disease Caused by Non-Tuberculous Mycobacteria. *Respiration*, *91*(5), 386–402. https://doi.org/10.1159/000445906

Weiskopf, K., Schnorr, P. J., Pang, W. W., Chao, M. P., Chhabra, A., Seita, J., … Weissman, I. L. (2016). Myeloid Cell Origins, Differentiation, and Clinical Implications. *Microbiology Spectrum*, *4*(5). https://doi.org/10.1128/microbiolspec.MCHD-0031-2016

Wu, X., & Zhang, Y. (2017). TET-mediated active DNA demethylation: mechanism, function and beyond. *Nature Reviews Genetics*, *18*(9), 517–534. https://doi.org/10.1038/nrg.2017.33

Xiao, H., Jiao, J., Wang, L., O'Brien, S., Newick, K., Wang, L.-C. S., … Beier, U. H. (2016). HDAC5 controls the functions of Foxp3(+) T-regulatory and CD8(+) T cells. *International Journal of Cancer*, *138*(10), 2477–2486. https://doi.org/10.1002/ijc.29979

Yan, B., Liu, Y., Bai, H., Chen, M., Xie, S., Li, D., … Zhou, J. (2017). HDAC6 regulates IL-17 expression in T lymphocytes: implications for HDAC6-targeted therapies. *Theranostics*, *7*(4), 1002–1009. https://doi.org/10.7150/thno.17615

Yang, Q., Tang, J., Pei, R., Gao, X., Guo, J., Xu, C., … Chen, J. (2019). Host HDAC4 regulates the antiviral response by inhibiting the phosphorylation of IRF3. *Journal of Molecular Cell Biology*, *11*(2), 158–169. https://doi.org/10.1093/jmcb/mjy035

Yang, X., Cao, X., Sheng, L., & Yang, Z. (2021). [Mechanism of histone deacetylase inhibitor tubastatin A promoting autophagy of Legionella pneumophila infected RAW264.7 cells]. *Xi bao yu fen zi mian yi xue za zhi = Chinese journal of cellular and molecular immunology*, *37*(8), 693–701.

Yao, Z., Zhang, Q., Li, X., Zhao, D., Liu, Y., Zhao, K., … Cao, X. (2014). Death domain-associated protein 6 (Daxx) selectively represses IL-6 transcription through histone deacetylase 1 (HDAC1)-mediated histone deacetylation in macrophages. *The Journal of Biological Chemistry*, *289*(13), 9372–9379. https://doi.org/10.1074/jbc.M113.533992

Zhang, Yanhua, Xie, H., Tang, W., Zeng, X., Lin, Y., Xu, L., … Yuan, D. (2019). Trichostatin A, a Histone Deacetylase Inhibitor, Alleviates Eosinophilic Meningitis Induced by Angiostrongylus cantonensis Infection in Mice. *Frontiers in Microbiology*, *10*, 2280. https://doi.org/10.3389/fmicb.2019.02280

Zhang, Yingqian, & Zhou, C. (2019). Formation and biological consequences of 5-Formylcytosine in genomic DNA. *DNA Repair*, *81*, 102649. https://doi.org/10.1016/J.DNAREP.2019.102649

Zughaier, S. M., Rouquette-Loughlin, C. E., & Shafer, W. M. (2020). Identification of a Neisseria gonorrhoeae Histone Deacetylase: Epigenetic Impact on Host Gene Expression. *Pathogens (Basel, Switzerland)*, *9*(2). https://doi.org/10.3390/pathogens9020132

FIGURE LEGENDS

Figure 1: Pathogens interfering with HDAC localization often promote HDAC degradation. Pathogens interact with HDACs through a variety of different processes: *Salmonella typhimurium* infections lead to an upregulation of the mTOR/AKT pathway, which disrupts SIRT1 nuclear shuttling. The following cytoplasmic accumulation promotes the degradation of SIRT1 in a lysosome dependent manner. The surface protein InlB of *L. monocytogenes* interacts with the eukaryotic c-Met receptor, thereby promoting the uptake of the bacteria and activating phosphatidylinositol 3-kinase (PI3K), which then causes a nuclear translocation of SIRT2. In the nucleus, SIRT2 deacetylates lysine 18 of histone H3 (H3K18), leading to changes in gene expression. The HIV protein Vpr is a protein essential for the viral entry in the nucleus. Furthermore, it promotes E3 ubiquitin ligase activity. HDAC1 is ubiquinated through this process, travels to the cytoplasm and is degraded by the proteasome. The C6 protein of the Vaccinia virus also promotes proteasomal degradation of a eukaryotic histone deacetylase, HDAC4.

Figure 2: Distribution of histone deacetylase proteins on the phylogeny of the genus *Legionella*. An HDAC domain search in 58 different *Legionella* species identified two different types of HDAC proteins named group 1 (orange), and group 2 (green). The phylogenetic tree shown is a species tree of the genus *Legionella* published in Gomez-Valero et al. 2019. Several strains (number noted next to species name) of the same species were collapsed due to high homology between their proteins. The length of the protein lines and domain symbols are proportional to the protein/domain size and the domain length is noted within the domain. In the species *L. gresiliensis* two proteins belonging to group 2 are present.

Table 1: Pathogens known to target different eukaryotic histone deacetylases

Pathogen	Effector	Target HDAC (complex)	Reference
Changes in HDAC activity			
Anaplasma phagocytophilium	AnkA	HDAC1	(Rennoll-Bankert et al., 2015)
Helicobacter pylori	Unknown	Unknown	(Ding et al., 2010)
Mycobacterium avium/tuberculosis	Unknown	HDAC1/2 (Sin3)	(Wang et al., 2005)
Listeria monocytogenes	LntA	HDAC1/2 (BAHD1)	(Lebreton et al., 2011)
Beta-herpesvirus	UL38 and UL29/28	HDAC1/2 (Mi-2/NuRD)	(Terhune et al., 2010)
Gamma-herpesvirus	orf36	HDAC1/2	(Mounce et al., 2013)
Herpes simplex virus 1	US3	HDAC2	(Walters et al., 2010)
Toxoplasma gondii	TgIST	HDAC1/2 (Mi-2/NuRD)	(Olias et al., 2016)
	TgNSM	HDAC3 (NCoR/SMRT)	(Rosenberg and Sibley, 2021)
	ROP18	HDAC3	(An et al., 2018)
Changes in HDAC localization			
Salmonella typhimurium	Unknown	SIRT1	(Ganesan et al., 2017)
Listeria monocytogenes	InlB	SIRT2	(Eskandarian et al., 2013)
Human immunodeficiency virus 1	Vpr	HDAC1/3	(Romani et al., 2016)
Vaccinia virus	C6	HDAC4	(Lu et al., 2019)
Changes in HDAC expression			
Mycobacterium tuberculosis	Unknown	HDAC6/11	(Wang et al., 2018)
	Unknown	SIRT1	(Cheng et al., 2017)
Hepatitis C virus	Unknown	HDAC9	(Chen et al., 2015)
Influenza A virus	PA-X	HDAC4	(Galvin and Husain, 2019)
Hepatitis B virus	HBx	HDAC1	(Fu et al., 2018)

Table 2: HDAC inhibitors shown to affect different pathogens

Inhibitor	Target HDAC	Pathogen	Reference
Suberanilohydroxamic acid (SAHA/Vorinostat)	Class I, II and IV	*Salmonella typhimurium*	(Ariffin et al., 2015)
		Escherichia coli	(Ariffin et al., 2015)
		Adenovirus	(Saha & Parks, 2019)
		Human papillomavirus	(Banerjee et al., 2018)
		Cryptosporidium parvum	(Guo et al., 2018)
		Leishmania infantum/donovani	(Corpas-López et al., 2019)
		Fusarium solani	(X. Li et al., 2019)
Trichostatin A (TSA)	Class I and II	*Salmonella typhimurium*	(Ariffin et al., 2015)
		Escherichia coli	(Ariffin et al., 2015)
		Angiostrongylus cantonensis	(Zhang et al., 2019)
Tubastatin A	HDAC6	*Salmonella typhimurium*	(Ariffin et al., 2015)
		Legionella pneumophila	(X. Yang et al., 2021)
Sodium butyrate	Class I	*Klebsiella pneumoniae*	(Chakraborty et al., 2017)
Tenovin-1	SIRT1 and SIRT 2	Arboviruses	(Hackett et al., 2019)
Sirtinol	SIRT1 and SIRT2	West Nile virus	(Hackett et al., 2019)

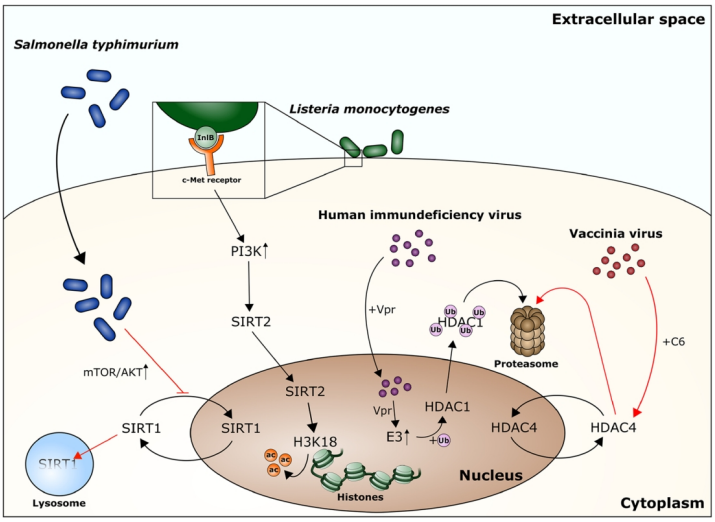

Pathogens interfering with HDAC localization often promote HDAC degradation.

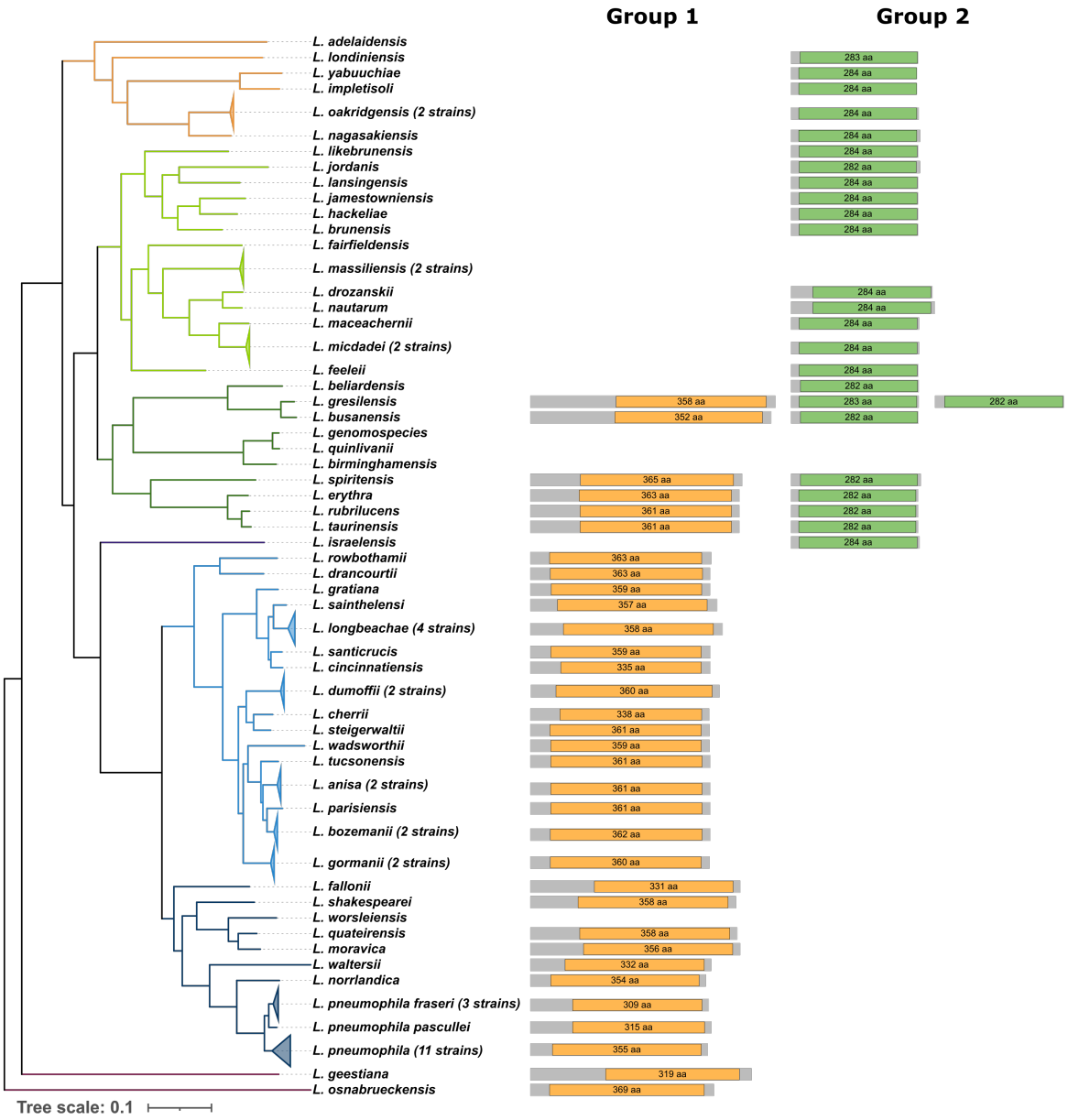
Group 1
Group 2
L. adelaidensis
L. londiniensis
L. yabuuchiae
L. impletisoli
L. oakridgensis (2 strains)
L. nagasakiensis
L. likebrunensis
L. jordanis
L. lansingensis
L. jamestowniensis
L. hackeliae
L. brunensis
L. fairfieldensis
L. massiliensis (2 strains)
L. drozanskii
L. nautarum
L. maceachernii
L. micdadei (2 strains)
L. feeleii
L. beliardensis
L. gresilensis
L. busanensis
L. genomospecies
L. quinlivanii
L. birminghamensis
L. spiritensis
L. erythra
L. rubrilucens
L. taurinensis
L. israelensis
L. rowbothamii
L. drancourtii
L. gratiana
L. sainthelensi
L. longbeachae (4 strains)
L. santicrucis
L. cincinnatiensis
L. dumoffii (2 strains)
L. cherrii
L. steigerwaltii
L. wadsworthii
L. tucsonensis
L. anisa (2 strains)
L. parisiensis
L. bozemanii (2 strains)
L. gormanii (2 strains)
L. fallonii
L. shakespearei
L. worsleiensis
L. quateirensis
L. moravica
L. waltersii
L. norrlandica
L. pneumophila fraseri (3 strains)
L. pneumophila pascullei
L. pneumophila (11 strains)
L. geestiana
L. osnabrueckensis
283 aa
284 aa
282 aa
358 aa
352 aa
365 aa
363 aa
361 aa
359 aa
357 aa
335 aa
360 aa
338 aa
362 aa
331 aa
356 aa
332 aa
354 aa
309 aa
315 aa
355 aa
319 aa
369 aa
Tree scale: 0.1

Aim of the PhD thesis

The influence of bacterial effectors on the host's epigenetic landscape has moved into the limelight in the past decade. Numerous strategies have been identified how pathogens manipulate gene transcription, but the goal is always the same, ensure their own survival and promote their replication.

For *L. pneumophila* it was shown that many secreted effectors interfere with cell signaling to disable the defenses that are aimed at controlling and eliminating invaders (Mondino et al., 2020a). As mentioned before, RomA is directly secreted by *L. pneumophila* to modify the host chromatin by methylating lysine 14 of histone H3 (H3K14), a usually acetylated residue, consequently leading to a down regulation of host response genes (Rolando et al., 2013).

The finding that RomA methylates a usually acetylated histone mark led to the question how deacetylation of this mark might happen to allow its subsequent methylation, and whether this is also induced by the bacteria directly or via recruiting host histone deacetylases (HDACs). An in-depth bioinformatics search for additional putative chromatin modifying effectors in the *L. pneumophila* genome, led to the identification of a protein predicted to code for a eukaryotic histone deacetylase, later named LphD (*Legionella pneumophila* histone deacetylase).

The main objective of this work was to understand if and how LphD targets host chromatin. Furthermore, to determine if LphD, together with RomA, might play a concerted role to modulate the host chromatin landscape to promote bacterial replication. To elucidate the function of LphD and its role during infection this project focused on three main objectives:

I. Decipher the functional role of the LphD in the eukaryotic cell

II. Solve the structure and the biochemical function of LphD

III. Understand the mechanisms of function of LphD in a context of multi-effector synergy as well as its implication in transcriptional changes during infection

Beside my main project on the characterization of LphD nuclear functions, I was also involved in two other projects during the time I spent in the lab. In particular, I was working on the characterization of a *L. longbeachae* effector (**Annex 1**) and in setting up a new animal model, zebrafish (*Danio rerio*), for *L. pneumophila* infection (**Annex 2**).

Results

Project Progress

As mentioned before, the project was split into three main objectives:

I. Decipher the functional role of the LphD in the eukaryotic cell

To determine the influence of LphD during *L. pneumophila* infection, we constructed a *lphD* knock out strain (Δ*lphD*). We then compared the ability to replicate of this strain with the wild type strain, using different infection models (*A. castellanii* and human THP-1 cells), showing that the Δ*lphD* strain exhibits a replication defect. In addition, we proofed that LphD is secreted into the host cell during infection and that this secretion is dependent on the Dot/Icm secretion system. Furthermore, we followed the intracellular localization of LphD in the host cell, first in transfected cells and later during infection. In both models we observed a clear nuclear localization of LphD, further supporting the hypothesis of its chromatin modifying function.

II. Solve the structure and the biochemical function of LphD

To determine the biochemical function, we first decided to construct a catalytic inactive version of LphD. Through sequence analysis and comparison to eukaryotic HDACs we predicted the catalytic center of the enzyme (Y392). By a single base pair mutation, we replaced this tyrosine residue with a phenylalanine, a mutation previously used to generate catalytically dead eukaryotic HDACs. We then set up a purification protocol to isolate LphD from *E. coli*. This purified LphD was then used for several different assays. We first showed that the enzyme indeed has lysine deacetylase activity in an *in vitro* assay. Moreover, the Y392F mutation completely abolished the enzymatic activity. Interestingly, we also observed that Trichostatin A (TSA) – a known inhibitor of eukaryotic Zn^{2+}-dependent HDACs – impedes the activity of LphD, highlighting its homology to this class of enzymes. To further investigate the enzyme kinetics, we set up a collaboration with Jérémy Berthelet and Fernando Rodrigues-Lima (Université de Paris). By comparing the catalytic efficiency of LphD on different acetylated histone H3 peptides, they revealed that LphD shows the highest efficiency for H3K14, the same residue targeted by RomA. In our lab we confirmed these results in the context of infection, showing that cells infected with *L. pneumophila* have lower levels of H3K14ac, and that this decrease is indeed dependent on the presence of LphD. This effect on acetylation seems to be

specific for H3K14, since other tested residues show no difference between the wild-type strain and the *lphD* knock out.

For the last part of this project, deciphering the structure of LphD, we set up a collaboration with Mathilde Ben Assaya and Anne Marie Wehenkel (Institut Pasteur). Through numerous tests they were able to improve the purification process, as well as optimize the crystallization conditions. They generated several crystals so far, however, the resolution obtained when analyzed in the synchrotron did not allow an in-depth analysis. This project is still on-going and they work tirelessly to further optimize the crystallization conditions. To get a first glimpse of the putative structure, they used the AlphaFold 2 artificial intelligence program.

III. Understand the mechanisms of function of the LphD in a context of multi-effector synergy as well as its implication on transcriptional changes during infection

To understand if LphD directly influences the activity of RomA, we analyzed the H3K14 methylation levels in cells infected with the Δ*lphD* strain. We observed a drastic decrease of H3K14me in the absence of LphD, further supporting the hypothesis of a synergy between LphD and RomA. In addition, we showed that LphD, as well as RomA, interacts with KAT7, a eukaryotic histone acetyl transferase known to target H3K14. This interaction confirmed in transfected cells as well as in the context of infection. To get a better understanding of the influence of both bacterial effectors in the transcriptional landscape of the cells, we performed RNA-seq of infected THP-1 cells in a time course experiment. The analyses of these data revealed dynamic changes in the transcription of the host cell within the first few hours of infection, mainly focused on the response to the bacterial intruders. Furthermore, we showed by using RT-qPCR, that LphD and RomA can influence gene transcription synergistically, but also independently from each other. These results highlight the fine-tuned regulation of the host's transcriptional response by *L. pneumophila* via the secretion of LphD and RomA.

This work is summarized in my main publication (*in preparation* for submission).

LphD crystal structure

As mentioned before, to determine the structure of LphD, we set up a collaboration with Mathilde Ben Assaya and Anne Marie Wehenkel (Structural Microbiology, Institut Pasteur). Together with the *Production and Purification of Recombinant Proteins Technological Platform* at Institut Pasteur, they developed the purification protocol for HIS_6-tagged LphD.

Crystallization screens were performed using LphD protein alone or in complex with the inhibitor Trichostatin A (TSA) (molar ratio 1:4) with the sitting-drop vapour diffusion method and a Mosquito nanolitre-dispensing crystallization robot (TTP Labtech). The apo-protein resulted in small needle-like crystals that could not be optimized and did not diffract. Small crystals arose for the protein-inhibitor complex in the following conditions crystallization condition: I) 0.2 M $MgCl_2$, 0.1 M MES pH 6.5, 25% PEG 4K, II) 22% (w/v) PEG 8k, 250 mM $MgCl_2$, 0.1 M MES pH 6.5. The crystals were cryo-protected in mother liquor containing 33% (v/v) ethylene glycol or glycerol33% (v/v) (**Figure 13**).

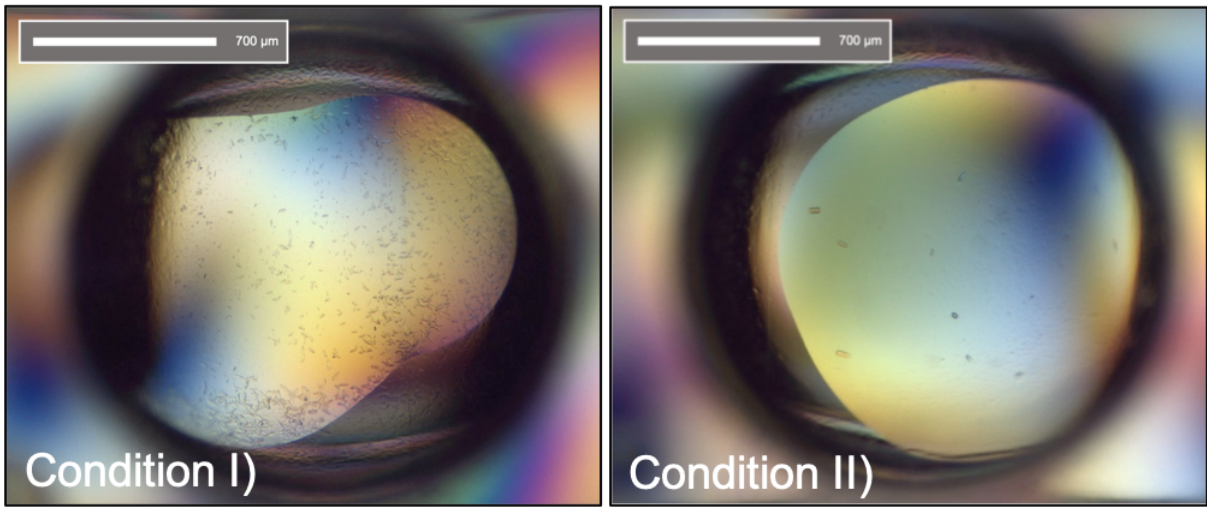

Figure 13: Crystallization of LphD under two different experimental conditions. Purified LphD – together with its inhibitor TSA (molar ratio 1:4) – was screened for crystallization under different conditions using the sitting-drop vapour diffusion method and a Mosquito nanoliter-dispensing crystallization robot. The two conditions are as follows: I) 0.2 M MgCl2, 0.1 M MES pH 6.5, 25% PEG 4K; II) 22% (w/v) PEG 8k, 250 mM MgCl2, 0.1 M MES pH 6.5.

The crystals were tested at the Soleil synchrotron (PX1 and 2), but diffracted poorly (only several spots at low resolution). We are currently optimizing the crystallization conditions to improve the diffraction properties. In parallel we have generated a structural model using AlphaFold 2 (Jumper et al., 2021). This model suggests that the N-and C-terminal flanking regions of the protein are disordered, and these limits could be used to design new constructs. In addition, when highlighting the catalytic tyrosine (Y392) and other conserved residues implicated in substrate binding in eukaryotic HDACs (H177/178, D218/330, N218, Y248) (Uba and Yelekçi, 2017), we can see that it is clearly localized in the probable binding pocket of the enzyme (**Figure 14**). Apart from the flanking regions that do not present a secondary structure,

the core of the protein is predicted with high confidence and will be used to derive structure-based hypotheses for future experiments.

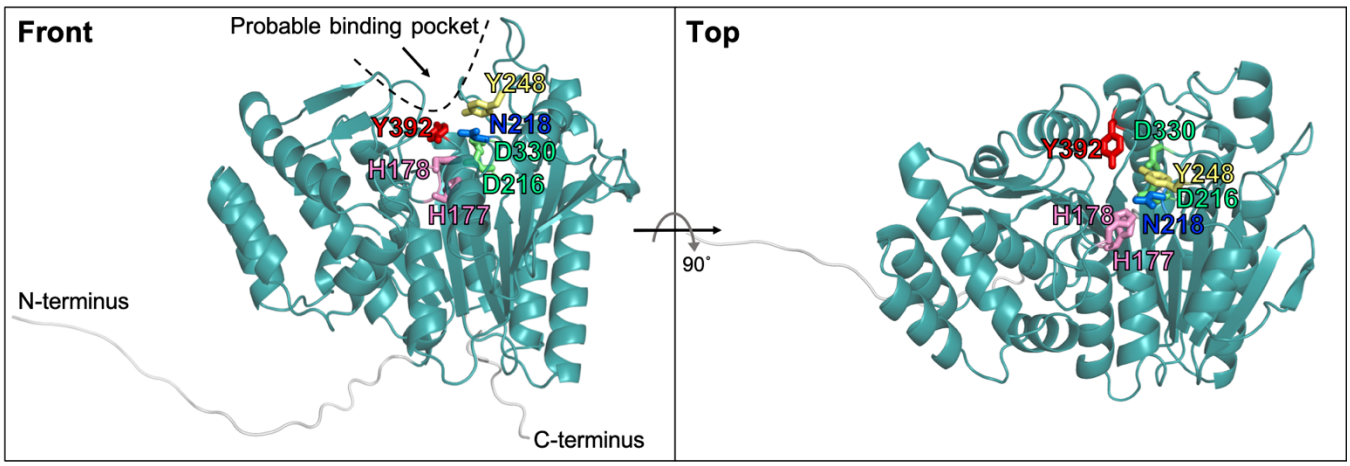

Figure 14: AlphaFold2 prediction of LphD structure. The structure of LphD shows the presence of a possible substrate binding pocket, also seen in eukaryotic HDACs. In addition, conserved residues (Y392 red; H177/178 pink; D216/330 green; N218 blue; Y248 yellow) know to be implicated in substrate binding are positioned within this probable binding pocket. The core of the protein – including the HDAC domain – is predicted with high confidence.

Moreover, we used the Phyre2 structure prediction tool to look for structurally similar proteins. This led to the identification of HDAC10 (of *Danio rerio*) as a possibly highly homologous protein (Kelley et al., 2015). When superposing the HDAC domain of LphD with the HDAC domain of a catalytic inactive HDAC10 (Y307F) (Hai et al., 2017), we can see a clear overlap in the position of the binding pockets as well as the position of the catalytic tyrosine (**Figure 15**).

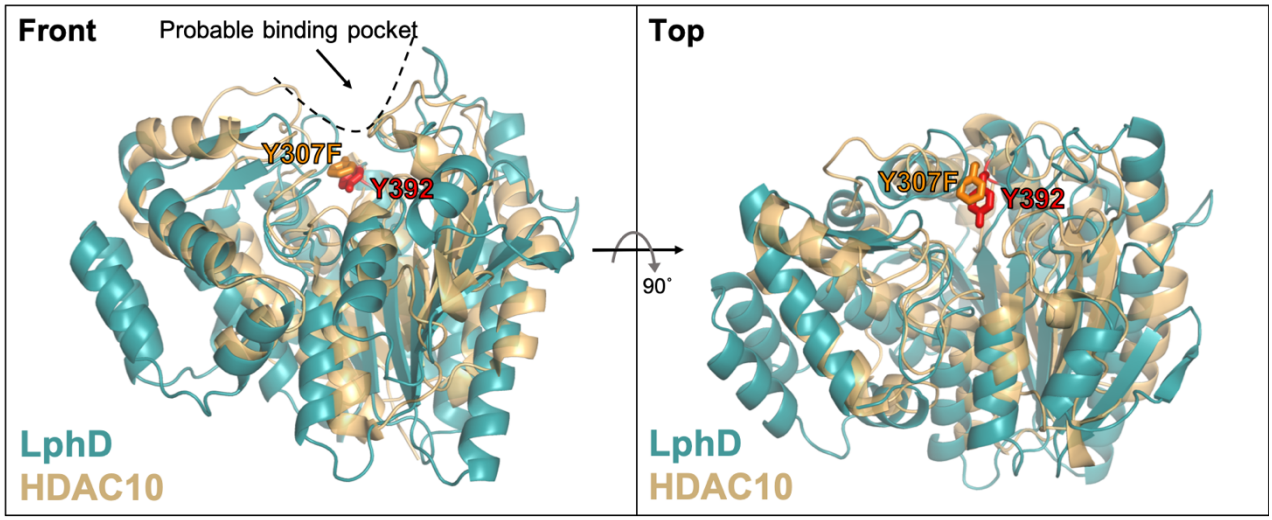

Figure 15: Superposition of the HDAC domains of LphD and HDAC10. The HDAC domain of a catalytic inactive HDAC10 (Y307F) from *Danio rerio* is superposed with the HDAC domain of LphD. In both proteins a clear overlap in the position of the binding pocket can be seen. In addition, when comparing the position of the catalytic residue of each HDAC domain (Y307F, orange for HDAC10; Y392 red for LphD) they closely colocalize, further highlighting the similarity between the two domains.

These results further highlight the similarity of the bacterial HDAC domain with its eukaryotic counterparts. In addition, future experiments can be designed to test the involvement of different amino acid residues in the activity of LphD.

Publication – Characterization of LphD and its synergy with RomA

TITLE

Two *Legionella pneumophila* effectors hijack the HBO1 complex to modify host chromatin during infection

Daniel SCHATOR [1,2], Sonia MONDINO [1], Jérémy BERTHELET[3], Giulia BRENNA[1], Fernando RODRIGUES-LIMA[3], Carmen BUCHRIESER [1*], Monica ROLANDO[1*]

1, Institut Pasteur, Université de Paris, CNRS UMR 3525, Unité Biologie des Bactéries Intracellulaires, F-75015 Paris, France

2, Sorbonne Université, Collège doctoral, F-75005 Paris, France

3, Université de Paris, BFA, UMR 8251, CNRS, 75013, Paris, France

Key words : *Legionella pneumophila*, histone deacetylase, epigenetic modifications, chromatin, HBO1, pathogenesis

* For correspondence:

Carmen Buchrieser and Monica Rolando

Institut Pasteur, Biologie des Bactéries Intracellulaires

28, rue du Dr. Roux, 75724 Paris Cedex 15, France

Tel: (33-1)-44-38-95-40

Fax: (33-1)-45-68-87-86

E-mail: *cbuch@pasteur.fr, mrolando@pasteur.fr*

ABSTRACT

Legionella pneumophila – a facultative intracellular bacterium – is the causative agent of a severe pneumonia called Legionnaires' disease. It has been shown that *L. pneumophila* directly modifies host chromatin by secreting RomA, a eukaryotic-like SET-domain methyltransferase. RomA specifically methylates a usually acetylated lysine residue on histone H3 (H3K14), a usually acetylated residue, leading to a transcriptional repression of the host's immune response. Here we show that *L. pneumophila* is directly involved in the process of H3K14 deacetylation, by secreting a histone deacetylase, which we named LphD. LphD targets the host cell nucleus and modifies host chromatin in synergy with RomA. Both bacterial effectors target the host chromatin by interacting with the HBO1 histone acetyltransferase complex, a complex known to target H3K14. RNA-seq analyses of wild-type *L. pneumophila* and mutants deleted of the two bacterial effectors revealed that RomA and LphD influence the expression of genes implicated in the host immune response in a cumulative way. Thus, we provide unique insight into how a bacterial pathogen manipulates their host to ensure survival in an otherwise hostile environment.

GRAPHICAL ABSTRACT

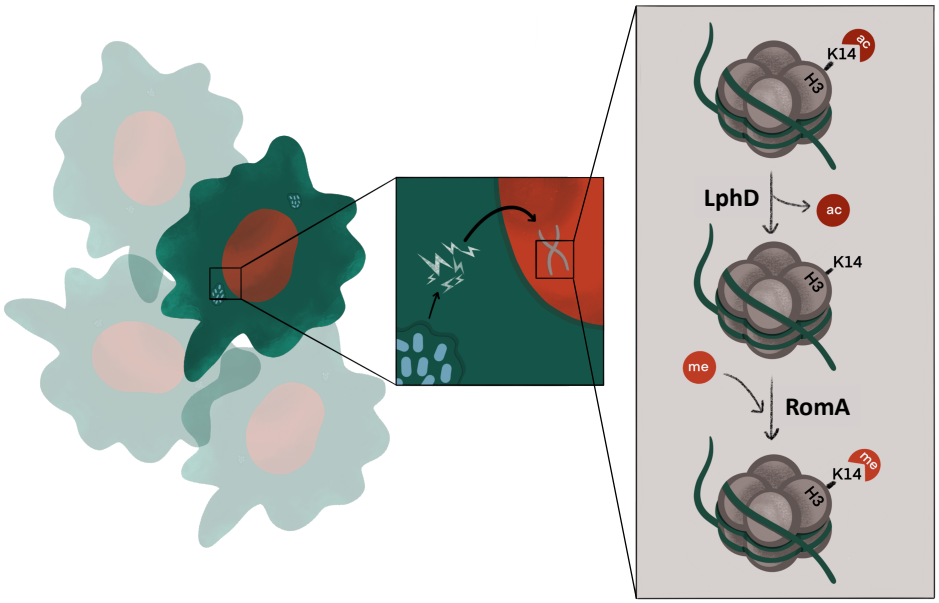

INTRODUCTION

The accessibility of chromatin to transcription factors and the subsequent changes in gene expression are a key regulatory mechanism in cells. The process of changing this accessibility is known as chromatin remodeling. The dynamic modification of histones, the small basic proteins that DNA is wrapped around to form chromatin, is one of the most studied mechanisms of chromatin remodeling. The so-called histone tails – peptide sequences reaching out of the core histone structure – are subjected to a variety of modifications (du Preez and Patterton, 2013). In fact, histones undergo various forms of post-translational modifications (PTMs), such as acetylation, methylation, ubiquitination and phosphorylation (Kouzarides, 2007). However, methylation and acetylation of the amino-terminal tail of histone proteins are the most studied and best characterized PTMs. They have been the first post-translational modifications discovered and were linked to altered rates of DNA transcription almost six decades ago (Allfrey et al., 1964; Murray, 1964). Importantly, combinations of acetylation and methylation of lysine residues in histone tails can function in a concerted manner with both cooperative or antagonistic functions. Methylation is associated to compaction of chromatin and reduced transcription (Rice and Allis, 2001). Acetylation impairs the affinity of histones to DNA thus, loosening chromatin compaction, promoting the recruitment of transcription factors (Mathis et al., 1978) and increasing the mobility of histones along the DNA (Cosgrove et al., 2004). Therefore, the balanced activity of enzyme classes involved in attaching (histone methyltransferases and histone acetyltransferases (HAT)) and removing (histone demethylases and histone deacetylases (HDAC)) these groups ensures the correct expression of specific genes at specific times.

Numerous different stimuli have been shown to influence the PTM levels of histones, an emerging topic is the manipulation of histone modifications by different pathogens. Histone acetylation has been shown to be a potent target for a variety of pathogens to promote their replication and the research on these processes has gained momentum in recent years (An et al., 2018; Galvin and Husain, 2019; Ganesan et al., 2017).

Legionella pneumophila, a facultative intracellular, Gram-negative bacterium that parasitizes free-living protozoa, is the causative agent of a severe atypical pneumonia in humans, called Legionnaires' disease (Mondino et al., 2020a). *L. pneumophila* has closely co-evolved with its eukaryotic hosts, giving rise to numerous mechanisms to manipulate the host and to thrive in this otherwise hostile intracellular environment. One consequence of *Legionella* co-evolution with its hosts is the presence of a high number of genes encoding eukaryotic-like proteins in the *Legionella* genome (Cazalet et al., 2004; de Felipe et al., 2005; Gomez-Valero et al., 2019).

A key factor for the manipulation of the host cell is the Dot/Icm type-IV secretion system (T4SS) which is highly conserved in the entire genus and is used by the bacteria to translocate more than 300 proteins into the host cell (Burstein et al., 2016; Ensminger, 2016; Gomez-Valero et al., 2019). Several of these secreted effectors represent eukaryotic-like proteins and have been functionally characterized in order to understand how *Legionella* spp. manipulate the host cell response thus, facilitating bacteria survival and replication (Mondino et al., 2020b). One of these secreted effectors, RomA, is a SET-domain histone methyltransferase that directly modifies host chromatin by tri-methylating lysine 14 on histone H3 (H3K14) (Rolando et al., 2013). This histone modification is present at very low levels in human cells (Zhao et al., 2018), however, its distribution is increased under specific conditions (*e.g.* stress response) (Zhu et al., 2021). The drastic increase in H3K14 methylation – due to RomA activity – revealed a new strategy *L. pneumophila* employs to subvert the host response. By secreting these so-called nucleomodulins, effectors targeting the host cell nucleus, the bacteria are able to vastly change the chromatin landscape (Bierne and Pourpre, 2020). In fact, RomA activity strongly affects the expression of several genes involved in the host's response to the infection (Rolando et al., 2013). However, it should be noted that K14 is a major acetylation site on histone H3, together with K9, K18, K23 and K27. Although histone marks are not necessarily explicit codes, they may still serve as epigenetic indicators of chromatin state associated with gene activation and repression (Kimura, 2013). In general, histone acetylation is correlated with transcriptional activation, being localized to transcription start sites and/or enhancers of potentially actively transcribed genes (Karmodiya et al., 2012). The fact that RomA targets a usually acetylated histone residue gave rise to the question of how the bacteria might influence the acetylation of H3K14 to enable its subsequent methylation. Due to the plethora of eukaryotic-like proteins in *L. pneumophila* we hypothesized that the bacteria might encode their own eukaryotic-like histone deacetylase (HDAC). Here we report that *L. pneumophila* encodes an HDAC-like protein that specifically targets H3K14 and works in synergy with RomA to ensure intracellular replication of the bacteria and finetune the host's gene expression to its own advantage.

RESULTS

L. pneumophila secretes the effector LphD, an active HDAC

Bioinformatic searches for *L. pneumophila* strain Paris genes encoding histone deacetylase-like domains, identified the gene *lpp2163* as a possible candidate. This gene encodes a 425 amino acid long protein – with residues 54-409 predicted to be a Zn^{2+}-dependent histone deacetylase domain – that we named LphD (*Legionella pneumophila* histone Deacetylase) (Schator et al., 2021). Indeed, the histone deacetylase domain contains conserved binding pocket residues and the active-site tyrosine (Y392), features found as part of the so-called charge relay system in eukaryotic histone deacetylases (**Figure S1**) (Uba and Yelekçi, 2017).

To determine if LphD indeed holds lysine deacetylase activity, we purified the full-length protein in *Escherichia coli* and performed a fluorometric enzymatic assay that allows the quantification of lysine deacetylation on an acetylated lysin side chain. **Figure 1A** shows that LphD exhibits strong *in vitro* lysine deacetylase activity in a dose-dependent manner. Furthermore, the single amino acid substitution (Y392F) on the predicted active site completely inactivates the enzyme. Adding Trichostatin A (TSA), a broad range inhibitor of Zn^{2+}-dependent histone deacetylases, LphD activity was drastically reduced (**Figure 1A**), further suggesting that LphD is a Zn^{2+}-dependent histone deacetylase.

To identify the substrate recognized by LphD, we performed an enzymatic activity assay and measured the catalytic efficiency of LphD on histone H3 peptides acetylated on different lysine residues (H3K4, H3K9, H3K14, H3K18, H3K23 and H3K27). We measured the activity of both LphD and LphD Y392F against these different peptides while varying the peptide concentration. We clearly observed the highest catalytic efficiency of LphD on H3K14, compared to the other tested residues (**Figure 1B**). The deacetylase activity of LphD on H3K14 was also confirmed on histone octamers isolated from human cells (**Figure 1C**, **Figure S2A**). In addition, the H3K14ac antibody was tested to ensure its specificity (**Figure S2B**).

Given that LphD is an active histone deacetylase targeting H3K14 *in vitro*, we characterized its function in an intracellular context. To assess whether LphD is indeed an effector secreted by the T4SS we infected THP-1 cells with an *L. pneumophila* strain expressing a β-lactamase-LphD fusion construct and measured the effector translocation by quantifying the number of cells exhibiting β-lactamase activity against a fluorescent substrate (CFF4) in their cytosol. A β-lactamase-RomA fusion protein was used as positive control. This clearly showed that LphD is a secreted effector (**Figure 2A**). By knocking out a central component of the Dot/Icm

secretion system (*dotA*), we could completely abolish the secretion of the LphD fusion protein, confirming that the secretion process is T4SS-dependent (**Figure 2A**). To assess the subcellular localization of LphD, we transiently transfected HeLa cells with an EGFP-LphD fusion product. The LphD fusion protein accumulates in the nucleus in transfected cells, compared to the cytosolic localization typically found for EGFP (**Figure 2B**). To note, the LphD-Y392F catalytic inactive mutant is still located in the nucleus of transfected cells (**Figure S2C**). To determine the nuclear localization of LphD during infection, we generated a specific anti-LphD antibody from rabbits (**Figure S2D**) to follow the translocation of LphD. This showed that, at late stages of the infection cycle, LphD accumulates in the host cell nucleus (**Figure 2C**). Furthermore, the nuclear accumulation of LphD in transfected cells, correlates with a drastic decrease in H3K14ac signal, an effect not seen in cells transfected with the Y392F mutant (**Figure 2D**).

To better assess the influence of LphD on the epigenetic status of H3K14 during infection, we isolated histones from cells infected either with *L. pneumophila* wild type or the Δ*lphD* strain and followed H3K14 acetylation as a function of time. **Figure 2E** shows that *L. pneumophila* wild type leads to a decrease in H3K14ac within 7 hours of infection, dependent on the presence of LphD, as the infection with the Δ*lphD* strain led to an increase in H3K14ac in the same timeframe (**Figure 2E**). Moreover, this is specific for H3K14, since other tested residues (H3K18 and H3K23) did not show a difference between the wild type and the Δ*lphD* infection (**Figure S3A, S3B**).

To evaluate the role of LphD in infection, we analyzed the replication of the wild-type strain compared to the Δ*lphD* strain in *Acanthamoeba castellanii*, a natural host of *L. pneumophila*, as well as in macrophages derived from THP-1 cells. This revealed that the Δ*lphD* strain has a slight but consistent growth defect compared to the wild-type strain (**Figure S3C** and **2F**). In contrast, when grown in liquid medium, both strains show the same growth rate (data not shown). To determine if the deficiency in intracellular replication is dependent on the presence of LphD, we trans-complemented the Δ*lphD* strain with the full length *lphD* under the control of its native promotor, which led to a complete reversion of the defective phenotype (**Figure 2G**). The over expression of the gene, due to the plasmid copy number, even induced a clear increase in the replication of the mutant, further supporting the conclusion that LphD plays a role in virulence and intracellular replication.

LphD and RomA modify H3K14 in synergy

As previously reported, the secreted effector RomA is able to specifically target and methylate H3K14 (Rolando et al., 2013). We observed a clear decrease in H3K14 acetylation in presence of RomA, thus, we wondered if this was due to a genome wide H3K14me accumulation, or a specific and targeted deacetylase activity, possibly driven by the bacteria. Given the activity of LphD, we hypothesized that the two effectors act in synergy to manipulate the host transcriptional response. We first investigated the influence of LphD on the activity of RomA by analyzing the H3K14 methylation level of extracted histones from cells infected with the *ΔlphD* strain. Indeed, this showed that the absence of LphD significantly reduces the level of H3K14me already in the early stages of infection (1-3 hours) (**Figure 3A**). This strongly suggests that the two effectors act in synergy to modify the host chromatin landscape.

LphD and RomA hijack the HBO1 complex

To investigate the mechanism by which LphD and RomA target host chromatin, we sought to identify host complexes that the two bacterial effectors may interact with. To isolate potential targets of LphD, we performed affinity chromatography by GFP-trap pull down, followed by protein identification by mass spectrometry. Pull-down experiments of HEK293T cells transfected with an EGFP-LphD construct followed by MS/MS analysis identified a total of 687 significantly enriched proteins, compared to the control (EGFP) (**Figure 3B**). To identify candidate binding proteins with increased confidence, we set a threshold for proteins with at least two unique peptides detected and that displayed a significant (false discovery rate <0.1) >4-fold change compared to control condition (GFP). Interestingly, among the set of potential LphD binding proteins, many of the identified peptides were derived from proteins that are known to be involved in epigenetic regulation of the cell (**Table S1**). In particular, the histone acetyl transferase (HAT) KAT7 (HBO1) was one of the most promising candidates (**Figure 3B**). KAT7 is the enzymatic subunit of the so-called HBO1 complex, comprised of KAT7, BRPF1-3, ING4/5 and MEAF6. This complex is well-known to bind histone H3, regulating the acetylation of K14 (**Figure 3C**) (Xiao et al., 2021). To validate the interaction between LphD and KAT7, we performed co-immunoprecipitations (Co-IP) using GFP-trap to pull down EGFP-LphD (or EGFP) and blotted for the binding of endogenous KAT7. **Figure 3D** shows that EGFP-LphD indeed interacts with endogenous KAT7, compared to EGFP alone. Reverse immunoprecipitation also verified KAT7/LphD complex formation in transfected cells (**Figure S4A**). Importantly we observed that the binding of LphD to KAT7 is independent of its enzymatic activity, as the catalytically inactive LphD-Y392F still binds KAT7. Furthermore,

histone H3 is immunoprecipitated as well, confirming that the complex occurs at the chromatin level (**Figure 3D**, for IP control see **Figure S4B**). To determine if LphD targets the entire HBO1 complex and if RomA also participates in it, we performed co-IP of EGFP-LphD and EGFP-RomA and checked for the presence of the different components of the HBO1 complex (**Figure 3E**, for IP control see **Figure S4C**). We observed that LphD immunoprecipitates all components of the HBO1 complex (BRPF1, KAT7, MEAF6 and ING5), whereas RomA seems to preferentially bind ING5 and partially KAT7. Importantly, we could concomitantly show that RomA and LphD both bind the HBO1 complex, as well as the target histone H3.

To corroborate these interactions in the context of infection, we decided to use a previously established method, based on the infection of HEK293T cells that stably express the macrophage Fcγ-RII receptor (Arasaki and Roy, 2010). The expression of this receptor enables HEK293T cells to engulf bacteria that have been opsonized with antibodies, allowing an efficient infection of HEK293T cells in combination with high transfection efficiency. We transfected these cells with either EGFP or EGFP-KAT7 and infected them using *L. pneumophila* wild type strain overexpressing a tagged form (V5) of LphD or RomA. When pulling down the EGFP proteins we clearly detected an enrichment of both bacterial proteins in the EGFP-KAT7 sample (**Figure 3F**). This confirms that LphD and RomA target the same endogenous complex (HBO1) to specifically modify H3K14 during infection.

RNA-seq reveals dynamic changes during infection with contribution of nucleomodulins

Here we show that *L. pneumophila* secretes at least two effectors that target K14 of histone H3 to modify the host chromatin. In order to investigate how K14 remodeling changes the response of the cell to infection, we performed RNA-seq experiments. THP-1 cells were infected with either *L. pneumophila* wild type (WT), Δ*lphD*, Δ*romA* or the double knockout (Δ*lphD* Δ*romA*) and the transcriptional response was analyzed 1, 3, 5, and 7 hours post-infection compared to non-infected cells.

First, we evaluated the transcriptional response of the cell to the *L. pneumophila* infection as a function of time (**Figure 4A-4C**) by assessing the overall changes of differently expressed genes (DEGs) with an adjusted $p<0.05$ and a shrunken $\log_2$ fold change >2 or <-2. The variance between the different time points shows that changes are quite drastic 1 h and 3 h post-infection, compared to the control condition (non-infected). However, the later time points – 5 h and 7 h

post-infection – show a lower level of variance. independent of the bacterial strain (**Figure 4A**, **S5A, S5B, S5C**).

The dynamics of the expression changes were then explored by comparing the 100 most up- and down-regulated genes (independent of their fold-change) per time point and their overlaps between time points (**Figure 4B)**. Interestingly, for both up- and down-regulated genes, the genes that are unique for 1 h post-infection represent the biggest group (up: 56, down: 83), indicating that the expression changes very rapidly during the first hours of infection. However, after 1 h post-infection the two conditions show very different results. For the up-regulated genes we can see that almost half of the genes (47) are shared by 3 h, 5 h and 7 h post-infection and almost a quarter (24) are shared by all four time points. This suggests that the up-regulation of gene expression adapts quickly within the first three hours, leading to a core set of genes that is continuously up-regulated during the course of infection. In contrast, the down-regulation seems to be a more dynamic process with no clear pattern. Each time point has its own set of uniquely expressed genes, with very little overlap to the other time points, especially when compared to the pattern seen with the up-regulated genes (**Figure 4B**).

Analyses of functional changes by using gene ontology (GO) profiling (clusterProfiler (Yu et al., 2012)) of *L. pneumophila* wild-type infected cells, compared to uninfected cells, show a clear pattern within several ontology groups conserved between the four time points, which are all connected to the host cell response to infection (**Figure 4C**). GO groups such as "response to lipopolysaccharide", "cellular response to chemokines" and "positive regulation of defense response" are strongly conserved over the course of infection, highlighting their importance in host cell defense. Interestingly, 1 h post-infection we observed the highest number of unique GO-terms. One term that stands out is connected to promoting T cell differentiation, a probable first step of the immune response to an intracellular pathogen like *L. pneumophila*. Starting at 3 h post-infection we see GO groups associated with production and regulation of interferon-gamma, followed shortly by leukocyte migration starting at 5 h post-infection. Lastly, 7 h post-infection reveals the regulation of cytokine production, whereas early time points focused on the production and regulation of chemokines (**Figure 4C**). The down-regulated genes do not share this clear step-wise pattern seen with the up-regulated genes. For the early time points (1 h and 3 h) the program is not able to determine specifically enriched GO-terms. Very few enriched GO-terms are observed for 5 h and 7 h post-infection, but none of them are clearly

connected to the infection process. Especially 7 h post-infection focuses on sensory perception and pain, a quite unexpected topic (**Figure S5D**).

We then compared the transcriptional response of the cell of the *L. pneumophila* wild-type infection to the ones infected with the Δ*lphD*, Δ*romA* and Δ*lphD*Δ*romA* knockout strain. **Figure 4C** shows the number of DEGs identified at different points after infection, for both wild-type and mutant strains. Again, we observed that a very small number of DEGs was identified at 1h post-infection, whereas at 3 hours a sudden increase for all the studied strains can be seen (**Figure 4D**). By looking at the total number of genes up- or down-regulated in *L. pneumophila* wild-type infected cells, compared to mutants, we did not observe any significant changes; we therefore analyzed the functional changes by comparing the GO-term results of the mutants with the wild type infected cells (**Figure 4E**). This revealed no direct overlap of the GO-terms between the two single knockouts, however, they are part of the same immunological processes, but belonging to different steps. Furthermore, the double knockout shows a mixture of GO-term of the two single knockouts, indicating that the presence of the two effectors causes a cumulative effect on the transcriptional response of the cell.

To confirm these results, a subset of genes was chosen for validation by RT-qPCR. The choice of these genes was based on their high fold change in the RNA-seq of the different knockout mutants and their possible involvement in the immune response (ADAM19, CCR2 and AJUBA). Furthermore, recently a list of DEGs in KAT7 knockout mutants of HEK293T and HeLa cells was published (Kueh et al., 2020). We cross-referenced these lists with the results of our RNA-seq and chose three additional candidate genes for validation by RT-qPCR (CCL2, CLEC2D and TXNIP). **Figure 4F** shows that LphD and RomA can act together, as the double knockout exhibits a cumulative effect (in transcriptional repression or induction), compared to single mutants for ADAM19, CCL2, CCR2 and AJUBA. However, for TXNIP and CLEC2D the double knockout has an effect that can be recapitulated by a single mutant (Δ*lphD* for TXNIP and Δ*romA* for CLED2D). This strongly suggests that the two proteins can also work independently from each other.

DISCUSSION

We identified here a new secreted nucleomodulins of *L. pneumophila*, named LphD, that encodes histone deacetylase activity. Importantly, LphD shows a high catalytic efficiency for H3K14 *in vitro* and targets the host cell nucleus during infection. In the nucleus, it deacetylates H3K14, thereby facilitating the methylation of this residue by another bacterial effector, the SET-domain methyltransferase RomA. Nuclear targeting of LphD to the nucleus does not depend on its enzymatic activity, as a catalytic inactive mutant (Y392F) shows the same localization (**Figure S2C**). However, the processes by which LphD targets the nucleus remains to be determined, as the deletion of a nuclear localization signal (NLS) – predicted at the N-terminus of the protein – did not affect its translocation to the nucleus (data not shown).

In vitro activities on short H3 peptides acetylated on different lysine residues showed a clear preference of LphD for H3K14 (**Figure 1A**), however, we cannot exclude the possibility that LphD has other targets than H3K14. In particular, non-histone targets should not be dismissed as many eukaryotic HDACs have been shown to target non-histone proteins. For example the tumor protein p53 and the immune response regulator MyD88 (Ito et al., 2002; Menden et al., 2019). Considering that acetylation is a very prevalent post-translational modification of proteins (Philp et al., 2014), its manipulations would be as a promising target for a pathogen like *L. pneumophila* to influence its host cell. Moreover, it has been previously shown that RomA indeed methylates also non-histone proteins, although the functional role of these modification is not established yet (Schuhmacher et al., 2018).

Importantly, we showed that LphD and RomA modify the same cellular target in synergy during infection. Other *L. pneumophila* effectors have been described to target the same cellular component to subsequently manipulate it. One example is the host small GTPase Rab1, which is sequentially modified by at least three effectors (Rolando and Buchrieser, 2012). Furthermore, we revealed that LphD and RomA have a common target in the host cell, namely H3K14. Moreover, we showed that both bacterial effectors bind the same cellular complex, HBO1, to target host chromatin (**Figure 3**). Indeed, they both co-immunoprecipitate with KAT7, a component of the HBO1 complex, a known regulator of H3K14 acetylation.
Our pulldown results show that LphD interacts with all components of the HBO1 complex, including its target, histone H3. RomA on the other hands seems to preferentially bind only to KAT7, ING5 and H3 (**Figure 3E**). However, as mentioned before, the analysis of possible interaction partners led not only to the identification of HBO1 but also suggested interaction

with several other complexes related to chromatin remodeling. Some of which, like the NuRD- and the Sin3-complex, are known to comprise eukaryotic histone deacetylases and thus, might be additional interaction partners for LphD (Adams et al., 2018; Kelly and Cowley, 2013). Further studies will elucidate whether additional possible interaction partners of LphD and RomA exist.

Many pathogens are known to indirectly manipulate histone acetylation to subvert the host immune response and promote their survival (Eskandarian et al., 2013; Rennoll-Bankert et al., 2015; Wang et al., 2018b). The analysis of the activity of LphD and RomA – with respect to the transcriptional response of the host cell to the infection – by RNA-seq experiments revealed dynamic changes in the mRNA landscape of the host within the first few hours of infection, thus showing a rapid response to the bacterial intruders.

The enriched GO-terms for the *L. pneumophila* mutant strains do not show overlap between the two single knockout mutants, however, this is due to the definition of GO terms, where single genes that are present in both conditions might be attributed to different GO terms, depending on the rest of the genes in these conditions. We therefore used RT-qPCR to confirm the RNA-seq results by choosing several genes related to immune response processes, three of which (CCL2, CLEC2D, and TXNIP) are known to be differently expressed in KAT7 knockout cells (Kueh et al., 2020).

The expression levels of ADAM19, AJUBA, CCR2 and CCL2 are up-regulated in the different knockout mutants, indicating that LphD and RomA are responsible for their down-regulation.

ADAM19 is a metalloprotease and a known sheddase for TNF-α, responsible for its release from the cellular membrane into the extracellular space (Zheng et al., 2004). This shows that LphD and RomA might not only directly influence the infected cell, but also manipulate bystander cells. Furthermore, it was shown that ADAM19 regulates CCL2 production as well as macrophage infiltration in the kidney (Wang et al., 2021).

AJUBA, a LIM-domain containing protein, has been described as a key regulator of NF-κB activation by modulating the assembly of the Czeta/p62/TRAF6 signaling complex (Feng and Longmore, 2005). NF-κB activation is a key characteristic of *L. pneumophila* infection and is positively correlated with bacterial virulence (Wang et al., 2018a).

CCR2 and CCL2 are a chemokine receptor/ligand pair with a multitude of immune related functions. They have been shown to be essential in the recruitment of NK cells to viral infection sites as well as the attraction of myeloid progenitors to the lung in a flagellin-dependent manner

(Lei et al., 2021; Shou et al., 2019). In addition, CCR2 deficiency has been linked to increased susceptibility of mice to another intracellular pathogen, *Francisella tularensis* LVS (Kurtz et al., 2021).

On the other hand, CLEC2D and TXNIP show decreased expression in the different knockout mutants, indicating that LphD and RomA positively influence their expression, albeit indirectly. CLEC2D (C-type lectin domain family member D), also known as LLT1 (Lectin like transcript 1), is a surface ligand mainly expressed on activated immune cells (Germain et al., 2011). It is well established that the interaction of LLT1 with NKRP1A – a receptor expressed on NK cells – inhibits NK cell mediated cytotoxic effects (Rosen et al., 2008). This phenotype was mostly described on different types of cancer (Malaer and Mathew, 2020; Mathew et al., 2016), but might also play a major role in the clearance of an intracellular pathogen like *L. pneumophila*. Indeed, it has been shown that NK cell activation during *L. pneumophila* infection leads to increased IFN-γ production, which subsequently promotes bactericidal activity of monocyte-derived cells (Brown et al., 2016).

Finally, TXNIP (thioredoxin-interacting protein) is a key regulator of oxidative stress by inhibiting the activity of thioredoxin, a strong antioxidant (Nishiyama et al., 1999). Interestingly, TXNIP has been shown to be down-regulated during *Brucella abortus* infection and thereby promoting the intracellular survival of the bacteria (Hu et al., 2020). In addition, TXNIP has been linked to phagosome acidification during infection with *Escherichia coli* in an NLRP3-dependent manner (Yoon et al., 2019). This is different to what observed, as the knockout strains actually showed lower expression of TXNIP, indicating that the two effectors promote its upregulation. However, it has also been shown that in NK cells, TXNIP blocks IFN-γ production during bacterial infection in a TAK-1 (transforming growth factor b-activated kinase 1)-dependent manner (Kim et al., 2020). It has been demonstrated that the production of IFN-γ by NK cells plays a key role in *L. pneumophila* clearance in a mouse model (Spörri et al., 2006). Interestingly, the Δ*romA* strain shows a stronger change in TXNIP expression than the Δ*lphD* and the Δ*lphD*Δ*romA* strain, indicating that the *lphD* knockout somehow hides the Δ*romA* phenotype. These results suggest that LphD and RomA not only directly influence the reaction of the infected cell, but can also manipulate the response of bystander cells.

In conclusion, this study provides exciting insight on how *L. pneumophila* modifies host chromatin by using two distinct chromatin remodelers. Both, LphD and RomA, are deployed by the bacteria to strategically influence the response of the host cell to the infection and promote bacterial replication in this otherwise hostile environment.

METHODS

Bacterial strains, growth conditions and cell culture

Legionella pneumophila strain Paris and mutants were cultured in N-(2-acetamido)-2-aminoethanesulfonic acid (ACES)-buffered yeast extract broth (BYE) or on ACES-buffered charcoal-yeast (BCYE) extract agar (Feeley et al., 1979). For *Escherichia coli* Luria-Bertani broth (LB) was used. When needed antibiotics were added: for *L. pneumophila* (*E. coli*): kanamycin 12.5 µg/ml (50 µg/ml), gentamycin 12.5 µg/ml, apramycin 15 µg/ml, chloramphenicol 10 µg/ml (10 µg/ml), and ampicillin (only for E. coli) 100 µg/ml.

The knockout of *lphD* in the wild type background to generate a single mutant followed by the knockout of *romA* to generate the double mutant, was performed as previously described (Sahr et al., 2012) and detailed in **Supp. Methods**. For the complementation construction, the full-length *lphD* with its own promotor was cloned into pBC-KS (Stratagene). Bacteria expressing EGFP were obtained by introducing EGFP under the control of the *flaA* promotor of *L. pneumophila* into pBC-KS backbone. To generate the catalytic inactive Y392F mutant of LphD, a single base pair mutation was performed using mismatched primers (217H and 217B, **Table S2**).

THP-1 cells were maintained in RPMI-1640 (Gibco), HeLa and HEK293T in DMEM GlutaMAX (Gibco), both containing 10% FBS (Eurobio Scientific) in a humid environment with 5% CO_2 at 37°C. *Acanthamoeba castellanii* (ATCC50738) were maintained in PYG 712 medium at 20°C. For the virulence replication assays, THP- and *A. castellanii* were infected as previously described (Lomma et al., 2010) and detailed in **Supp. Methods**. Cell transfections were performed by using FuGENE (Promega) following the recommendations of the manufacturer.

β-lactamase translocation assay and immunofluorescence analysis

β-lactamase assays were performed in THP1 infected cells as previously described (Charpentier et al., 2009) and as detailed in **Supp Methods**. For immunofluorescence analyses, cells are fixed with 4% para-formaldehyde in PBS for 15 minutes at room temperature, followed by quenching (PBS-50 mM NH_4Cl for 10 minutes). Cells are permeabilized with 0.1% Triton X-100 and blocked for 30 minutes with 5% BSA in PBS. The cells are incubated with the respective primary antibodies overnight at 4°C. They are washed three times using PBS and then stained with DAPI and secondary antibodies for 30 minutes at room temperature, followed by mounting to glass slides using Mowiol (SIGMA). Immunosignals were analyzed with a

457 Leica SP8 Microscope at 63× magnification. Images were processed using ImageJ software.
458 Antibodies used in this study are listed in **Table S3**.
459
460 **LphD purification**
461 N-terminal HIS_6-tagged LphD was expressed in *E. coli* BL21 C41 following an auto-induction
462 protocol (Studier, 2005). After 4 hours at 37°C cells were grown for 20 hours at 20°C in 2YT
463 complemented autoinduction medium containing 50 μg/ml kanamycin. Cells were harvested
464 and flash frozen in liquid nitrogen. Cell pellets were resuspended in 50ml lysis buffer (50 mM
465 HEPES pH8, 500 mM KCl, 5% glycerol, 1 mM $MgCl_2$, benzonase, lysozyme, 1 mM DTT and
466 supplemented with EDTA-free protease inhibitor cocktails (ROCHE)) at 4°C and disrupted by
467 sonication (6 x 60 seconds). The lysate was centrifuged for 60 min at 10.000 x g at 4°C. The
468 cleared lysate was loaded onto a Ni-NTA affinity chromatography column (HisTrap FF crude,
469 GE Healthcare) equilibrated in Buffer A (50 mM Hepes pH8, 500 mM KCl, 5% glycerol, 10
470 mM imidazole, 1 mM DTT). HIS_6-tagged proteins were eluted with a linear gradient of buffer
471 B (50 mM Hepes pH8, 500 mM KCl, 5% glycerol, 1 M imidazole, 1 mM DTT). The eluted
472 fractions containing the protein of interest were pooled and dialysed at 4°C overnight in SEC
473 buffer (20 mM HEPES pH8, 300 mM KCl, 5% glycerol, 2 mM TCEP). The HIS_6-tag was not
474 removed as this led to precipitation of the protein. After dialysis, the protein was concentrated
475 and loaded onto a Superdex 75 16/60 size exclusion (SEC) column (GE Healthcare). The peak
476 corresponding to the protein was concentrated to about 12 mg/ml and flash frozen in liquid
477 nitrogen and stored at -80°C.
478
479 ***In vitro* enzymatic assays**
480 Purified HIS_6-LphD was used to perform *in vitro* enzymatic assays against FAM-conjugated
481 H3-derived acetylated peptides, followed by RP-UFLC (see **Supp Methods**) or with Fluor de
482 Lys® deacetylase assay (Enzo Life Sciences). Briefly, different amount of purified LphD and
483 catalytically dead LphD Y392F were incubated with the substrate for 30 minutes at 37°C and
484 the signal was read using a plate reader (TECAN). Trichostatin-A (TSA) was added at 5 μM.
485 The kinetic parameters of LphD on H3-derived peptides were determined by UFL in a 96-wells
486 ELISA. Briefly, LphD (7.7 nM) was mixed with different concentrations of acetylated H3
487 peptides (ranging from 12.5 to 200 μM final) for 15 minutes at 30°C and the reaction was
488 stopped by adding 50 μL of $HClO_4$ (15% v/v in water). Finally, 10 μl of the reaction mix were
489 automatically injected into the RP-UFLC column and initial velocities (V_i, $\mu M.min^{-1}$) were
490 determined as described above. V_i were then plotted against substrate peptide concentrations

and curves were non-linearly fitted using Michaelis–Menten equation $\frac{V_m*[S]}{K_m+[S]}$ (OriginPro 8.0). K_m (enzyme Michaelis's constant), V_m (enzyme maximal initial velocity) and k_{cat} (enzyme turnover) values were extrapolated from these fits. A catalytic dead version of the enzyme was used as a negative deacetylation control (Duval et al., 2015).

In vitro histone deacetylating assays were performed on 250 ng of highly-acetylated purified histones (extracted as described in **Supp Methods**) and 10 ng LphD (WT or catalytic dead) in LphD purification buffer at 30°C. At different time points (0, 1, 2, 3, 4 and 5 minutes), the reaction was stopped with the addition of 10 μL Laemmli sample buffer. Samples were analyzed by western blot and the α-H3K14ac signal quantified.

Histone modification analysis

For the analysis of histone modifications during infection, THP-1 cells in suspension were infected with *Legionella pneumophila* wild type and a Δ*lphD* strain, both containing a plasmid for the expression of EGFP under the control of the *flaA* promotor at an MOI of 50. After 30 minutes, Gentamicin is added (100 μg/ml) to kill extracellular bacteria. Cells are then sorted by FACS (S3e, BIORAD) as previously described (Rolando and Buchrieser, 2019). Histones of infected cells were isolated as previously described with some modifications (Luense et al., 2016). Briefly, THP-1 cells ($3x10^6$) were incubated at 4°C with hypotonic lysis buffer (10 mM Tris–HCl pH 8.0, 1 mM KCl, 1.5 mM $MgCl_2$, with protease inhibitors) for two hours while rotating. Subsequently, nuclei were pelleted and resuspended in 0.4 M sulfuric acid - incubate overnight at 4°C. The supernatant was precipitated with 33% trichloroacetic acid (TCA) on ice. Pelleted histones were washed twice with ice-cold acetone and were then resuspended in DNase/RNase free water. Sample quality of acid extraction was visualized on a Coomassie-stained 12% SDS-PAGE. Histone modification signal (H3K14ac, H3K14me, H3K18ac, H3K23ac) is assessed by western blot and normalized to signal of histone H1. Samples are then compared to non-infected controls.

Co-immunoprecipitation experiments

For the GFP-pulldown HEK293T cells were seeded in 10 cm dishes and transfected 24 or 48 hours with 3 μg of the different EGFP construct expression plasmids. Transfected cells were washed three times with PBS before lysis in RIPA buffer (20 mM HEPES-HCl pH 7.4, 150 mM NaCl, 5 mM EDTA, 1% Triton X-100, 0.1% SDS, 1% Na-deoxycholate). For the verification of protein interaction during infection we modified the previously established protocol by Arasaki et al. (Arasaki and Roy, 2010). Briefly, we transiently transfected HEK293-

FcγRII cells with either EGFP or a EGFP-KAT7 fusion product. After 48 hours of transfection, the cells were washed and fresh DMEM with IPTG (1 mM) was added. The bacteria – *L. pneumophila* over-expressing either V5-LphD or V5-RomA – are pre-opsonized by incubating them with an anti-FlaA antibody for 30 minutes at 37°C. Then the cells are infected with MOI 50. After one hour, the cells are washed and fresh DMEM (with 1 mM IPTG) is added. After 7 hours of infection, the cells are collected and lysed in RIPA buffer.

To facilitate the lysis, cells were sonicated using a Bioruptor® Pico sonication device (Diagenode) for 15 cycles of 30 seconds ON/OFF. Lysates were precleared and the pulldown was performed using GFP-trap magnetic agarose beads (Chromotek) following the manufacturer's instructions at 4°C overnight. Proteins were eluted in 30 µl Laemmli buffer and then analyzed by western blot or the beads directly processed for MS/MS analyses (see **Supp Methods**).

Western blotting

Sample proteins are prepared in Laemmli sample buffer containing 400 mM β-mercaptoethanol and loaded on SDS PAGE gels, followed by a transfer onto a nitrocellulose membrane (0.2 µm). Ponceau S staining was carried out to ensure equal protein loading. Membranes were blocked with 5% non-fat milk in TBS-Tween 0.5% for 1 hour and incubated with the respective primary antibody overnight at 4°C. Antibodies used are listed in **Table S3**. Membranes are washed and probed with horseradish peroxidase-coupled antibody against either mouse IgG or rabbit IgG (1:2500 in 5% non-fat milk TBS-Tween) for 1 hour. The proteins were then visualized by chemiluminescence detection using HRP Substrate spray reagent (Advansta) on the G:BOX instrument (Syngene). Images were processed and quantified using MultiGauge V3.0 and ImageJ softwares.

RNA-sequencing, GO-term analyses and RT-qPCR

For the RNA-seq and RT-qPCR, THP-1 monocytes were infected with either *L. pneumophila* wild type, Δ*lphD*, Δ*romA* or Δ*lphD*-Δ*romA*, all of which were expressing EGFP. After 1 h, 3 h, 5 h, and 7 h post-infection, the infected cells were enriched by FACS and stored at -80°C. RNA-seq and data analysis was performed by Active Motif. In short, total RNA was isolated from samples using the Qiagen RNeasy Mini Kit (Qiagen). For each sample, 1 µg of total RNA was then used in the TruSeq Stranded mRNA Library kit (Illumina). Libraries were sequenced on Illumina NextSeq 500 as paired-end 42-nt reads. Sequence reads were analyzed with the STAR alignment – DESeq2 software pipeline. Genes that were differently regulated in the RNA-seq

were analyzed for possible GO term groups using the clusterProfiler package in R (Yu et al., 2012). The function *compareCluster* with its standard setting was used to assess enriched biological processes within those differently regulated genes under the different experimental conditions. To remove possible redundant GO terms, the *simplify* function was used, again with standard settings. The resulting lists were visualized in dot plots or upset plots, also using R (Lex et al., 2014). For the RT-qPCR the RNA was isolated using the Arcturus® PicoPure® RNA isolation kit (Thermo Fisher Scientific). RT-PCR was performed using 2.5 μg of RNA. qPCR primers (**Table S2**) were designed to span an exon-exon junction to minimize amplification of genomic DNA. qPCR was performed using SYBR-Green Master Mix (Thermo Fisher Scientific) and mRNA expression was calculated using the $2^{-\Delta\Delta Ct}$ method(Livak and Schmittgen, 2001). Results were normalized to human GAPDH, ACTB and 36B4.

SUPPLEMENTAL METHODS

Mutant and Complementation Constructions

To construct the Δ*lphD* mutant strain the chromosomal gene *lphD* of the wild-type strain was replaced by introducing a gentamycin (GenR) resistance cassette. The mutant allele was constructed using a 3-steps PCR. Briefly, three overlapping fragments (*lphD* upstream region- primers 195H and 196H, antibiotic cassette-primers 52H and 52B, *lphD* downstream region- primers 195B and 196B; **Table S2**) were amplified independently and purified on agarose gels. The three resulting PCR products were mixed at the same molar concentration (15nM) and a second PCR with flanking primer pairs (primers 195H and 195B; **Table S2**) was performed. The resulting PCR product, the gentamycin resistance cassette flanked by 500 bp regions homologous to *lphD* was introduced into strain *L. pneumophila* Paris by natural competence for chromosomal recombination. Strains that had undergone allelic exchange were selected by plating on BCYE containing gentamycin and the mutant was verified by PCR and sequencing. To resulting mutant was then used to generate the Δ*lphD* Δ*romA* double knockout strain, using a new set of primers (*romA* upstream region- primers 11H and 66H, kanamycin antibiotic resistance cassette-primers 60H and 60B, *romA* downstream region- primers 11B and 66B; **Table S2**).

Cell Culture and Infection Assay

Acanthamoeba castellanii ATCC50739 was cultured at 20°C in PYG 712 medium [2% proteose peptone, 0.1% yeast extract, 0.1 M glucose, 4 mM $MgSO_4$, 0.4 M $CaCl_2$, 0.1% sodium citrate dihydrate, 0.05 mM $Fe(NH_4)_2(SO_4)_2 \bullet 6H_2O$, 2.5 mM NaH_2PO_3, 2.5 mM K_2HPO_3]. *A. castellanii* were washed once with infection buffer (PYG 712 medium without proteose peptone, glucose and yeast extract) and seeded at a concentration of $4x10^6$ cells per T25 flask. *L. pneumophila* wild-type and mutant strains were grown on BCYE agar to stationary phase, diluted in infection buffer and mixed with *A. castellanii* at an MOI of 0.1. Intracellular multiplication was monitored plating a sample at different time points on BCYE plates and the number of intracellular bacteria was counted. The human monocyte (THP-1) were maintained in 5% CO_2 at 37°C in RPMI 1640 medium GlutaMAX medium (Invitrogen) supplemented with 10% fetal bovine serum (Biowest). In THP-1 cell infection assays cells were seeded into 12-well tissue culture trays (Falcon, BD lab ware) at a density of $2x10^5$ cells/well. THP-1 cells were pretreated with 0.8 μM phorbol 12-myristate 13-acetate (PMA, Sigma) for 72 h to induce differentiation into macrophage-like adherent cells. Stationary phase *L. pneumphila* were resuspended in serum free medium and added to cells at an MOI of 10. After 2 hours of

incubation, infected cells were washed with PBS before incubation with serum-free medium. At 2 h, 24 h, 48 h and 72 hours the supernatant was collected and the cells were lysed with 0.1% TritonX-100. The infection efficiency was monitored by determining the number of colony-forming units (cfu) of the different *L. pneumophila* strains after plating on BCYE agar.

β-lactamase translocation assays

Around 1×10^5 THP-1 cells are seeded in a 96-well plate and differentiated for 72 hours using 10 nM phorbol 12-myristate 13-acetate (PMA). One day before infection *Legionella pneumophila* wild type carrying responding plasmids for the expression of either β-lactamase alone or a β-lactamase LphD fusion are cultured in BYE broth containing chloramphenicol and IPTG to induce protein production. After differentiation the cells are washed and fresh RPMI medium with IPTG (1 mM) is added. Cells are infected with the β-lactamase fusion protein expressing bacteria at an MOI of 50. Spin the plates for 5 minutes at 300 g and then incubate the plate for 2 hours at 37°C in a humidified 5% CO_2 atmosphere. After this incubation, LiveBLAzer CCF4-AM solution (Thermo Fisher Scientific) is added to all the wells and the plate is incubated in the dark at room temperature for 2 hours. The cells are washed and cell dissociation solution (SIGMA) is added. After another incubation of 30 minutes at 37°C with 5% CO_2 the samples are analyzed by flow cytometry (MACS Quant, Miltenyi Biotec). Non-infected cells are used as negative control.

UFLC-mediated LphD deacetylase activity assay

In order to quantify LphD deacetylase activity, we synthetized six 5-fluorescein amidite (5-FAM)-conjugated acetylated peptide substrates based on the human H3.1 sequence and centered on various lysine residues of interest:

ARTK_{ac}QTARRSK-(5-FAM), referred to as H3K4ac peptide

(5-FAM)-QTARK_{ac}STGG-NH_2, referred to as H3K9ac peptide

(5-FAM)-STGGK_{ac}APRR-NH_2, referred to as H3K14ac peptide

(5-FAM)-RAPRK_{ac}QLAT-NH_2, referred to as H3K18ac peptide

(5-FAM)-QLATK_{ac}AARR-NH_2, referred to as H3K23ac peptide

(5-FAM)-TRAARK_{ac}SAPAT-NH_2, referred to as H3K27ac peptide

Non-acetylated versions of these peptides were also synthetized as detection standards.

Samples containing H3 peptides and their acetylated forms were separated by RP-UFLC (Shimadzu) using Shim-pack XR-ODS column 2.0 x 100 mm 12 nm pores at 40°C. The mobile phase used for the separation consisted of the mix of 2 solvents: A was water with 0.12%

trifluoroacetic acid (TFA) and B was acetonitrile with 0.12% TFA. Separation was performed by an isocratic flow depending on the peptide:

- → 83 % A/17 % B, rate of 1 ml/min, 6 min run for H3K4ac peptide
- → 80 % A/20 % B, rate of 1 ml/min, 6 min run for H3K9ac, H3K14ac, H3K18ac, H3K27ac peptides
- → 79 % A/21 % B, rate of 1 ml/min, 8 min run for H3K23ac peptide

H3 acetylated peptides (substrates) and their non-acetylated forms (products) were monitored by fluorescence emission (λ = 530 nm) after excitation at λ = 485 nm and quantified by integration of the peak absorbance area, employing a calibration curve established with various known concentrations of peptides.

Highly-acetylated histone extraction

HEK293T cells were cultivated in RPMI 1640 medium with 10 % heat-inactivated fetal bovine serum (FBS) and 1 mM L-glutamine at 37°C under 5 % CO_2. For endogenous histone extraction, cells were seeded at 30 000 cells/cm² in a 100 cm² Petri dish (VWR). The next day, cells were treated with 20 mM sodium butyrate and 6 μM Trichostatin A (TSA). Cells were then put back in the incubator at 37°C and 5 % CO_2 for 30 min before being harvested. Cells were lysed with cell lysis buffer (PBS 1x, 1% Triton X-100, 20 mM sodium butyrate, 6 μM TSA, protease inhibitors) for 30 min at 4°C, sonicated (2 sec, 10 % power) and centrifuged (15 min, 15500 g, 4°C). 500 μL of 0.2 N HCl was then put on remaining pellets. The mixture was sonicated 3 times (3 sec, 10 % power) and incubated overnight at 4°C. The next day, samples were centrifuged (15 min, 15500 g, 4°C) and the supernatant (containing extracted histones) was buffer exchanged three times into Tris 50 mM, 50 mM NaCl, pH 8 using MiniTrap G-25 desalting columns (GE Healthcare) and stored with protease inhibitor at -20°C until use.

Mass spectrometry analysis of GFP co-IP

MS grade Acetonitrile (ACN), MS grade H_2O and MS grade formic acid (FA) was acquired from Thermo Chemical.

Proteins on magnetic beads were digested overnight at 37°C with 1μl (0.2 μg/μL) of trypsin (Promega) in a 25-mM NH_4HCO_3 buffer per sample. The resulting peptides were desalted using ZipTip µ-C18 Pipette Tips (Pierce Biotechnology).

Samples were analyzed using an Orbitrap Fusion equipped with an easy spray ion source and coupled to a nano-LC Proxeon 1200 (Thermo Fisher Scientific). Peptides were loaded with an online preconcentration method and separated by chromatography using a Pepmap-RSLC C18

column (0.75 x 750 mm, 2 µm, 100 Å) from Thermo Fisher Scientific, equilibrated at 50°C and operating at a flow rate of 300 nl/min. Peptides were eluted by a gradient of solvent A (H_2O, 0.1 % FA) and solvent B (ACN/H_2O 80/20, 0.1% FA), the column was first equilibrated 5 min with 95 % of A, then B was raised to 28 % in 105 min and to 40% in 15 min. Finally, the column was washed with 95% B during 20 min and re-equilibrated at 95% A during 10 min. Peptide masses were analyzed in the Orbitrap cell in full ion scan mode, at a resolution of 120,000, a mass range of *m/z* 350-1550 and an AGC target of 4.10^5. MS/MS were performed in the top speed 3s mode. Peptides were selected for fragmentation by Higher-energy C-trap Dissociation (HCD) with a Normalized Collisional Energy of 27% and a dynamic exclusion of 60 seconds. Fragment masses were measured in an Ion trap in the rapid mode, with and an AGC target of $1x10^4$. Monocharged peptides and unassigned charge states were excluded from the MS/MS acquisition. The maximum ion accumulation times were set to 100 ms for MS and 35 ms for MS/MS acquisitions, respectively.

Label-free quantification was done on Progenesis QI for Proteomics (Waters) in Hi-3 mode for protein abundance calculation. MGF peak files from Progenesis were processed by Proteome Discoverer 2.4 with the Sequest search engine. A custom database was created using the Swissprot/TrEMBL protein database release 2019_08 with the *Homo sapiens* taxonomy and including LphD, both from the *Legionella pneumophila* taxonomy. A maximum of 2 missed cleavages was authorized. Precursor and fragment mass tolerances were set to respectively 7 ppm and 0.5 Da. Spectra were filtered using a 1% FDR using the percolator node.

Production of anti-LphD antibodies in rabbit

Rabbit polyclonal antibodies to LphD where generated for this study (Thermo Fisher). Briefly, the purified HIS_6-LphD was injected in a rabbit for a protocol of 90 days. The produced antibody was qualitatively evaluated by affinity purified ELISA: the purified antibody is tittered by indirect ELISA against the protein bound to the solid-phase to measure the reactivity of the antibodies after elution.

ACKNOWLEDGMENTS

Work in the CB laboratory is financed by the Institut Pasteur, the *Fondation pour la Recherche Médicale* (FRM) grant N° EQU201903007847 and the *Agence Nationale de la Recherche* grant n°ANR-10-LABX-62-IBEID to CB and grant n° ANR-18-CE15-0005-. DS was funded by a Sorbonne University doctoral contract. We thank Jacques Monod Institute, the UMR 7592 Paris University/CNRS and the region Île-de-France for support. We also thank the group of Craig Roy for providing the HEK293-FcγRII cells.

REFERENCES

Adams, G.E., Chandru, A., and Cowley, S.M. (2018). Co-repressor, co-activator and general transcription factor: the many faces of the Sin3 histone deacetylase (HDAC) complex. Biochem. J. *475*, 3921–3932.

Allfrey, V.G., Faulkner, R., and Mirsky, A.E. (1964). ACETYLATION AND METHYLATION OF HISTONES AND THEIR POSSIBLE ROLE IN THE REGULATION OF RNA SYNTHESIS. Proc. Natl. Acad. Sci. U. S. A. *51*, 786–794.

An, R., Tang, Y., Chen, L., Cai, H., Lai, D.-H., Liu, K., Wan, L., Gong, L., Yu, L., Luo, Q., et al. (2018). Encephalitis is mediated by ROP18 of *Toxoplasma gondii* , a severe pathogen in AIDS patients. Proc. Natl. Acad. Sci. *115*, E5344–E5352.

Arasaki, K., and Roy, C.R. (2010). Legionella pneumophila Promotes Functional Interactions between Plasma Membrane Syntaxins and Sec22b. Traffic *11*, 587–600.

Bierne, H., and Pourpre, R. (2020). Bacterial Factors Targeting the Nucleus: The Growing Family of Nucleomodulins. Toxins (Basel). *12*.

Brown, A.S., Yang, C., Fung, K.Y., Bachem, A., Bourges, D., Bedoui, S., Hartland, E.L., and van Driel, I.R. (2016). Cooperation between Monocyte-Derived Cells and Lymphoid Cells in the Acute Response to a Bacterial Lung Pathogen. PLoS Pathog. *12*, e1005691.

Burstein, D., Amaro, F., Zusman, T., Lifshitz, Z., Cohen, O., Gilbert, J.A., Pupko, T., Shuman, H.A., and Segal, G. (2016). Genomic analysis of 38 Legionella species identifies large and diverse effector repertoires. Nat. Genet. *48*, 167–175.

Cazalet, C., Rusniok, C., Brüggemann, H., Zidane, N., Magnier, A., Ma, L., Tichit, M., Jarraud, S., Bouchier, C., Vandenesch, F., et al. (2004). Evidence in the Legionella pneumophila genome for exploitation of host cell functions and high genome plasticity. Nat. Genet. *36*, 1165–1173.

Charpentier, X., Gabay, J.E., Reyes, M., Zhu, J.W., Weiss, A., and Shuman, H.A. (2009). Chemical genetics reveals bacterial and host cell functions critical for type IV effector translocation by Legionella pneumophila. PLoS Pathog. *5*, e1000501.

Cosgrove, M.S., Boeke, J.D., and Wolberger, C. (2004). Regulated nucleosome mobility and the histone code. Nat. Struct. Mol. Biol. *11*, 1037–1043.

Cui, L., Jiang, X., Zhang, C., Li, D., Yu, S., Wan, F., Ma, Y., Guo, W., and Shan, Z. (2019). Ketamine induces endoplasmic reticulum stress in rats and SV-HUC-1 human uroepithelial cells by activating NLRP3/TXNIP aix. Biosci. Rep. *39*.

Duval, R., Fritsch, L., Bui, L.-C., Berthelet, J., Guidez, F., Mathieu, C., Dupret, J.-M., Chomienne, C., Ait-Si-Ali, S., and Rodrigues-Lima, F. (2015). An acetyltransferase assay for CREB-binding protein based on reverse phase–ultra-fast liquid chromatography of fluorescent histone H3 peptides. Anal. Biochem. *486*, 35–37.

Ensminger, A.W. (2016). Legionella pneumophila, armed to the hilt: justifying the largest arsenal of effectors in the bacterial world. Curr. Opin. Microbiol. *29*, 74–80.

Eskandarian, H.A., Impens, F., Nahori, M.-A., Soubigou, G., Coppee, J.-Y., Cossart, P., and Hamon, M.A. (2013). A Role for SIRT2-Dependent Histone H3K18 Deacetylation in Bacterial Infection. Science (80-.). *341*, 1238858–1238858.

Feeley, J.C., Gibson, R.J., Gorman, G.W., Langford, N.C., Rasheed, J.K., Mackel, D.C., and Baine, W.B. (1979). Charcoal-yeast extract agar: primary isolation medium for Legionella pneumophila. J. Clin. Microbiol. *10*, 437–441.

de Felipe, K.S., Pampou, S., Jovanovic, O.S., Pericone, C.D., Ye, S.F., Kalachikov, S., and Shuman, H.A. (2005). Evidence for Acquisition of Legionella Type IV Secretion Substrates via Interdomain Horizontal Gene Transfer. J. Bacteriol. *187*, 7716–7726.

Feng, Y., and Longmore, G.D. (2005). The LIM protein Ajuba influences interleukin-1-induced NF-kappaB activation by affecting the assembly and activity of the protein kinase Czeta/p62/TRAF6 signaling complex. Mol. Cell. Biol. *25*, 4010–4022.

Galvin, H.D., and Husain, M. (2019). Influenza A virus-induced host caspase and viral PA-X antagonise the antiviral host factor, histone deacetylase 4. J. Biol. Chem.

Ganesan, R., Hos, N.J., Gutierrez, S., Fischer, J., Stepek, J.M., Daglidu, E., Krönke, M., and Robinson, N. (2017).

Salmonella Typhimurium disrupts Sirt1/AMPK checkpoint control of mTOR to impair autophagy. PLoS Pathog. *13*, e1006227.

Germain, C., Meier, A., Jensen, T., Knapnougel, P., Poupon, G., Lazzari, A., Neisig, A., Håkansson, K., Dong, T., Wagtmann, N., et al. (2011). Induction of lectin-like transcript 1 (LLT1) protein cell surface expression by pathogens and interferon-γ contributes to modulate immune responses. J. Biol. Chem. *286*, 37964–37975.

Gomez-Valero, L., Rusniok, C., Carson, D., Mondino, S., Pérez-Cobas, A.E., Rolando, M., Pasricha, S., Reuter, S., Demirtas, J., Crumbach, J., et al. (2019). More than 18,000 effectors in the Legionella genus genome provide multiple, independent combinations for replication in human cells. Proc. Natl. Acad. Sci. U. S. A. *116*, 2265–2273.

Hu, H., Tian, M., Li, P., Guan, X., Lian, Z., Yin, Y., Shi, W., Ding, C., and Yu, S. (2020). Brucella Infection Regulates Thioredoxin-Interacting Protein Expression to Facilitate Intracellular Survival by Reducing the Production of Nitric Oxide and Reactive Oxygen Species. J. Immunol. *204*, 632–643.

Ito, A., Kawaguchi, Y., Lai, C.-H., Kovacs, J.J., Higashimoto, Y., Appella, E., and Yao, T.-P. (2002). MDM2-HDAC1-mediated deacetylation of p53 is required for its degradation. EMBO J. *21*, 6236–6245.

Karmodiya, K., Krebs, A.R., Oulad-Abdelghani, M., Kimura, H., and Tora, L. (2012). H3K9 and H3K14 acetylation co-occur at many gene regulatory elements, while H3K14ac marks a subset of inactive inducible promoters in mouse embryonic stem cells. BMC Genomics *13*, 424.

Kelly, R.D.W., and Cowley, S.M. (2013). The physiological roles of histone deacetylase (HDAC) 1 and 2: complex co-stars with multiple leading parts. Biochem. Soc. Trans. *41*, 741–749.

Kim, D.O., Byun, J.-E., Kim, W.S., Kim, M.J., Choi, J.H., Kim, H., Choi, E., Kim, T.-D., Yoon, S.R., Noh, J.-Y., et al. (2020). TXNIP Regulates Natural Killer Cell-Mediated Innate Immunity by Inhibiting IFN-γ Production during Bacterial Infection. Int. J. Mol. Sci. *21*.

Kimura, H. (2013). Histone modifications for human epigenome analysis. J. Hum. Genet. *58*, 439–445.

Kouzarides, T. (2007). Chromatin Modifications and Their Function. Cell *128*, 693–705.

Kueh, A.J., Eccles, S., Tang, L., Garnham, A.L., May, R.E., Herold, M.J., Smyth, G.K., Voss, A.K., and Thomas, T. (2020). HBO1 (KAT7) Does Not Have an Essential Role in Cell Proliferation, DNA Replication, or Histone 4 Acetylation in Human Cells. Mol. Cell. Biol. *40*.

Kurtz, S.L., De Pascalis, R., Meierovics, A.I., and Elkins, K.L. (2021). Deficiency in CCR2 increases susceptibility of mice to infection with an intracellular pathogen, Francisella tularensis LVS, but does not impair development of protective immunity. PLoS One *16*, e0249142.

Lei, X., Palomero, J., de Rink, I., de Wit, T., van Baalen, M., Xiao, Y., and Borst, J. (2021). Flagellin/TLR5 Stimulate Myeloid Progenitors to Enter Lung Tissue and to Locally Differentiate Into Macrophages. Front. Immunol. *12*, 621665.

Lex, A., Gehlenborg, N., Strobelt, H., Vuillemot, R., and Pfister, H. (2014). UpSet: Visualization of Intersecting Sets. IEEE Trans. Vis. Comput. Graph. *20*, 1983–1992.

Livak, K.J., and Schmittgen, T.D. (2001). Analysis of Relative Gene Expression Data Using Real-Time Quantitative PCR and the 2−ΔΔCT Method. Methods *25*, 402–408.

Lomma, M., Dervins-Ravault, D., Rolando, M., Nora, T., Newton, H.J., Sansom, F.M., Sahr, T., Gomez-Valero, L., Jules, M., Hartland, E.L., et al. (2010). The Legionella pneumophila F-box protein Lpp2082 (AnkB) modulates ubiquitination of the host protein parvin B and promotes intracellular replication. Cell. Microbiol. *12*, 1272–1291.

Luense, L.J., Wang, X., Schon, S.B., Weller, A.H., Lin Shiao, E., Bryant, J.M., Bartolomei, M.S., Coutifaris, C., Garcia, B.A., and Berger, S.L. (2016). Comprehensive analysis of histone post-translational modifications in mouse and human male germ cells. Epigenetics Chromatin *9*, 24.

Malaer, J.D., and Mathew, P.A. (2020). Role of LLT1 and PCNA as Natural Killer Cell Immune Evasion Strategies of HCT 116 Cells. Anticancer Res. *40*, 6613–6621.

Mathew, S.O., Chaudhary, P., Powers, S.B., Vishwanatha, J.K., and Mathew, P.A. (2016). Overexpression of LLT1 (OCIL, CLEC2D) on prostate cancer cells inhibits NK cell-mediated killing through LLT1-NKRP1A (CD161) interaction. Oncotarget *7*, 68650–68661.

Mathis, D.J., Oudet, P., Wasylyk, B., and Chambon, P. (1978). Effect of histone acetylation on structure and in vitro transcription of chromatin. Nucleic Acids Res. *5*, 3523–3547.

Menden, H., Xia, S., Mabry, S.M., Noel-MacDonnell, J., Rajasingh, J., Ye, S.Q., and Sampath, V. (2019). Histone deacetylase 6 regulates endothelial MyD88-dependent canonical TLR signaling, lung inflammation, and alveolar remodeling in the developing lung. Am. J. Physiol. Cell. Mol. Physiol. *317*, L332–L346.

Mondino, S., Schmidt, S., Rolando, M., Escoll, P., Gomez-Valero, L., and Buchrieser, C. (2020a). Legionnaires' Disease: State of the Art Knowledge of Pathogenesis Mechanisms of Legionella. Annu. Rev. Pathol. *15*, 439–466.

Mondino, S., Schmidt, S., and Buchrieser, C. (2020b). Molecular Mimicry: a Paradigm of Host-Microbe Coevolution Illustrated by Legionella. MBio *11*.

Murray, K. (1964). The Occurrence of iε-N-Methyl Lysine in Histones. Biochemistry *3*, 10–15.

Neves-Costa, A., and Moita, L.F. (2013). TET1 is a negative transcriptional regulator of IL-1β in the THP-1 cell line. Mol. Immunol. *54*, 264–270.

Nishiyama, A., Matsui, M., Iwata, S., Hirota, K., Masutani, H., Nakamura, H., Takagi, Y., Sono, H., Gon, Y., and Yodoi, J. (1999). Identification of thioredoxin-binding protein-2/vitamin D(3) up-regulated protein 1 as a negative regulator of thioredoxin function and expression. J. Biol. Chem. *274*, 21645–21650.

Philp, A., Rowland, T., Perez-Schindler, J., and Schenk, S. (2014). Understanding the acetylome: translating targeted proteomics into meaningful physiology. Am. J. Physiol. Cell Physiol. *307*, C763-73.

du Preez, L.L., and Patterton, H.-G. (2013). Secondary Structures of the Core Histone N-terminal Tails: Their Role in Regulating Chromatin Structure. (Springer, Dordrecht), pp. 37–55.

Rennoll-Bankert, K.E., Garcia-Garcia, J.C., Sinclair, S.H., and Dumler, J.S. (2015). Chromatin-bound bacterial effector ankyrin A recruits histone deacetylase 1 and modifies host gene expression. Cell. Microbiol. *17*, 1640–1652.

Rice, J.C., and Allis, C.D. (2001). Histone methylation versus histone acetylation: new insights into epigenetic regulation. Curr. Opin. Cell Biol. *13*, 263–273.

Rolando, M., and Buchrieser, C. (2012). Post-translational modifications of host proteins by Legionella pneumophila: a sophisticated survival strategy. Future Microbiol. *7*, 369–381.

Rolando, M., and Buchrieser, C. (2019). Sorting of Phagocytic Cells Infected with Legionella pneumophila. Methods Mol. Biol. *1921*, 179–189.

Rolando, M., Sanulli, S., Rusniok, C., Gomez-Valero, L., Bertholet, C., Sahr, T., Margueron, R., and Buchrieser, C. (2013). Legionella pneumophila effector RomA uniquely modifies host chromatin to repress gene expression and promote intracellular bacterial replication. Cell Host Microbe *13*, 395–405.

Rosen, D.B., Cao, W., Avery, D.T., Tangye, S.G., Liu, Y.-J., Houchins, J.P., and Lanier, L.L. (2008). Functional consequences of interactions between human NKR-P1A and its ligand LLT1 expressed on activated dendritic cells and B cells. J. Immunol. *180*, 6508–6517.

Sahr, T., Rusniok, C., Dervins-Ravault, D., Sismeiro, O., Coppee, J.-Y., and Buchrieser, C. (2012). Deep sequencing defines the transcriptional map of L. pneumophila and identifies growth phase-dependent regulated ncRNAs implicated in virulence. RNA Biol. *9*, 503–519.

Schator, D., Gomez-Valero, L., Buchrieser, C., and Rolando, M. (2021). Epigenetic reprogramming: histone deacetylases as targets of pathogens and therapeutics. *submitted*.

Schuhmacher, M.K., Rolando, M., Bröhm, A., Weirich, S., Kudithipudi, S., Buchrieser, C., and Jeltsch, A. (2018). The Legionella pneumophila Methyltransferase RomA Methylates Also Non-histone Proteins during Infection. J. Mol. Biol. *430*, 1912–1925.

Shou, Q., Fu, H., Huang, X., and Yang, Y. (2019). PARP-1 controls NK cell recruitment to the site of viral infection. JCI Insight *4*.

Spörri, R., Joller, N., Albers, U., Hilbi, H., and Oxenius, A. (2006). MyD88-dependent IFN-gamma production by NK cells is key for control of Legionella pneumophila infection. J. Immunol. *176*, 6162–6171.

Studier, F.W. (2005). Protein production by auto-induction in high density shaking cultures. Protein Expr. Purif. *41*, 207–234.

Uba, A.İ., and Yelekçi, K. (2017). Exploration of the binding pocket of histone deacetylases: the design of potent and isoform-selective inhibitors. Turkish J. Biol. = Turk Biyol. Derg. *41*, 901–918.

Wang, H., Lu, J., Li, K., Ren, H., Shi, Y., Qin, T., Duan, X., and Fang, M. (2018a). The virulence of *Legionella pneumophila* is positively correlated with its ability to stimulate NF-κB activation. Future Microbiol. *13*, 1247–1259.

Wang, J., Nie, W., Xie, X., Bai, M., Ma, Y., Jin, L., Xiao, L., Shi, P., Yang, Y., Jose, P.A., et al. (2021). MicroRNA-874-3p/ADAM (A Disintegrin and Metalloprotease) 19 Mediates Macrophage Activation and Renal Fibrosis After Acute Kidney Injury. Hypertens. (Dallas, Tex. 1979) HYPERTENSIONAHA12016900.

Wang, X., Wu, Y., Jiao, J., and Huang, Q. (2018b). Mycobacterium tuberculosis infection induces IL-10 gene expression by disturbing histone deacetylase 6 and histonedeacetylase 11 equilibrium in macrophages. Tuberculosis *108*, 118–123.

Xiao, Y., Li, W., Yang, H., Pan, L., Zhang, L., Lu, L., Chen, J., Wei, W., Ye, J., Li, J., et al. (2021). HBO1 is a versatile histone acyltransferase critical for promoter histone acylations. Nucleic Acids Res.

Yoon, S.-J., Jo, D.H., Park, S.-H., Park, J.-Y., Lee, Y.-K., Lee, M.-S., Min, J.-K., Jung, H., Kim, T.-D., Yoon, S.R., et al. (2019). Thioredoxin-Interacting Protein Promotes Phagosomal Acidification Upon Exposure to Escherichia coli Through Inflammasome-Mediated Caspase-1 Activation in Macrophages. Front. Immunol. *10*, 2636.

Yu, G., Wang, L.-G., Han, Y., and He, Q.-Y. (2012). clusterProfiler: an R package for comparing biological themes among gene clusters. OMICS *16*, 284–287.

Zhao, B., Xu, W., Rong, B., Chen, G., Ye, X., Dai, R., Li, W., Chen, J., Cai, J., Song, L., et al. (2018). H3K14me3 genomic distributions and its regulation by KDM4 family demethylases. Cell Res. *28*, 1118–1120.

Zheng, Y., Saftig, P., Hartmann, D., and Blobel, C. (2004). Evaluation of the contribution of different ADAMs to tumor necrosis factor alpha (TNFalpha) shedding and of the function of the TNFalpha ectodomain in ensuring selective stimulated shedding by the TNFalpha convertase (TACE/ADAM17). J. Biol. Chem. *279*, 42898–42906.

Zhu, Q., Yang, Q., Lu, X., Wang, H., Tong, L., Li, Z., Liu, G., Bao, Y., Xu, X., Gu, L., et al. (2021). SETD2-mediated H3K14 trimethylation promotes ATR activation and stalled replication fork restart in response to DNA replication stress. Proc. Natl. Acad. Sci. U. S. A. *118*.

878 **FIGURES**
879

Figure 1

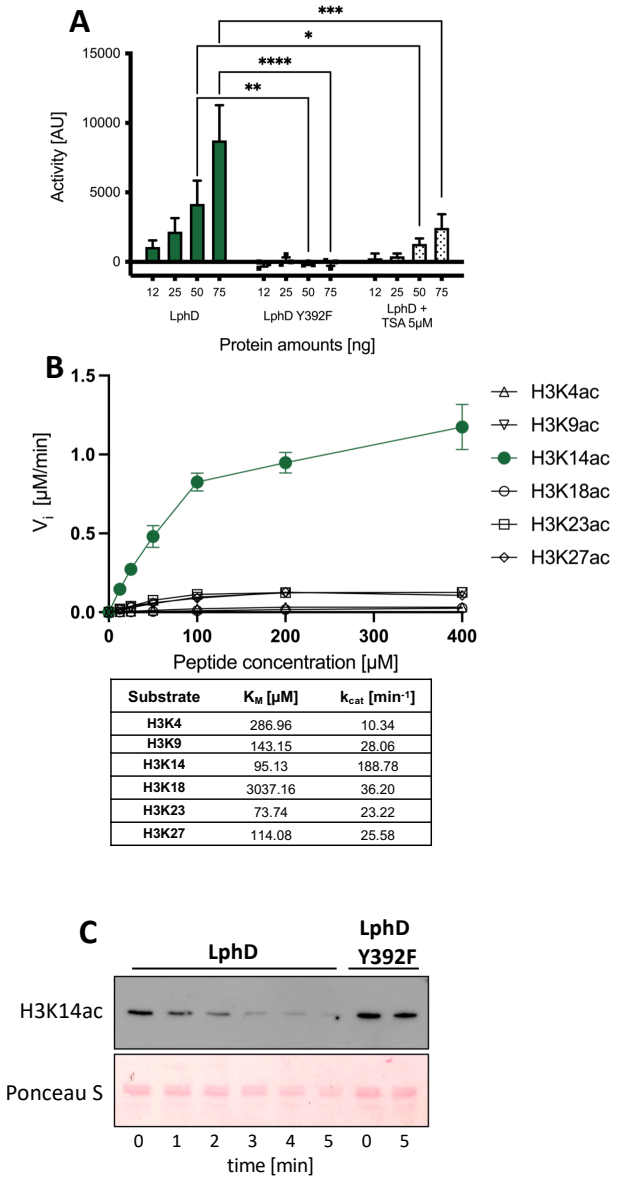

Substrate	K_M [µM]	k_{cat} [min^{-1}]
H3K4	286.96	10.34
H3K9	143.15	28.06
H3K14	95.13	188.78
H3K18	3037.16	36.20
H3K23	73.74	23.22
H3K27	114.08	25.58

880
881

882

Figure 2

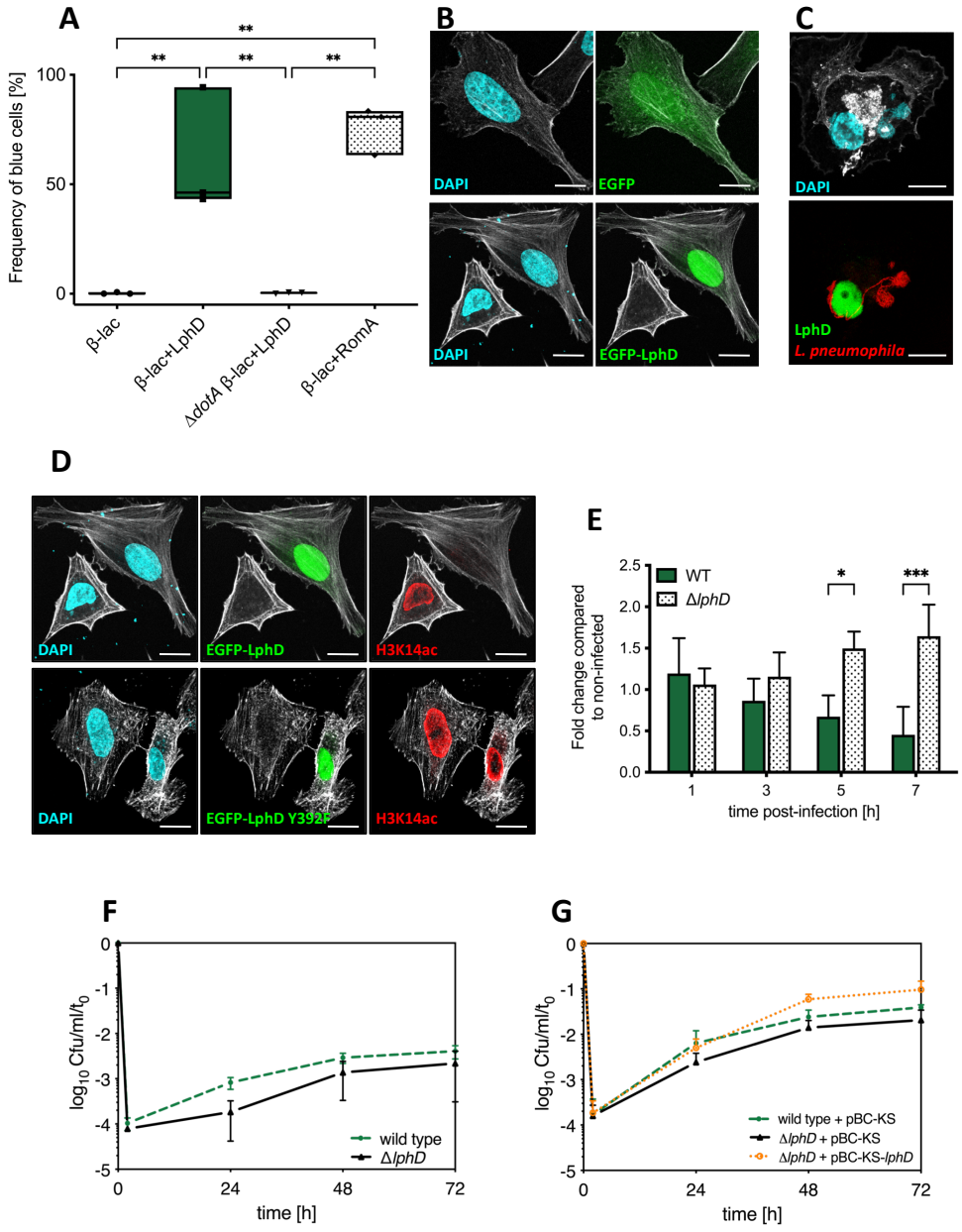

883
884

885

Figure 3

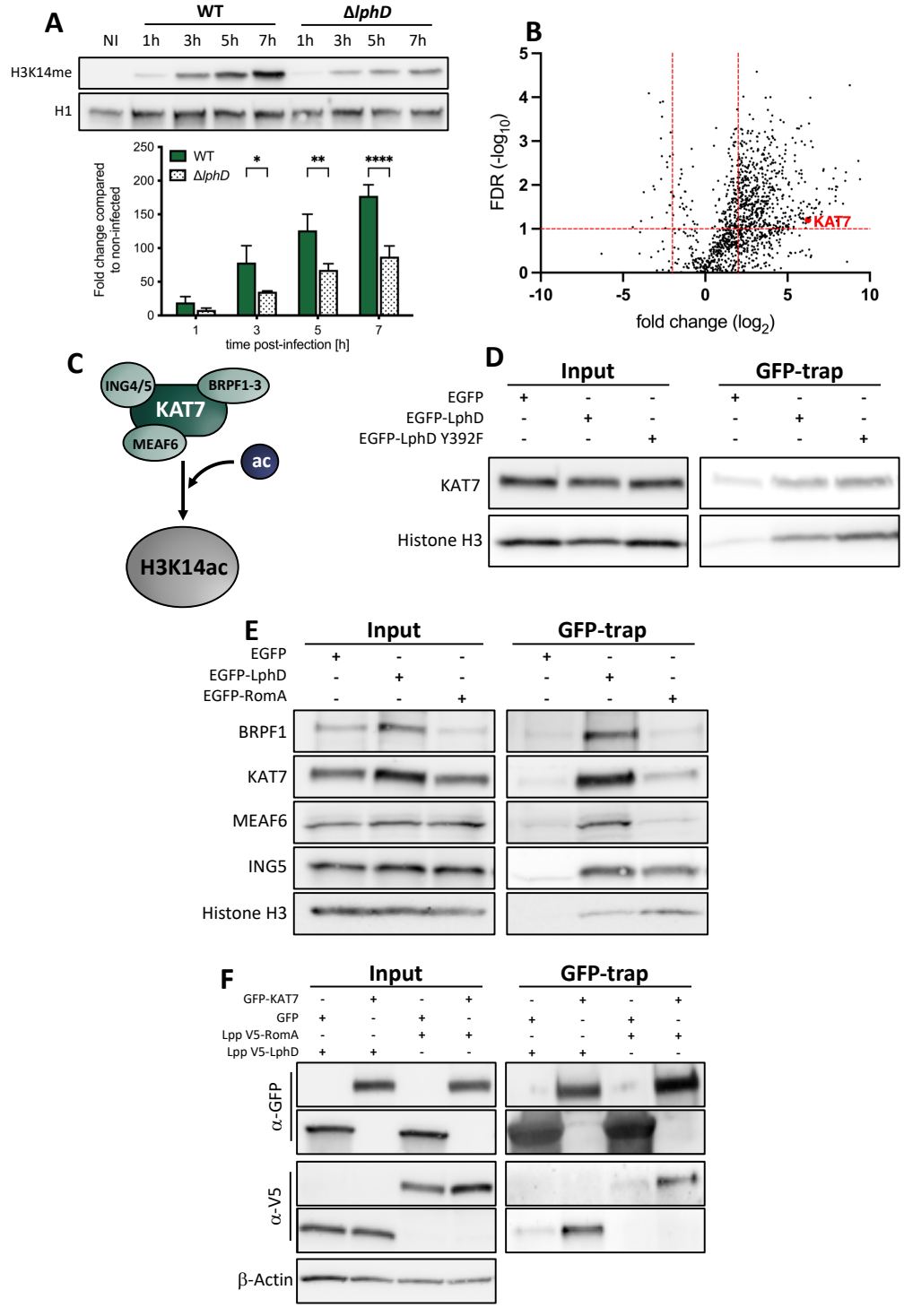

886
887

Figure 4

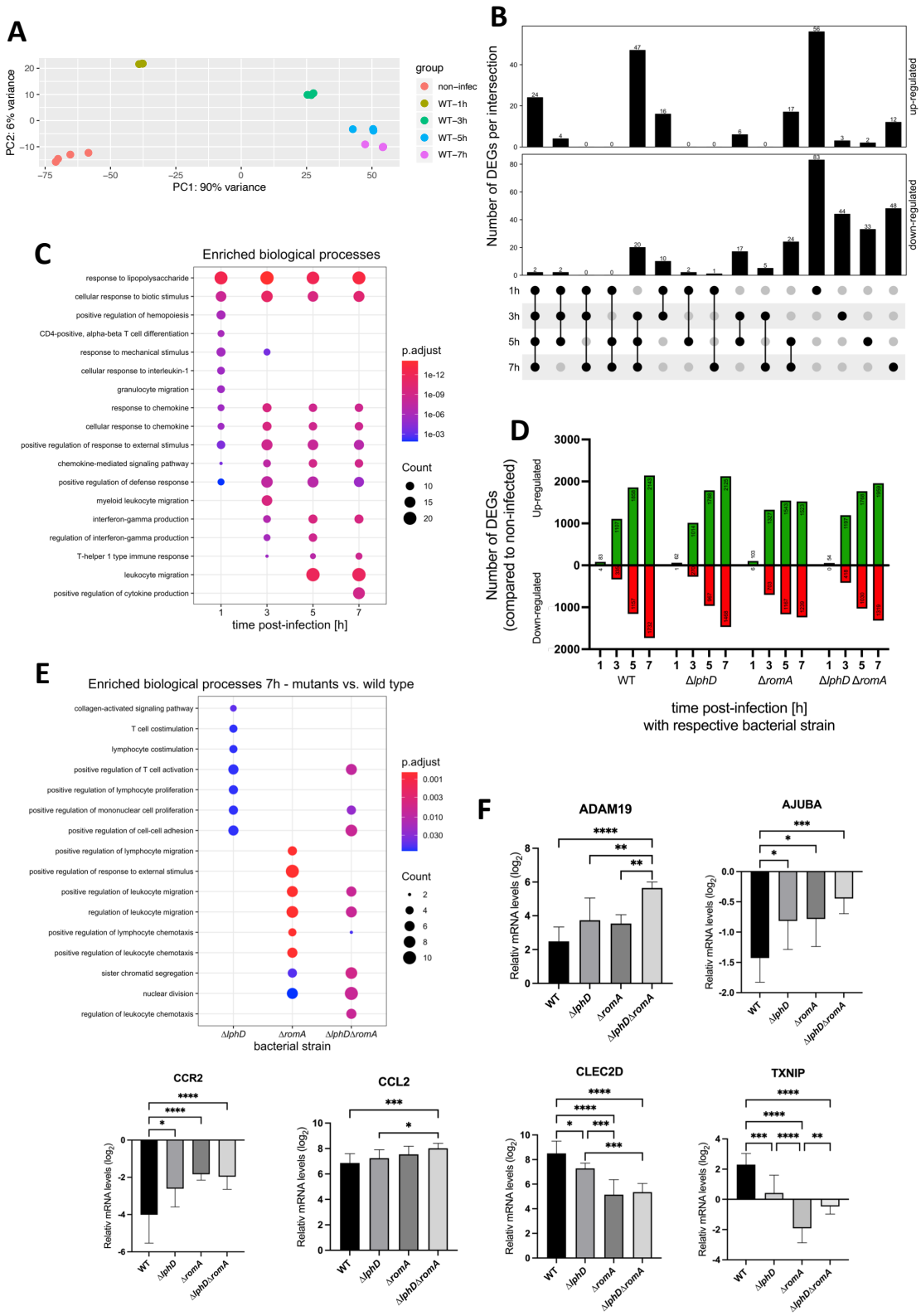
A
PC2: 6% variance
PC1: 90% variance
group
non−infec
WT−1h
WT−3h
WT−5h
WT−7h
B
Number of DEGs per intersection
up-regulated
down-regulated
1h
3h
5h
7h
C
Enriched biological processes
response to lipopolysaccharide
cellular response to biotic stimulus
positive regulation of hemopoiesis
CD4-positive, alpha-beta T cell differentiation
response to mechanical stimulus
cellular response to interleukin-1
granulocyte migration
response to chemokine
cellular response to chemokine
positive regulation of response to external stimulus
chemokine-mediated signaling pathway
positive regulation of defense response
myeloid leukocyte migration
interferon-gamma production
regulation of interferon-gamma production
T-helper 1 type immune response
leukocyte migration
positive regulation of cytokine production
time post-infection [h]
p.adjust
Count
D
Number of DEGs
(compared to non-infected)
Up-regulated
Down-regulated
WT
ΔlphD
ΔromA
ΔlphD ΔromA
time post-infection [h]
with respective bacterial strain
E
Enriched biological processes 7h - mutants vs. wild type
collagen-activated signaling pathway
T cell costimulation
lymphocyte costimulation
positive regulation of T cell activation
positive regulation of lymphocyte proliferation
positive regulation of mononuclear cell proliferation
positive regulation of cell-cell adhesion
positive regulation of lymphocyte migration
positive regulation of response to external stimulus
positive regulation of leukocyte migration
regulation of leukocyte migration
positive regulation of lymphocyte chemotaxis
positive regulation of leukocyte chemotaxis
sister chromatid segregation
nuclear division
regulation of leukocyte chemotaxis
ΔlphD
ΔromA
ΔlphDΔromA
bacterial strain
p.adjust
Count
F
ADAM19
AJUBA
CCR2
CCL2
CLEC2D
TXNIP
Relativ mRNA levels (log2)
WT
ΔlphD
ΔromA
ΔlphDΔromA

SUPP FIGURES

Figure S1

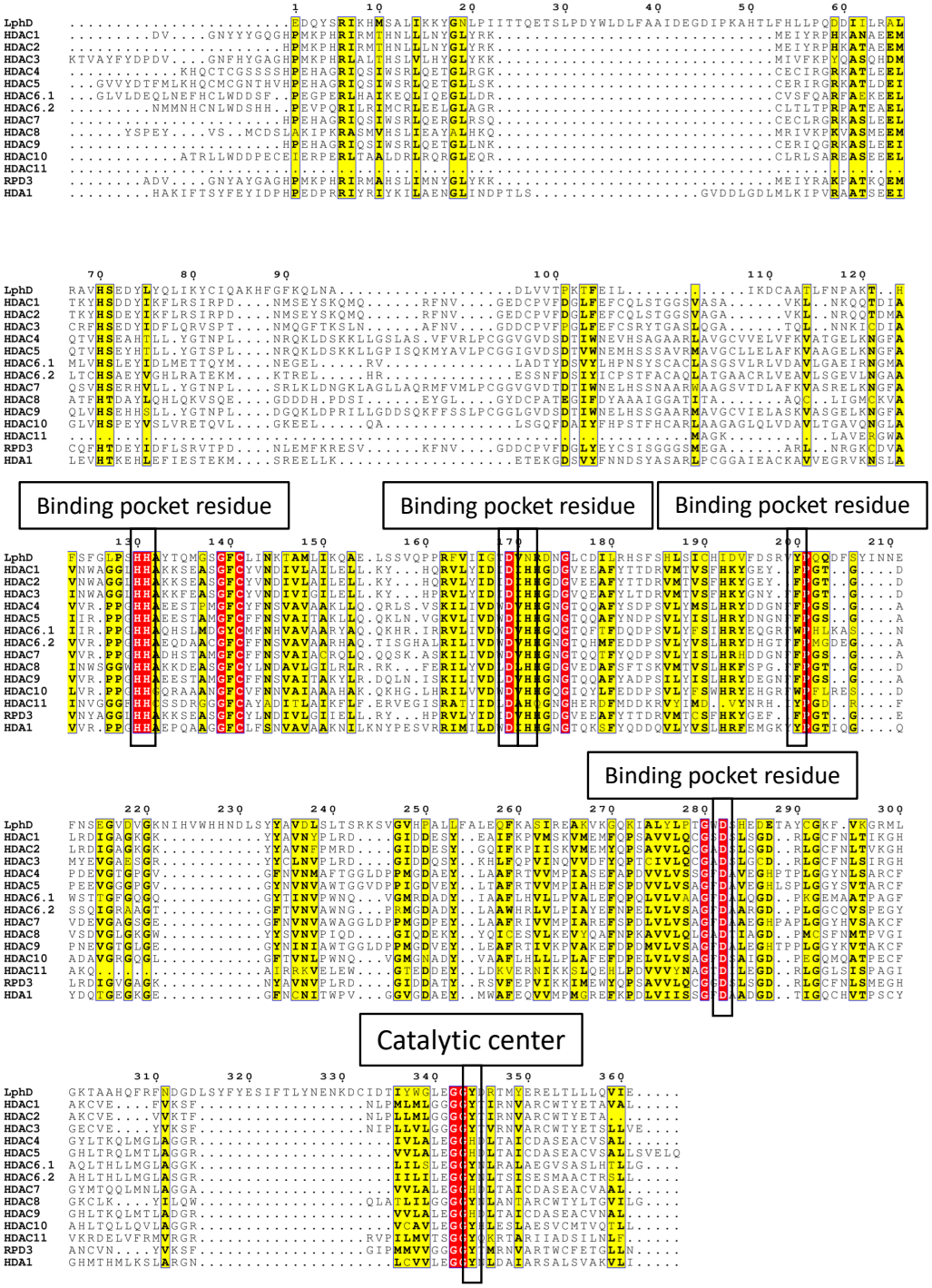

895

Figure S2

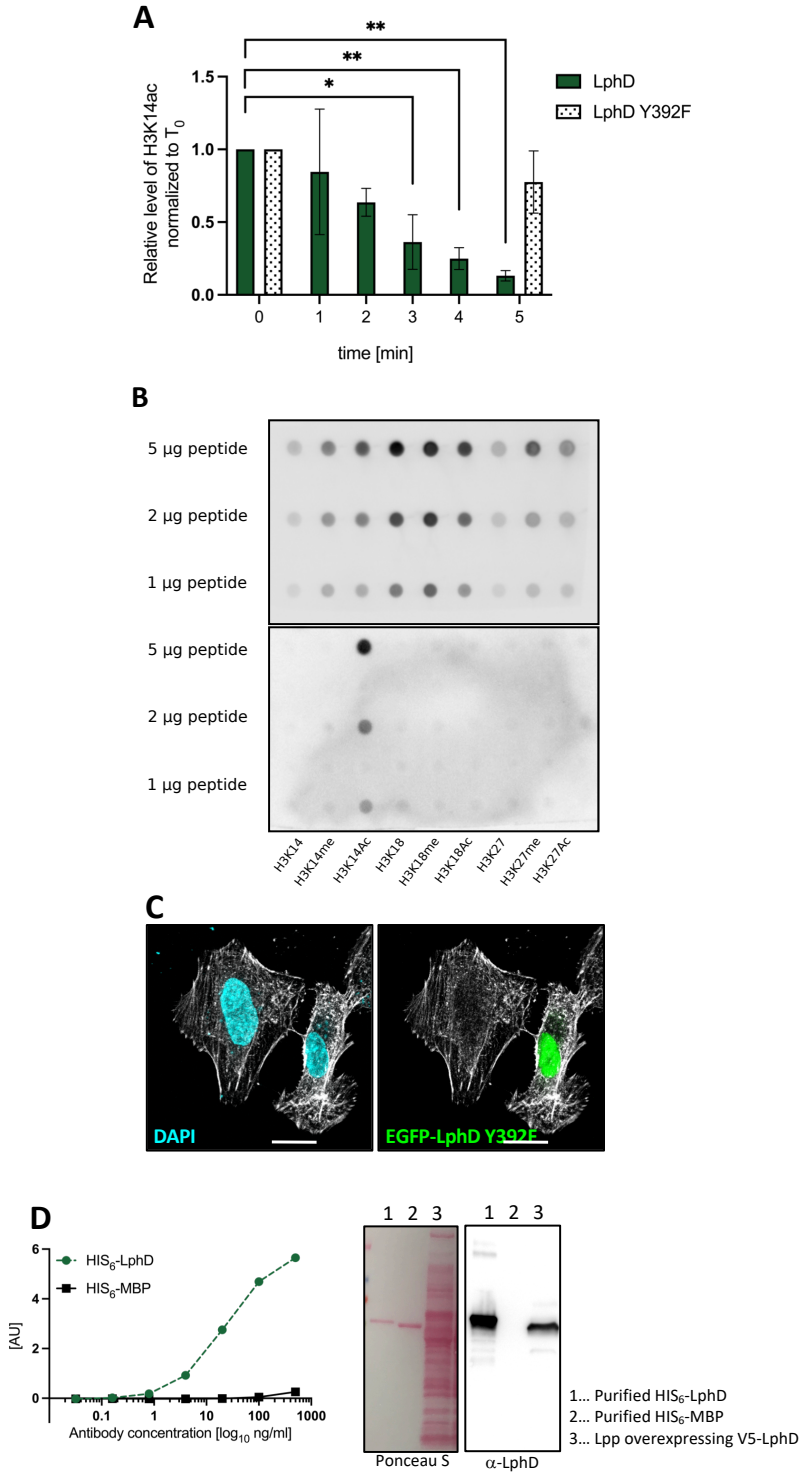

896

Figure S3

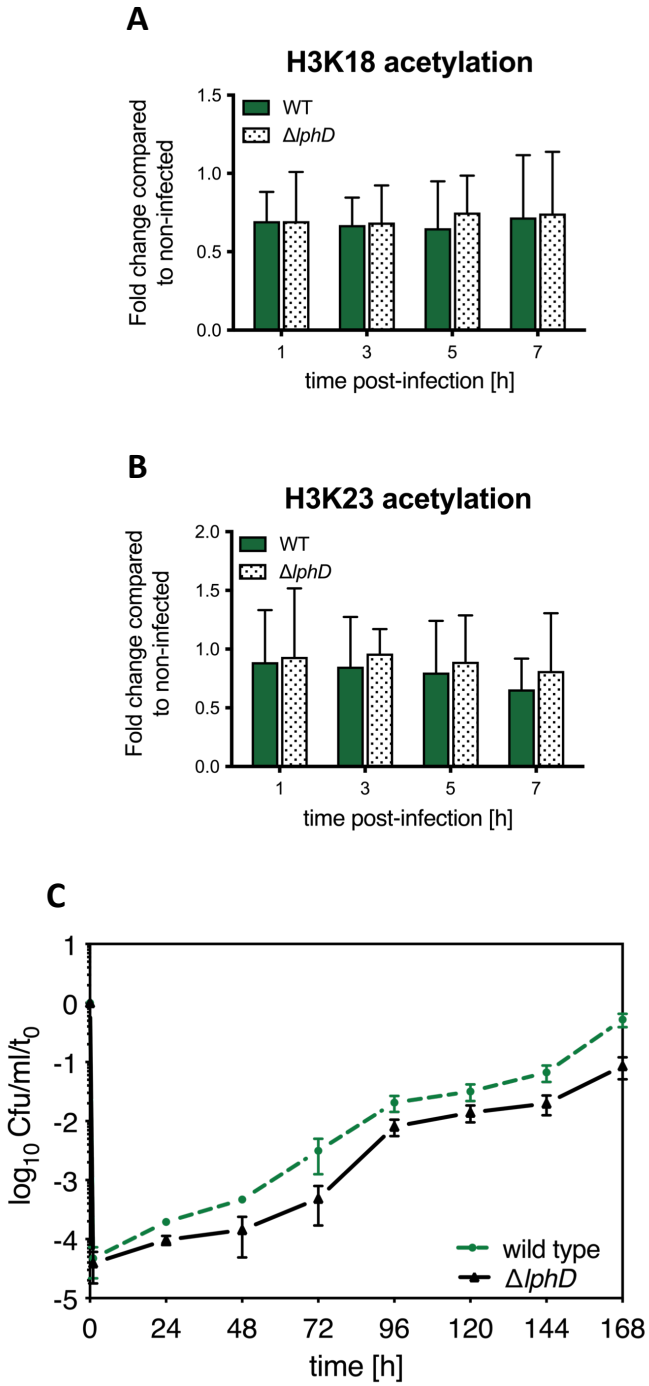
A
H3K18 acetylation
WT
ΔlphD
Fold change compared to non-infected
1.5
1.0
0.5
0.0
1
3
5
7
time post-infection [h]
B
H3K23 acetylation
WT
ΔlphD
Fold change compared to non-infected
2.0
1.5
1.0
0.5
0.0
1
3
5
7
time post-infection [h]
C
log10 Cfu/ml/t0
1
0
-1
-2
-3
-4
-5
0
24
48
72
96
120
144
168
time [h]
wild type
ΔlphD

Figure S4

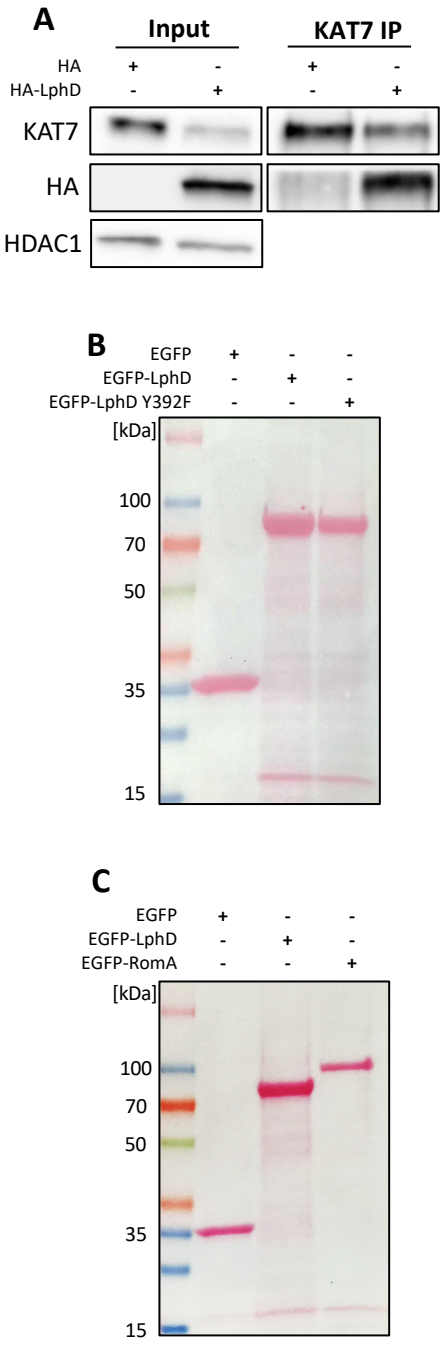

899
900
901

902

Figure S5

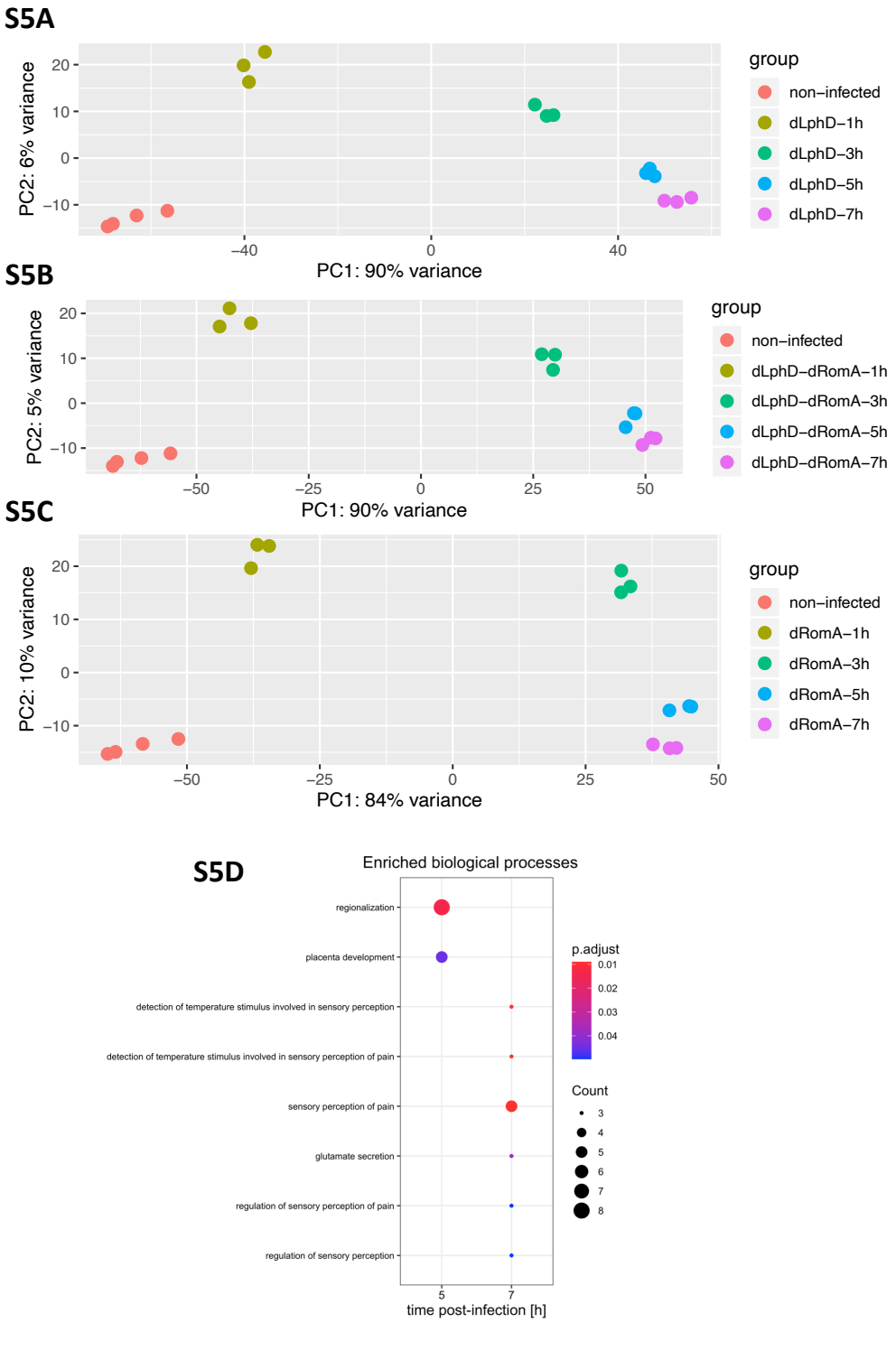

903
904
905

SUPP TABLES

Table S1: LphD interacting proteins identified through GFP-trap analysis directly connected to epigenetic regulation.

Protein	Epigenetic complex	FDR	Fold change
KAT7	HBO1	0.06	75.70
HDAC2	NuRD/Sin3	0.08	8.44
MTA2	NuRD	0.03	5.41
SAP18	Sin3	0.005	9.46
PRKDC	DNA-PK	0.005	4.71
XRCC5	DNA-PK	0.02	14.47
SSRP1	FACT	0.02	3.08
SUPT16H	FACT	0.001	3.39
EED	PRC2/EED-EZH2	0.03	32.19
SUZ12	PRC2/EED-EZH2	0.002	15.45
EZH2	PRC2/EED-EZH2	0.09	9.17

930 **Table S2:** Primers used in this study

Primer	Sequence (5'-3')	Purpose	Reference
52H	GATGAAGGCACGAACCCAGTTGACA	Deletion of *lphD* gene	This study
52B	CGGCTTGAACGAATTGTTAGGTGGC	Deletion of *lphD* gene	This study
195H	GACCCTCGACTTAATTGGATAACGG	Deletion of *lphD* gene	This study
195B	GGAGGGTAAACGGAAAACAAACTG	Deletion of *lphD* gene	This study
196H	GCCACCTAACAATTCGTTCAAGCCGGGTGATC TAAGCTACTTCTATGAATCCATATTC	Deletion of *lphD* gene	This study
196B	TGTCAACTGGGTTCGTGCCTTCATCGTTTCCTG AGTTGTAATAATTGGTAAATTCC	Deletion of *lphD* gene	This study
11H	TCCAATATACAAGCATTCATGTGCTATCTG	Deletion of *romA* gene	(Rolando et al., 2013)
11B	GAAGTTTCTCGAATTCTTTGGACAAGC	Deletion of *romA* gene	(Rolando et al., 2013)
60H	CATCGATGAATTGTGTCTCAAAA	Deletion of *romA* gene	(Rolando et al., 2013)
60B	GTCCCGTCAAGTCAGCGTA	Deletion of *romA* gene	(Rolando et al., 2013)
66H	TTTTGAGACACAATTCATCGATG GCTCTATTT TGCATGTGATTTTCATT	Deletion of *romA* gene	(Rolando et al., 2013)
66B	TACGCTGACTTGACGGGAC GCAAGTTTTTTTG ATTTGATATTTCCTG	Deletion of *romA* gene	(Rolando et al., 2013)
217H	ATCTATTGGGGCTTGGAAGGTGGATTTGACAG GACCATGTATGAA	Base pair substitution (LphD Y392F)	This study
217B	TTCATACATGGTCCTGTCAAATCCACCTTCCAA GCCCCAATAGAT	Base pair substitution (LphD Y392F)	This study
222H	GGATCCGAAAGTAGCGCCTCTTGTCTTGATA	Complementation of *lphD*	This study
222B	GGTACCTTAACAGGACATATTATGCGAATTGG	Complementation of *lphD*	This study
CCL2_2_fwd	ACCTTCATTCCCCAAGGGC	qPCR analysis of *CCL2* mRNA	This study
CCL2_2_rev	CTCCTTGGCCACAATGGTCT	qPCR analysis of *CCL2* mRNA	This study
CCR2_1_fwd	TTCCAGGAATTCTTCGGCCT	qPCR analysis of *CCR2* mRNA	This study
CCR2_1_rev	GCAATCCTACAGCCAAGAGC	qPCR analysis of CCR2 mRNA	This study
TXNIP_2_fwd	GCCACACTTACCTTGCCA AT	qPCR analysis of *TXNIP* mRNA	(Cui et al., 2019)
TXNIP_2_rev	TTGGATCCAGGAACGCTA AC	qPCR analysis of *TXNIP* mRNA	(Cui et al., 2019)
AJUBA_2_fwd	GCTTTGCTTCGCCTGACG	qPCR analysis of *AJUBA* mRNA	This study
AJUBA_2_rev	CCATAGATGCCTTTGTTGCACT	qPCR analysis of *AJUBA* mRNA	This study
ADAM19_2_fwd	GGGACTGGGCTCTTCAGTTT	qPCR analysis of *ADAM19* mRNA	This study
ADAM19_2_rev	GTCCTGGTCTCGTCGATTCT	qPCR analysis of *ADAM19* mRNA	This study
CLEC2D_1_fwd	TCTGAATTGCCTGCAAACCC	qPCR analysis of *CLEC2D* mRNA	This study
CLEC2D_1_rev	GGCATGCAGCTTGAAGACAT	qPCR analysis of *CLEC2D* mRNA	This study
ACTB_2_fwd	GTTGTCGACGACGAGCG	qPCR analysis of *ACTB* mRNA	(Rolando et al., 2013)
ACTB_2_rev	GCACAGAGCCTCGCCTT	qPCR analysis of *ACTB* mRNA	(Rolando et al., 2013)
36B4_1_fwd	TGGCAGCATCTACAACCCTG	qPCR analysis of *36B4* mRNA	(Rolando et al., 2013)
36B4_1_rev	AAGGTGTAATCCGTCTCCACAGA	qPCR analysis of *36B4* mRNA	(Rolando et al., 2013)
GAPDH_fwd	GAGTCAACGGATTTGGTCGT	qPCR analysis of *GAPDH* mRNA	(Neves-Costa and Moita, 2013)
GAPDH_rev	TTGATTTTGGAGGGATCTCG	qPCR analysis of *GAPDH* mRNA	(Neves-Costa and Moita, 2013)

931

932

933 **Table S3:** Antibodies and dyes used in this study.

Target	Manufacturer	Product code
Western blot:		
β-Actin	Sigma	A5316
BRPF1	Active Motif	61541
EGFP	Thermo Fisher	A11122
H1	Active Motif	61201
H3	Active Motif	39163
H3K14ac	Milipore	07-353
H3K14me2	Euromedex	H3-2B10
H3K18ac	Active Motif	39755
H3K23ac	Active Motif	39131
HA	Sigma	H6908
ING5	Active Motif	91329
KAT7	Santa Cruz Biotechnology	sc-39846
MEAF6	Thermo Fisher	PA5-40704
V5	Thermo Fisher	46-0705
anti-Mouse HRP-conjugated	Cell signaling	7076S
anti-Rabbit HRP-conjugated	Cell signaling	7074S
Immunofluorescence:		
LphD	Thermo Fisher	Custom (see **Supp Methods**)
Alexa488 goat anti-Rabbit	Thermo Fisher	A32731
Alexa546 goat anti-Rabbit	Thermo Fisher	A11010
DAPI	Thermo Fisher	D21490
Alexa633 phalloidin	Thermo Fisher	A22284

934
935
936
937
938
939
940
941
942
943
944
945
946
947

FIGURE LEGENDS

Figure 1

(**A**) Fluor de Lys® HDAC activity assay of LphD. Increasing amounts of purified LphD and its predicted catalytic inactive mutant (LphD Y392F) were used to assess the lysine deacetylase activity *in vitro*. Trichostatin A (TSA), a known HDAC inhibitor, was added to LphD as a control (n = 3, * $p < 0.05$, ** $p < 0.01$, *** $p < 0.01$, **** $p < 0.0001$). (**B**) Top: Steady-state kinetics of purified LphD on fluorogenic H3 peptide substrates acetylated at different lysine residues (H3K4ac, H3K9ac, H3K14ac, H3K18ac, H3K23ac, H3K27ac). Bottom: Michaelis-Menten constants (K_M and k_{cat}) were individually calculated for each peptide from non-linear regression fit using OriginPro and are embedded below the graph. Data represents mean value ± SD (n = 3). (**C**) Representative western blot of LphD activity on H3K14ac levels on histone octamers. Wild type protein (LphD) is compared to the catalytic inactive mutant (LphD Y392F). H3K14ac levels are assessed every minute for 5 minutes. Ponceau S staining of H3 is used as loading control.

Figure 2

(**A**) β-lactamase secretion assay for LphD. Percentage of blue cells after 2 hours of infection with *L. pneumophila* wild type or Δ*dotA* overexpressing expressing either β-lactamase alone (β-lac), β-lactamase fused to LphD (β-lac+LphD) or β-lactamase fused to RomA (β-lac+RomA). Cells were incubated with LiveBLAzer CCF4-AM solution (Thermo Fisher Scientific) and analyzed by flow cytometry (n = 3, ** $p < 0.01$). (**B**) Immunofluorescence analysis of subcellular localization of EGFP-LphD. HeLa cells were transfected either with EGFP (top) or EGFP-LphD (bottom). Nuclei are stained by DAPI (cyan) and actin cytoskeleton with phalloidin (gray). Scale bars 10 μm. (**C**) Immunofluorescence analysis of subcellular localization of LphD during infection. Differentiated THP-1 cells were infected with *L. pneumophila* wildtype expressing LphD and DsRed. DAPI (cyan), LphD (green), *L. pneumophila* (red), and phalloidin (gray). Scale bars 10 μm. (**D**) Immunofluorescence analysis of H3K14ac in LphD transfected cells. HeLa cells were either transfected with EGFP-LphD (top) or EGFP-LphD Y392F (bottom) and then stained for H3K14ac using a specific antibody. DAPI (cyan), EGFP-LphD/LphD Y392F (green), H3K14ac (red), and phalloidin (gray). Scale bars 10 μm. (**E**) Quantification of western blot signal for H3K14 acetylation. THP-1 cells were infected with *L. pneumophila* wild type (green) or Δ*lphD* (white) strain expressing EGFP. Cells

were sorted at different times post-infection, as indicated, by FACS, histones were isolated and analyzed by western blot. Histone H1 was used as loading control and signal is normalized to non-infected cells. Data are represented as mean ± SD. (n = 3, * $p < 0.05$, *** $p < 0.001$). (**F**) Intracellular replication in THP-1 cells (MOI = 10) of wild type *L. pneumophila* (dashed green line, circles) and the Δ*lphD* (solid black line, squares) mutant. Replication was determined by recording the number of colony-forming units (cfu) through plating on buffered charcoal yeast extract (BCYE) agar (log_{10} ratio cfu/t_0, n = 3). Data are represented as mean ± SD. (**G**) Complementation analysis after infection of THP-1 cells (MOI = 10) with the *L. pneumophila* wild type and Δ*lphD* mutant carrying the empty vector pBC-KS (dashed green and solid black lines, respectively), or Δ*lphD* carrying the complementing plasmid pBC-KS-*lphD* (dotted orange) (log_{10} ratio cfu/t_0, n = 3). Data are represented as mean ± SD.

Figure 3

(**A**) Representative western blot signal for H3K14 methylation (top) and quantification (n = 3, * $p < 0.05$, ** $p < 0.01$, **** $p < 0.0001$) (bottom). THP-1 cells were infected with *L. pneumophila* wild type (green) or Δ*lphD* (white) strain expressing EGFP. Cells were sorted at different times post-infection by FACS, histones were isolated and analyzed by western blot. Histone H1 was used as loading control and signal is compared to non-infected cells. Data are represented as mean ± SD. (**B**) Volcano plot of EGFP-LphD interacting proteins. The log_2 fold change of EGFP-LphD to control (GFP) is plotted against the $-log_{10}$ of the false discovery rate (FDR). Protein selected for further tests (KAT7) is highlighted in red. Thresholds were set at log_2 fold change > 2 and false discovery rate < 0.1 (dashed red lines). (**C**) Schematic representation of the HBO1 histone acetyltransferase complex in the configuration with BRPF1-3 targeting H3K14. (**D**) Immunoblots showing the interaction of LphD with KAT7 and histone H3. Co-immunoprecipitation using GFP-trap beads (GFP-trap) in HEK293T cells transfected with EGFP, EGFP-LphD, or EGFP-LphD Y392F. Input shows the expression level of endogenous KAT7 and Histone H3 in total lysates. (**E**) Immunoblots showing the interaction of LphD and RomA with the HBO1 complex and histone H3. Co-immunoprecipitation using GFP-trap beads in HEK293T cells transfected with EGFP, EGFP-LphD, or EGFP-RomA. Samples were analyzed for the presence of the different components of the HBO1 complex (BRPF1, KAT7, MEAF6, ING5) as well as its target, histone H3. Input shows the expression level of endogenous HBO1 components and histone H3 in total lysates (**F**) Immunoblots showing the interaction of LphD and RomA with KAT7 and Histone H3 during infection. Co-immunoprecipitation using GFP-trap beads in HEK293T cells transfected with either EGFP or

EGFP-KAT7 followed by infection with *L. pneumophila* wild type over-expressing either V5-LphD or V5-RomA. EGFP proteins were pulled down using GFP-trap beads and samples were analyzed for the presence of V5-LphD or V5-RomA. Input shows the expression level in total lysates of transfected EGFP-KAT7, V5-fusion proteins, as well as β-actin (loading control).

Figure 4

(**A**) Principal component analysis (PCA) plot of RNA-seq results of *L. pneumophila* wild type (WT) infected THP-1 cells over a time course, as indicated. Each dot represents a sample and each color represents a sample group. (**B**) Upset plot of intersection of sets of genes at multiple time points comparing the 100 most up- and down-regulated genes in *L. pneumophila* wild type infected cells. Each column represents the number differently expressed genes (DEGs) corresponding to a single time point (last four columns) or set of time points (dots connected by lines below the X axis). The number of genes in each set appears above the column, while the time points shared are indicated in the graphic below the column. (**C**) Dot plot of enriched biological processes of the 100 most up-regulated genes of THP-1 cells infected with *L. pneumophila* wild type at different time points compared to non-infected cells. Dot size represents the gene count per GO-term and color represents adjusted p-value. (**D**) Bar graph of the number of DEGs (up-regulated = green, down-regulated = red) compared to non-infected cells. Comparison of each time point (1 h, 3 h, 5 h, and 7 h post-infection) for each tested infection condition (wild type (WT), Δ*lphD*, Δ*romA*, and Δ*lphD*Δ*romA*). (**E**) Dot plot of enriched biological processes of the 100 most up-regulated genes of THP-1 cells infected seven hours with *L. pneumophila* knockout mutants (Δ*lphD*, Δ*romA*, and Δ*lphD*Δ*romA*) compared to wild type infected cells. Dot size represents the gene count per GO-term and color represents adjusted p-value (p.adjust). (**F**) Relative mRNA expression for selected genes after seven hours infection with wild type (WT), Δ*lphD*, Δ*romA*, and Δ*lphD*Δ*romA* strains, compared to non-infected cells (set to 0). Transcript levels were assessed by RT-qPCR and normalized to those of ActB, GAPDH and 36B4. Data are represented as mean ± SD (n = 9, * $p < 0.05$, ** $p < 0.01$, *** $p < 0.01$, **** $p < 0.0001$).

SUPP FIGURES LEGENDS

(**S1**) Multiple sequence alignment of various HDAC domains, including LphD and several eukaryotic HDACs (Accession numbers: *Homo sapiens*: HDAC1 #Q6IT96, HDAC2 #Q92769, HDAC3 #O15379, HDAC4 #P56524, HDAC5 #Q9UQL6, HDAC6.1 #Q9UBN7, HDAC6.2 #Q9UBN7, HDAC7 #Q8WUI4, HDAC8 #Q9BY41, HDAC9 #Q9UKV0, HDAC10 #Q969S8, HDAC11 #Q96DB2; *Saccharomyces cerevisiae*: Rpd3 # P32561, HDA1 #P53973). Analysis also includes two yeast HDACs (Rpd3 and HDA1), which are the basis of general HDAC classification. Alignment was performed using SeaView and visualization with ESPript. Red boxes with white characters mean strict identity between all samples, bold characters mean high in-group similarity and yellow boxes mean high across-group similarity. Binding pocket residues (charge relay system) and the catalytic center are marked with black boxes.

(**S2A**) Quantification of LphD activity on H3K14ac levels using histone octamers in function of time (minutes) and compared to LphD Y392F. Octamers are incubated with the enzymes and the reaction was stopped after the indicated times. The H3K14ac signal was quantified after immunoblot detection. Data are represented as mean ± SD (n = 3, ** $p < 0.01$).

(**S2B**) Validation of H3K14ac antibody specificity by dot blot experiments, using different amounts of several H3 peptides (H3K14, H3K14me, H3K14ac, H3K18, H3K18me, H3K18ac, H3K27, H3K27me, H3K27ac).

(**S2C**) Immunofluorescence analysis of subcellular localization of EGFP-LphD Y392F in transfected HeLa cells. Nuclei are stained by DAPI (cyan) and actin cytoskeleton with phalloidin (gray). Scale bars 10 μm.

(**S2D**) Validation of custom anti-LphD antibody produced in rabbit. Left: Titer determination of polyclonal antibodies by ELISA comparing binding activity to purified HIS_6-LphD, compared to HIS_6-MBP. Right: Specificity testing by western blot using anti-LphD antibody. Line 1: purified HIS_6-LphD, Line 2: purified HIS_6-MBP, Line 3: *L. pneumophila* extract overexpressing V5-LphD.

(**S3A** and **S3B**) Quantification of western blot signal for H3K18 acetylation (**S3A**) and H3K23 acetylation (**S3B**) during infection. THP-1 cells were infected with *L. pneumophila* wild type

(green) or Δ*lphD* (white) strain expressing EGFP. Cells were sorted at different times post-infection by FACS, histones were isolated and analyzed by western blot. Histone H1 was used as loading control and signal is compared to non-infected cells (n = 3). Data are represented as mean ± SD. (**S3C**) Intracellular replication in *A. castellanii* (MOI = 0.1) of wild type (dashed green line, circles) *L. pneumophila* and Δ*lphD* (solid black line, squares) strain. Replication was determined by recording the number of colony-forming units (cfu) through plating on buffered charcoal yeast extract (BCYE) agar (log_{10} ratio cfu/t_0, n = 3). Data are represented as mean ± SD.

(**S4A**) Immunoblots showing the interaction of LphD with KAT7. Co-immunoprecipitation of endogenous KAT7 in HEK293T cells transfected with 3xHA or 3xHA-LphD. Input shows the expression level of endogenous KAT7 and HA-LphD in total lysates, as well as histone H1 (loading control). Co-IP samples were analyzed for the presence of 3xHA-LphD.

(**S4B**) IP control of Figure 3D. Ponceau S staining of GFP-trap samples showing the corresponding immunoprecipitated products (EGFP = 27 kDa, EGFP-LphD = 75 kDa, EGFP-LphD Y392F = 75 kDa).

(**S4C**) IP control of Figure 3E. Ponceau S staining of GFP-trap samples showing the corresponding immunoprecipitated products (EGFP = 27 kDa, EGFP-LphD = 75 kDa, EGFP-RomA = 88 kDa).

(**S5A**, **S5B** and **S5C**) Principal component analysis (PCA) plot of RNA-seq results of *L. pneumophila* Δ*lphD* (**S4A**), Δ*romA* (**S4B**) and Δ*lphD*Δ*romA* (**S4C**) infected THP-1 cells over a time course, as indicated. Each dot represents a sample and each color represents a sample group.

(**S5D**) Dot plot of enriched biological processes of the 100 most down-regulated genes of THP-1 cells infected with *L. pneumophila* wild type at different time points (hours) compared to non-infected cells. Dot size corresponds to gene count and the color to the adjusted p-value (p.adjust).

Conclusion and perspectives

Legionella pneumophila has closely co-evolved with its eukaryotic hosts. This co-evolution gave rise to the countless strategies employed by the bacteria to invade their host cells, establish a protected niche – the *Legionella* containing vacuole – and enable bacterial replication within this self-made environment (Escoll et al., 2013; Isberg et al., 2009). One of the main virulence factors in *L. pneumophila* is the type-IVB secretion system Dot/Icm. To date, more than 330 proteins have been predicted to be secreted by the Dot/Icm system, which corresponds to around 10% of the *L. pneumophila* genome (Burstein et al., 2009; Ensminger, 2016; Escoll et al., 2016; Finsel and Hilbi, 2015; Lifshitz et al., 2013; Qiu and Luo, 2017; Zhu et al., 2011). The broad range of secreted proteins, as well as their redundancy in function, highlight the ability of the bacteria to survive in a wide variety of eukaryotic hosts. This is achieved by targeting numerous different host cell pathways and manipulating them to impede the host cell response as well as promote bacterial growth. A unique feature of members of the genus *Legionella* is the large number of eukaryotic-like proteins encoded in their genome. So far, 137 eukaryotic domains have been described in the genus *Legionella*, encompassing more than 250 different proteins (Gomez-Valero et al., 2019). The functions of these secreted eukaryotic-like proteins range from influencing intracellular trafficking and manipulating signal transduction, to salvaging host metabolites and directly interfering with gene transcription (Hubber and Roy, 2010; Isberg et al., 2009; Mondino et al., 2020b). One of these effectors, a SET-domain methyltransferase called RomA, was described to target and the host cell nucleus and induce chromatin changes. RomA specifically methylates lysine 14 of histone 3 (H3K14), causing transcriptional repression of a subset of genes involved in the host cell response to the bacterial invasion (Rolando et al., 2013). H3K14 methylation usually occurs at very low levels in the host but accumulates very quickly during infection, which might be caused by low levels of the corresponding demethylase (Zhao et al., 2018; Zhu et al., 2021). However, the fact that H3K14 is usually acetylated in eukaryotic cells – a modification connected to active transcription – led to the question how the bacteria efficiently methylate this residue. In eukaryotic cells, the process of removing acetyl moieties from histones is regulated by histone deacetylases (HDAC). One possibility was that the bacteria intercept the natural turnover of this residue, due to highly dynamic changes in these modifications. The other option was that *L. pneumophila* might encode its own secreted HDAC to facilitate the deacetylation of H3K14 at specific genome regions, consequently enabling their methylation by RomA.

Indeed, a bioinformatical search of the *L. pneumophila* genome revealed that the bacteria encode a protein with a predicted HDAC domain, which we called LphD. Furthermore, this HDAC domain shows high similarity to eukaryotic HDACs, especially the Zn^{+2}-dependent classes. In addition, phylogenetic analysis revealed that this HDAC-like protein is widely distributed in the whole *Legionella* genus. Interestingly, further analysis revealed that there are two distinct groups of HDAC-like proteins in the genus *Legionella*, which, due to their low homology, seem to have been acquired on two separate occasions during evolution (Schator et al., 2021). Group 2, which includes LphD, shows a lower level of homology to possible eukaryotic ancestor proteins, whereas group 1 seems to be more conserved and shows high homology to members of HDAC class II. The fact that HDAC-like proteins are widely distributed within the genus, strongly suggests that they have an important role in the life cycle of the bacteria.

The aim of my PhD thesis was to characterize the role and function of LphD during infection and to assess whether it acts in synergy with RomA to modify histone and alter gene transcription. HDACs have been described before as targets of a variety of pathogens to manipulate their host and ensure their own survival (An et al., 2018; Ganesan et al., 2017; Grabiec and Potempa, 2018; He et al., 2017; Kong et al., 2017; Murata et al., 2012; Rennoll-Bankert et al., 2015; Terhune et al., 2010; Walters et al., 2010; Wang et al., 2005; Zhou et al., 2011). However, very rarely it has been shown that pathogens encode their own HDAC-like proteins to directly manipulate the host. One recently published example is Gc-HDAC, an HDAC-like protein encoded by *Neisseria gonorrhoeae* that interferes with epigenetic modifications at the promoters of certain proinflammatory genes, thereby promoting bacterial immune evasion (Zughaier et al., 2020). In addition, the synergy of LphD and RomA represents the first documented case of two bacterial effectors directly targeting host chromatin and modifying it step-by-step to impede the host cell response to bacterial infection.

First, we assessed the intracellular localization of LphD during infection. We demonstrated that LphD is indeed secreted during infection in a Dot/Icm-dependent manner and it localizes to the host cell nucleus. However, the exact mechanism of nuclear localization is not known yet. The protein encodes a putative nuclear localization signal (NLS) predicted in the N-terminal part (amino acids 2-22), however we confirmed that the deletion of this signal does not influence the localization of the protein. We cannot exclude the presence of another NLS not detected by classical NLS-finding algorithms, and additional experiments on truncated version of the protein must be performed to clearly define how LphD might actively reach the nucleus. In fact, to exert their functions, almost all eukaryotic class I HDACs need to be in the

nucleus, but this localization not always occurs via an NLS: some of them reach the nucleus together with other proteins/HDACs. One example is HDAC3 that is recruited by HDACs 4, 5 and 7 through complex formation via SMRT and No-CoR (Fischle et al., 2001; Yang et al., 2002).

HDAC translocation, especially HDAC class IIa, is also regulated by serine phosphorylation. It has been shown for several eukaryotic HDACs that their intracellular localization is dependent on protein kinases, such as CaMKII (Ca^{2+}/calmodulin-dependent protein kinase), and phosphatases like PP2A (protein phosphatase 2) (Martin et al., 2008; McKinsey et al., 2000; Paroni et al., 2008). LphD contains several possible phosphorylation sites and their involvement in nuclear transport could be assessed by using phosphoablation mutants. Another regulator of HDAC nuclear import is CSE1L (chromosome segregation 1 like): CSE1L has been reported to export importin α from the nucleus to the cytoplasm, where it can bind NLS-containing proteins, enabling a new cycle of nuclear transport (Cook et al., 2005; Kutay et al., 1997; Stewart, 2007). It was shown that if CSE1L expression is downregulated, HDAC1/2/8 mislocalized to the cytoplasm. However, other HDACs (HDAC3/5/10) – also containing NLS – do not change their localization during CSE1L depletion (Dong et al., 2018). The exact mechanism of this phenotype is yet to be understood. Nonetheless, determining the possible involvement of CSE1L on the intracellular localization of LphD might give us a better understanding how the protein targets the nucleus and elucidate the possible involvement of importin α in this process.

Next, we analyzed the HDAC domain sequence of LphD. Several amino acids are conserved in LphD, when compared to its eukaryotic counterparts. One of these conserved amino acids is the catalytic site tyrosine (Y392). In addition, several other amino acid residues, all part of the so-called charge relay system (Uba and Yelekçi, 2017) – a crucial component of HDAC catalysis – are conserved in LphD. Moreover, when using the AlphaFold 2 model of LphD, we can see that all these conserved residues (H177/178, D216/330, N218, Y248/392) localize in what is predicted to be the binding pocket of the enzyme. These results will be confirmed as soon as we obtain the crystal structure of LphD. For the moment we are focusing on crystalizing LphD in presence of TSA, however, it would be interesting – as a next step – to co-crystalize the catalytic inactive form of LphD (Y392F) with an H3 peptide, corresponding to the N-terminal histone tail.

We then could show that purified LphD has lysine deacetylase activity in an *in vitro* assay and that this activity is indeed dependent on the predicted catalytic tyrosine, Y392. To determine which histone residue is targeted by LphD, we set up a collaboration with Jérémy

Berthelet and Fernando Rodrigues-Lima. Using fluorescently-tagged acetylated histone peptides and incubating them with purified LphD or a catalytic inactive mutant (LphD Y392F), followed by HPLC analysis, they could determine that LphD shows the highest efficiency for H3K14, when compared to other known acetylation marks of H3 (K4, K9, K18, K23, K27). However, this experiment does not exclude the possibility of LphD targeting residues on other histone proteins. This aspect of LphD might raise new questions, since this activity would be completely independent of the activity of RomA, which is limited in its activity on histones to H3K14 (Rolando et al., 2013). Also, non-histone targets should be investigated, since it is known that HDAC activity, contrary to their name, is not limited to histones. The best understood example of HDACs targeting non-histone proteins is HDAC6, which deacetylates α-tubulin, thereby regulating chemotactic cell movement and cell motility (Hubbert et al., 2002). We also see an example for non-histone targeting with RomA, which was shown to methylate AROS, a regulator of histone deacetylase SIRT1 (Schuhmacher et al., 2018).

We next assessed the influence of LphD on bacterial virulence and determine its possible synergy with RomA. For this, we demonstrated that a Δ*lphD* strain shows a slight reduction in virulence as seen in replication assays in *A. castellanii* as well as human THP-1 cells. In addition, the complementation of this knockout actually led to an increase in virulence, further supporting the idea of the importance of LphD in *L. pneumophila* replication. To get a better understanding of the synergy between the two bacterial effectors we compared the deacetylation and methylation of H3K14 in cells infected with wild type *L. pneumophila* or the Δ*lphD* strain. In wild type infected cells, we could see a LphD-dependent decrease in acetylation, specifically of H3K14. Moreover, the Δ*lphD* strain shows a drastic impediment not only in H3K14 acetylation, but also in its methylation, which further supports the theory of synergistic effects between LphD and RomA. However, it is not known how the secretion of these two effectors is regulated and timed. A recent publication shows that effector secretion might be regulated by c-di-GMP levels and that the secretion is following the functional consequence of the effectors and that it is independent of effector concentration (Allombert et al., 2021). Nonetheless, there are still many questions that remain unanswered concerning effector secretion regulation and little is known about this process (Kim et al., 2020; Meir et al., 2020). Two-component systems like LetAS and PmrAB have been implicated to regulate the expression of specific effectors (Segal, 2013), and Dot/Icm components like IcmS and IcmW have been shown to control the secretion of specific subsets of effectors (Cambronne and Roy, 2007). However, due to the low abundance of effectors and the small amounts that are secreted during infection, it is very difficult to determine secretion kinetics without

artificially over-expressing the protein in question. Nonetheless, the prospect of a possible timed secretion of LphD and RomA, to first facilitate deacetylation of H3K14, followed by its methylation, represents a unique opportunity to assess secretion regulation in *L. pneumophila*.

To determine possible eukaryotic interaction partners, we transfected HEK293T cells with GFP or a GFP-LphD fusion construct, pulled down GFP proteins with GFP-trap beads, and analyzed those pulldowns by MS/MS for bound eukaryotic proteins. This led to the identification of KAT7, a histone acetyltransferase known to target H3K14, in a complex called HBO1 (Kueh et al., 2011). KAT7 activity is connected to the promotor regions of highly transcribed genes and has recently been shown to have a wide variety of activities besides histone acetylation, for example histone propionylation and histone butyrylation (Partridge et al., 2020; Xiao et al., 2021). The interaction of LphD, as well as RomA, with KAT7 and other components of the HBO1 complex was confirmed in transfection followed by co-IP. In addition, the interaction of KAT7 with both bacterial effectors was also shown during infection. Interestingly, in transfection experiments RomA seems not to bind every component of the complex, like LphD does. The reason for this is still unknown, but one possible explanation could be that the binding of RomA initiates structural changes in the HBO1 complex, either through its binding directly or through PTMs, leading to the loss of different components of the complex. This hypothesis could be tested by transfecting cells with RomA and performing co-IPs targeting the different components of the HBO1 complex and determining possible changes in its composition.

Moreover, a possible regulation of KAT7 activity by the two bacterial effectors cannot be excluded. Not much is known about the regulation of KAT7 activity, however, the activity of its homologue KAT8, was shown to be regulated by autoacetylation of a lysine residue, which is conserved in KAT7 (Sun et al., 2011; Yuan et al., 2012). As mentioned before, the investigation of non-histone targets of LphD could lead to very interesting results, and KAT7 could be one of those non-histone targets. It might be possible that LphD is not only hijacking the HBO1 complex to target the host chromatin, but in addition, deacetylates and thereby inactivates KAT7 to further impede histone acetylation. This multifunctional approach of LphD could ensure to minimize histone acetylation as efficiently as possible, thus promoting the subsequent methylation. In addition, other complexes connected to epigenetic regulation, like NuRD and Sin3A, have been identified during the GFP-pulldown. These complexes are known to contain eukaryotic HDACs, so they represent promising interaction partners of LphD (Adams et al., 2018; Torchy et al., 2015). Further experiments are necessary to investigate the possible interplay of LphD with these complexes.

The analysis of the RNA-seq experiments revealed drastic changes in the host's transcriptional response to *L. pneumophila* infection. However, if we compare up- and down-regulated genes at these early stages of infection we can see that the up-regulation seems more robust, with around half of the genes being shared between the last three time points and a quarter shared between all time points. Whereas, in the group of down-regulated genes, genes unique for each time point represent the biggest groups. This indicates that the process of transcriptional up-regulation in response to an infection is highly organized and comprises a core set of genes involved in the immune response, a behavior that cannot be seen in the down-regulated genes. The analysis of enriched GO terms (biological process) for the 100 most up- and down-regulated genes only further supports this idea. For the up-regulation we see a strong enrichment in GO terms related to immune response with the biggest set of unique GO terms at 1 h post-infection. This set includes terms related to CD4+ T cell differentiation, a previously described phenomenon in *L. pneumophila* infection (Trunk and Oxenius, 2012). Interestingly, another enriched GO term at early time points is "response to mechanical stimulus". However, this can be easily explained if we look at the genes attributed to this GO term. "Response to mechanical stimulus" includes genes such as CXCL10, NFKBIA (NF-κB inhibitor a) and IL1B, all of which can also be assigned to other, more expected GO terms. Later time points focus on overall immune response processes, such as interferon gamma production and regulation, as well as leukocyte migration. The results of this RNA-seq, concerning the reaction of the cell to an infection by *L. pneumophila* provide exciting insight into the early processes during bacterial invasion. Moreover, the cornucopia of results provided by these experiments can be used to further investigate the interplay between *L. pneumophila* and its host on a transcriptional level.

Although we show a clear synergy between LphD and RomA, this does not limit the possible interactions to these two proteins. *L. pneumophila* encodes several other putative nucleomodulins that might target histones. These putative secreted effectors are part of the PRMT (protein arginine methyl-transferase), DOT1 (histone lysine methyltranferase), HAT (histone acetyltransferases), and LSD1 (lysine-demethylase) families and could be part of a bigger interaction network of secreted effectors all targeting the host cell nucleus. The possible synergy of LphD with any of these effectors should be assessed to get a better understanding of LphD beyond its synergy with RomA.

Another aspect of this project that could be further investigated is the role of LphD and RomA during the infection of amoebae. We could clearly see a growth defect of the Δ*lphD* strain in *A. castellanii*, however no further experiments were possible due to the limited resources available for amoebae. Moreover, very little is known about the epigenetic landscape

of *A. castellanii*, and even less is known about its regulation. A more thorough examination of the role of LphD and RomA in this context, could reveal new exciting results on how the bacteria manipulate different hosts with the same set of effectors.

Taken together, the results of my PhD work have, on one hand, brought new insight in how bacterial pathogens – in this case *L. pneumophila* – manipulate the chromatin landscape of the host cell, and, on the other hand, opened many new and exciting questions regarding the exact molecular mechanism. Answers to these questions might not only elucidate how pathogens manipulate host cell functions, but also contribute to discovering new host cell pathways. Moreover, the identification of new bacterial activities modifying host chromatin will help us to better understand the strategies employed by *L. pneumophila*, and possibly other bacteria, to modulate the host response for its advantage. Furthermore, inhibiting these chromatin modifying activities could represent a promising new target to treat bacterial infections, considering the ever-growing threat of antibiotic resistances.

References

Abu-Zant, A., Jones, S., Asare, R., Suttles, J., Price, C., Graham, J., and Kwaik, Y.A. (2007). Anti-apoptotic signalling by the Dot/Icm secretion system of L. pneumophila. Cell. Microbiol. *9*, 246–264.

Adams, G.E., Chandru, A., and Cowley, S.M. (2018). Co-repressor, co-activator and general transcription factor: the many faces of the Sin3 histone deacetylase (HDAC) complex. Biochem. J. *475*, 3921–3932.

Al-Quadan, T., Price, C.T., and Abu Kwaik, Y. (2012). Exploitation of evolutionarily conserved amoeba and mammalian processes by Legionella. Trends Microbiol. *20*, 299–306.

Alberts, B., Johnson, A., Lewis, J., Raff, M., Roberts, K., and Walter, P. (2002). Chromosomal DNA and Its Packaging in the Chromatin Fiber. In Molecular Biology of the Cell. 4th Edition., (Garland Science), p.

Alli, O.A., Gao, L.Y., Pedersen, L.L., Zink, S., Radulic, M., Doric, M., and Abu Kwaik, Y. (2000). Temporal pore formation-mediated egress from macrophages and alveolar epithelial cells by Legionella pneumophila. Infect. Immun. *68*, 6431–6440.

Allombert, J., Jaboulay, C., Michard, C., Andréa, C., Charpentier, X., Vianney, A., and Doublet, P. (2021). Deciphering Legionella effector delivery by Icm/Dot secretion system reveals a new role for c-diGMP signaling. BioRxiv 754762.

Alvarez, M.C., Ladeira, M.S.P., Scaletsky, I.C.A., Pedrazzoli, J., and Ribeiro, M.L. (2013). Methylation pattern of THBS1, GATA-4, and HIC1 in pediatric and adult patients infected with Helicobacter pylori. Dig. Dis. Sci. *58*, 2850–2857.

Amor, J.C., Swails, J., Zhu, X., Roy, C.R., Nagai, H., Ingmundson, A., Cheng, X., and Kahn, R.A. (2005). The structure of RalF, an ADP-ribosylation factor guanine nucleotide exchange factor from Legionella pneumophila, reveals the presence of a cap over the active site. J. Biol. Chem. *280*, 1392–1400.

Ampel, N.M., Ruben, F.L., and Norden, C.W. (1985). Cutaneous Abscess Caused by Legionella micdadei in an Immunosuppressed Patient. Ann. Intern. Med. *102*, 630.

An, R., Tang, Y., Chen, L., Cai, H., Lai, D.-H., Liu, K., Wan, L., Gong, L., Yu, L., Luo, Q., et al. (2018). Encephalitis is mediated by ROP18 of *Toxoplasma gondii* , a severe pathogen in AIDS patients. Proc. Natl. Acad. Sci. *115*, E5344–E5352.

Anand, C.M., Skinner, A.R., Malic, A., and Kurtz, J.B. (1983). Interaction of L. pneumophilia and a free living amoeba (Acanthamoeba palestinensis). J. Hyg. (Lond). *91*, 167–178.

Arasaki, K., and Tagaya, M. (2017). Legionella blocks autophagy by cleaving STX17 (syntaxin 17). Autophagy *13*, 2008–2009.

Arbibe, L., Kim, D.W., Batsche, E., Pedron, T., Mateescu, B., Muchardt, C., Parsot, C., and Sansonetti, P.J. (2007). An injected bacterial effector targets chromatin access for transcription factor NF-κB to alter transcription of host genes involved in immune responses. Nat. Immunol. *8*, 47–56.

Arents, G., and Moudrianakis, E.N. (1993). Topography of the histone octamer surface: repeating structural motifs utilized in the docking of nucleosomal DNA. Proc. Natl. Acad. Sci. U. S. A. *90*, 10489–10493.

Aurass, P., Gerlach, T., Becher, D., Voigt, B., Karste, S., Bernhardt, J., Riedel, K., Hecker, M., and Flieger, A. (2016). Life Stage-specific Proteomes of Legionella pneumophila Reveal a Highly Differential Abundance of Virulence-associated Dot/Icm effectors. Mol. Cell. Proteomics *15*, 177–200.

Baldi, S., Korber, P., and Becker, P.B. (2020). Beads on a string-nucleosome array arrangements and folding of the chromatin fiber. Nat. Struct. Mol. Biol. *27*, 109–118.

Bangsborg, J.M., Uldum, S., Jensen, J.S., and Bruun, B.G. (1995). Nosocomial legionellosis in three heart-lung transplant patients: Case reports and environmental observations. Eur. J. Clin. Microbiol. Infect. Dis. *14*, 99–104.

Barbaree, J.M., Fields, B.S., Feeley, J.C., Gorman, G.W., and Martin, W.T. (1986). Isolation of protozoa from water associated with a legionellosis outbreak and demonstration of intracellular multiplication of Legionella pneumophila. Appl. Environ. Microbiol. *51*, 422–424.

Bargellini, A., Marchesi, I., Marchegiano, P., Richeldi, L., Cagarelli, R., Ferranti, G., and Borella, P. (2013). A culture-proven case of community-acquired legionella pneumonia apparently classified as nosocomial: diagnostic and public health implications. Case Rep. Med. *2013*, 303712.

Barton, M., McKelvie, B., Campigotto, A., and Mullowney, T. (2017). Legionellosis following water birth in a hot tub in a Canadian neonate. CMAJ *189*, E1311–E1313.

von Baum, H., Ewig, S., Marre, R., Suttorp, N., Gonschior, S., Welte, T., Lück, C., and Group, C.N. for C.A.P.S. (2008). Community-Acquired *Legionella* Pneumonia: New Insights from the German Competence Network for Community Acquired Pneumonia. Clin. Infect. Dis. *46*, 1356–1364.

Bellinger-Kawahara, C., and Horwitz, M.A. (1990). Complement component C3 fixes selectively to the major outer membrane protein (MOMP) of Legionella pneumophila and mediates phagocytosis of liposome-MOMP complexes by human monocytes. J. Exp. Med. *172*, 1201–1210.

Belotserkovskaya, R., Oh, S., Bondarenko, V.A., Orphanides, G., Studitsky, V.M., and Reinberg, D. (2003). FACT Facilitates Transcription-Dependent Nucleosome Alteration. Science (80-.). *301*, 1090–1093.

Benitez, A.J., and Winchell, J.M. (2016). Rapid detection and typing of pathogenic nonpneumophila Legionella spp. isolates using a multiplex real-time PCR assay. Diagn. Microbiol. Infect. Dis. *84*, 298–303.

Berger, K.H., and Isberg, R.R. (1993). Two distinct defects in intracellular growth complemented by a single genetic locus in Legionella pneumophila. Mol. Microbiol. *7*, 7–19.

Best, A., Price, C., Ozanic, M., Santic, M., Jones, S., and Abu Kwaik, Y. (2018). A Legionella pneumophila amylase is essential for intracellular replication in human macrophages and amoebae. Sci. Rep. *8*, 6340.

Bierne, H., and Cossart, P. (2012). When bacteria target the nucleus: the emerging family of nucleomodulins. Cell. Microbiol. *14*, 622–633.

Bierne, H., and Pourpre, R. (2020). Bacterial Factors Targeting the Nucleus: The Growing Family of Nucleomodulins. Toxins (Basel). *12*.

Bierne, H., Tham, T.N., Batsche, E., Dumay, A., Leguillou, M., Kernéis-Golsteyn, S., Regnault, B., Seeler, J.S., Muchardt, C., Feunteun, J., et al. (2009). Human BAHD1 promotes heterochromatic gene silencing. Proc. Natl. Acad. Sci. U. S. A. *106*, 13826–13831.

Bird, A. (2007). Perceptions of epigenetics. Nature *447*, 396–398.

Böck, D., Hüsler, D., Steiner, B., Medeiros, J.M., Welin, A., Radomska, K.A., Hardt, W.-D., Pilhofer, M., and Hilbi, H. (2021). The Polar Legionella Icm/Dot T4SS Establishes Distinct Contact Sites with the Pathogen Vacuole Membrane. MBio *12*, e0218021.

Bourquin, F., Riezman, H., Capitani, G., and Grütter, M.G. (2010). Structure and function of sphingosine-1-phosphate lyase, a key enzyme of sphingolipid metabolism. Structure *18*, 1054–1065.

Bozue, J.A., and Johnson, W. (1996). Interaction of Legionella pneumophila with Acanthamoeba castellanii: uptake by coiling phagocytosis and inhibition of phagosome-lysosome fusion. Infect. Immun. *64*, 668–673.

Brabender, W., Hinthorn, D.R., Asher, M., Lindsey, N.J., and Liu, C. (1983). Legionella pneumophila Wound Infection. JAMA J. Am. Med. Assoc. *250*, 3091.

Bradley, B.T., and Bryan, A. (2019). Emerging respiratory infections: The infectious disease pathology of SARS, MERS, pandemic influenza, and Legionella. Semin. Diagn. Pathol. *36*, 152–159.

Brenner, D.J., Steigerwalt, A.G., and McDade, J.E. (1979). Classification of the Legionnaires' Disease Bacterium: Legionella pneumophila, genus novum, species nova, of the Family Legionellaceae, familia nova. Ann. Intern. Med. *90*, 656.

Bruin, J.P., Koshkolda, T., IJzerman, E.P.F., Luck, C., Diederen, B.M.W., Den Boer, J.W., and Mouton, J.W. (2014). Isolation of ciprofloxacin-resistant Legionella pneumophila in a patient with severe pneumonia. J. Antimicrob. Chemother. *69*, 2869–2871.

De Buck, E., Anne, J., and Lammertyn, E. (2007). The role of protein secretion systems in the virulence of the intracellular pathogen Legionella pneumophila. Microbiology *153*, 3948–3953.

Bundock, P., den Dulk-Ras, A., Beijersbergen, A., and Hooykaas, P.J. (1995). Trans-kingdom T-DNA transfer from Agrobacterium tumefaciens to Saccharomyces cerevisiae. EMBO J. *14*, 3206–3214.

Burstein, D., Zusman, T., Degtyar, E., Viner, R., Segal, G., and Pupko, T. (2009). Genome-scale identification of Legionella pneumophila effectors using a machine learning approach. PLoS Pathog. *5*, e1000508.

Burstein, D., Amaro, F., Zusman, T., Lifshitz, Z., Cohen, O., Gilbert, J.A., Pupko, T., Shuman, H.A., and Segal, G. (2016). Genomic analysis of 38 Legionella species identifies large and diverse effector repertoires. Nat. Genet. *48*, 167–175.

Cambronne, E.D., and Roy, C.R. (2007). The Legionella pneumophila IcmSW complex interacts with multiple Dot/Icm effectors to facilitate type IV translocation. PLoS Pathog. *3*, e188.

Cameron, R.L., Pollock, K.G.J., Lindsay, D.S.J., and Anderson, E. (2016). Comparison of Legionella longbeachae and Legionella pneumophila cases in Scotland; implications for diagnosis, treatment and public health response. J. Med. Microbiol. *65*, 142–146.

Campodonico, E.M., Chesnel, L., and Roy, C.R. (2005). A yeast genetic system for the identification and characterization of substrate proteins transferred into host cells by the Legionella pneumophila Dot/Icm system. Mol. Microbiol. *56*, 918–933.

Carratala, J., Gudiol, F., Pallares, R., Dorca, J., Verdaguer, R., Ariza, J., and Manresa, F. (1994). Risk factors for nosocomial Legionella pneumophila pneumonia. Https://Doi.Org/10.1164/Ajrccm.149.3.8118629.

Cazalet, C., Rusniok, C., Brüggemann, H., Zidane, N., Magnier, A., Ma, L., Tichit, M., Jarraud, S., Bouchier, C., Vandenesch, F., et al. (2004). Evidence in the Legionella pneumophila genome for exploitation of host cell functions and high genome plasticity. Nat. Genet. *36*, 1165–1173.

Ceccato, A., Di Giannatale, P., Nogas, S., and Torres, A. (2021). Safety considerations of current drug treatment strategies for nosocomial pneumonia. Expert Opin. Drug Saf. *20*, 181–190.

Chen, J.R., Francisco, R.B., and Miller, T.E. (1977). Legionnaires' disease: nickel levels. Science *196*, 906–908.

Chen, P., Li, W., and Li, G. (2021). Structures and Functions of Chromatin Fibers. Annu. Rev. Biophys. *50*, 95–116.

Cherfils, J., and Zeghouf, M. (2013). Regulation of small GTPases by GEFs, GAPs, and GDIs. Physiol. Rev. *93*,

269–309.
Cianciotto, N.P. (2009). Many substrates and functions of type II secretion: lessons learned from *Legionella pneumophila*. Future Microbiol. *4*, 797–805.
Cianciotto, N.P. (2014). Type II Secretion and Legionella Virulence. In Molecular Mechanisms in Legionella Pathogenesis, H. Hilbi, ed. (Berlin, Heidelberg: Springer Berlin Heidelberg), pp. 81–102.
Cianciotto, N.P., and Fields, B.S. (1992). Legionella pneumophila mip gene potentiates intracellular infection of protozoa and human macrophages. Proc. Natl. Acad. Sci. U. S. A. *89*, 5188–5191.
Collier, S.A., Deng, L., Adam, E.A., Benedict, K.M., Beshearse, E.M., Blackstock, A.J., Bruce, B.B., Derado, G., Edens, C., Fullerton, K.E., et al. (2021). Estimate of Burden and Direct Healthcare Cost of Infectious Waterborne Disease in the United States. Emerg. Infect. Dis. *27*, 140–149.
Collins, S.L., Afshar, B., Walker, J.T., Aird, H., Naik, F., Parry-Ford, F., Phin, N., Harrison, T.G., Chalker, V.J., Sorrell, S., et al. (2016). Heated birthing pools as a source of Legionnaires' disease. Epidemiol. Infect. *144*, 796–802.
Cook, A., Fernandez, E., Lindner, D., Ebert, J., Schlenstedt, G., and Conti, E. (2005). The structure of the nuclear export receptor Cse1 in its cytosolic state reveals a closed conformation incompatible with cargo binding. Mol. Cell *18*, 355–367.
Corpas-López, V., Díaz-Gavilán, M., Franco-Montalbán, F., Merino-Espinosa, G., López-Viota, M., López-Viota, J., Belmonte-Reche, E., Pérez-del Palacio, J., de Pedro, N., Gómez-Vidal, J.A., et al. (2019). A nanodelivered Vorinostat derivative is a promising oral compound for the treatment of visceral leishmaniasis. Pharmacol. Res. *139*, 375–383.
Correia, A.M., Ferreira, J.S., Borges, V., Nunes, A., Gomes, B., Capucho, R., Gonçalves, J., Antunes, D.M., Almeida, S., Mendes, A., et al. (2016). Probable Person-to-Person Transmission of Legionnaires' Disease. N. Engl. J. Med. *374*, 497–498.
Costa, T.R.D., Harb, L., Khara, P., Zeng, L., Hu, B., and Christie, P.J. (2021). Type IV secretion systems: Advances in structure, function, and activation. Mol. Microbiol. *115*, 436–452.
Cross, K.E., Mercante, J.W., Benitez, A.J., Brown, E.W., Diaz, M.H., and Winchell, J.M. (2016). Simultaneous detection of Legionella species and L. anisa, L. bozemanii, L. longbeachae and L. micdadei using conserved primers and multiple probes in a multiplex real-time PCR assay. Diagn. Microbiol. Infect. Dis. *85*, 295–301.
Cunha, B.A., and Cunha, C.B. (2017). Legionnaire's Disease: A Clinical Diagnostic Approach. Infect. Dis. Clin. North Am. *31*, 81–93.
David, S., Rusniok, C., Mentasti, M., Gomez-Valero, L., Harris, S.R., Lechat, P., Lees, J., Ginevra, C., Glaser, P., Ma, L., et al. (2016). Multiple major disease-associated clones of Legionella pneumophila have emerged recently and independently. Genome Res. *26*, 1555–1564.
Derré, I., and Isberg, R.R. (2004). Legionella pneumophila replication vacuole formation involves rapid recruitment of proteins of the early secretory system. Infect. Immun. *72*, 3048–3053.
Dillon, S.C., Zhang, X., Trievel, R.C., and Cheng, X. (2005). The SET-domain protein superfamily: protein lysine methyltransferases. Genome Biol. *6*, 227.
Domínguez, J., Galí, N., Matas, L., Pedroso, P., Hernández, A., Padilla, E., and Ausina, V. (1999). Evaluation of a Rapid Immunochromatographic Assay for the Detection of Legionella Antigen in Urine Samples. Eur. J. Clin. Microbiol. Infect. Dis. *18*, 896–898.
Dong, Q., Li, X., Wang, C.-Z., Xu, S., Yuan, G., Shao, W., Liu, B., Zheng, Y., Wang, H., Lei, X., et al. (2018). Roles of the CSE1L-mediated nuclear import pathway in epigenetic silencing. Proc. Natl. Acad. Sci. U. S. A. *115*, E4013–E4022.
Dournon, E., Bure, A., Kemeny, J.L., Pourriat, J.L., and Valeyre, D. (1982). Legionella pneumophila peritonitis. Lancet *319*, 1363.
Durie, C.L., Sheedlo, M.J., Chung, J.M., Byrne, B.G., Su, M., Knight, T., Swanson, M., Lacy, D.B., and Ohi, M.D. (2020). Structural analysis of the Legionella pneumophila Dot/Icm type IV secretion system core complex. Elife *9*.
Von Dwingelo, J., Chung, I.Y.W., Price, C.T., Li, L., Jones, S., Cygler, M., and Abu Kwaik, Y. (2019). Interaction of the Ankyrin H Core Effector of Legionella with the Host LARP7 Component of the 7SK snRNP Complex. MBio *10*.
Edelstein, P.H. (1984). Laboratory diagnosis of Legionnaires disease. In Legionalla: Proceedings of the 2nd International Symposium, (Washington, DC: American Society for Microbiology), pp. 3–5.
Elliott, J.A., and Winn, W.C. (1986). Treatment of alveolar macrophages with cytochalasin D inhibits uptake and subsequent growth of Legionella pneumophila. Infect. Immun. *51*, 31–36.
Ensminger, A.W. (2016). Legionella pneumophila, armed to the hilt: justifying the largest arsenal of effectors in the bacterial world. Curr. Opin. Microbiol. *29*, 74–80.
Escoll, P., Rolando, M., Gomez-Valero, L., and Buchrieser, C. (2013). From Amoeba to Macrophages: Exploring the Molecular Mechanisms of Legionella pneumophila Infection in Both Hosts. (Springer, Berlin,

Heidelberg), pp. 1–34.
Escoll, P., Mondino, S., Rolando, M., and Buchrieser, C. (2016). Targeting of host organelles by pathogenic bacteria: a sophisticated subversion strategy. Nat. Rev. Microbiol. *14*, 5–19.
Escoll, P., Song, O.-R., Viana, F., Steiner, B., Lagache, T., Olivo-Marin, J.-C., Impens, F., Brodin, P., Hilbi, H., and Buchrieser, C. (2017). Legionella pneumophila Modulates Mitochondrial Dynamics to Trigger Metabolic Repurposing of Infected Macrophages. Cell Host Microbe *22*, 302-316.e7.
Eylert, E., Herrmann, V., Jules, M., Gillmaier, N., Lautner, M., Buchrieser, C., Eisenreich, W., and Heuner, K. (2010). Isotopologue Profiling of Legionella pneumophila: ROLE OF SERINE AND GLUCOSE AS CARBON SUBSTRATES. J. Biol. Chem. *285*, 22232–22243.
Feldman, M., Zusman, T., Hagag, S., and Segal, G. (2005). Coevolution between nonhomologous but functionally similar proteins and their conserved partners in the Legionella pathogenesis system. Proc. Natl. Acad. Sci. U. S. A. *102*, 12206–12211.
de Felipe, K.S., Pampou, S., Jovanovic, O.S., Pericone, C.D., Ye, S.F., Kalachikov, S., and Shuman, H.A. (2005). Evidence for Acquisition of Legionella Type IV Secretion Substrates via Interdomain Horizontal Gene Transfer. J. Bacteriol. *187*, 7716–7726.
Fields, B.S. (1996). The molecular ecology of legionellae. Trends Microbiol. *4*, 286–290.
Fields, B.S., Shotts, E.B., Feeley, J.C., Gorman, G.W., Martin, W.T., and Martin, W.T. (1984). Proliferation of Legionella pneumophila as an intracellular parasite of the ciliated protozoan Tetrahymena pyriformis. Appl. Environ. Microbiol. *47*, 467–471.
Finsel, I., and Hilbi, H. (2015). Formation of a pathogen vacuole according to Legionella pneumophila: how to kill one bird with many stones. Cell. Microbiol. *17*, 935–950.
Fischle, W., Dequiedt, F., Fillion, M., Hendzel, M.J., Voelter, W., and Verdin, E. (2001). Human HDAC7 Histone Deacetylase Activity Is Associated with HDAC3in Vivo. J. Biol. Chem. *276*, 35826–35835.
Flendrie, M., Jeurissen, M., Franssen, M., Kwa, D., Klaassen, C., and Vos, F. (2011). Septic Arthritis Caused by Legionella dumoffii in a Patient with Systemic Lupus Erythematosus-Like Disease. J. Clin. Microbiol. *49*, 746–749.
Fraser, D.W., Tsai, T.R., Orenstein, W., Parkin, W.E., Beecham, H.J., Sharrar, R.G., Harris, J., Mallison, G.F., Martin, S.M., McDade, J.E., et al. (1977). Legionnaires' Disease - Description of an Epidemic of Pneumonia. N. Engl. J. Med. *297*, 1189–1197.
Fraser, T.G., Zembower, T.R., Lynch, P., Fryer, J., Salvalaggio, P.R.O., Yeldandi, A. V, and Stosor, V. (2004). Cavitary Legionella pneumonia in a liver transplant recipient. Transpl. Infect. Dis. *6*, 77–80.
Fu, K.P., and Neu, H.C. (1979). Inactivation of beta-lactam antibiotics by Legionella pneumophila. Antimicrob. Agents Chemother. *16*, 561–564.
Fuche, F., Vianney, A., Andrea, C., Doublet, P., and Gilbert, C. (2015). Functional type 1 secretion system involved in Legionella pneumophila virulence. J. Bacteriol. *197*, 563–571.
Fujitani, S., Sun, H.-Y., Yu, V.L., and Weingarten, J.A. (2011). Pneumonia due to Pseudomonas aeruginosa: part I: epidemiology, clinical diagnosis, and source. Chest *139*, 909–919.
Ganesan, R., Hos, N.J., Gutierrez, S., Fischer, J., Stepek, J.M., Daglidu, E., Krönke, M., and Robinson, N. (2017). Salmonella Typhimurium disrupts Sirt1/AMPK checkpoint control of mTOR to impair autophagy. PLoS Pathog. *13*, e1006227.
Garau, J. (2005). Role of beta-lactam agents in the treatment of community-acquired pneumonia. Eur. J. Clin. Microbiol. Infect. Dis. *24*, 83–99.
García-Fulgueiras, A., Navarro, C., Fenoll, D., García, J., González-Diego, P., Jiménez-Buñuales, T., Rodriguez, M., Lopez, R., Pacheco, F., Ruiz, J., et al. (2003). Legionnaires' disease outbreak in Murcia, Spain. Emerg. Infect. Dis. *9*, 915–921.
Ge, J., Xu, H., Li, T., Zhou, Y., Zhang, Z., Li, S., Liu, L., and Shao, F. (2009). A Legionella type IV effector activates the NF-kappaB pathway by phosphorylating the IkappaB family of inhibitors. Proc. Natl. Acad. Sci. U. S. A. *106*, 13725–13730.
George, J.R., Pine, L., Reeves, M.W., and Harrell, W.K. (1980). Amino acid requirements of Legionella pneumophila. J. Clin. Microbiol. *11*, 286–291.
Ghosal, D., Chang, Y.-W., Jeong, K.C., Vogel, J.P., and Jensen, G.J. (2017). In situ structure of the Legionella Dot/Icm type IV secretion system by electron cryotomography. EMBO Rep. *18*, 726–732.
Ghosh, R.P., Horowitz-Scherer, R.A., Nikitina, T., Shlyakhtenko, L.S., and Woodcock, C.L. (2010). MeCP2 Binds Cooperatively to Its Substrate and Competes with Histone H1 for Chromatin Binding Sites. Mol. Cell. Biol. *30*, 4656–4670.
Gibson, F.C., Tzianabos, A.O., and Rodgers, F.G. (1994). Adherence of Legionella pneumophila to U-937 cells, guinea-pig alveolar macrophages, and MRC-5 cells by a novel, complement-independent binding mechanism. Can. J. Microbiol. *40*, 865–872.
Gillmaier, N., Schunder, E., Kutzner, E., Tlapák, H., Rydzewski, K., Herrmann, V., Stämmler, M., Lasch, P., Eisenreich, W., and Heuner, K. (2016). Growth-related Metabolism of the Carbon Storage Poly-3-

hydroxybutyrate in Legionella pneumophila. J. Biol. Chem. *291*, 6471–6482.
Glick, T.H., Gregg, M.B., Berman, B., Mallison, G., Rhodes, W.W., and Kassanoff, I. (1978). Pontiac fever: an epidemic of unknown etiology in a health department. Am. J. Epidemiol. *107*, 149–160.
Gomez-Valero, L., Rusniok, C., Cazalet, C., and Buchrieser, C. (2011). Comparative and functional genomics of legionella identified eukaryotic like proteins as key players in host-pathogen interactions. Front. Microbiol. *2*, 208.
Gomez-Valero, L., Rusniok, C., Carson, D., Mondino, S., Pérez-Cobas, A.E., Rolando, M., Pasricha, S., Reuter, S., Demirtas, J., Crumbach, J., et al. (2019). More than 18,000 effectors in the Legionella genus genome provide multiple, independent combinations for replication in human cells. Proc. Natl. Acad. Sci. U. S. A. *116*, 2265–2273.
Grabiec, A.M., and Potempa, J. (2018). Epigenetic regulation in bacterial infections: targeting histone deacetylases. Crit. Rev. Microbiol. *44*, 336–350.
Graves, J.D., and Krebs, E.G. (1999). Protein phosphorylation and signal transduction. Pharmacol. Ther. *82*, 111–121.
Guy, S.D., Worth, L.J., Thursky, K.A., Francis, P.A., and Slavin, M.A. (2011). Legionella pneumophila lung abscess associated with immune suppression. Intern. Med. J. *41*, 715–721.
Hägele, S., Köhler, R., Merkert, H., Schleicher, M., Hacker, J., and Steinert, M. (2000). Dictyostelium discoideum: a new host model system for intracellular pathogens of the genus Legionella. Cell. Microbiol. *2*, 165–171.
Hai, Y., Shinsky, S.A., Porter, N.J., and Christianson, D.W. (2017). Histone deacetylase 10 structure and molecular function as a polyamine deacetylase. Nat. Commun. *8*, 15368.
Hall, L.L., and Lawrence, J.B. (2010). XIST RNA and architecture of the inactive X chromosome: implications for the repeat genome. Cold Spring Harb. Symp. Quant. Biol. *75*, 345–356.
He, Q., Li, G., Wang, X., Wang, S., Hu, J., Yang, L., He, Y., Pan, Y., Yu, D., and Wu, Y. (2017). A Decrease of Histone Deacetylase 6 Expression Caused by Helicobacter Pylori Infection is Associated with Oncogenic Transformation in Gastric Cancer. Cell. Physiol. Biochem. *42*, 1326–1335.
Heidtman, M., Chen, E.J., Moy, M.-Y., and Isberg, R.R. (2009). Large-scale identification of *Legionella pneumophila* Dot/Icm substrates that modulate host cell vesicle trafficking pathways. Cell. Microbiol. *11*, 230–248.
Herrmann, V., Eidner, A., Rydzewski, K., Blädel, I., Jules, M., Buchrieser, C., Eisenreich, W., and Heuner, K. (2011). GamA is a eukaryotic-like glucoamylase responsible for glycogen- and starch-degrading activity of Legionella pneumophila. Int. J. Med. Microbiol. *301*, 133–139.
Hiller, M., Lang, C., Michel, W., and Flieger, A. (2018). Secreted phospholipases of the lung pathogen Legionella pneumophila. Int. J. Med. Microbiol. *308*.
Horwitz, M.A. (1984). Phagocytosis of the Legionnaires' disease bacterium (Legionella pneumophila) occurs by a novel mechanism: engulfment within a pseudopod coil. Cell *36*, 27–33.
Huang, L., Boyd, D., Amyot, W.M., Hempstead, A.D., Luo, Z.-Q., O'Connor, T.J., Chen, C., Machner, M., Montminy, T., and Isberg, R.R. (2011). The E Block motif is associated with Legionella pneumophila translocated substrates. Cell. Microbiol. *13*, 227–245.
Hubber, A., and Roy, C.R. (2010). Modulation of Host Cell Function by *Legionella pneumophila* Type IV Effectors. Annu. Rev. Cell Dev. Biol. *26*, 261–283.
Hubbert, C., Guardiola, A., Shao, R., Kawaguchi, Y., Ito, A., Nixon, A., Yoshida, M., Wang, X.-F., and Yao, T.-P. (2002). HDAC6 is a microtubule-associated deacetylase. Nature *417*, 455–458.
Husmann, L.K., and Johnson, W. (1992). Adherence of Legionella pneumophila to guinea pig peritoneal macrophages, J774 mouse macrophages, and undifferentiated U937 human monocytes: role of Fc and complement receptors. Infect. Immun. *60*, 5212–5218.
Ibranosyan, M., Beraud, L., Lemaire, H., Ranc, A.-G., Ginevra, C., Jarraud, S., and Descours, G. (2019). The clinical presentation of Legionella arthritis reveals the mode of infection and the bacterial species: case report and literature review. BMC Infect. Dis. *19*, 864.
Isberg, R.R., O'Connor, T.J., and Heidtman, M. (2009). The Legionella pneumophila replication vacuole: making a cosy niche inside host cells. Nat. Rev. Microbiol. *7*, 13–24.
Izzo, A., Kamieniarz, K., and Schneider, R. (2008). The histone H1 family: specific members, specific functions? *389*, 333–343.
Jaulhac, B., Nowicki, M., Bornstein, N., Meunier, O., Prevost, G., Piemont, Y., Fleurette, J., and Monteil, H. (1992). Detection of Legionella spp. in bronchoalveolar lavage fluids by DNA amplification. J. Clin. Microbiol. *30*, 920–924.
Jeong, K.C., Ghosal, D., Chang, Y.-W., Jensen, G.J., and Vogel, J.P. (2017). Polar delivery of Legionella type IV secretion system substrates is essential for virulence. Proc. Natl. Acad. Sci. U. S. A. *114*, 8077–8082.
Jia, X., Ren, H., Nie, X., Li, Y., Li, J., and Qin, T. (2019). Antibiotic Resistance and Azithromycin Resistance Mechanism of Legionella pneumophila Serogroup 1 in China. Antimicrob. Agents Chemother. *63*.

Jones, P.A. (2012). Functions of DNA methylation: islands, start sites, gene bodies and beyond. Nat. Rev. Genet. *13*, 484–492.

Jose, L., Ramachandran, R., Bhagavat, R., Gomez, R.L., Chandran, A., Raghunandanan, S., Omkumar, R.V., Chandra, N., Mundayoor, S., and Kumar, R.A. (2016). Hypothetical protein Rv3423.1 of *Mycobacterium tuberculosis* is a histone acetyltransferase. FEBS J. *283*, 265–281.

Jumper, J., Evans, R., Pritzel, A., Green, T., Figurnov, M., Ronneberger, O., Tunyasuvunakool, K., Bates, R., Žídek, A., Potapenko, A., et al. (2021). Highly accurate protein structure prediction with AlphaFold. Nature *596*, 583–589.

Kagan, J.C., Stein, M.-P., Pypaert, M., and Roy, C.R. (2004). Legionella subvert the functions of Rab1 and Sec22b to create a replicative organelle. J. Exp. Med. *199*, 1201–1211.

Kao, W.-F., Wang, J.-T., Sheng, W.-H., and Chen, Y.-C. (2019). Community-acquired Legionnaires' disease at a medical center in northern Taiwan. J. Microbiol. Immunol. Infect. *52*, 465–470.

Kaufmann, A.F., McDade, J.E., Patton, C.M., Bennett, J. V., Skaliy, P., Feeley, J.C., Anderson, D.C., Potter, M.E., Newhouse, V.F., Gregg, M.B., et al. (1981). Pontiac fever: isolation of the etiologic agent (Legionella pneumophila) and demonstration of its mode of transmission. Am. J. Epidemiol. *114*, 337–347.

Kelley, L.A., Mezulis, S., Yates, C.M., Wass, M.N., and Sternberg, M.J.E. (2015). The Phyre2 web portal for protein modeling, prediction and analysis. Nat. Protoc. *10*, 845–858.

Khokher, W., Kesireddy, N., Adunse, J., Mudiyanselage, P.H., Iftikhar, S., and Assaly, R. (2021). Legionella pneumophila as a cause of cavitary lung disease in systemic lupus erythematous. Lupus *30*, 1010–1012.

Kim, H., Kubori, T., Yamazaki, K., Kwak, M.-J., Park, S.-Y., Nagai, H., Vogel, J.P., and Oh, B.-H. (2020). Structural basis for effector protein recognition by the Dot/Icm Type IVB coupling protein complex. Nat. Commun. *11*, 2623.

Kimura, H. (2013). Histone modifications for human epigenome analysis. J. Hum. Genet. *58*, 439–445.

King, C.H., Fields, B.S., Shotts, E.B., and White, E.H. (1991). Effects of cytochalasin D and methylamine on intracellular growth of Legionella pneumophila in amoebae and human monocyte-like cells. Infect. Immun. *59*, 758–763.

Kitabayashi, J., Shirasaki, T., Shimakami, T., Nishiyama, T., Welsch, C., Funaki, M., Murai, K., Sumiyadorj, A., Takatori, H., Kitamura, K., et al. (2020). Upregulation of the Long Noncoding RNA HULC by Hepatitis C Virus and Its Regulation of Viral Replication. J. Infect. Dis.

Kohler, R.B., Zimmerman, S.E., Wilson, E., Allen, S.D., Edelstein, P.H., Wheat, L.J., and White, A. (1981). Rapid radioimmunoassay diagnosis of Legionnaires' disease: detection and partial characterization of urinary antigen. Ann. Intern. Med. *94*, 601–605.

Kong, L., Qiu, X., Kang, J., Wang, Y., Chen, H., Huang, J., Qiu, M., Zhao, Y., Kong, G., Ma, Z., et al. (2017). A Phytophthora Effector Manipulates Host Histone Acetylation and Reprograms Defense Gene Expression to Promote Infection. Curr. Biol. *27*, 981–991.

Krinos, C., High, A.S., and Rodgers, F.G. (1999). Role of the 25 kDa major outer membrane protein of Legionella pneumophila in attachment to U-937 cells and its potential as a virulence factor for chick embryos. J. Appl. Microbiol. *86*, 237–244.

Kueh, A.J., Dixon, M.P., Voss, A.K., and Thomas, T. (2011). HBO1 is required for H3K14 acetylation and normal transcriptional activity during embryonic development. Mol. Cell. Biol. *31*, 845–860.

Kuiper, M.W., Wullings, B.A., Akkermans, A.D.L., Beumer, R.R., and van der Kooij, D. (2004). Intracellular Proliferation of *Legionella pneumophila* in *Hartmannella vermiformis* in Aquatic Biofilms Grown on Plasticized Polyvinyl Chloride. Appl. Environ. Microbiol. *70*, 6826–6833.

Kutay, U., Bischoff, F.R., Kostka, S., Kraft, R., and Görlich, D. (1997). Export of importin alpha from the nucleus is mediated by a specific nuclear transport factor. Cell *90*, 1061–1071.

Kyung Lee, M., Armstrong, D.A., Hazlett, H.F., Dessaint, J.A., Mellinger, D.L., Aridgides, D.S., Christensen, B.C., and Ashare, A. (2020). Exposure to extracellular vesicles from Pseudomonas aeruginosa result in loss of DNA methylation at enhancer and DNase hypersensitive site regions in lung macrophages. Epigenetics 1–14.

L, X., X, S., A, B., S, B., MS, S., and ZQ, L. (2010). Inhibition of host vacuolar H+-ATPase activity by a Legionella pneumophila effector. PLoS Pathog. *6*.

Lang, C., Hiller, M., and Flieger, A. (2017). Disulfide loop cleavage of Legionella pneumophila PlaA boosts lysophospholipase A activity. Sci. Rep. *7*, 16313.

Lawrence, M., Daujat, S., and Schneider, R. (2016). Lateral Thinking: How Histone Modifications Regulate Gene Expression. Trends Genet. *32*, 42–56.

Lebreton, A., Lakisic, G., Job, V., Fritsch, L., Tham, T.N., Camejo, A., Matteï, P.-J., Regnault, B., Nahori, M.-A., Cabanes, D., et al. (2011). A Bacterial Protein Targets the BAHD1 Chromatin Complex to Stimulate Type III Interferon Response. Science (80-.). *331*, 1319–1321.

Li, T., Lu, Q., Wang, G., Xu, H., Huang, H., Cai, T., Kan, B., Ge, J., and Shao, F. (2013). SET-domain bacterial effectors target heterochromatin protein 1 to activate host rDNA transcription. EMBO Rep. *14*, 733–740.

Lifshitz, Z., Burstein, D., Peeri, M., Zusman, T., Schwartz, K., Shuman, H.A., Pupko, T., and Segal, G. (2013). Computational modeling and experimental validation of the Legionella and Coxiella virulence-related type-IVB secretion signal. Proc. Natl. Acad. Sci. U. S. A. *110*, E707-15.

Losick, V.P., and Isberg, R.R. (2006). NF-kappaB translocation prevents host cell death after low-dose challenge by Legionella pneumophila. J. Exp. Med. *203*, 2177–2189.

Lowry, P.W., Blankenship, R.J., Gridley, W., Troup, N.J., and Tompkins, L.S. (1991). A Cluster of Legionella Sternal-Wound Infections Due to Postoperative Topical Exposure to Contaminated Tap Water. N. Engl. J. Med. *324*, 109–113.

Luger, K., Mäder, A.W., Richmond, R.K., Sargent, D.F., and Richmond, T.J. (1997). Crystal structure of the nucleosome core particle at 2.8 Å resolution. Nature *389*, 251–260.

Lurie-Weinberger, M.N., Gomez-Valero, L., Merault, N., Glöckner, G., Buchrieser, C., and Gophna, U. (2010). The origins of eukaryotic-like proteins in Legionella pneumophila. Int. J. Med. Microbiol. *300*, 470–481.

Lyko, F. (2018). The DNA methyltransferase family: a versatile toolkit for epigenetic regulation. Nat. Rev. Genet. *19*, 81–92.

Mariner, P.D., Walters, R.D., Espinoza, C.A., Drullinger, L.F., Wagner, S.D., Kugel, J.F., and Goodrich, J.A. (2008). Human Alu RNA is a modular transacting repressor of mRNA transcription during heat shock. Mol. Cell *29*, 499–509.

Marra, A., Blander, S.J., Horwitz, M.A., and Shuman, H.A. (1992). Identification of a Legionella pneumophila locus required for intracellular multiplication in human macrophages. Proc. Natl. Acad. Sci. U. S. A. *89*, 9607–9611.

Marrie, T.J., and Hoffman, P.S. (2011). Legionellosis. Trop. Infect. Dis. Princ. Pathog. Pract. 215–218.

Martin, M., Potente, M., Janssens, V., Vertommen, D., Twizere, J.-C., Rider, M.H., Goris, J., Dimmeler, S., Kettmann, R., and Dequiedt, F. (2008). Protein phosphatase 2A controls the activity of histone deacetylase 7 during T cell apoptosis and angiogenesis. Proc. Natl. Acad. Sci. *105*, 4727 LP – 4732.

Mastroeni, D., Grover, A., Delvaux, E., Whiteside, C., Coleman, P.D., and Rogers, J. (2010). Epigenetic changes in Alzheimer's disease: decrements in DNA methylation. Neurobiol. Aging *31*, 2025–2037.

McDade, J.E., Shepard, C.C., Fraser, D.W., Tsai, T.R., Redus, M.A., and Dowdle, W.R. (1977). Legionnaires' disease: isolation of a bacterium and demonstration of its role in other respiratory disease. N. Engl. J. Med. *297*, 1197–1203.

McDade, J.E., Brenner, D.J., and Bozeman, F.M. (1979). Legionnaires' Disease Bacterium Isolated in 1947. Ann. Intern. Med. *90*, 659.

McGhee, J.D., Nickol, J.M., Felsenfeld, G., and Rau, D.C. (1983). Higher order structure of chromatin: Orientation of nucleosomes within the 30 nm chromatin solenoid is independent of species and spacer length. Cell *33*, 831–841.

McKinsey, T.A., Zhang, C.-L., Lu, J., and Olson, E.N. (2000). Signal-dependent nuclear export of a histone deacetylase regulates muscle differentiation. Nature *408*, 106–111.

Meir, A., Macé, K., Lukoyanova, N., Chetrit, D., Hospenthal, M.K., Redzej, A., Roy, C., and Waksman, G. (2020). Mechanism of effector capture and delivery by the type IV secretion system from Legionella pneumophila. Nat. Commun. *11*, 2864.

Melé, M., Mattioli, K., Mallard, W., Shechner, D.M., Gerhardinger, C., and Rinn, J.L. (2017). Chromatin environment, transcriptional regulation, and splicing distinguish lincRNAs and mRNAs. Genome Res. *27*, 27–37.

Mentasti, M., Cassier, P., David, S., Ginevra, C., Gomez-Valero, L., Underwood, A., Afshar, B., Etienne, J., Parkhill, J., Chalker, V., et al. (2017). Rapid detection and evolutionary analysis of Legionella pneumophila serogroup 1 sequence type 47. Clin. Microbiol. Infect. *23*, 264.e1-264.e9.

Mentula, S., Pentikäinen, J., Perola, O., and Ruotsalainen, E. (2014). Legionella longbeachae infection in a persistent hand-wound after a gardening accident. JMM Case Reports *1*, e004374.

Mérault, N., Rusniok, C., Jarraud, S., Gomez-Valero, L., Cazalet, C., Marin, M., Brachet, E., Aegerter, P., Gaillard, J.L., Etienne, J., et al. (2011). Specific Real-Time PCR for Simultaneous Detection and Identification of *Legionella pneumophila* Serogroup 1 in Water and Clinical Samples. Appl. Environ. Microbiol. *77*, 1708–1717.

Mercante, J.W., and Winchell, J.M. (2015). Current and Emerging Legionella Diagnostics for Laboratory and Outbreak Investigations. Clin. Microbiol. Rev. *28*, 95–133.

Mercer, T.R., and Mattick, J.S. (2013). Structure and function of long noncoding RNAs in epigenetic regulation. Nat. Struct. Mol. Biol. *20*, 300–307.

Mercuro, N.J., and Veve, M.P. (2020). Clinical Utility of Lefamulin: If Not Now, When? Curr. Infect. Dis. Rep. *22*, 25.

Ming, X., Zhu, B., and Li, Y. (2021). Mitotic inheritance of DNA methylation: more than just copy and paste. J. Genet. Genomics *48*, 1–13.

Molmeret, M., Horn, M., Wagner, M., Santic, M., and Abu Kwaik, Y. (2005). Amoebae as training grounds for

intracellular bacterial pathogens. Appl. Environ. Microbiol. *71*, 20–28.
Molofsky, A.B., and Swanson, M.S. (2004). Differentiate to thrive: lessons from the Legionella pneumophila life cycle. Mol. Microbiol. *53*, 29–40.
Mondino, S., Schmidt, S., Rolando, M., Escoll, P., Gomez-Valero, L., and Buchrieser, C. (2020a). Legionnaires' Disease: State of the Art Knowledge of Pathogenesis Mechanisms of Legionella. Annu. Rev. Pathol. *15*, 439–466.
Mondino, S., Schmidt, S., and Buchrieser, C. (2020b). Molecular Mimicry: a Paradigm of Host-Microbe Coevolution Illustrated by Legionella. MBio *11*.
Morales, A., Mathur-Wagh, U., Tran, A., Cui, I., DeSimone, R.A., Jenkins, S.G., Westblade, L.F., and Jones, S. (2018). Cavitary Pulmonary Nodules in an Immunocompromised Patient With Urothelial Carcinoma of the Bladder. Clin. Infect. Dis. *67*, 1631–1634.
Morrison, O., and Thakur, J. (2021). Molecular Complexes at Euchromatin, Heterochromatin and Centromeric Chromatin. Int. J. Mol. Sci. *22*.
Moyer, B.D., Allan, B.B., and Balch, W.E. (2001). Rab1 interaction with a GM130 effector complex regulates COPII vesicle cis--Golgi tethering. Traffic *2*, 268–276.
Muder, R.R., and Yu, V.L. (2002). Infection Due to *Legionella* Species Other Than *L. pneumophila*. Clin. Infect. Dis. *35*, 990–998.
Muder, R.R., Yu, V.L., and Fang, G.D. (1989). Community-acquired Legionnaires' disease. Semin. Respir. Infect. *4*, 32–39.
Mujtaba, S., Winer, B.Y., Jaganathan, A., Patel, J., Sgobba, M., Schuch, R., Gupta, Y.K., Haider, S., Wang, R., and Fischetti, V.A. (2013). Anthrax SET protein: a potential virulence determinant that epigenetically represses NF-κB activation in infected macrophages. J. Biol. Chem. *288*, 23458–23472.
Murata, T., Kondo, Y., Sugimoto, A., Kawashima, D., Saito, S., Isomura, H., Kanda, T., and Tsurumi, T. (2012). Epigenetic Histone Modification of Epstein-Barr Virus BZLF1 Promoter during Latency and Reactivation in Raji Cells. J. Virol. *86*, 4752–4761.
Murga, R., Forster, T.S., Brown, E., Pruckler, J.M., Fields, B.S., and Donlan, R.M. (2001). Role of biofilms in the survival of Legionella pneumophila in a model potable-water system. Microbiology *147*, 3121–3126.
Nagai, H., Kagan, J.C., Zhu, X., Kahn, R.A., and Roy, C.R. (2002). A bacterial guanine nucleotide exchange factor activates ARF on Legionella phagosomes. Science *295*, 679–682.
Nagai, H., Cambronne, E.D., Kagan, J.C., Amor, J.C., Kahn, R.A., and Roy, C.R. (2005). A C-terminal translocation signal required for Dot/Icm-dependent delivery of the Legionella RalF protein to host cells. Proc. Natl. Acad. Sci. U. S. A. *102*, 826–831.
Naito, T., Suda, T., Saga, K., Horii, T., and Chida, K. (2007). Reactive Legionella pneumophila arthritis diagnosed by polymerase chain reaction. Rheumatol. Int. *27*, 415–416.
Newsome, A.L., Baker, R.L., Miller, R.D., and Arnold, R.R. (1985). Interactions between Naegleria fowleri and Legionella pneumophila. Infect. Immun. *50*, 449–452.
Newton, H.J., Sansom, F.M., Bennett-Wood, V., and Hartland, E.L. (2006). Identification of Legionella pneumophila-specific genes by genomic subtractive hybridization with Legionella micdadei and identification of lpnE, a gene required for efficient host cell entry. Infect. Immun. *74*, 1683–1691.
Newton, H.J., Ang, D.K.Y., van Driel, I.R., and Hartland, E.L. (2010). Molecular Pathogenesis of Infections Caused by Legionella pneumophila. Clin. Microbiol. Rev. *23*, 274–298.
Nhu Nguyen, T.M., Ilef, D., Jarraud, S., Rouil, L., Campese, C., Che, D., Haeghebaert, S., Ganiayre, F., Marcel, F., Etienne, J., et al. (2006). A Community-Wide Outbreak of Legionnaires Disease Linked to Industrial Cooling Towers—How Far Can Contaminated Aerosols Spread? J. Infect. Dis. *193*, 102–111.
Olins, D.E., and Olins, A.L. (1978). Nucleosomes: The Structural Quantum in Chromosomes: Virtually all the DNA of eukaryotic cells is organized into a repeating array of nucleohistone particles called nucleosomes. These chromatin subunits are close-packed into higher-order fibers and are mod. Am. Sci. *66*, 704–711.
Oliva, G., Sahr, T., and Buchrieser, C. (2018). The Life Cycle of L. pneumophila: Cellular Differentiation Is Linked to Virulence and Metabolism. Front. Cell. Infect. Microbiol. *8*, 3.
Panzitt, K., Tschernatsch, M.M.O., Guelly, C., Moustafa, T., Stradner, M., Strohmaier, H.M., Buck, C.R., Denk, H., Schroeder, R., Trauner, M., et al. (2007). Characterization of HULC, a novel gene with striking up-regulation in hepatocellular carcinoma, as noncoding RNA. Gastroenterology *132*, 330–342.
Paroni, G., Cernotta, N., Dello Russo, C., Gallinari, P., Pallaoro, M., Foti, C., Talamo, F., Orsatti, L., Steinkühler, C., and Brancolini, C. (2008). PP2A Regulates HDAC4 Nuclear Import. Mol. Biol. Cell *19*, 655–667.
Partridge, E.C., Chhetri, S.B., Prokop, J.W., Ramaker, R.C., Jansen, C.S., Goh, S.-T., Mackiewicz, M., Newberry, K.M., Brandsmeier, L.A., Meadows, S.K., et al. (2020). Occupancy maps of 208 chromatin-associated proteins in one human cell type. Nature *583*, 720–728.
Pashaei-Asl, R., Khodadadi, K., Pashaei-Asl, F., Haqshenas, G., Ahmadian, N., Pashaiasl, M., and Hajihosseini Baghdadabadi, R. (2017). Legionella Pneumophila and Dendrimers-Mediated Antisense Therapy. Adv. Pharm. Bull. *7*, 179–187.

Payne, N.R., and Horwitz, M.A. (1987). Phagocytosis of Legionella pneumophila is mediated by human monocyte complement receptors. J. Exp. Med. *166*, 1377–1389.

Pearson, G., Robinson, F., Beers Gibson, T., Xu, B.E., Karandikar, M., Berman, K., and Cobb, M.H. (2001). Mitogen-activated protein (MAP) kinase pathways: regulation and physiological functions. Endocr. Rev. *22*, 153–183.

Pedro-Botet, L., and Yu, V.L. (2006). Legionella: macrolides or quinolones? Clin. Microbiol. Infect. *12*, 25–30.

Pennini, M.E., Perrinet, S., Dautry-Varsat, A., and Subtil, A. (2010). Histone methylation by NUE, a novel nuclear effector of the intracellular pathogen Chlamydia trachomatis. PLoS Pathog. *6*, e1000995.

Perkins, N.D. (2007). Integrating cell-signalling pathways with NF-kappaB and IKK function. Nat. Rev. Mol. Cell Biol. *8*, 49–62.

Portal, E., Descours, G., Ginevra, C., Mentasti, M., Afshar, B., Chand, M., Day, J., Echahidi, F., Franzin, L., Gaia, V., et al. (2021). *Legionella* antibiotic susceptibility testing: is it time for international standardization and evidence-based guidance? J. Antimicrob. Chemother. *76*, 1113–1116.

Postepska-Igielska, A., Giwojna, A., Gasri-Plotnitsky, L., Schmitt, N., Dold, A., Ginsberg, D., and Grummt, I. (2015). LncRNA Khps1 Regulates Expression of the Proto-oncogene SPHK1 via Triplex-Mediated Changes in Chromatin Structure. Mol. Cell *60*, 626–636.

Postnikov, Y., and Bustin, M. (2010). Regulation of chromatin structure and function By HMGN proteins. Biochim. Biophys. Acta - Gene Regul. Mech. *1799*, 62–68.

Prasad, A., and Prasad, M. (2021). Host-virus interactions mediated by long non-coding RNAs. Virus Res. *298*, 198402.

Prashar, A., Bhatia, S., Tabatabaeiyazdi, Z., Duncan, C., Garduño, R.A., Tang, P., Low, D.E., Guyard, C., and Terebiznik, M.R. (2012). Mechanism of invasion of lung epithelial cells by filamentous *L egionella pneumophila*. Cell. Microbiol. *14*, 1632–1655.

du Preez, L.L., and Patterton, H.-G. (2013). Secondary Structures of the Core Histone N-terminal Tails: Their Role in Regulating Chromatin Structure. (Springer, Dordrecht), pp. 37–55.

Qin, W., Scicluna, B.P., and van der Poll, T. (2021). The Role of Host Cell DNA Methylation in the Immune Response to Bacterial Infection. Front. Immunol. *12*, 696280.

Qiu, J., and Luo, Z.-Q. (2017). Legionella and Coxiella effectors: strength in diversity and activity. Nat. Rev. Microbiol. *15*, 591–605.

Quaile, A.T., Stogios, P.J., Egorova, O., Evdokimova, E., Valleau, D., Nocek, B., Kompella, P.S., Peisajovich, S., Yakunin, A.F., Ensminger, A.W., et al. (2018). The Legionella pneumophila effector Ceg4 is a phosphotyrosine phosphatase that attenuates activation of eukaryotic MAPK pathways. J. Biol. Chem. *293*, 3307–3320.

Radford, E.J. (2018). Exploring the extent and scope of epigenetic inheritance. Nat. Rev. Endocrinol. *14*, 345–355.

Rasmussen, K.D., and Helin, K. (2016). Role of TET enzymes in DNA methylation, development, and cancer. Genes Dev. *30*, 733–750.

Rennoll-Bankert, K.E., Garcia-Garcia, J.C., Sinclair, S.H., and Dumler, J.S. (2015). Chromatin-bound bacterial effector ankyrin A recruits histone deacetylase 1 and modifies host gene expression. Cell. Microbiol. *17*, 1640–1652.

Ridenour, D.A., Cirillo, S.L.G., Feng, S., Samrakandi, M.M., and Cirillo, J.D. (2003). Identification of a gene that affects the efficiency of host cell infection by Legionella pneumophila in a temperature-dependent fashion. Infect. Immun. *71*, 6256–6263.

Robinson, C.G., and Roy, C.R. (2006). Attachment and fusion of endoplasmic reticulum with vacuoles containing Legionella pneumophila. Cell. Microbiol. *8*, 793–805.

Robinson, P.J.J., Fairall, L., Huynh, V.A.T., and Rhodes, D. (2006). EM measurements define the dimensions of the "30-nm" chromatin fiber: Evidence for a compact, interdigitated structure. Proc. Natl. Acad. Sci. *103*, 6506 LP – 6511.

Rodgers, F.G., and Gibson, F.C. (1993). Opsonin-independent adherence and intracellular development of Legionella pneumophila within U-937 cells. Can. J. Microbiol. *39*, 718–722.

Rogers, J., Dowsett, A.B., Dennis, P.J., Lee, J. V, and Keevil, C.W. (1994). Influence of temperature and plumbing material selection on biofilm formation and growth of Legionella pneumophila in a model potable water system containing complex microbial flora. Appl. Environ. Microbiol. *60*, 1585–1592.

Rolando, M., and Buchrieser, C. (2014). Legionella pneumophila type IV effectors hijack the transcription and translation machinery of the host cell. Trends Cell Biol. *24*, 771–778.

Rolando, M., Sanulli, S., Rusniok, C., Gomez-Valero, L., Bertholet, C., Sahr, T., Margueron, R., and Buchrieser, C. (2013). Legionella pneumophila effector RomA uniquely modifies host chromatin to repress gene expression and promote intracellular bacterial replication. Cell Host Microbe *13*, 395–405.

Rolando, M., Escoll, P., Nora, T., Botti, J., Boitez, V., Bedia, C., Daniels, C., Abraham, G., Stogios, P.J., Skarina, T., et al. (2016). Legionella pneumophila S1P-lyase targets host sphingolipid metabolism and restrains

autophagy. Proc. Natl. Acad. Sci. U. S. A. *113*, 1901–1906.
Rothmeier, E., Pfaffinger, G., Hoffmann, C., Harrison, C.F., Grabmayr, H., Repnik, U., Hannemann, M., Wölke, S., Bausch, A., Griffiths, G., et al. (2013). Activation of Ran GTPase by a Legionella Effector Promotes Microtubule Polymerization, Pathogen Vacuole Motility and Infection. PLoS Pathog. *9*, e1003598.
Rowbotham, T.J. (1980). Preliminary report on the pathogenicity of Legionella pneumophila for freshwater and soil amoebae. J. Clin. Pathol. *33*, 1179–1183.
Russo, V.E.A., Martienssen, R.A., and Riggs, A.D. (1996). Overview of epigenetic mechanisms. In Epigenetic Mechanisms of Gene Regulation, (Cold Spring Harbor Laboratory Press), pp. 29–45.
Sathapatayavongs, B., Kohler, R.B., Wheat, L.J., White, A., Winn, W.C., Girod, J.C., and Edelstein, P.H. (1982). Rapid diagnosis of Legionnaires' disease by urinary antigen detection: Comparison of ELISA and radioimmunoassay. Am. J. Med. *72*, 576–582.
Sauer, J.-D., Bachman, M.A., and Swanson, M.S. (2005). The phagosomal transporter A couples threonine acquisition to differentiation and replication of Legionella pneumophila in macrophages. Proc. Natl. Acad. Sci. U. S. A. *102*, 9924–9929.
Schator, D., Gomez-Valero, L., Buchrieser, C., and Rolando, M. (2021). Epigenetic reprogramming: histone deacetylases as targets of pathogens and therapeutics. *submitted*.
Schlanger, G., Lutwick, L.I., Kurzman, M., Hoch, B., and Chandler, F.W. (1984). Sinusitis caused by Legionella pneumophila in a patient with the acquired immune deficiency syndrome. Am. J. Med. *77*, 957–960.
Schmerer, N., and Schulte, L.N. (2021). Long noncoding RNAs in bacterial infection. WIREs RNA e1664.
Schuhmacher, M.K., Rolando, M., Bröhm, A., Weirich, S., Kudithipudi, S., Buchrieser, C., and Jeltsch, A. (2018). The Legionella pneumophila Methyltransferase RomA Methylates Also Non-histone Proteins during Infection. J. Mol. Biol. *430*, 1912–1925.
Segal, G. (2013). The Legionella pneumophila two-component regulatory systems that participate in the regulation of Icm/Dot effectors. Curr. Top. Microbiol. Immunol. *376*, 35–52.
Shadoud, L., Almahmoud, I., Jarraud, S., Etienne, J., Larrat, S., Schwebel, C., Timsit, J.-F., Schneider, D., and Maurin, M. (2015). Hidden Selection of Bacterial Resistance to Fluoroquinolones In Vivo: The Case of Legionella pneumophila and Humans. EBioMedicine *2*, 1179–1185.
Shadrach, W.S., Rydzewski, K., Laube, U., Holland, G., Ozel, M., Kiderlen, A.F., and Flieger, A. (2005). Balamuthia mandrillaris, free-living ameba and opportunistic agent of encephalitis, is a potential host for Legionella pneumophila bacteria. Appl. Environ. Microbiol. *71*, 2244–2249.
Shahbazian, M.D., and Grunstein, M. (2007). Functions of site-specific histone acetylation and deacetylation. Annu. Rev. Biochem. *76*, 75–100.
Shames, S.R., Bhavsar, A.P., Croxen, M.A., Law, R.J., Mak, S.H.C., Deng, W., Li, Y., Bidshari, R., de Hoog, C.L., Foster, L.J., et al. (2011). The pathogenic Escherichia coli type III secreted protease NleC degrades the host acetyltransferase p300. Cell. Microbiol. *13*, 1542–1557.
Shivaji, T., Sousa Pinto, C., San-Bento, A., Oliveira Serra, L.A., Valente, J., Machado, J., Marques, T., Carvalho, L., Nogueira, P.J., Nunes, B., et al. (2014). A large community outbreak of Legionnaires disease in Vila Franca de Xira, Portugal, October to November 2014. Euro Surveill. *19*, 20991.
Silveira, T.N., and Zamboni, D.S. (2010). Pore Formation Triggered by *Legionella* spp. Is an Nlrc4 Inflammasome-Dependent Host Cell Response That Precedes Pyroptosis. Infect. Immun. *78*, 1403–1413.
Simon, S., Wagner, M.A., Rothmeier, E., Müller-Taubenberger, A., and Hilbi, H. (2014). Icm/Dot-dependent inhibition of phagocyte migration by Legionella is antagonized by a translocated Ran GTPase activator. Cell. Microbiol. *16*, 977–992.
Singh, R., Bassett, E., Chakravarti, A., and Parthun, M.R. (2018). Replication-dependent histone isoforms: a new source of complexity in chromatin structure and function. Nucleic Acids Res. *46*, 8665–8678.
Song, F., Chen, P., Sun, D., Wang, M., Dong, L., Liang, D., Xu, R.-M., Zhu, P., and Li, G. (2014). Cryo-EM Study of the Chromatin Fiber Reveals a Double Helix Twisted by Tetranucleosomal Units. Science (80-.). *344*, 376–380.
Speir, M., Vince, J.E., and Naderer, T. (2014). Programmed cell death in Legionella infection. Future Microbiol. *9*, 107–118.
Starnbach, M.N., Falkow, S., and Tompkins, L.S. (1989). Species-specific detection of Legionella pneumophila in water by DNA amplification and hybridization. J. Clin. Microbiol. *27*, 1257–1261.
Staynov, D.Z., Dunn, S., Baldwin, J.P., and Crane-Robinson, C. (1983). Nuclease digestion patterns as a criterion for nucleosome orientation in the higher order structure of chromatin. FEBS Lett. *157*, 311–315.
Steinert, M., Emödy, L., Amann, R., and Hacker, J. (1997). Resuscitation of viable but nonculturable Legionella pneumophila Philadelphia JR32 by Acanthamoeba castellanii. Appl. Environ. Microbiol. *63*, 2047–2053.
Stewart, M. (2007). Molecular mechanism of the nuclear protein import cycle. Nat. Rev. Mol. Cell Biol. *8*, 195–208.
Sturgill-Koszycki, S., and Swanson, M.S. (2000). Legionella pneumophila replication vacuoles mature into acidic, endocytic organelles. J. Exp. Med. *192*, 1261–1272.

Sun, B., Guo, S., Tang, Q., Li, C., Zeng, R., Xiong, Z., Zhong, C., and Ding, J. (2011). Regulation of the histone acetyltransferase activity of hMOF via autoacetylation of Lys274. Cell Res. *21*, 1262–1266.

Sutherland, M.C., Nguyen, T.L., Tseng, V., and Vogel, J.P. (2012). The Legionella IcmSW complex directly interacts with DotL to mediate translocation of adaptor-dependent substrates. PLoS Pathog. *8*, e1002910.

Terhune, S.S., Moorman, N.J., Cristea, I.M., Savaryn, J.P., Cuevas-Bennett, C., Rout, M.P., Chait, B.T., and Shenk, T. (2010). Human cytomegalovirus UL29/28 protein interacts with components of the NuRD complex which promote accumulation of immediate-early RNA. PLoS Pathog. *6*, e1000965–e1000965.

Terranova, W., Cohen, M., and Fraser, D. (1978). 1974 outbreak of Legionnaires' Disease diagnosed in 1977: Clinical and Epidemiological Features. Lancet *312*, 122–124.

Tesh, M.J., Morse, S.A., and Miller, R.D. (1983). Intermediary metabolism in Legionella pneumophila: utilization of amino acids and other compounds as energy sources. J. Bacteriol. *154*, 1104–1109.

Thacker, S.B., Bennett, J. V., Tsai, T.F., Fraser, D.W., McDade, J.E., Shepard, C.C., Williams, K.H., Stuart, W.H., Dull, H.B., and Eickhoff, T.C. (1978). An Outbreak in 1965 of Severe Respiratory Illness Caused by the Legionnaires' Disease Bacterium. J. Infect. Dis. *138*, 512–519.

Thurneysen, C., and Boggian, K. (2014). Legionella pneumophila Serogroup 1 Septic Arthritis With Probable Endocarditis in an Immunodeficient Patient. JCR J. Clin. Rheumatol. *20*, 297–298.

Torchy, M.P., Hamiche, A., and Klaholz, B.P. (2015). Structure and function insights into the NuRD chromatin remodeling complex. Cell. Mol. Life Sci. *72*, 2491–2507.

Touati, E. (2010). When bacteria become mutagenic and carcinogenic: lessons from H. pylori. Mutat. Res. *703*, 66–70.

Trunk, G., and Oxenius, A. (2012). Innate instruction of CD4+ T cell immunity in respiratory bacterial infection. J. Immunol. *189*, 616–628.

Uba, A.İ., and Yelekçi, K. (2017). Exploration of the binding pocket of histone deacetylases: the design of potent and isoform-selective inhibitors. Turkish J. Biol. = Turk Biyol. Derg. *41*, 901–918.

Vanderlaan, J., and Hall, P. (2020). Systematic Review of Case Reports of Poor Neonatal Outcomes With Water Immersion During Labor and Birth. J. Perinat. Neonatal Nurs. *34*, 311–323.

Vandersmissen, L., De Buck, E., Saels, V., Coil, D.A., and Anné, J. (2010). A Legionella pneumophila collagen-like protein encoded by a gene with a variable number of tandem repeats is involved in the adherence and invasion of host cells. FEMS Microbiol. Lett. *306*, 168–176.

Veve, M.P., and Wagner, J.L. (2018). Lefamulin: Review of a Promising Novel Pleuromutilin Antibiotic. Pharmacotherapy *38*, 935–946.

Vieira, O. V, Botelho, R.J., and Grinstein, S. (2002). Phagosome maturation: aging gracefully. Biochem. J. *366*, 689–704.

Vogel, J.P., Andrews, H.L., Wong, S.K., and Isberg, R.R. (1998). Conjugative transfer by the virulence system of Legionella pneumophila. Science *279*, 873–876.

Voth, K.A., Chung, I.Y.W., Straaten, K., Li, L., Boniecki, M.T., and Cygler, M. (2019). The structure of *Legionella* effector protein LpnE provides insights into its interaction with Oculocerebrorenal syndrome of Lowe (OCRL) protein. FEBS J. *286*, 710–725.

Walters, M.S., Kinchington, P.R., Banfield, B.W., and Silverstein, S. (2010). Hyperphosphorylation of histone deacetylase 2 by alphaherpesvirus US3 kinases. J. Virol. *84*, 9666–9676.

Wang, L., Wu, G., Qin, X., Ma, Q., Zhou, Y., Liu, S., and Tan, Y. (2015). Expression of Nodal on Bronchial Epithelial Cells Influenced by Lung Microbes Through DNA Methylation Modulates the Differentiation of T-Helper Cells. Cell. Physiol. Biochem. *37*, 2012–2022.

Wang, Y., Curry, H.M., Zwilling, B.S., and Lafuse, W.P. (2005). Mycobacteria inhibition of IFN-gamma induced HLA-DR gene expression by up-regulating histone deacetylation at the promoter region in human THP-1 monocytic cells. J. Immunol. *174*, 5687–5694.

Watanabe, K., Nakao, R., Fujishima, M., Tachibana, M., Shimizu, T., and Watarai, M. (2016). Ciliate Paramecium is a natural reservoir of Legionella pneumophila. Sci. Rep. *6*, 24322.

Weber, S., Steiner, B., Welin, A., and Hilbi, H. (2018). Legionella-Containing Vacuoles Capture PtdIns(4)P-Rich Vesicles Derived from the Golgi Apparatus. MBio *9*.

Weber, S.S., Ragaz, C., and Hilbi, H. (2009). The inositol polyphosphate 5-phosphatase OCRL1 restricts intracellular growth of Legionella, localizes to the replicative vacuole and binds to the bacterial effector LpnE. Cell. Microbiol. *11*, 442–460.

Wedemann, G., and Langowski, J. (2002). Computer simulation of the 30-nanometer chromatin fiber. Biophys. J. *82*, 2847–2859.

Weiss, D., Boyd, C., Rakeman, J.L., Greene, S.K., Fitzhenry, R., McProud, T., Musser, K., Huang, L., Kornblum, J., Nazarian, E.J., et al. (2017). A Large Community Outbreak of Legionnaires' Disease Associated With a Cooling Tower in New York City, 2015. Public Health Rep. *132*, 241–250.

Westbrook, R.H., and Dusheiko, G. (2014). Natural history of hepatitis C. J. Hepatol. *61*, S58-68.

Wilmes, D., Coche, E., Rodriguez-Villalobos, H., and Kanaan, N. (2018). Bacterial pneumonia in kidney

transplant recipients. Respir. Med. *137*, 89–94.
Wu, X., and Zhang, Y. (2017). TET-mediated active DNA demethylation: mechanism, function and beyond. Nat. Rev. Genet. *18*, 517–534.
Wutz, A. (2011). Gene silencing in X-chromosome inactivation: advances in understanding facultative heterochromatin formation. Nat. Rev. Genet. *12*, 542–553.
Xiao, Y., Li, W., Yang, H., Pan, L., Zhang, L., Lu, L., Chen, J., Wei, W., Ye, J., Li, J., et al. (2021). HBO1 is a versatile histone acyltransferase critical for promoter histone acylations. Nucleic Acids Res.
Xu, D., Joglekar, A.P., Williams, A.L., and Hay, J.C. (2000). Subunit structure of a mammalian ER/Golgi SNARE complex. J. Biol. Chem. *275*, 39631–39639.
Yang, W.-M., Tsai, S.-C., Wen, Y.-D., Fejer, G., and Seto, E. (2002). Functional domains of histone deacetylase-3. J. Biol. Chem. *277*, 9447–9454.
Yao, R.-W., Wang, Y., and Chen, L.-L. (2019). Cellular functions of long noncoding RNAs. Nat. Cell Biol. *21*, 542–551.
Yaseen, I., Kaur, P., Nandicoori, V.K., and Khosla, S. (2015). Mycobacteria modulate host epigenetic machinery by Rv1988 methylation of a non-tail arginine of histone H3. Nat. Commun. *6*, 8922.
Yu, V.L., Plouffe, J.F., Pastoris, M.C., Stout, J.E., Schousboe, M., Widmer, A., Summersgill, J., File, T., Heath, C.M., Paterson, D.L., et al. (2002). Distribution of *Legionella* Species and Serogroups Isolated by Culture in Patients with Sporadic Community-Acquired Legionellosis: An International Collaborative Survey. J. Infect. Dis. *186*, 127–128.
Yuan, H., Rossetto, D., Mellert, H., Dang, W., Srinivasan, M., Johnson, J., Hodawadekar, S., Ding, E.C., Speicher, K., Abshiru, N., et al. (2012). MYST protein acetyltransferase activity requires active site lysine autoacetylation. EMBO J. *31*, 58–70.
Zhang, W., Wang, H., Liu, B., Jiang, M., Gu, Y., Yan, S., Han, X., Hou, A.Y., Tang, C., Jiang, Z., et al. (2021). Differential DNA Methylation Profiles in Patients with Temporal Lobe Epilepsy and Hippocampal Sclerosis ILAE Type I. J. Mol. Neurosci.
Zhao, B., Xu, W., Rong, B., Chen, G., Ye, X., Dai, R., Li, W., Chen, J., Cai, J., Song, L., et al. (2018). H3K14me3 genomic distributions and its regulation by KDM4 family demethylases. Cell Res. *28*, 1118–1120.
Zhao, J., Beyrakhova, K., Liu, Y., Alvarez, C.P., Bueler, S.A., Xu, L., Xu, C., Boniecki, M.T., Kanelis, V., Luo, Z.-Q., et al. (2017). Molecular basis for the binding and modulation of V-ATPase by a bacterial effector protein. PLoS Pathog. *13*, e1006394.
Zhou, B.-R., Jiang, J., Feng, H., Ghirlando, R., Xiao, T.S., and Bai, Y. (2015). Structural Mechanisms of Nucleosome Recognition by Linker Histones. Mol. Cell *59*, 628–638.
Zhou, G., Te, D., and Roizman, B. (2011). The CoREST/REST Repressor Is both Necessary and Inimical for Expression of Herpes Simplex Virus Genes. MBio *2*, e00313-10.
Zhu, Q., Yang, Q., Lu, X., Wang, H., Tong, L., Li, Z., Liu, G., Bao, Y., Xu, X., Gu, L., et al. (2021). SETD2-mediated H3K14 trimethylation promotes ATR activation and stalled replication fork restart in response to DNA replication stress. Proc. Natl. Acad. Sci. U. S. A. *118*.
Zhu, W., Banga, S., Tan, Y., Zheng, C., Stephenson, R., Gately, J., and Luo, Z.-Q. (2011). Comprehensive identification of protein substrates of the Dot/Icm type IV transporter of Legionella pneumophila. PLoS One *6*, e17638.
Zughaier, S.M., Rouquette-Loughlin, C.E., and Shafer, W.M. (2020). Identification of a Neisseria gonorrhoeae Histone Deacetylase: Epigenetic Impact on Host Gene Expression. Pathog. (Basel, Switzerland) *9*.
(1977a). Legionnaire's disease. Lancet *309*, 1295–1296.
(1977b). Special issue : Follow-up on respiratory illness - Philidelphia. Morb. Mortal. Wkly. Rep. *26*.
(2021). Australia's notifiable disease status, 2016: Annual report of the National Notifiable Diseases Surveillance System.

Annexes

Annex 1

LEGIONELLA LONGBEACHAE SECRETES A RAB GTPASE PROTEIN TO HIJACK NLRP3 DURING INFECTION

In preparation

INTRODUCTION AND AIM OF THE PROJECT

When first join the lab for my Master thesis in January 2018, I was working in collaboration with *Sonia Mondino*, Postdoc in the lab, on the characterization of a secreted effector of *L. longbeachae*.

L. longbeachae is the second most common cause of Legionnaires' disease after *L. pneumophila.* Especially in Australia, New Zealand and Japan, *L. longbeachae* accounts for around 30% of all cases. Yet, *L. longbeachae* has not been studied to the same extent, leading to rather limited insight into its mode of infection and other aspects of its biology. While the research conducted on *L. pneumophila* can contribute to a better understanding of *L. longbeachae*, however, this does not replace research performed specifically on *L. longbeachae*, due to several key differences between the two species.

The aim of the project was the determination of the role of a secreted bacterial Rab-like small GTPase, RabL, during infection and assess its influence on bacterial virulence. I was involved in determining the intracellular localization of RabL during infection, by constructing an expression plasmid enabling the overexpression of V5-tagged RabL and following its translocation in the host cell by immunofluorescence microscopy.

In addition, I helped to exclude the involvement of specific phosphorylation sites of RabL in its intracellular localization when expressed ectopically in human cells, as well as its involvement in Golgi disruption during *L. longbeachae* infection. Last but not least, I was implicated in confirming the interaction of RabL with possible eukaryotic partners in the host cell.

This publication is *in preparation* and promises to grant an exciting new insight in host-pathogen interaction and manipulation of intracellular trafficking by pathogens.

Legionella longbeachae secretes a Rab GTPase protein to hijack NLRP3 during infection

Sonia MONDINO[1], Pedro ESCOLL[1,§], Daniel SCHATOR[1,2,§], Silke SCHMIDT[1,2], Gustavo F S Quirino[3], Monica ROLANDO[1], Laura GOMEZ-VALERO[1], Lena Oesterlin[4,5], Bruno Goud[4,5], Dario ZAMBONI[3], Carmen BUCHRIESER[1]; *in preparation*

1, Institut Pasteur, Université de Paris, CNRS UMR 3525, Unité Biologie des Bactéries Intracellulaires, F-75015 Paris, France
2, Sorbonne Université, Collège doctoral, F-75005 Paris, France
3, Department of Cell Biology, Ribeirão Preto Medical School, University of São Paulo, Ribeirão Preto, São Paulo, Brazil
4, Institut Curie, Mécanismes moléculaires du transport intracellulaire, Paris, France
5, CNRS UMR 144, Paris, France

§, these authors contributed equally to this study

Abstract

Legionella spp. are environmental bacteria and accidental human pathogens that can cause a severe pneumonia, termed Legionnaires' disease. These bacteria replicate intracellularly in free living amoebae and human alveolar macrophages within a distinct compartment known as the *Legionella*-containing vacuole (LCV). The LCV resembles an endoplasmic reticulum (ER) structure due to the recruitment of vesicles from the host secretory pathway, partly by targeting Rab GTPases. Despite *L. pneumophila* secretes several protein effectors that modulate Rab function during infection, most of them are not conserved in the *L. longbeachae* genome. Instead, this understudied species harbours a novel family of eukaryotic Rab-like effector proteins with unknown function. Here we show that one of these proteins, named RabL, is a T4SS-dependent effector with intrinsic GTPase activity. RabL localizes to the Golgi when ectopically expressed in mammalian cells, but it is not involved in Golgi disruption during *L. longbeachae* infection. Moreover, RabL was required for efficient replication in C57BL/6 murine lungs, highlighting an important virulence role for this effector. Determination of RabL *in vivo* interactome by tandem affinity purification allowed us to identify STARD3NL and NLRP3 as RabL partners in macrophages. STARD3NL mediates ER-endosome contacts and consequently endosome dynamics in eukaryotic cells. However, no differences in ER-recruitment to LCV were observed in an *L. longbeachae rabL* mutant strain, suggesting that RabL-STARD3NL interaction modulates other trafficking pathways in infection. Conversely, further analyses demonstrated that RabL is important for IL-1β secretion in infected macrophages, suggesting a role of this protein in NLRP3-mediated inflammasome activation. Thus, RabL is a eukaryotic Rab-like virulence factor crucial for *L. longbeachae* infection *in vivo*.

Annex 2

ZEBRAFISH LARVAE AS A POWERFUL MODEL TO DISSECT PROTECTIVE INNATE IMMUNITY IN RESPONSE TO *LEGIONELLA PNEUMOPHILA* INFECTION

Submitted to PLOS Biology

INTRODUCTION AND AIM OF THE PROJECT

In the lab, we aimed at establishing a new animal model for *L. pneumophila* infection. At this time, very few animal models are available for this purpose, and all of them have significant drawbacks. We wanted to assess if a common model organism, like the zebrafish (*Danio rerio*) could be used as a new tool to better understand how *L. pneumophila* infects eukaryotic organisms and how the innate immune system reacts to this bacterial invasion. In this project, led by *Flávia Viana*, I was involved in preparing the bacteria for the infection of the zebrafish larvae, as well as the following analyses of bacterial burden in the larvae after several days of infection. The publication associated with this project was recently submitted at PLOS biology and illustrates that zebrafish larvae represent an innovative *L. pneumophila* infection model that closely mimics important aspects of human infection.

Zebrafish larvae as a powerful model to dissect protective innate immunity in response to *Legionella pneumophila* infection

Flávia Viana[1,§,#,*], Laurent Boucontet[2,§], Daniel Schator[1,3], Valerio Laghi[2], Marine Ibranosyan[4], Sophie Jarraud[4,5], Emma Colucci-Guyon[2,€,*] and Carmen Buchrieser[1,€,*]

[1]Institut Pasteur, Biologie des Bactéries Intracellulaires and CNRS UMR 3525, 75724, Paris, France, [2]Institut Pasteur, Unité Macrophages et Développement de l'Immunité and CNRS UMR 3738, Paris, France, [3]Sorbonne Université, Collège doctoral, 75005 Paris, France, [4]National Reference Centre of *Legionella*, Institute of Infectious Agents, Hospices Civils de Lyon, Lyon, France, [4] Hospices Civils de Lyon, Centre National de Référence des Legionella, Lyon, France, [5]Centre International de Recherche en Infectiologie, Université Lyon 1, UMR CNRS 5308, Inserm U1111, ENS de Lyon, Lyon, France

#Present Address: Wellcome-Wolfson Institute for Experimental Medicine, Queen's University Belfast, Belfast, United Kingdom

§ These authors contributed equally

€ Co-last authors

* Corresponding author's: cbuch@pasteur.fr, emma.colucci@pasteur.fr, f.d.m.viana@gmail.com

Key words: *Legionella pneumophila*, zebrafish, innate immune response; live imaging; neutrophils; macrophages

Lead contact:
Carmen Buchrieser
Institut Pasteur
Biologie des Bactéries Intracellulaires
28, rue du Dr. Roux,
75724 Paris Cedex 15, France
Tel: (33-1)-45-68-83-72
E-mail: *cbuch@pasteur.fr*

Abstract

The zebrafish has become a powerful model organism to study host-pathogen interactions. Here, we developed a zebrafish model of *Legionella pneumophila* infection to dissect innate immune responses. We show that *L. pneumophila* cause zebrafish larvae death in a dose dependent manner, and that macrophages are the first line of defence, with neutrophils cooperating to clear the infection. When either macrophages or neutrophils are depleted, the larvae become lethally sensitive to *L. pneumophila*. As observed in human infections, the adaptor signalling molecule Myd88 is not required to control disease in the larvae. Furthermore, proinflammatory cytokines IL-1β and TNFα were upregulated during infection, recapitulating key immune responses seen in human infection. We also uncovered a previously undescribed phenotype in zebrafish larvae, whereby bloodborne, wild type *L. pneumophila* invade and grow in the larval yolk region but not a T4SS mutant. Zebrafish larva represent an innovative *L. pneumophila* infection model closely mimicking important aspects of human infection.

.

INTRODUCTION

Legionella pneumophila, a gram negative, facultative intracellular bacterium inhabits natural, freshwater sources [1,2]. As an environmental, aquatic microbe *L. pneumophila* replicates intracellularly in aquatic protozoa [3]. Most interestingly, in contrast to other intracellular pathogens *L. pneumophila* is not adapted to a single host, but it exhibits a broad host range including Amoebozoa (amoebae), Percolozoa (excavates) and Ciliophora (ciliated protozoa) [3,4]. In the environment *L. pneumophila* can also be found within biofilms where it acquires nutrients from this mixed community, but it can also survive in a planktonic form for a certain time as well [5]. As fresh water and man-made systems are connected, *L. pneumophila* can also contaminate artificial water systems. Protected in its protozoan hosts *L. pneumophila* survives water disinfectants and may gain access to humans *via* aerosols produced by different man-made structures and devices. The inhalation of *L. pneumophila* contaminated aerosols can cause a severe pneumonia, the so-called Legionnaires' disease [6]. However, not every infection leads to disease. Disease outcome is determined by virulence of the bacterial strain, bacterial burden in the inhaled aerosols and most importantly by the host immune status. Host factors determining susceptibility include age above 50, smoking and/or having chronic lung disease, being immunocompromised and genetic factors that alter the immune response [2,7,8].

Once the bacteria reach the lungs of susceptible individuals, they can infect alveolar macrophages and replicate therein. After being phagocytosed *L. pneumophila* avoids lysosomes and establishes an endoplasmic reticulum derived vacuole named the *Legionella* containing vacuole (LCV) [9,10]. The LCV, a safe haven for bacterial replication, is established by utilizing the Dot/Icm type IV secretion system (T4SS) that injects over 350 proteins into the host cell [9-11]. These effector proteins manipulate a myriad of host pathways to recruit vesicles derived from the endoplasmic reticulum to the LCV, to supply the bacteria with nutrients, restrain autophagy and supress apoptosis or to subvert the host cell immune response [9-11]. A surprising high number of these effectors mimic host proteins and encode eukaryotic functions helping *L. pneumophila* to subvert numerous host pathways in remarkable diverse ways [11-13]

Intracellular bacterial replication and innate immune responses have been studied *in vitro* using both murine and human cell lines and *in vivo* using different animal models of *L. pneumophila* infection. However, results obtained with these models cannot be easily extrapolated to what is observed in human disease. Studies in invertebrate models, for example in *Galleria mellonella* and *Caenorhabditis elegans*, [14,15] require further validation in more developed models as their immune system greatly differs from that of vertebrates. More interestingly, mouse infection fails to recall the human disease phenotype, as most inbred mice strains are naturally resistant to *L. pneumophila* [16]. Very early after the discovery of *L. pneumophila* the guinea pig model of Legionnaires' disease was developed. Guinea pigs are highly susceptible to *L. pneumophila* when infected through injection into

the peritoneum [6] or when exposed to *L. pneumophila* containing aerosols [6]. Several studies thereafter have shown that the guinea pig infection model recalls human disease and allows to study the immune response to *L. pneumophila* infection [17,18]. However, the guinea pig model is now rarely used due to the limited availability of specific immunological reagents for these animals and the demanding laboratory and husbandry requirements to work with guinea pigs.

Since the above-mentioned models, including the widely used murine models, are limited for studying *L. pneumophila* infection *in vivo* and discrepancies exist between results obtained in mouse or human cells, the development of new, alternative models for *Legionella* infection is important. The zebrafish (*Danio rerio*) originally introduced as a model organism in developmental biology has emerged in recent years as a powerful non-mammalian model to study nearly every aspect of biology, including immune cell behaviour and host-pathogen interactions [19,20]. Zebrafish are evolutionary closer to humans than fruit flies and nematodes, easier to manipulate than mice and their immune system is remarkably similar to the one of mammals, making them an attractive laboratory model for immunology and infection biology [19,20]. Its popularity is also due to its small size and the natural translucency of its embryos and larvae, which makes it possible to follow leukocyte behaviour and infection onset at the level of the whole organism in real-time and high resolution [21]. Additionally, although adult organisms display a fully developed immune system with both active innate and adaptive branches, studies can also be conducted at the early stages of life (embryonic or larvae) when the organism solely relies on innate immunity, allowing to dissect the mechanisms arising from different immune responses [21-23]. Thus, we sought to examine whether the zebrafish could be an alternative model for analysing host-pathogen interactions and the innate immune response to *L. pneumophila* infection.

We show that *L. pneumophila* infection of zebrafish larvae recapitulate human disease onset, as infected wild-type larvae are generally able to clear the infection, but immunocompromised fish fail to do so. Both macrophages and neutrophils quickly interact and engulf injected *L. pneumophila*. Macrophage-depleted larvae show a dramatic increase of bacterial burden concomitant with host death, pointing to a crucial role of macrophages in controlling the infection. Interestingly, we discovered a new infection phenotype, as *L. pneumophila* replicates in the larvae yolk region, where it seems to be able to avoid the immune response of the host.

RESULTS

L. pneumophila infection induces mortality in zebrafish larvae in a dose dependent manner

To analyse whether *L. pneumophila* can cause disease in zebrafish larvae we microinjected larvae 72 hours post fertilisation (hpf) intravenously in the caudal vessels near the cloaca (UGO) (Fig 1A), with 10^3 or 10^4 CFU of wild type (WT) *L. pneumophila* strain Paris expressing GFP (WT-GFP) or the type IV

secretion system (T4SS) deficient isogenic mutant expressing GFP (Δ*dotA*-GFP). The infected larvae were kept at 28°C and were monitored regularly until 72 hours post infection (hpi) to record survival or death using a stereomicroscope. Larvae infected with doses of up to $3x10^3$ CFU of WT-GFP (defined as low dose, LD) all survived (100% survival). In contrast, larvae infected intravenously with doses of 10^4 CFU (defined as high dose, HD) resulted in approximately 30% of death within 72 hpi (Fig 1B). Importantly, all larvae injected with LD or HD of the Δ*dotA*-GFP strain survived for the entire time of observation (Fig 1B) indicating that the T4SS is important for replication in zebrafish larvae as it is in other infection models and in humans.

We then set up a method to monitor the bacterial burden of the infected zebrafish larvae. The progression of the infection was followed by analysing the bacterial load at 0, 24, 48 and 72 hpi comparing three different methods. First, we quantified the pixel counts of GFP fluorescence of live larvae images (Fig. S1A), secondly, we analysed the number of GFP expressing bacteria present in lysed infected larvae by FACS (Fig. S1B) and thirdly we plated serial dilutions of homogenates of euthanized larvae on BCYE medium (Fig S1C). The results obtained with the three methods were comparable (Fig S1). We choose to routinely monitor the *L. pneumophila* load of zebrafish larvae by FACS. As shown in Fig. 1C, larvae injected with LD of WT-GFP progressively eliminate the bacteria, by 24 hpi. Similarly, with high doses of Δ*dotA*-GFP were progressively cleared by 24 hpi. In contrast, some zebrafish larvae injected with HD of WT-GFP were unable to eliminate the bacteria at 72hpi, and the bacterial burden even increased by 48-72 hpi (Fig 1C). We also monitored infected larvae by fluorescent microscopy. Immediately upon injection (20 min to 2 hpi), bacteria were detectable as small foci, probably associated with professional phagocytes (Fig. 1D). By 24 hpi, in both, larvae injected with LD of WT-GFP as well as larvae injected with HD of the avirulent Δ*dotA*-GFP strain, the GFP signal declined becoming undetectable by 48 hpi, suggesting that the bacteria were progressively cleared. Despite showing the same pattern 24 hpi, larvae injected with HD of WT-GFP displayed a radically different progression of infection at 48 hpi, as bacterial proliferation started in a fraction of the infected larvae as seen by an increase in GFP signal. Most interestingly, in these larvae, bacterial proliferation occurred mainly in the yolk region while the bacterial load in the body decreased simultaneously. These bacterial foci in the yolk increased dramatically over time, causing death of the infected larvae by 72 hpi (Fig 1D).

Collectively our results indicate that *L. pneumophila* WT, but not the T4SS mutant induces death of zebrafish larvae. Larvae that were unable to control infection by 72 hpi, showed a unique phenotype, an increase of the bacterial burden in the yolk region.

Bloodstream L. pneumophila establishes a proliferative niche in the yolk region causing a persistent infection

To characterise the *L. pneumophila* foci identified in the yolk region of zebrafish larvae, we used high resolution fluorescent microscopy of HD of WT-GFP bloodstream injected in 72hpf Tg*(mfap4::mCherryF)* (herein referred as *mfap4*:mCherryF) (red macrophages) or Tg(*Lyz::DsRed)*^{nz50} (herein referred as *lyz*:DsRed)(red neutrophils) or Tg(*kdrl*::mCherry)^{is5} (red blood vessels) larvae. Upon injection of HD of WT-GFP, bacteria were progressively eliminated by the rest of the body and appeared growing in the yolk region between 48 and 72hpi, with macrophages accumulating there (Fig. 2A). We observed that *L. pneumophila* foci in the yolk region are highly complex, aggregate-like structures of long, filamentous bacteria growing in the yolk cell region and not in the visceral organs of the zebrafish larva. Macrophages were recruited to the yolk region containing *L. pneumophila,* (Fig. 2B, D Movie S1). Similarly, upon injection of HD of WT-GFP in *lyz*:DsRed larvae (red neutrophils), neutrophils were recruited to and accumulated around the growing bacterial aggregates, but seem unable to engulf them (Fig 2E, Movie S2).Moreover, confocal microscopy revealed that *L. pneumophila* exhibits grow in aggregates, and that these growing complex bacterial structures localize in the yolk and or in the yolk tube (Fig. 2F, Movie S3). Upon injection HD of WT-GFP in Tg(*kdrl*::mCherry)^{is5} (red blood vessels) larvae, we also showed that, the fast growing bacterial aggregates interact with the blood vessels (Fig 2G, Movie S4). It should be noted that the yolk is the only food source of the larvae during this developmental stage. The fast proliferation of the bacteria in the yolk region probably depletes its nutritional content, leading to larvae death (Fig 2, Movie S1). Strikingly, zebrafish larvae infected with the T4SS deficient Δ*dotA* mutant strain, did neither develop bacterial colonisation of the yolk nor larval death. This outcome was independent of the used dose, suggesting that zebrafish susceptibility to *L. pneumophila* infection and yolk penetration depends on a functional T4SS system.

Thus, blood-borne *L. pneumophila* is able to invade the yolk sac of zebrafish larvae, a previously undescribed phenotype of bacterial infection in this model. Once in the yolk, the bacteria replicate extensively, forming complex, organized, aggregate-like structures that cannot be removed by macrophages and neutrophils, thereby avoiding he host's immune control and clearance, eventually leading to death of the larvae.

Infection of zebrafish larvae with high doses of L. pneumophila leads to macrophage and neutrophil death

In human infection, alveolar macrophages are the primary cell type infected by *L. pneumophila* supporting its intracellular replication. Following infection, neutrophils are recruited to the lung and are key players for controlling infection as they possess antimicrobial activity and kill *L. pneumophila*

[24]. To analyse whether zebrafish infection mirrors human infection we monitored the interaction of zebrafish macrophages or neutrophils with the bacteria *in vivo*. The transgenic zebrafish larvae *mfap4*:mCherryF and *lyz*:DsRed were injected with low or high doses of WT-GFP or with high doses of Δ*dotA*-GFP. Infected larvae were monitored using widefield fluorescence microscopy and the number of leukocytes per larva was assessed by counting fluorescent macrophages and neutrophils over time until 72hpi. We observed that upon injection of high dose WT-GFP, the macrophage count decreased dramatically at 24hpi and then remained stable (Fig. 3A, B). Neutrophil counts gave similar results, as there was a dramatic decrease observed in neutrophil numbers starting at 24hpi, in particular after injection of high doses of WT bacteria Fig. 3C, D). Interestingly, upon infection with low doses of WT the neutrophil numbers decreased dramatically only at 24hpi but increased at 48hpi and 72hpi (Fig. 3D). In contrast macrophage and neutrophil counts remained unaffected upon injection of equal amounts of the avirulent Δ*dotA* strain, suggesting that phagocyte death is linked to a functional T4SS system.

Taken together, these results show that high dose *L. pneumophila* infection leads to a decrease in the number of professional phagocytes dependent on the T4SS, similar to what is seen during human infection by *L. pneumophila* and *Mycobacterium tuberculosis* [24,25]

Macrophages are the primary cells to phagocytise blood-borne L. pneumophila and neutrophils co-operate to decrease bacterial load

As macrophages and neutrophils are likely the phagocytes that interact with *L. pneumophila* we analysed phagocyte-*L. pneumophila* interactions *in vivo* by injecting *mfap4*:mCherryF or *lyz*:DsRed 72hpf larvae with WT-GFP or Δ*dotA*-GFP and recorded phagocyte-*L. pneumophila* interactions using high resolution confocal microscopy. This showed that upon injection of LD WT-GFP, macrophages immediately contacted and engulfed blood-borne bacteria, and the initial bacterial load was thereby unchanged for 8hpi. The GFP signal of the engulfed bacteria was present for a long time in macrophages, suggesting that live bacteria persist in macrophages *in vivo* over a certain period of time. However, macrophages were continuously recruited to the site of infection and by 16hpi the bacteria were mostly undetectable (Fig. 4A top panel, Movie S5). Macrophages that had engulfed a large amount of *L. pneumophila* stopped moving and rounded-up, suggesting cell death. Similarly, the inhibition of the migration of phagocytes by *L. pneumophila* has been observed previously during infection of RAW 264.7 macrophages and the amoeba *Dictyostelium discoideum* and *Acanthamoeba castellanii*, [26,27]. In contrast, zebrafish infected with HD of WT-GFP were not able to restrict the bacterial growth by 16hpi. HD of *L pneumophila* formed big aggregates, that were not easily engulfed and cleared by macrophages (Fig 4A, bottom panel, Movie S5). Remarkably, macrophages were very efficient in engulfing and rapidly clearing high doses of blood-borne Δ*dotA*-GFP bacteria. By 10hpi

most of the bacteria had been engulfed and cleared as suggested by the diffuse GFP staining in phagocytes (Fig. 4A, bottom panel, Movie S5). However, upon infection with a HD WT-GFP, bacteria were not completely cleared but persisted, and at 72hpi *L. pneumophila* was found in macrophages, suggesting that the bacteria are also replicating in macrophages of zebrafish larvae. Indeed, high resolution confocal microscopy showed that at 72hpi, *L. pneumophila* can also be found inside of macrophages in replicative vacuoles (Fig. S2).

The analyses of *L. pneumophila*-neutrophil interactions showed that these engulfed the bacteria trapped in the mesenchyme around the site of injection, but they were less efficient at clearing blood-borne bacteria. This is similar to what has been previously observed for infection of zebrafish larvae with *Escherichia coli* or *Shigella flexneri* [22,28]. Indeed, upon infection with a high dose of WT-GFP, *L. pneumophila* persisted in neutrophils and massive death of infected neutrophils occurred (Fig. 4B, second panel, Movies S6). In sharp contrast, neutrophils very efficiently engulfed and cleared large amounts of Δ*dotA*-GFP aggregated and trapped in the mesenchyme (Fig. 4B, lower panel, Movie S6) as well as low doses of WT-GFP (Fig 4B upper panel, Movie S6).

Altogether this shows that upon bloodstream injection of *L. pneumophila*, macrophages and neutrophils efficiently cooperate to eliminate the majority of bacteria within 20-24 hpi, with macrophages playing the primary role. However, *L. pneumophila* is also able to persist and replicate in macrophages. In contrast, neutrophils interact with *L. pneumophila* by quickly engulfing bacteria trapped in the mesenchyme near the site of injection but are less efficient in clearing blood-borne bacteria.

Macrophages are the first line defence restricting L. pneumophila infection

In humans, innate immune responses, based essentially on the activities of professional phagocytes and pro-inflammatory cytokine induction, are the key players to control and restrict *L. pneumophila* proliferation. Thus, human disease develops primarily in immunocompromised individuals [10]. To investigate whether the phagocytes of the innate immune system, macrophages and neutrophils, are also responsible for controlling *L. pneumophila* infection in zebrafish larvae, we selectively and transiently depleted macrophages or neutrophils, respectively and infected these "immunocompromised" larvae with *L. pneumophila*. Depletion of macrophages was achieved by knocking down the expression of s*pi1b*, a transcription factor involved in early myeloid progenitor formation. A low dose of s*pi1b* morpholino was reported to impact macrophages without affecting neutrophils [29]. We monitored the effect of low doses s*pi1b* morpholino injection on macrophage and neutrophil populations in double transgenic larvae with green neutrophils (*mpx*:GFP) and red

263 macrophages (*mfap4*:mCherryF). The specific depletion of the two cell types was confirmed by
264 counting macrophages and neutrophils 72hpf (Fig S3A).
265 We then infected macrophage depleted larvae (s*pi1b* knockdown) by intravenous injection of
266 LD or HD of WT-GFP. Independently of the infection dose, a dramatic decrease in survival occurred,
267 as even injection of low doses of WT-GFP resulted in the death of 30% of the larvae (Fig 5A). When
268 injecting high doses of WT-GFP nearly all of the infected larvae died by 72hpi, with the earliest
269 deaths starting 48hpi (Fig 5A). In contrast, s*pi1b* knockdown larvae injected with high doses of Δ*dotA*-
270 GFP did not show impaired survival (Fig 5A). The increased mortality correlated with an increased
271 bacterial burden in s*pi1b* knockdown larvae compared to control larvae as judged from counting
272 bacteria growing on BCYE agar from homogenates of individual larvae by FACS analyses (Fig 5B).
273 Intravital imaging of infected s*pi1b* knock down larvae also showed that both low and high doses of
274 WT-GFP failed to be cleared and that the bacteria established a replicative niche in the yolk, where
275 they proliferated extensively (Fig 5C). This highlights, that macrophages are critical to restrict the
276 onset of infection and *L. pneumophila* proliferation *in vivo*. Furthermore, these results also suggest
277 that neutrophils, which are not depleted in s*pi1b* knockdown larvae, fail to control *L. pneumophila*
278 infection in the absence of macrophages.
279 We next analysed the role of neutrophils in controlling the infection. Neutrophil
280 development was disrupted by knocking down the G-CSF/GCSFR pathway using *csf3R* morpholino,
281 previously reported to decrease up to 70% of the neutrophils present [30-32]. We then monitored the
282 efficiency of the *csf3R* morpholino knockdown in double transgenic larvae confirming that 75% of the
283 neutrophil population was depleted, while macrophage numbers were only slightly decreased (Fig
284 S3B). When HD Δ*dotA*-GFP was injected, neutrophil-depleted larvae survived, and the bacterial
285 burden remained unchanged, similar to what we had observed in infections of macrophage-depleted
286 larvae (Fig. 5D, E). However, when neutrophil-depleted larvae were injected with HD WT-GFP, larvae
287 survival significantly decreased and bacterial burdens increased at 48hpi (Fig. 5D, E). Neutrophil-
288 depleted fish larvae showed an intermediate phenotype, displaying less survival and higher bacterial
289 burden than in WT infected control larvae (Fig. 1A) but more survival and lower bacterial burden
290 than in macrophage-depleted larvae (Fig. 5D, E). Intravital imaging showed that csf3R knockdown
291 larvae that were unable to control *L. pneumophila* infection showed bacterial proliferation in the yolk
292 comparable to WT control larvae (Fig 5F).
293 These results show that both neutrophils and macrophages are required for restricting and
294 controlling *L. pneumophila* infection in the zebrafish model, but macrophages play the key role.
295 Although neutrophils contributed less to clear the bacteria upon bloodstream injection, neutrophils
296 might impact the infection outcome through cytokine release that can modulate macrophage
297 activity.

Key pro-inflammatory cytokines are induced upon L. pneumophila infection of zebrafish larvae

Proinflammatory cytokines produced by infected and bystander cells during *L. pneumophila* infection of humans and mice play crucial roles in orchestrating host defences to control infection [33,34]. Infected cells produce IL-1α and IL-1β through a mechanism involving MyD88-dependent translational bypass. In contrast, bystander cells produce IL-6, TNF-α and IL-12 in an IL-1 receptor (IL-1R) dependant way [33,35]. To determine the pro-inflammatory responses of zebrafish larvae during *L. pneumophila* infection, we analysed *il1b*, *tnfa*, and *ifng1/2* (orthologues of mammalian *Ifng*) gene expression levels over time by qRT-PCR on RNA isolated from individual infected larvae. We found that infection of zebrafish larvae with LD or HD of WT-GFP induced a rapid (by 6hpi) and robust induction of *il1b* and *tnfa* gene expression. In larvae injected with low doses of WT-GFP the expression levels started to decrease by 24hpi, and gradually became undetectable at 72hpi. In contrast, larvae injected with HD of WT-GFP, expression of *il1b* and *tnfa* did not decrease over time (Fig. S3A and B) and a significant induction of *ifng1* was observed at 48hpi (Fig. S3C) but not of *ifng2* (Fig. S3D). In parallel, we scored the bacterial burden of the infected larvae before pro-inflammatory cytokine measurement at each time point under the microscope, which consistently showed that larvae with increased *il1b* and *tnfa* induction had also high bacterial burdens in the yolk and were not controlling the infection. These pro-inflammatory responses were T4SS dependent, as zebrafish larvae infected with HD of Δ*dotA*-GFP did not show significant induction of transcription of *tnfa*, *il1b* and *ing1/2* (Fig. S3 A-D).

Collectively, these results reveal, that key pro-inflammatory cytokines known to orchestrate the host response during *L. pneumophila* infection in humans are also induced in zebrafish larvae, and that cytokine gene induction is sustained when uncontrolled *L. pneumophila* proliferation occurs.

The immune response of zebrafish larvae to L. pneumophila infection is independent of MyD88 signalling

In innate immunity, the myeloid differentiation factor 88 (MyD88) plays a pivotal role in immune cell activation through Toll-like receptors (TLRs). MyD88-deficient mice are highly susceptible to *L. pneumophila* infection [36-39], however this is not the case when human macrophages are depleted of MyD88 [40]. Therefore, we sought to analyse which role MyD88 plays in zebrafish larvae during *L. pneumophila* infection. We injected *myd88-/-* and control larvae with LD or HD of WT-GFP, or with HD of Δ*dotA*-GFP and monitored larvae survival and bacterial burden over time as described in Figure 1. Our results show that susceptibility to infection of *myd88-/-* larvae injected with HD of WT-GFP, was comparable to that of WT larvae (Fig. 6A). Similarly, both control and *myd88-/-* larvae injected with LD WT-GFP or with the avirulent Δ*dotA*-GFP bacteria did not develop an infection, and the

bacterial burden decreased over time indicating that bacteria were cleared (Fig. 6A, B). To determine if pro-inflammatory responses were affected in the absence of MyD88 signalling, we analysed *il1b* and *tnfa* gene expression levels over time in control and *myd88*-/- larvae. Our results showed that *il1b* and *tnfa* gene expression levels were comparable in control and *myd88*-/- infected larvae for all conditions tested (LD WT-GFP and HD Δ*dotA*-GFP (Fig 6C, D).

Taken together, our results suggest that MyD88 signalling is not required for the innate immune response against *L. pneumophila* infection in the zebrafish larvae, which recapitulates human infection. However, MyD88 signalling may also be functionally compensated by other immune signalling pathways.

***Legionella pneumophila* replication in the yolk of zebrafish larvae is T4SS dependent**

Interestingly, replication of *L. pneumophila* mainly took place in the yolk region of infected zebrafish larvae (Movie S1-4, Fig. 2), dependent on a functioning T4SS as Δ*dotA*-GFP failed be detected in the yolk. To investigate whether the secretion mutant would be able to grow in the yolk cell when reaching it, we injected LD and HD of WT-GFP or Δ*dotA*-GFP directly into the yolk cell cytoplasm of 72hpf *lys*:DsRed zebrafish larvae (Fig. S4A). WT-GFP replicated extensively in the yolk region with low and high dose infections leading to rapid bacterial proliferation followed by a marked increase of the bacterial burden and death of the larvae (Fig. 7A, B). Surprisingly, Δ*dotA*-GFP did not replicate in the yolk even when injected directly but persisted over 72hpi. This result suggests that T4SS system is not only crucial for crossing the yolk sac syncytium but that its effectors are also necessary to obtain nutrients from the environment to allow replication. To further analyze this hypothesis, we selected a mutant in the gene encoding a sphingosine-1 phosphate lyase, (WT, Δ*spl)* [41] as we reasoned that this enzyme might be implicated in degrading sphingolipids present in the yolk of zebrafish larvae and thereby might aid *L. pneumophila* to obtain nutrients. Injection of Δ*spl* in the yolk sac region, and analyses of larvae death as compared to WT or Δ*dotA* showed that survival of zebrafish larvae injected with the Δ*spl* was slightly higher than with WT injected larvae (Fig. S4B), suggesting that the T4SS effector *Lp*Spl might be implicated in nutrient acquisition in the yolk environment.

Interestingly, the first isolation of *L. pneumophila* was achieved by inoculating the yolk region of embryonated eggs probably due to the richness in nutrients provided by the yolk [6]. Later yolk sacs of embryonated hen's eggs were used to produce polyvalent antigens for the diagnosis of *L. pneumophila* [42]. Thus, we decided to analyse *L. pneumophila* WT and Δ*dotA* phenotypes in the yolk sac of embryonated chicken eggs (ECE). We inoculated ECE directly in the yolk region with WT and with the Δ*dotA* strain at a concentration of 9.2 $\log_{10}$ CFU/mL and 9.1 $\log_{10}$ CFU/mL, respectively and assessed mortality of the embryos daily. The total mortality during the 6-day observation period in WT-GFP infected eggs was significantly higher (88.9%) than in the Δ*dotA*-infected eggs (14.3%;

p=0.010) or PBS inoculated control eggs (28.6%; *p*=0.010 and *p*=0.021, respectively), which were not significantly different from each other (p=0.253) (Fig. S4C). The highest mortality was observed at 2 days post infection in WT inoculated eggs with 55.6% mortality *versus* 0% in Δ*dotA* or 28.6% mortality in PBS inoculated eggs. Quantification of *L. pneumophila* in the yolk sac region at the day of mortality or at day 6 post infection revealed that the number of bacteria in the yolk sac of WT-infected ECE, was significantly higher than that in the yolk sac of those infected with the Δ*dotA* strain (7.8 $\log_{10}$ CFU/mL and 5.9 $\log_{10}$ CFU/mL, respectively, p=0.0127) (Fig. S4D). Controls inoculated with PBS (n=2) showed no *L. pneumophila* growth. Thus, like in zebrafish larvae only the WT strain is able to replicate in the yolk region and of inducing mortality in the embryos, while the T4SS mutant strain persists but is not able to replicate and does not induce high embryo mortality. This result further supports the finding that the T4SS system is crucial for obtaining nutrients when lipids are the major energy source available.

We next monitored neutrophil behaviour in the yolk-injected *lyz*:DsRed larvae in which neutrophils are labelled red. This showed that replication of WT-GFP in the yolk coincides with neutrophil death (Fig. 7C and D). The yolk cell is a single large cell where leukocytes were described to be unable to enter [43], but interestingly, macrophages and neutrophils were highly recruited to the yolk of WT-GFP infected larvae (Figure 2B-E), suggesting that *L. pneumophila* is sensed by the immune system even when replicating in the yolk, and could induce neutrophil death “at distance”. It is likely neutrophils can partly counteract *L. pneumophila* growth in the yolk by degranulating “at distance”, as previously shown in a zebrafish notochord infection model using non-pathogenic *E. coli* [32].

Our results suggest that the *L. pneumophila* T4SS plays a crucial role for the bacteria to pass from the blood circulation into the yolk and that T4SS effectors play an important role to obtain nutrients for bacterial proliferation.

DISCUSSION

In this study, we developed a zebrafish larva infection model for *L. pneumophila* and have analysed host pathogen interactions and the innate immune response of the host. We have found that a successful infection of zebrafish larvae by *L. pneumophila* depends on the infection site, the infection dose, the T4SS Dot/Icm and the host innate immune response, in particular macrophages and neutrophils. Wild type zebrafish larvae are susceptible to infection in a dose dependent manner, as larvae infected with a highly concentrated bacterial inoculum displayed bacterial dissemination and replication, concomitant with host death. However, as only about 30% of the larvae displayed this phenotype, the innate host defence of the larvae against *L. pneumophila* infection is relatively efficient. Thus, similar to what is observed in *L. pneumophila* infection of immune competent

individuals, the development of Legionnaire's disease is determined not only by the infection dose but also by the capacity of the host immune system to quickly and efficiently respond to infection.

Only blood borne bacteria are able to proliferate and induce mortality in zebrafish larvae. Once in the blood circulation, bacteria are actively engulfed and eliminated by both macrophages and neutrophils. However, some bacteria resist intracellular killing and replicate extensively inside macrophages (Fig. S2), get released into the blood flow and circulate in the zebrafish larvae. Some reach the yolk sac syncytium and T4SS competent *L. pneumophila* are able to cross this barrier and enter the yolk sac region. Once in the yolk, *L. pneumophila* gains a significant advantage in the pathogen-host arms race and establishes a replicative niche where it proliferates extensively. Indeed, in the yolk sac region *L. pneumophila* is protected from the host immune system as professional phagocytes are unable to enter in the yolk. Proliferation of the bacteria leads to host death, likely due to exhaustion of the nutrients present in the yolk, which are key in supporting the larvae development and due to the physical compression of the visceral developing organs, in particular the gastro-intestinal tract, exerted by the growing bacterial aggregate. Interestingly, we have also observed that in few cases the infected larvae were able to extrude the bacterial aggregates growing in the yolk and survived. This host defence mechanism has also been reported in a caudal fin model of *Mycobacterium marinum* infection, where infected zebrafish larvae extruded the bacteria-containing granuloma [44].

To our knowledge, the establishment of a replicative niche in the yolk upon injection in the bloodstream is unique to *L. pneumophila.* Most interestingly, direct yolk sac injection revealed that only the WT strain but not the T4SS knockout strain is able to replicate and establish a persistent infection, irrespective of the dose injected. This result points towards the involvement of the T4SS system and its secreted effectors in infection, replication and nutrient uptake in the yolk environment. Further analyses of this phenotype in embryonated chicken eggs, a commonly used model for antigen preparation, showed again, that only WT *L. pneumophila* are able to replicate in the yolk sac region, confirming the importance of the T4SS in nutrient uptake in addition to its known role in infection (Fig. S4A, B, C). *L. pneumophila* is known to mainly use amino acids as carbon and energy sources for growth [45] and secreted T4SS effectors have been shown to aid in amino acid uptake [46], however, fatty acids, glucose and/or glycerol also serve as carbon sources during the later stages of the life cycle of *L. pneumophila* [47,48], but no effectors connected to the uptake of these nutrients have been identified yet. The yolk cell is composed of a complex and dynamic mixture of different lipids on which the zebrafish larvae rely on for nutrition throughout development in the early larva phase. Cholesterol and phosphatidylcholine are the main constituents until 120hpf, with triacylglycerol, phosphatidylinositol, phosphatidylethanolamine, diacyl-glycerol, cholesteryl esters and sphingomyelins also present in significant concentrations [49]. *L. pneumophila* is known to secrete

437 several effectors with lipolytic activity through its T4SS which could be important for growth in a lipid
438 rich environment like the yolk (Hiller et al., 2018). In a first attempt to identify one of these effectors
439 we analysed the growth of a *L. pneumophila* mutant in a gene encoding a sphingosine-1 phosphate
440 lyase (*Lp*Spl) [41] compared to the WT strain after direct injection in the zebrafish larvae yolk sac.
441 Indeed, a small difference in larvae mortality was observed for the Δ*spl* strain, suggesting that *Lp*Spl
442 is one of several effectors that might participate in nutrient acquisition from lipids (Fig. S4B).
443 However, further analyses are needed to identify all effectors implicated in this phenotype.
444 Studies of *Legionella* infection in humans, guinea pigs and mouse lungs have shown that
445 *L. pneumophila* interacts closely with neutrophils and mononuclear phagocytes [50,51]. Professional
446 phagocytes are the main replication niche for *L. pneumophila* with monocytes and macrophages, in
447 particular alveolar macrophages, representing the main cells for replication in the lungs [52-55]. *In vivo*
448 studies in mice have shown that upon lung infection with *L. pneumophila* neutrophils, cDCs,
449 monocytes, and monocyte-like cells are rapidly recruited to the infection site, but although all these
450 cells seem to engulf the bacteria, *L. pneumophila* appears to be able to translocate effectors only into
451 neutrophils and alveolar macrophages. In zebrafish macrophages appear during the first days of
452 development, followed by neutrophils a day later forming together an efficient immune system that
453 protects the developing fish [23,56-58]. Therefore, the zebrafish larva offers a unique possibility to
454 interrogate the role of innate immune responses to infection [21]. Indeed, macrophage depleted larvae
455 showed a dramatically increased susceptibility to *L. pneumophila* infection as nearly 100% of larvae
456 inoculated with HD of WT and 30% of larvae inoculated with LD of *L. pneumophila* died from the
457 infection. Hence, macrophages are the first line of infection control against *L. pneumophila* and are
458 essential for restricting and controlling blood-borne infections, similar to what was observed for
459 *Burkholderia cenocepacia or Staphylococcus aureus* infection [59,60]. In contrast, when neutrophils were
460 depleted, the innate immune response was impaired to a lesser extent, suggesting that neutrophils
461 are required to ensure an effective innate immune response and, that macrophages alone are not
462 able to contain high burdens of *L. pneumophila* infection (Fig. 5).
463 Human innate immune signalling relies strongly on activation of Toll-like receptors (TLRs) and
464 respective adaptor molecules, all of which are highly conserved in the zebrafish [61,62]. One of these
465 adaptors is MyD88, known as a central player in interleukin 1 receptor (IL-1R) and TLR signalling in
466 humans and mammalian models [63]. MyD88 signalling is crucial for mice to combat *L. pneumophila*
467 infection, as it triggers the early secretion of inflammatory cytokines, neutrophil recruitment, and the
468 host immune response to the infection. Consequently, mice that lack MyD88 are highly susceptible
469 to infection [35-38]. However, in MyD88 depleted human macrophages *L. pneumophila* replication is not
470 different to replication in WT cells [40] Here we show, that *L. pneumophila* infected *myd88-/-* zebrafish
471 larvae have the same replication phenotype as WT larvae. Thus, Myd88 signalling does not play a key

role or may be redundant in the control of the innate immune response to *L. pneumophila* in zebrafish larvae, indicating that zebrafish mirrors human infection better than the mouse model. In the mouse model infected macrophages are incapable of producing cytokines, such as tumor necrosis factor (TNF) and interleukin-12 (IL-12), which are necessary to control infection. In contrast, infection of zebrafish larvae with WT *L. pneumophila* induced a rapid (by 6hpi) and robust induction of *il1b* and *tnfa* gene expression. However, it is thought that IL-1 released initially by *L. pneumophila*-infected macrophages drives the production of critical cytokines by bystander cells [33]. Infection of zebrafish larvae with HD of WT *L. pneumophila* induced a rapid (by 6hpi) and robust induction of *il1b* and *tnfa* gene expression whereas WT LD infection leads only to a short induction of *Il1b* transcript levels at 6hpi before declining to CTRL levels at later time points, suggesting that a short boost of IL-1β is sufficient to control LD of *L. pneumophila*. However, for a high load of *L. pneumophila* even a high and long-term induction of IL-1β is not allowing to control the infection, suggesting that the self-regulation of the immune response may be abrogated leading to a constant activation of IL-1β expression. Moreover, gene expression analyses also confirms that Myd88 has no influence on the control of the infection, as no difference in the transcript levels of *il1b*, *tnfa, ifng1 or infg2* was observed further suggesting that activation of the IL1R and certain TLR pathways are not crucial for *L. pneumophila* clearance in zebrafish larvae. One may even hypothesise that IL-1β release could be beneficial for *L. pneumophila* replication, as it was shown that IL-1β also may indicate an activation of the metabolic state of the bystander cells as it was shown that IL-1β induces a shift towards more metabolically active cells and increased cellular glucose uptake [64], which could aid *L. pneumophila* replication.

In conclusion, we have set up a new infection model for *L. pneumophila* that mimics human infection better than the mouse model. The unique advantages of the zebrafish provide now exciting possibilities to further explore different aspects of the relationship between, *L. pneumophila* and its host: the dynamics of bacterial dissemination, the interactions of the bacteria with macrophages and neutrophils, as well as the host immune response by intravital imaging.

EXPERIMENTAL PROCEDURES

Ethics Statement. Animal experiments were performed according to European Union guidelines for handling of laboratory animals ((http://ec.europa.eu/environment/chemicals/lab_animals/home_en.htm) and were approved by the Institut Pasteur Animal Care and Use Committee. and the French Ministry of Research (APAFIS#31827). The inoculation of embryonated chicken eggs is a standard procedure in diagnostics for the multiplication and antigen production of *Legionella* and is not covered by the national law for animal experiments in France (Décret n° 2013-118 du 1er février 2013).

Zebrafish care and maintenance. Wild-type AB fish, initially obtained from the Zebrafish International Resource Center (Eugene, OR), Tg(*Lyz::DsRed)*[nz50] [65], Tg*(mfap4::mCherryF*) (ump6Tg) [32] Tg(mpx:GFP)[i114] [66] , Tg(kdrl::mCherry)[is5] [67] and *myd88*[*hu3568*] mutant line (obtained from the Hubrecht Laboratory and the Sanger Institute Zebrafish Mutation Resource) [68], were raised in our facility. Eggs were obtained by natural spawning, bleached according to standard protocols, and kept in Petri dishes containing Volvic source water and, from 24 hours post fertilization (hpf) onwards 0.003% 1-phenyl-2-thiourea (PTU) (Sigma-Aldrich) was added to prevent pigmentation. Embryos were reared at 28°C or 24°C according to the desired speed of development; infected larvae were kept at 28°C. Timings in the text refer to the developmental stage at the reference temperature of 28.5°C. Larvae were anesthetized with 200µg/ml tricaine (Sigma-Aldrich) during the injection procedure as well as during *in vivo* imaging and processing for bacterial burden evaluation or cytokine expression studies.

Bacterial strains and growth conditions. *Legionella pneumophila* strain Paris carrying the pNT28 plasmid encoding for green fluorescent protein (constitutive GFP) [69], wild-type (WT-GFP) or Δ*dotA*-GFP were plated from -80°C glycerol stocks on N-(2-acetamido)-2-aminoethanesulfonic acid (ACES)-buffered charcoal yeast-extract (BCYE) medium supplemented with 10 µg/ml of chloramphenicol and cultured for 3 days at 37°C. Suspensions were prepared by resuspending bacteria in sterile 1x Phosphate Buffered Saline (PBS) and adjusting the OD 600 according to the desired bacterial concentrations for injection.

Morpholino injections. Morpholino antisense oligonucleotides (Gene Tools LLC, Philomath, OR, USA) were injected at the one to two cell stage as described [70]A low dose (4ng) of spi1b (previously named pu1) translation blocking morpholino (GATATACTGATACTCCATTGGTGGT) [71] blocks macrophage development only, but can also block neutrophil development when it is injected at a higher dose (20ng in 2nl). The csf3r translation blocking morpholino (GAACTGGCGGATCTGTAAAGACAAA) (4ng) [30] was injected to block neutrophil development. Control morphants were injected with 4ng control morpholino, with no known target (GAAAGCATGGCATCTGGATCATCGA).

Zebrafish infections. The volume of injected suspension was deduced from the diameter of the drop obtained after mock microinjection, as described in [70]. Bacteria were recovered by centrifugation, washed, resuspended at the desired concentration in PBS. 72h post-fertilization (hpf) anesthetized zebrafish larvae were microinjected iv or in the yolk with 0.5-1nl of bacterial suspension at the desired dose (~10^3 bacteria/nl for Low Dose (LD) and ~10^4 bacteria/nl for High Dose (HD) as described [22,28]. Infected larvae were transferred into individual wells (containing 1ml of Volvic water +

0.003% PTU in 24-well culture plates), incubated at 28°C and regularly observed under a stereomicroscope.

Evaluation of the bacterial burden in infected larvae. Infected zebrafish larvae were collected at 0, 24, 48 and 72hpi and lysed for analysing the bacterial burden by FACS. Each larva was placed in a 1.5 ml Eppendorf tube and anesthetized with tricaine (200µg/ml), washed with 1ml of sterile water and placed in 150 µl of sterile water. Larvae were then homogenized using a pestle motor mixer (Argos). Each sample was transferred to an individual well of a 96 well plate, counted on a MACSQuant VYB FACS (Miltenyi Biotec) and data analysed using FlowJo version 7.6.5. For CFU enumeration, serial dilutions were plated on BCYE agar plates supplemented with Chloramphenicol and the *Legionella* Selective Supplement GVPN (Sigma). Plates were incubated for 4-5 days at 37°C and colonies with the appropriate morphology and colour were scored using the G-Box imaging system (Syngene) and colonies enumerated using the Gene Tools software (Syngene).

***Dissociation of zebrafish larvae for FACS analysis of macrophages*.** Three to five Tg*(mfap4::mCherryF)* larvae were pooled in single 1.5 ml Eppendorf tubes and anesthetized with tricaine. The supernatant was discarded, and the larvae were resuspended in 1ml of 1x trypsin-EDTA solution (SIGMA) and incubated in a dry heat block at 30°C for 10 - 20 min. Every 2 minutes, the suspensions were homogenised by pipetting, until full homogenisation was reached. $CaCl_2$ (final concentration of 2µM) and foetal bovine serum (final concentration of 10%) were added to each tube and samples were kept on ice. Lysates were filtered using 40 µm strainers, washed with 20 ml ice cold 1X PBS and centrifuged 5 min at 1500 g, 4°C. Remaining pellets were resuspended in 250 µl 1X PBS and analysed with a MACSQuant VYB FACS (Miltenyi Biotec).

Live imaging, image processing and analysis. Quantification of total neutrophils and/or macrophages on living transgenic reporter larvae was performed upon infection as previously described [28]. Briefly, bright field, DsRed and GFP images of whole living anesthetized larvae were taken using a Leica Macrofluo™ Z16 APOA (zoom 16:1) equipped with a Leica PlanApo 2.0X lens, and a Photometrics® CoolSNAP™ *HQ2* camera. Images were captured using Metavue software 7.5.6.0 (MDS Analytical Technologies). Then larvae were washed and transferred in a new 24 wells plate filled with 1ml of fresh water per well, incubated at 28°C and imaged again under the same conditions the day after. Pictures were analysed, and Tg(*lyzC::DsRed*) neutrophils or Tg(*mfap4::mCherryF*) macrophages manually counted using the ImageJ software (V 1.52a). Counts shown in figures are numbers of cells per image.

575 The bacterial burden was measured by counting the total number of pixels corresponding to
576 the GFP channel (Metavue software 7.5.6.0). Briefly, images corresponding to the GFP channel were
577 adjusted to a fixed threshold that allowed to abrogate the background of the autofluorescence of the
578 yolk. The same threshold was used for all images of one experiment. Histogram in the Analyze menu
579 was used to obtain the number of black and white pixels. As shown in figure S1A, number of white
580 pixels corresponding to *L. pneumophila* are plotted using GraphPad Prism® software.
581 High resolution confocal live imaging of injected larvae was performed as previously
582 described [72]. Briefly, injected larvae were positioned in lateral or ventral position in 35 mm glass-
583 bottom-Dishes (Ibidi Cat#: 81158). Larvae were immobilized using a 1% low-melting-point agarose
584 (Promega; Cat#: V2111) solution and covered with Volvic water containing tricaine. A Leica SP8
585 confocal microscope equipped with two PMT and Hybrid detector, a 20X IMM objective (HC PL APO
586 CS2 20X/0.75), a X–Y motorized stage and with the LAS-X software was used to live image injected
587 larvae. To generate images of the whole larvae, a mosaic of confocal z-stack of images was taken
588 with the 20X objective using the Tile Scan tool of the LAS-X software and was stitched together using
589 the Mosaic Merge tool of the LAS-X software. All samples were acquired using the same settings,
590 allowing comparisons of independent experiments. After acquisition, larvae were washed and
591 transferred in a new 24-well plate filled with 1 ml of fresh water per well, incubated at 28°C and
592 imaged again under the same conditions over time. A Leica SPE inverted confocal microscope and a
593 40x oil immersion oil immersion objective (ACS APO 40 × 1.15 UV) was also used to live image larvae
594 infected with *L. pneumophila* Δ*dotA*-GFP (Figure 4).
595 The 4D files generated by the time-lapse acquisitions were processed, cropped, analysed,
596 and annotated using the LAS-X and LAS-AF Leica software. Acquired Z-stacks were projected using
597 maximum intensity projection and exported as AVI files. Frames were captured from the AVI files and
598 handled with Photoshop software to mount figures. AVI files were also cropped and annotated with
599 ImageJ software. Files generated with the LAS-X software were also processed and analysed with the
600 Imaris software version9.5 (Bitplane, OXFORD Instruments) for 3D reconstruction, surfacing and
601 volume rendering.
602
603 ***qRT-PCR to measure gene expression of cytokine encoding genes .*** RNA was extracted from
604 individual larvae using the RNeasy® Mini Kit (Qiagen). cDNA was obtained using M-MLV H- reverse-
605 transcriptase (Promega) with a dT_{17} primer. Quantitative PCR was performed on an ABI7300
606 thermocycler (Applied Biosystems) using TakyonTM ROX SYBR® 2X MasterMix (Eurogentec) in a final
607 volume of 10 µl. Primers used: *ef1a (housekeeping gene used for normalization):*
608 GCTGATCGTTGGAGTCAACA and ACAGACTTGACCTCAGTGGT*; il1b*: GAGACAGACGGTGCTGTTTA and

609 GTAAGACGGCACTGAATCCA*; tnfa*: TTCACGCTCCATAAGACCCA and CAGAGTTGTATCCACCTGTTA*; ifng-*
610 *1-1*: ACCAGCTGAATTCTAAGCCAA and TTTTCGCCTTGACTGAGTGAA; *ifng-2:* GAATCTTGAGGAAAGTG
611 AGCA and TCGTTTTCCTTGATCGCCCA
612
613 ***Statistical analysis.*** Normal distributions were analysed with the Kolmogorov– Smirnov and the
614 Shapiro–Wilk tests. To evaluate difference between means of normally distributed data (for
615 neutrophil and macrophage numbers), an analysis of variance followed by Bonferroni's multiple
616 comparison tests was used. For bacterial burdens (CFU/FACS counts), values were Log10
617 transformed. Values of FACS and CFU counts did not pass the normality test, data were analysed
618 following the Mann-Whitney test. For cytokine expression and bacterial burdens, non-Gaussian data
619 were analysed with the Kruskal– Wallis test followed by Dunn's multiple comparison test. $P < 0.05$
620 was considered statistically significant (symbols: **** $P < 0.0001$; ***$P < 0.001$; **$P < 0.01$; *$P <$
621 0.05). Survival data were plotted using the Kaplan–Meier estimator and log-rank (Mantel–Cox) tests
622 were performed to assess differences between groups. Statistical analyses were performed using
623 GraphPad Prism® software. Statistical analyses for *in ovo* experiments, were performed using
624 GraphPrism version 7. Comparison of survival curves between different infection groups was carried
625 out with the Log-rank (Mantel-Cox) test. Comparisons of the means of *L. pneumophila* CFU counts
626 between groups were performed by the Mann–Whitney test. A p-value under 0.05 was considered
627 statistically significant.
628
629 **Inoculation and quantification of *L. pneumophila* strains in *in ovo* experiments.** Fertilized chicken
630 eggs purchased from a local producer (Saint-Maurice-sur-Dargoire, Rhône, France) were incubated at
631 35°C in an egg incubator (Maino, Italy) to maintain normal embryonic development. Eggs were
632 pathogen and antibiotic free. On day 0, 23 embryonated chicken eggs (ECE) were inoculated at 8
633 days of embryonation (DOE) with either *L. pneumophila* WT (n=9), *L. pneumophila ΔdotA* (n=7) or
634 sterile PBS as control (n=7). *L. pneumophila* concentration in WT and Δ*dotA* suspensions before ECE
635 injection was quantified at 9.2 $\log_{10}$ CFU/mL and 9.1 $\log_{10}$ CFU/mL, respectively. *L. pneumophila*
636 concentration in the yolk sac of ECE directly after injection were estimated, considering both the
637 measured inoculum counts and the yolk sac volumes (median (interquartile range) [IQR] volume, 30
638 [28.7-31.2] mL), at 7.4 and 7.3 $\log_{10}$ CFU/mL in the WT and Δ*dotA* groups, respectively. Two-day
639 cultures of Lpp-WT and Lpp-Δ*dotA* on BCYE at 36°C were suspended in PBS at a DO = 2.5 McFarland
640 (9 $\log_{10}$ CFU/mL) and 0.5 mL of suspensions or PBS as negative control were inoculated in the yolk sac
641 of ECE. After inoculation, ECE were candled every 24 hours to assess embryo viability until day-6 post
642 infection. Embryos that died the day after inoculation (n=2, corresponding to one WT-infected and
643 one *ΔdotA*-infected embryo) were discarded for *L. pneumophila* quantification as death was probably

644 due to bad inoculation. Dead embryos were stored at 4°C overnight prior to harvesting the yolk sacs.
645 Remaining live embryos at 6-days post injection were euthanized by refrigeration overnight and the
646 yolk sacs were collected. After measuring their volume, yolk sacs were crushed using gentleMACS™
647 Octo Dissociator (Miltenyi Biotec, Germany) and 100 µL of serial dilutions at 10^{-2}, 10^{-4} and 10^{-6} were
648 automatically plated using easySpiral® automatic plater (Interscience, France) in triplicates on BCYE
649 agar. *L. pneumophila* were quantified after 5 days-incubation using Scan® 1200 Automatic HD colony
650 counter (Interscience, France).
651
652 **Author contributions**
653 FV, LB, DS, VL, MI and ECG performed the experiments, FV, SJ, LB, ECG and CB designed the
654 experiments, FV, LB, ECG analyzed the experiments, VL performed IMARIS analysis of the raw
655 confocal high resolution acquisition data, FV, ECG and CB wrote the article, ECG and CB supervised
656 the work and acquired funds.
657
658 **Competing Interest**
659 The authors declare there are no competing interests.
660
661 **ACKNOWLEDGEMENTS**
662 We thank Pedro Escoll and Jean-Pierre Levraud for help and ideas in the initial set up of the project
663 and Tobias Sahr for critical reading and helpful discussions and Yohann Rolin and Noël Aimar for their
664 excellent care of the fish. Work in the CB laboratory is financed by the Institut Pasteur, the Fondation
665 pour la Recherche Médicale (FRM) grant N° EQU201903007847 and the grant n°ANR-10-LABX-62-
666 IBEID. Work in ECG group is financed by Institut Pasteur, CNRS, and ANR grant N° 17-CE15-0026.
667 Valerio Laghi is funded by ANR grant TIFAsomes. We wish to thank the fish facility (Yohann Rolin and
668 Noël Aimar) for their excellent care of the fish. The funders, other than the authors, did not play any
669 role in the study or in the preparation of the article or decision to publish.
670
671 **REFERENCES**
672 1 Fliermans, C. B. Ecology of Legionella: From Data to Knowledge with a Little Wisdom. *Microb Ecol*
673 **32**, 203-228 (1996).
674 2 Cunha, B. A., Burillo, A. & Bouza, E. Legionnaires' disease. *Lancet* **387**, 376-385,
675 doi:10.1016/S0140-6736(15)60078-2 (2016).
676 3 Rowbotham, T. J. Preliminary report on the pathogenicity of *Legionella pneumophila* for
677 freshwater and soil amoebae. *J Clin Pathol* **33**, 1179-1183 (1980).
678 4 Boamah, D. K., Zhou, G., Ensminger, A. W. & O'Connor, T. J. From Many Hosts, One Accidental
679 Pathogen: The Diverse Protozoan Hosts of *Legionella*. *Frontiers in cellular and infection*
680 *microbiology* **7**, 477, doi:10.3389/fcimb.2017.00477 (2017).

5 Mampel, J. *et al.* Planktonic replication is essential for biofilm formation by *Legionella pneumophila* in a complex medium under static and dynamic flow conditions. *Appl Environ Microbiol* **72**, 2885-2895, doi:10.1128/AEM.72.4.2885-2895.2006 (2006).

6 McDade, J. E. *et al.* Legionnaires' disease: isolation of a bacterium and demonstration of its role in other respiratory disease. *N Engl J Med* **297**, 1197-1203 (1977).

7 Lanternier, F. *et al.* Legionnaire's Disease in Compromised Hosts. *Infect Dis Clin North Am* **31**, 123-135, doi:10.1016/j.idc.2016.10.014 (2017).

8 Naujoks, J., Lippmann, J., Suttorp, N. & Opitz, B. Innate sensing and cell-autonomous resistance pathways in Legionella pneumophila infection. *Int J Med Microbiol* **308**, 161-167, doi:10.1016/j.ijmm.2017.10.004 (2018).

9 Isberg, R. R., O'Connor, T. J. & Heidtman, M. The *Legionella pneumophila* replication vacuole: making a cosy niche inside host cells. *Nat Rev Microbiol* **7**, 13-24, doi:nrmicro1967 [pii]10.1038/nrmicro1967 (2009).

10 Mondino, S. *et al.* Legionnaires' Disease: State of the Art Knowledge of Pathogenesis Mechanisms of Legionella. *Annu Rev Pathol* **15**, 439-466, doi:10.1146/annurev-pathmechdis-012419-032742 (2020).

11 Ensminger, A. W. *Legionella pneumophila*, armed to the hilt: justifying the largest arsenal of effectors in the bacterial world. *Curr Opin Microbiol* **29**, 74-80, doi:10.1016/j.mib.2015.11.002 (2016).

12 Cazalet, C. *et al.* Evidence in the *Legionella pneumophila* genome for exploitation of host cell functions and high genome plasticity. *Nat Genet* **36**, 1165-1173 (2004).

13 Mondino, S., Schmidt, S. & Buchrieser, C. Molecular Mimicry: a Paradigm of Host-Microbe Coevolution Illustrated by Legionella. *mBio* **11**, doi:10.1128/mBio.01201-20 (2020).

14 Brassinga, A. K. *et al. Caenorhabditis* is a metazoan host for *Legionella*. *Cell Microbiol* **12**, 343-361, doi:CMI1398 [pii]10.1111/j.1462-5822.2009.01398.x (2009).

15 Harding, C. R. *et al. Legionella pneumophila* pathogenesis in the *Galleria mellonella* infection model. *Infect Immun* **80**, 2780-2790, doi:10.1128/IAI.00510-12 (2012).

16 Brown, A. S., van Driel, I. R. & Hartland, E. L. Mouse Models of Legionnaires' Disease. *Curr Top Microbiol* **376**, 271-291, doi:10.1007/82_2013_349 (2014).

17 Breiman, R. F. & Horwitz, M. A. Guinea pigs sublethally infected with aerosolized *Legionella pneumophila* develop humoral and cell-mediated immune responses and are protected against lethal aerosol challenge. A model for studying host defense against lung infections caused by intracellular pathogens. *J Exp Med* **165**, 799-811 (1987).

18 Weeratna, R. *et al.* Human and guinea pig immune responses to Legionella pneumophila protein antigens OmpS and Hsp60. *Infect Immun* **62**, 3454-3462 (1994).

19 Masud, S., Torraca, V. & Meijer, A. H. Modeling Infectious Diseases in the Context of a Developing Immune System. *Curr Top Dev Biol* **124**, 277-329, doi:10.1016/bs.ctdb.2016.10.006 (2017).

20 Torraca, V. & Mostowy, S. Zebrafish Infection: From Pathogenesis to Cell Biology. *Trends in Cell Biology* **28**, 143-156, doi:10.1016/j.tcb.2017.10.002 (2018).

21 Gomes, M. C. & Mostowy, S. The Case for Modeling Human Infection in Zebrafish. *Trends in Microbiology* **28**, 10-18, doi:10.1016/j.tim.2019.08.005 (2020).

22 Colucci-Guyon, E., Tinevez, J. Y., Renshaw, S. A. & Herbomel, P. Strategies of professional phagocytes in vivo: unlike macrophages, neutrophils engulf only surface-associated microbes. *J Cell Sci* **124**, 3053-3059, doi:10.1242/jcs.082792 (2011).

23 Herbomel, P., Thisse, B. & Thisse, C. Ontogeny and behaviour of early macrophages in the zebrafish embryo. *Development* **126**, 3735-3745 (1999).

24 Liu, X. & Shin, S. Viewing *Legionella pneumophila* Pathogenesis through an Immunological Lens. *J Mol Biol* **431**, 4321-4344, doi:10.1016/j.jmb.2019.07.028 (2019).

25 Cohen, S. B. *et al.* Alveolar Macrophages Provide an Early *Mycobacterium tuberculosis* Niche and Initiate Dissemination. *Cell Host Microbe* **24**, 439-446 e434, doi:10.1016/j.chom.2018.08.001 (2018).

26 Mengue, L. *et al. Legionella pneumophila* decreases velocity of Acanthamoeba castellanii. *Exp Parasitol* **183**, 124-127, doi:10.1016/j.exppara.2017.07.013 (2017).

27 Simon, S., Wagner, M. A., Rothmeier, E., Muller-Taubenberger, A. & Hilbi, H. Icm/Dot-dependent inhibition of phagocyte migration by *Legionella* is antagonized by a translocated Ran GTPase activator. *Cell Microbiol* **16**, 977-992, doi:10.1111/cmi.12258 (2014).

28 Mostowy, S. *et al.* The zebrafish as a new model for the in vivo study of *Shigella flexneri* interaction with phagocytes and bacterial autophagy. *PLoS Pathog* **9**, e1003588, doi:10.1371/journal.ppat.1003588 (2013).

29 Su, F. *et al.* Differential regulation of primitive myelopoiesis in the zebrafish by Spi-1/Pu.1 and C/ebp1. *Zebrafish* **4**, 187-199, doi:10.1089/zeb.2007.0505 (2007).

30 Ellett, F., Pase, L., Hayman, J. W., Andrianopoulos, A. & Lieschke, G. J. mpeg1 promoter transgenes direct macrophage-lineage expression in zebrafish. *Blood* **117**, e49-56, doi:10.1182/blood-2010-10-314120 (2011).

31 Palha, N. *et al.* Real-time whole-body visualization of Chikungunya Virus infection and host interferon response in zebrafish. *PLoS Pathog* **9**, e1003619, doi:10.1371/journal.ppat.1003619 (2013).

32 Phan, Q. T. *et al.* Neutrophils use superoxide to control bacterial infection at a distance. *Plos Pathogens* **14**, doi:ARTN e100715710.1371/journal.ppat.1007157 (2018).

33 Copenhaver, A. M., Casson, C. N., Nguyen, H. T., Duda, M. M. & Shin, S. IL-1R signaling enables bystander cells to overcome bacterial blockade of host protein synthesis. *Proc Natl Acad Sci U S A* **112**, 7557-7562, doi:10.1073/pnas.1501289112 (2015).

34 Friedman, H., Yamamoto, Y. & Klein, T. W. *Legionella pneumophila* pathogenesis and immunity. *Semin Pediatr Infect Dis* **13**, 273-279, doi:10.1053/spid.2002.127206 (2002).

35 Asrat, S., de Jesus, D. A., Hempstead, A. D., Ramabhadran, V. & Isberg, R. R. Bacterial pathogen manipulation of host membrane trafficking. *Annu Rev Cell Dev Biol* **30**, 79-109, doi:10.1146/annurev-cellbio-100913-013439 (2014).

36 Archer, K. A., Alexopoulou, L., Flavell, R. A. & Roy, C. R. Multiple MyD88-dependent responses contribute to pulmonary clearance of Legionella pneumophila. *Cell Microbiol* **11**, 21-36, doi:CMI1234 [pii]10.1111/j.1462-5822.2008.01234.x (2009).

37 Archer, K. A. & Roy, C. R. MyD88-dependent responses involving toll-like receptor 2 are important for protection and clearance of Legionella pneumophila in a mouse model of Legionnaires' disease. *Infect Immun* **74**, 3325-3333, doi:74/6/3325 [pii]10.1128/IAI.02049-05 (2006).

38 Hawn, T. R., Smith, K. D., Aderem, A. & Skerrett, S. J. Myeloid differentiation primary response gene (88)- and toll-like receptor 2-deficient mice are susceptible to infection with aerosolized Legionella pneumophila. *J Infect Dis* **193**, 1693-1702, doi:10.1086/504525 (2006).

39 Sporri, R., Joller, N., Albers, U., Hilbi, H. & Oxenius, A. MyD88-dependent IFN-gamma production by NK cells is key for control of Legionella pneumophila infection. *J Immunol* **176**, 6162-6171, doi:176/10/6162 [pii] (2006).

40 Mallama, C. A., McCoy-Simandle, K. & Cianciotto, N. P. The Type II Secretion System of *Legionella pneumophila* Dampens the MyD88 and Toll-Like Receptor 2 Signaling Pathway in Infected Human Macrophages. *Infect Immun* **85**, doi:10.1128/IAI.00897-16 (2017).

41 Rolando, M. *et al. Legionella pneumophila* S1P-lyase targets host sphingolipid metabolism and restrains autophagy. *Proc Natl Acad Sci U S A* **113**, 1901-1906, doi:10.1073/pnas.1522067113 (2016).

42 Fallon, R. J. & Abraham, W. H. Polyvalent heat-killed antigen for the diagnosis of infection with *Legionella pneumophila*. *J Clin Pathol* **35**, 434-438, doi:10.1136/jcp.35.4.434 (1982).

43 Levraud, J. P. *et al.* Real-time observation of *Listeria monocytogenes*-phagocyte interactions in living zebrafish larvae. *Infect Immun* **77**, 3651-3660, doi:10.1128/IAI.00408-09 (2009).

44 Hosseini, R. *et al.* Efferocytosis and extrusion of leukocytes determine the progression of early mycobacterial pathogenesis. *J Cell Sci* **129**, 3385-3395, doi:10.1242/jcs.135194 (2016).

45 Tesh, M. J. & Miller, R. D. Amino acid requirements for *Legionella pneumophila* growth. *J Clin Microbiol* **13**, 865-869 (1981).

784 46 Fonseca, M. V. & Swanson, M. S. Nutrient salvaging and metabolism by the intracellular pathogen
785 *Legionella pneumophila*. *Frontiers in cellular and infection microbiology* **4**, 12,
786 doi:10.3389/fcimb.2014.00012 (2014).
787 47 Hauslein, I., Manske, C., Goebel, W., Eisenreich, W. & Hilbi, H. Pathway analysis using (13) C-
788 glycerol and other carbon tracers reveals a bipartite metabolism of *Legionella pneumophila*. *Mol*
789 *Microbiol* **100**, 229-246, doi:10.1111/mmi.13313 (2016).
790 48 Hauslein, I. *et al. Legionella pneumophila* CsrA regulates a metabolic switch from amino acid to
791 glycerolipid metabolism. *Open Biol* **7**, doi:10.1098/rsob.170149 (2017).
792 49 Fraher, D. *et al.* Zebrafish Embryonic Lipidomic Analysis Reveals that the Yolk Cell Is Metabolically
793 Active in Processing Lipid. *Cell Rep* **14**, 1317-1329, doi:10.1016/j.celrep.2016.01.016 (2016).
794 50 Brieland, J. *et al.* Replicative *Legionella pneumophila* lung infection in intratracheally inoculated
795 A/J mice. A murine model of human Legionnaires' disease. *Am J Pathol* **145**, 1537-1546 (1994).
796 51 Glavin, F. L., Winn, W. C., Jr. & Craighead, J. E. Ultrastructure of lung in Legionnaires' disease.
797 Observations of three biopsies done during the Vermont epidemic. *Ann Intern Med* **90**, 555-559,
798 doi:10.7326/0003-4819-90-4-555 (1979).
799 52 Horwitz, M. A. Formation of a novel phagosome by the Legionnaires' disease bacterium
800 (*Legionella pneumophila*) in human monocytes. *J Exp Med* **158**, 1319-1331 (1983).
801 53 Horwitz, M. A. & Silverstein, S. C. Legionnaires' disease bacterium (*Legionella pneumophila*)
802 multiples intracellularly in human monocytes. *J Clin Invest* **66**, 441-450 (1980).
803 54 Jager, J. *et al.* Human lung tissue explants reveal novel interactions during *Legionella pneumophila*
804 infections. *Infect Immun* **82**, 275-285, doi:10.1128/IAI.00703-13 (2014).
805 55 Copenhaver, A. M. *et al.* Alveolar macrophages and neutrophils are the primary reservoirs for
806 *Legionella pneumophila* and mediate cytosolic surveillance of type IV secretion. *Infect Immun* **82**,
807 4325-4336, doi:10.1128/IAI.01891-14 (2014).
808 56 Bennett, C. M. *et al.* Myelopoiesis in the zebrafish, *Danio rerio*. *Blood* **98**, 643-651,
809 doi:10.1182/blood.v98.3.643 (2001).
810 57 Le Guyader, D. *et al.* Origins and unconventional behavior of neutrophils in developing zebrafish.
811 *Blood* **111**, 132-141, doi:10.1182/blood-2007-06-095398 (2008).
812 58 Willett, C. E., Cortes, A., Zuasti, A. & Zapata, A. G. Early hematopoiesis and developing lymphoid
813 organs in the zebrafish. *Dev Dyn* **214**, 323-336, doi:10.1002/(SICI)1097-
814 0177(199904)214:4<323::AID-AJA5>3.0.CO;2-3 (1999).
815 59 Mesureur, J. *et al.* Macrophages, but not neutrophils, are critical for proliferation of *Burkholderia*
816 *cenocepacia* and ensuing host-damaging inflammation. *PLoS Pathog* **13**, e1006437,
817 doi:10.1371/journal.ppat.1006437 (2017).
818 60 Prajsnar, T. K., Cunliffe, V. T., Foster, S. J. & Renshaw, S. A. A novel vertebrate model of
819 *Staphylococcus aureus* infection reveals phagocyte-dependent resistance of zebrafish to non-host
820 specialized pathogens. *Cell Microbiol* **10**, 2312-2325, doi:10.1111/j.1462-5822.2008.01213.x
821 (2008).
822 61 Jault, C., Pichon, L. & Chluba, J. Toll-like receptor gene family and TIR-domain adapters in *Danio*
823 *rerio*. *Mol Immunol* **40**, 759-771, doi:10.1016/j.molimm.2003.10.001 (2004).
824 62 Meijer, A. H. *et al.* Expression analysis of the Toll-like receptor and TIR domain adaptor families of
825 zebrafish. *Mol Immunol* **40**, 773-783, doi:10.1016/j.molimm.2003.10.003 (2004).
826 63 Akira, S. & Takeda, K. Toll-like receptor signalling. *Nat Rev Immunol* **4**, 499-511,
827 doi:10.1038/nri1391 (2004).
828 64 Wik, J. A. *et al.* Inflammatory activation of endothelial cells increases glycolysis and oxygen
829 consumption despite inhibiting cell proliferation. *FEBS Open Bio* **11**, 1719-1730,
830 doi:10.1002/2211-5463.13174 (2021).
831 65 Hall, C., Flores, M. V., Storm, T., Crosier, K. & Crosier, P. The zebrafish lysozyme C promoter drives
832 myeloid-specific expression in transgenic fish. *Bmc Dev Biol* **7**, doi:Artn 4210.1186/1471-213x-7-
833 42 (2007).
834 66 Renshaw, S. A. *et al.* A transgenic zebrafish model of neutrophilic inflammation. *Blood* **108**, 3976-
835 3978, doi:10.1182/blood-2006-05-024075 (2006).

836 67 van Leeuwen, L. M. *et al.* A transgenic zebrafish model for the in vivo study of the blood and
837 choroid plexus brain barriers using claudin 5. *Biol Open* **7**, doi:10.1242/bio.030494 (2018).
838 68 van der Vaart, M., van Soest, J. J., Spaink, H. P. & Meijer, A. H. Functional analysis of a zebrafish
839 myd88 mutant identifies key transcriptional components of the innate immune system. *Dis Model*
840 *Mech* **6**, 841-854, doi:10.1242/dmm.010843 (2013).
841 69 Tiaden, A. *et al.* The *Legionella pneumophila* response regulator LqsR promotes host cell
842 interactions as an element of the virulence regulatory network controlled by RpoS and LetA. *Cell*
843 *Microbiol* **9**, 2903-2920, doi:CMI1005 [pii]10.1111/j.1462-5822.2007.01005.x (2007).
844 70 Levraud, J. P., Colucci-Guyon, E., Redd, M. J., Lutfalla, G. & Herbomel, P. In vivo analysis of
845 zebrafish innate immunity. *Methods Mol Biol* **415**, 337-363, doi:10.1007/978-1-59745-570-1_20
846 (2008).
847 71 Brannon, M. K. *et al. Pseudomonas aeruginosa* Type III secretion system interacts with phagocytes
848 to modulate systemic infection of zebrafish embryos. *Cell Microbiol* **11**, 755-768,
849 doi:10.1111/j.1462-5822.2009.01288.x (2009).
850 72 Colucci-Guyon, E. *et al.* Spatiotemporal analysis of mycolactone distribution i*n vivo* reveals partial
851 diffusion in the central nervous system. *PLoS Negl Trop Dis* **14**, e0008878,
852 doi:10.1371/journal.pntd.0008878 (2020).
853

854

855 **FIGURES LEGENDS**

856

857 **Figure 1. Zebrafish larvae are susceptible to intravenous *L. pneumophila* infection in a dose**
858 **dependend manner**. **A)** Scheme of the experimental set up of bacterial infection using zebrafish. A
859 72hpf zebrafish larva is shown. Bacteria are injected in the bloodstream (iv) via the caudal vein
860 (green arrow). **B)** Survival curves (established from three independent experiments) of zebrafish
861 larvae injected with WT-GFP Low Dose (WT LD) (blue curve, n=60) or High Dose (HD) (red curve,
862 n=60), or with Δ*dotA*-GFP Low Dose (Δ*dotA* LD) (green curve, n=12) or High Dose (Δ*dotA* HD) (green
863 curve, n=36), and incubated at 28°C. Non-injected fish (CTRL, black curve; n= 24). Three independent
864 experiments. **C**) Bacterial burden quantification by enumerating live bacteria in homogenates from
865 individual larvae infected with WT-GFP Low Dose (blue symbols) or High Dose (red symbols), or with
866 Δ*dotA*-GFP High Dose (green symbols) measured by FACS immediately after *L. pneumophila* injection
867 and 24h, 48h and 72h post *L. pneumophila* injection. n=10 larvae for each condition. **D)**
868 Representative images of *L. pneumophila* dissemination, determined by live imaging using a
869 fluorescence stereomicroscope, of zebrafish AB larvae infected with a LD or a HD of WT-GFP, or a HD
870 of Δ*dotA*-GFP. The same infected larvae were live imaged 4h, 24h, 48h, and 72h post injection of the
871 different *L. pneumophila* strains. GFP fluorescence of the injected bacteria is shown.

872

873 **Figure 2. Bloodstream *L. pneumophila* establish a proliferative niche in the yolk causing a persistent**
874 **local infection**. Characterization of the *L. pneumophila* foci growing in the yolk region of zebrafish
875 larvae. Maximum intensity projection of confocal acquisition using high resolution fluorescent
876 microscope. **A)** 72hpf *mfap4*: mCherry larva (red macrophages) injected in the bloodstream with HD
877 of WT-GFP and followed over time with confocal fluorescent microscopy. **B)** Imaris 3D reconstruction
878 and volume rendering of the *L. pneumophila* growth in the yolk of the same infected larva at 72hpi,
879 shown laterally. Inset shows the maximum intensity projection of the *L. pneumophila* foci in the same
880 larva mounted ventrally. **C)** Scheme of 72hpf larva indicating with green dots the yolk sustaining
881 *L. pneumophila* growing. **D**) Imaris 3D reconstruction and volume rendering of the *L. pneumophila*
882 growth (GFP labelling) in the yolk of the same infected larva at 72hpi, showed ventrally. **E)** Imaris 3D
883 reconstruction and volume rendering of the *L. pneumophila* growth in the yolk of *lyz*:DsRed (red
884 neutrophils) infected larva at 72hpi, showed laterally. **F)** Imaris 3D reconstruction and volume
885 rendering of the *L. pneumophila* growth (GFP labelling) in the yolk of wild type AB infected larva at
886 72hpi, showed laterally. Overlay of GFP and mCherry, or DsRed fluorescence is shown (2B, E, G), and
887 BF is shown to help to visualize the yolk region and host anatomy (2A, D, F). See also related Movies
888 S1-S4.

889 **Figure 3. *L. pneumophila* high dose infection results in (systemic) macrophage and neutrophil**
890 **death. A)** Representative images of *L. pneumophila* dissemination, determined by live imaging using
891 a fluorescence stereomicroscope of zebrafish Tg*(mfap4::mCherryF*) larvae infected with a Low Dose
892 or a HD of WT-GFP, or a HD of Δ*dotA*-GFP. The same infected larvae were live imaged 4h, 24h, 48h,
893 and 72h post *L. pneumophila* injection. Overlay of GFP and mCherry fluorescence is shown.
894 **B)** Macrophage counts in uninfected larvae (black symbols) or upon Low Dose (blue symbols) or High
895 Dose of WT-GFP (red symbols), or High Dose (green symbols) of Δ*dotA* -GFP injections. Macrophages
896 were counted manually from images taken on live infected larvae, using ImageJ software, and results
897 were plotted using GraphPad Prism® software. Mean±SEM are also shown (horizontal bars). Data
898 plotted are from two pooled independent experiments (n=12 larvae scored for each condition).
899 **C)** Representative images of *L. pneumophila* dissemination, determined by live imaging using a
900 fluorescence stereomicroscope, of zebrafish Tg(*LysC::DsRed)*^{nz50} larvae infected with a Low Dose or a
901 High Dose of WT-GFP or a High Dose of Δ*dotA*-GFP. The same infected larvae were live imaged 4h,
902 24h, 48h, and 72h post *L. pneumophila* injection. Overlay of GFP and DsRed fluorescence is shown.
903 **D)** Neutrophil counts in uninfected (CTRL, black symbols) or upon Low Dose or High Dose of WT-GFP
904 (blue or red symbols), or High Dose of Δ*dotA*-GFP (green symbols) injections. Data plotted in the
905 same way as for macrophage counts, are from two pooled independent experiments (n=10 larvae
906 scored for each condition).
907
908 **Figure 4. Live imaging of macrophage and neutrophil interaction with** *L. pneumophila*
909 Frames extracted from maximum intensity projection of *in vivo* time-lapse confocal fluorescent
910 microscopy of 72hpf Tg*(mfap4::mCherryF*) larvae injected in the bloodstream (iv) with a LD, HD (of WT-
911 GFP or a HD of Δ*dotA*-GFP (upper panel) or Tg(*LysC::DsRed)*^{nz50} in the bloodstream (iv) with a LD, HD of
912 WT-GFP or a HD of Δ*dotA*-GFP (lower panel) to follow macrophage and neutrophil interaction with *L.*
913 *pneumophila* respectively. Images were taken from time lapse at different time points (0hpi, 2hpi,
914 4hpi, 8hpi and 16hpi). Overlay of green (*L. pneumophila*) and red (leucocytes) fluorescence of the
915 caudal area of the larvae (region boxed in the scheme on the right of the panel) is shown. Scale bar:
916 50μm. See also related Movies S5, S6.
917
918 **Figure 5. Macrophages are crucial to restrict *Legionella pneumophila* dissemination**
919 **A)** Survival curves of CTRL morphant zebrafish larvae injected with a Low Dose (LD) (blue dashed
920 curve, n=34 larvae) or a High Dose (HD) (red dashed curve, n=34) of WT-GFP, or with a HD (green
921 dashed curve, n=24) of Δ*dotA* -GFP, and spi1b morphant zebrafish larvae injected with a LD (blue
922 curve, n=48) or a HD (red curve, n=48) of WT-GFP, or with a High Dose (HD) (green curve, n=48) of
923 Δ*dotA* -GFP. Non-injected CTRL morphant fish (black dashed curve, n=48), and spi1b morphant fish

(black curves, n=48) were used as control. Infected and control larvae were incubated at 28°C. Data plotted are from two pooled independent experiments. **B)** and **E**) Bacterial burden quantification by enumerating live bacteria in homogenates from individual larvae infected with LD of WT-GFP (blue symbols) or HD (red symbols), or with LD of Δ*dotA*-GFP (magneta symbols) or HD (green symbols), measured by plating onto BCYE agar plates supplemented with Chloramphenicol and the *Legionella* Selective Supplement GVPN immediately after *L. pneumophila* injection and 24h, 48h and 48h post *L. pneumophila* injection. n=10 larvae for each condition. **D)** Survival curves of CTRL morphant zebrafish larvae injected with a LD (blue dashed curve, n=36) or a HD (red dashed curve, n=36) of WT-GFP, or with a HD (green dashed curve, n=24) of Δ*dotA* -GFP, and csf3r morphant zebrafish larvae injected with a LD (blue curve, n=24) or a HD (red curve, n=36) of WT-GFP, or with a HD (green curve, n=36) of Δ*dotA* -GFP. Non-injected CTRL morphant fish (black dashed curve, n=48), and csf3r morphant fish (black curve, n=36) were used as control. Data plotted are from two pooled independent experiments. **C)** and **F)** Representative images of *L. pneumophila* dissemination, determined by live imaging using a fluorescence stereomicroscope, of Tg*(mfap4::mCherryF*) *spe1b* morphant larvae (**C**) and of Tg(*LysC::DsRed)*^{nz50} (**F)** csf3r morphant larvae non infected, or infected with a LD or a HD of WT-GFP, or a HD of Δ*dotA*-GFP. The same infected larvae were live imaged 4h, 24h, 48h, and 72h post *L. pneumophila* injection. Overlay of GFP and mCherry fluorescence is shown.

Figure 6. Zebrafish larva Immunity to *L. pneumophila* is independent from signalling through MyD88 or compensated by other signalling pathways. **A**) Survival curves of CTRL zebrafish larvae injected with WT-GFP Low Dose (LD) (blue dashed curve) or High Dose (HD) (red dashed curve), or with Δ*dotA* -GFP HD (green dashed curve), and *myd88*^{hu3568} mutant zebrafish larvae injected with WT-GFP LD (blue curve) or HD (red curve), or with Δ*dotA* -GFP HD (green curve). Non-injected CTRL larvae (black dashed curves), and *myd88*^{hu3568} mutant larvae (black curves) were used as control. Infected and control larvae (n= 72 fish for *myd88*^{hu3568} mutant conditions and n= 57 fish for CTRL conditions) were incubated at 28°C. Data plotted are from 3 pooled independent experiments. **B)** Bacterial Burden of *myd88*^{hu3568} mutant zebrafish larvae are the same as what is observed for control larvae. Bacterial burden quantification by enumerating live bacteria in homogenates from individual larvae infected with WT-GFP LD (blue symbols) or HD (red symbols), or with Δ*dotA* -GFP HD (green symbols) were measured by plating onto BCYE agar plates supplemented with Chloramphenicol and the *L. pneumophila* Selective Supplement GVPN immediately after *Legionella* injection and 24h, 48h and 48h post *Legionella* injection. n=15 larvae for each condition. **C-D)** Cytokine (*il1b*, *tnfa*) induction was measured from individual *myd88*^{hu3568} mutant larvae injected with a HD (red curves) of WT-GFP and non-injected fish as control (CTRL, black curves). The same colours are used in individual CTRL zebrafish with dashed curves. Data plotted are from one experiment (n=5 larvae for each condition);

individual values are shown, and curves correspond to the medians. There is no statistically significant difference between CTRL and *myd88*^{hu3568} mutant curves over time for all the conditions analysed.

Figure 7. *L. pneumophila* replication in the yolk of zebrafish larvae is T4SS dependent. **A)** Survival curves of zebrafish larvae injected with WT-GFP Low Dose (LD) (blue curve) or High Dose (HD) (red curve), or with Δ*dotA*-GFP LD (magenta curve) or HD (green curve). Non-injected larvae (black curves) were used as control. n= 48 larvae per conditions. All larvae were incubated at 28°C. Data plotted are from two pooled independent experiments. **B**) Bacterial burden quantification of zebrafish larvae injected with *L. pneumophila* in the yolk cell, by enumerating live bacteria in homogenates from individual larvae infected with WT-GFP LD (blue symbols) or HD (red symbols), or with Δ*dotA*-GFP Low Dose (LD) (magenta symbols) or HD (green symbols). They were measured by plating onto BCYE agar plates supplemented with Chloramphenicol and the *Legionella* Selective Supplement GVPN immediately after *L. pneumophila* injection and 24h, 48h and 48h post *Legionella* injection. n=10 larvae for each condition. **C-D**) Representative images of *L. pneumophila* dissemination, determined by live imaging using a fluorescence stereomicroscope, of Tg(*LysC::DsRed)*^{nz50} not infected zebrafish larvae, or infected with a Low Dose of WT-GFP or Δ*dotA* -GFP (C), or infected with a High Dose of WT-GFP or Δ*dotA* -GFP (D). The same infected larvae were live imaged 4h, 24h, 48h, and 72h post *L. pneumophila* injection. Overlay of GFP and mCherry fluorescence is shown.

Figure 1

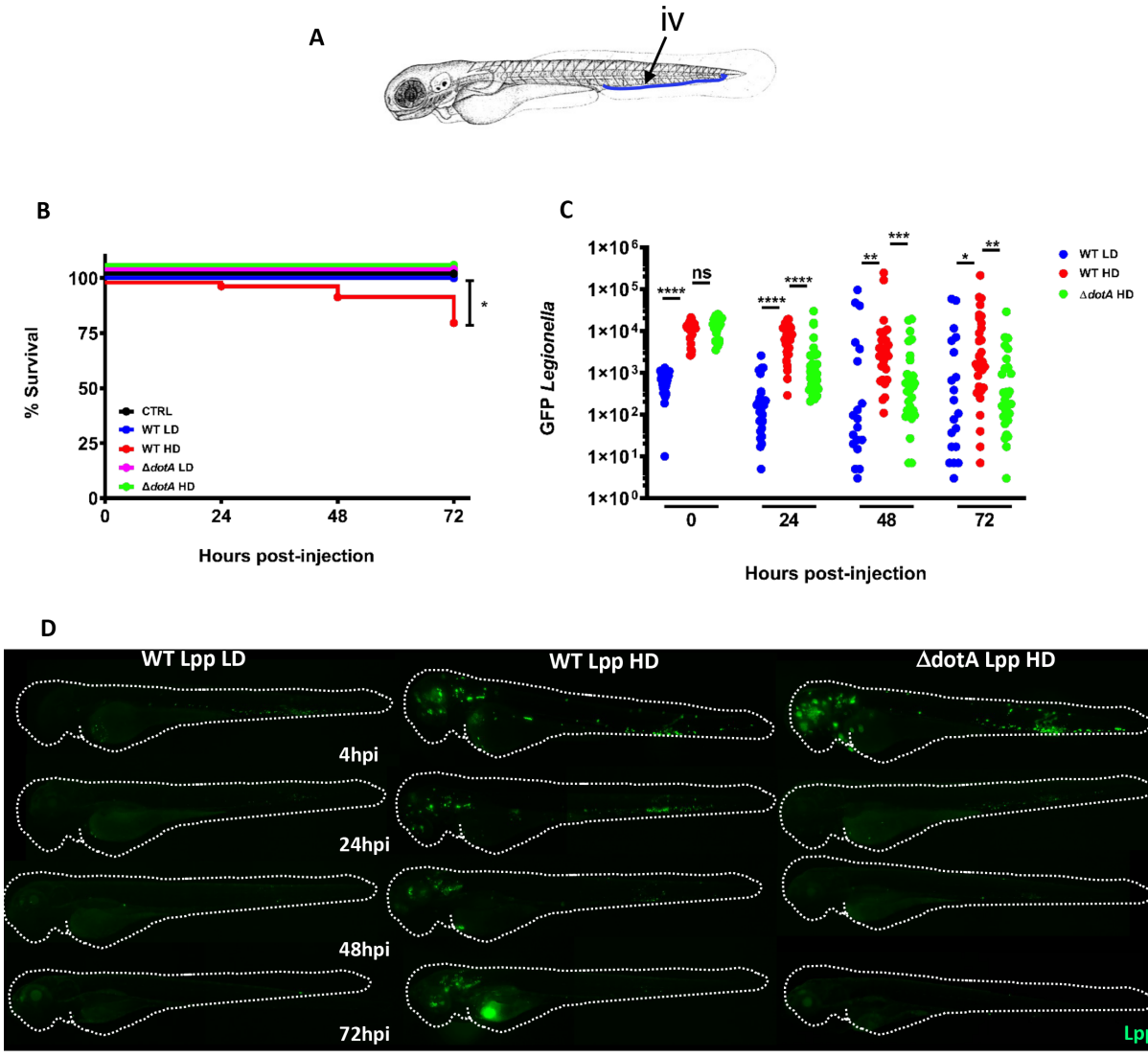
A
iv
B
% Survival
100
75
50
25
0
0
24
48
72
Hours post-injection
CTRL
WT LD
WT HD
ΔdotA LD
ΔdotA HD
*
C
GFP Legionella
1×10⁶
1×10⁵
1×10⁴
1×10³
1×10²
1×10¹
1×10⁰
ns
****
****
****
**
***
*
**
0
24
48
72
Hours post-injection
WT LD
WT HD
ΔdotA HD
D
WT Lpp LD
WT Lpp HD
ΔdotA Lpp HD
4hpi
24hpi
48hpi
72hpi
Lpp

Figure 2

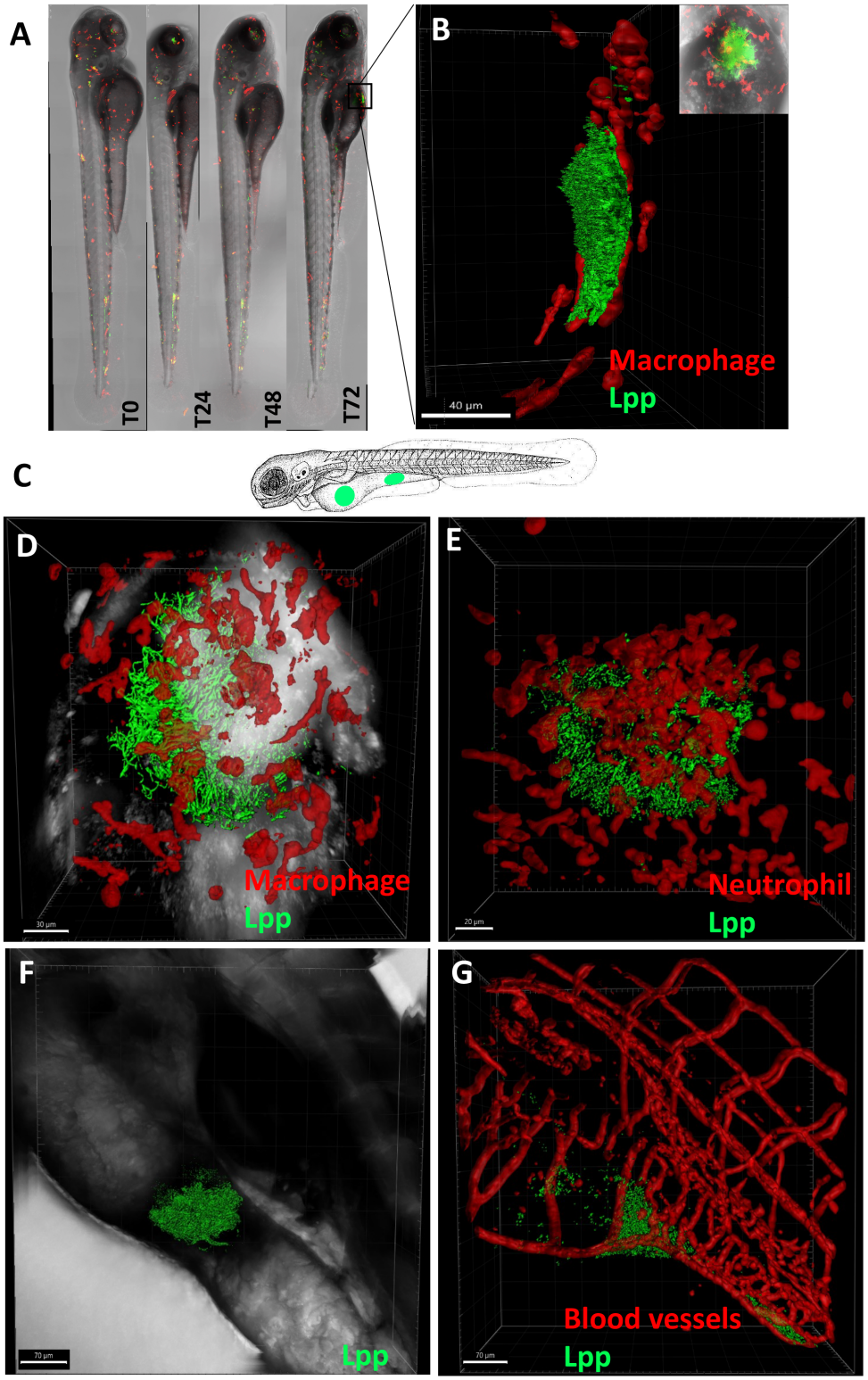
A
T0
T24
T48
T72
B
Macrophage
Lpp
40 µm
C
D
Macrophage
Lpp
30 µm
E
Neutrophil
Lpp
20 µm
F
Lpp
70 µm
G
Blood vessels
Lpp
70 µm

Figure 3

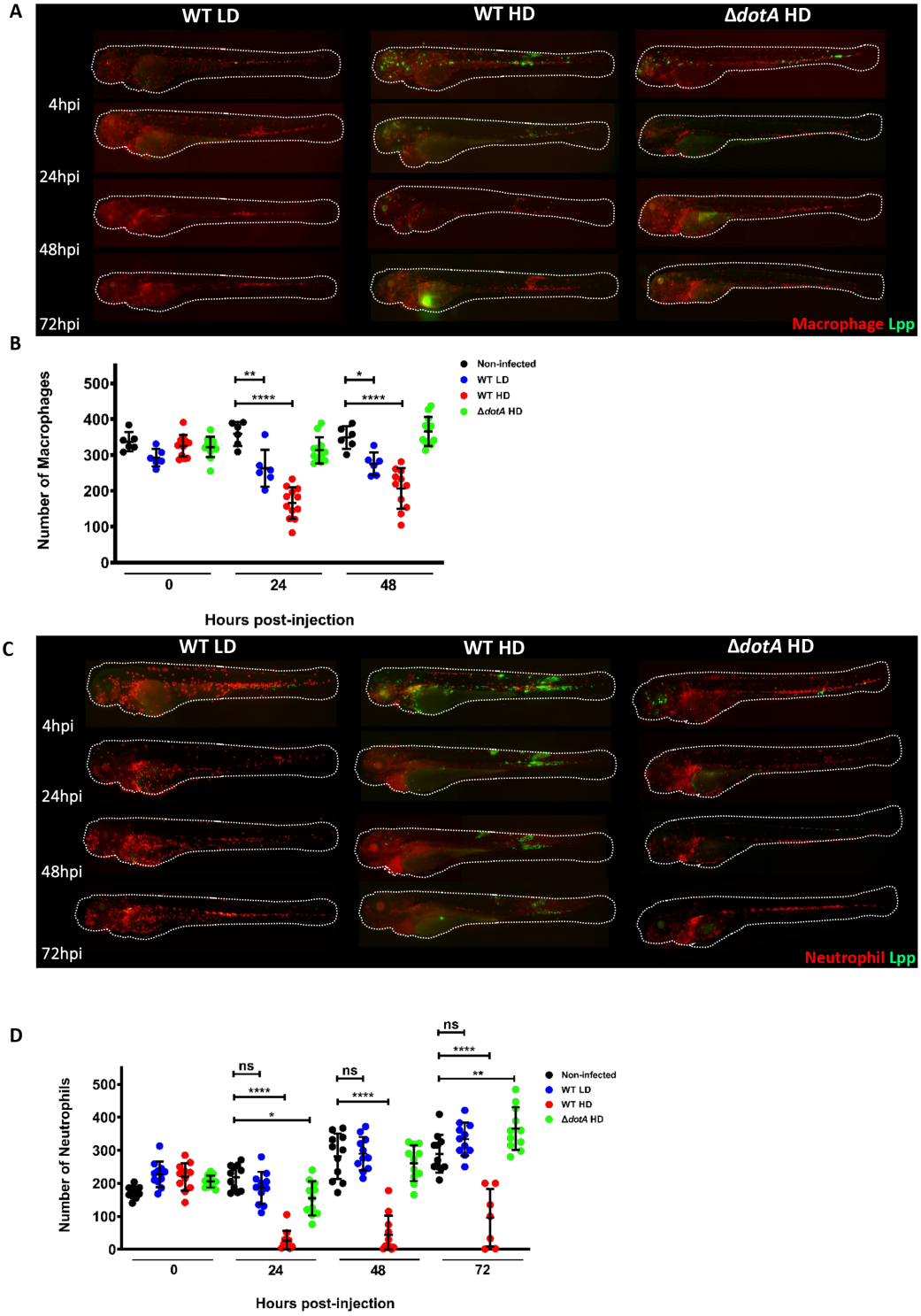
A
WT LD
WT HD
ΔdotA HD
4hpi
24hpi
48hpi
72hpi
Macrophage Lpp
B
Number of Macrophages
Non-infected
WT LD
WT HD
ΔdotA HD
Hours post-injection
C
WT LD
WT HD
ΔdotA HD
4hpi
24hpi
48hpi
72hpi
Neutrophil Lpp
D
Number of Neutrophils
Non-infected
WT LD
WT HD
ΔdotA HD
Hours post-injection

Figure 4

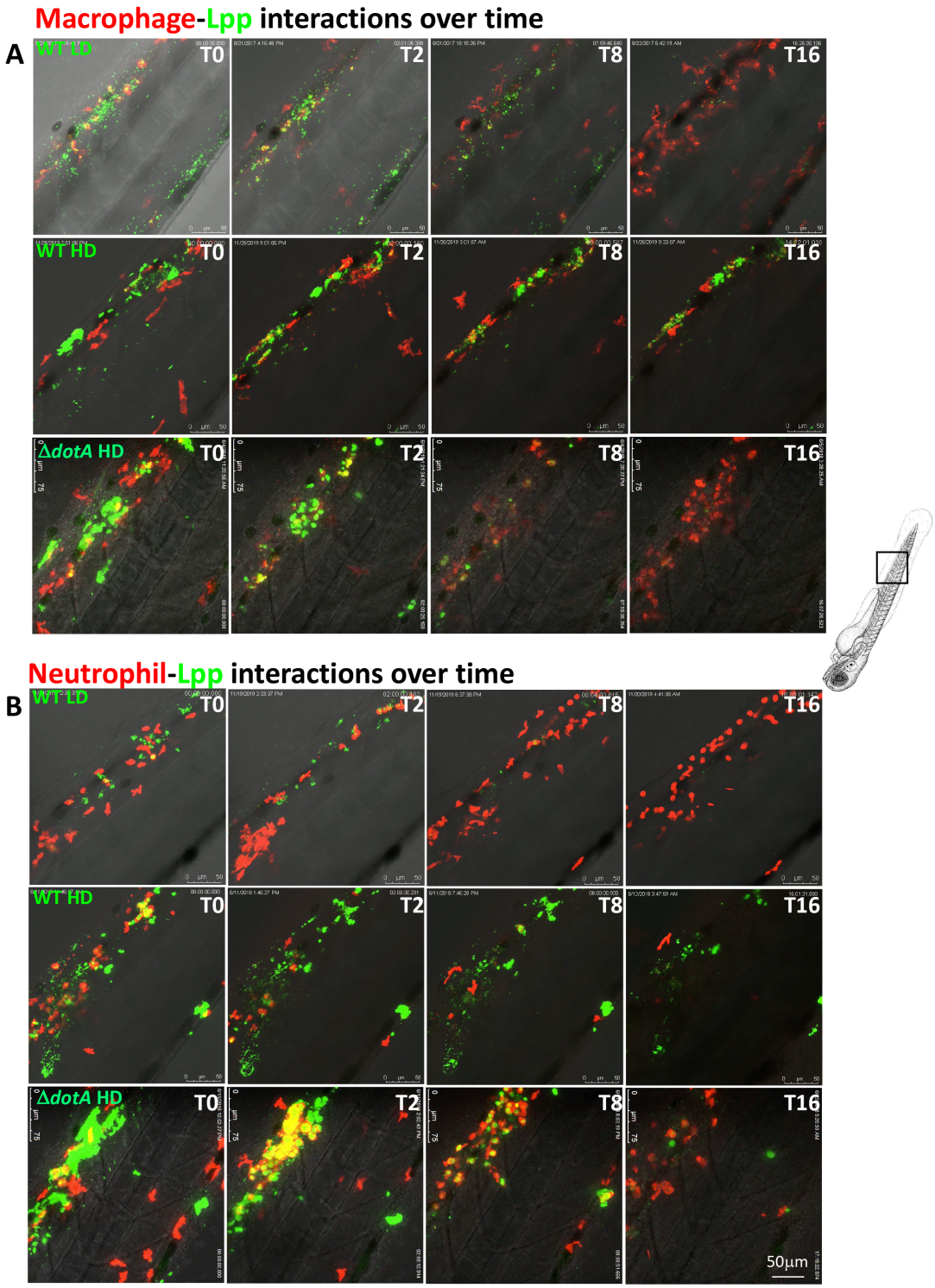
Macrophage-Lpp interactions over time
A
WT LD
T0
T2
T8
T16
WT HD
T0
T2
T8
T16
ΔdotA HD
T0
T2
T8
T16
Neutrophil-Lpp interactions over time
B
WT LD
T0
T2
T8
T16
WT HD
T0
T2
T8
T16
ΔdotA HD
T0
T2
T8
T16
50µm

Figure 5

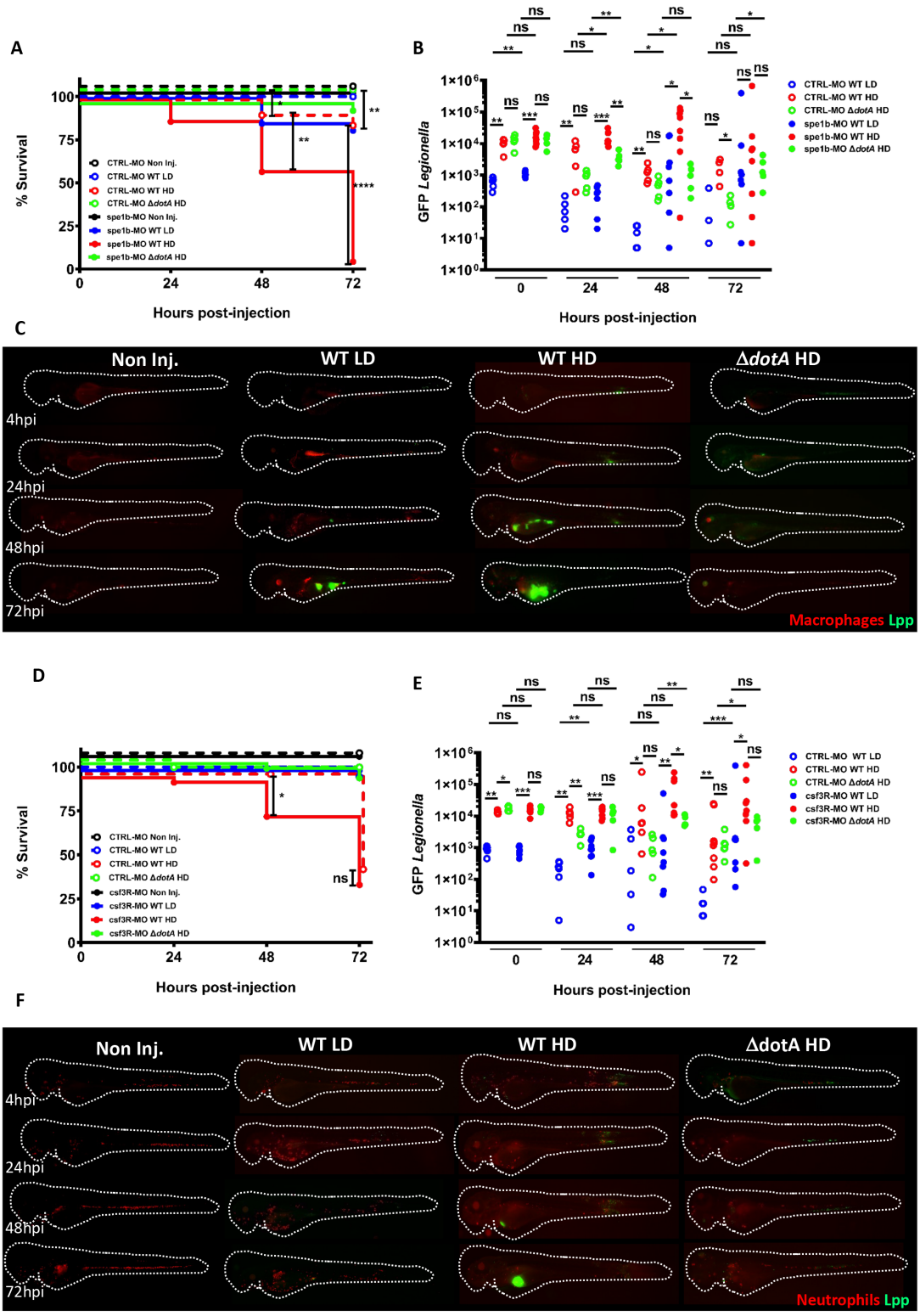
A
% Survival
Hours post-injection
CTRL-MO Non Inj.
CTRL-MO WT LD
CTRL-MO WT HD
CTRL-MO ΔdotA HD
spe1b-MO Non Inj.
spe1b-MO WT LD
spe1b-MO WT HD
spe1b-MO ΔdotA HD
B
GFP Legionella
Hours post-injection
C
Non Inj.
WT LD
WT HD
ΔdotA HD
4hpi
24hpi
48hpi
72hpi
Macrophages Lpp
D
% Survival
Hours post-injection
csf3R-MO Non Inj.
csf3R-MO WT LD
csf3R-MO WT HD
csf3R-MO ΔdotA HD
E
GFP Legionella
Hours post-injection
F
Non Inj.
WT LD
WT HD
ΔdotA HD
Neutrophils Lpp

Figure 6

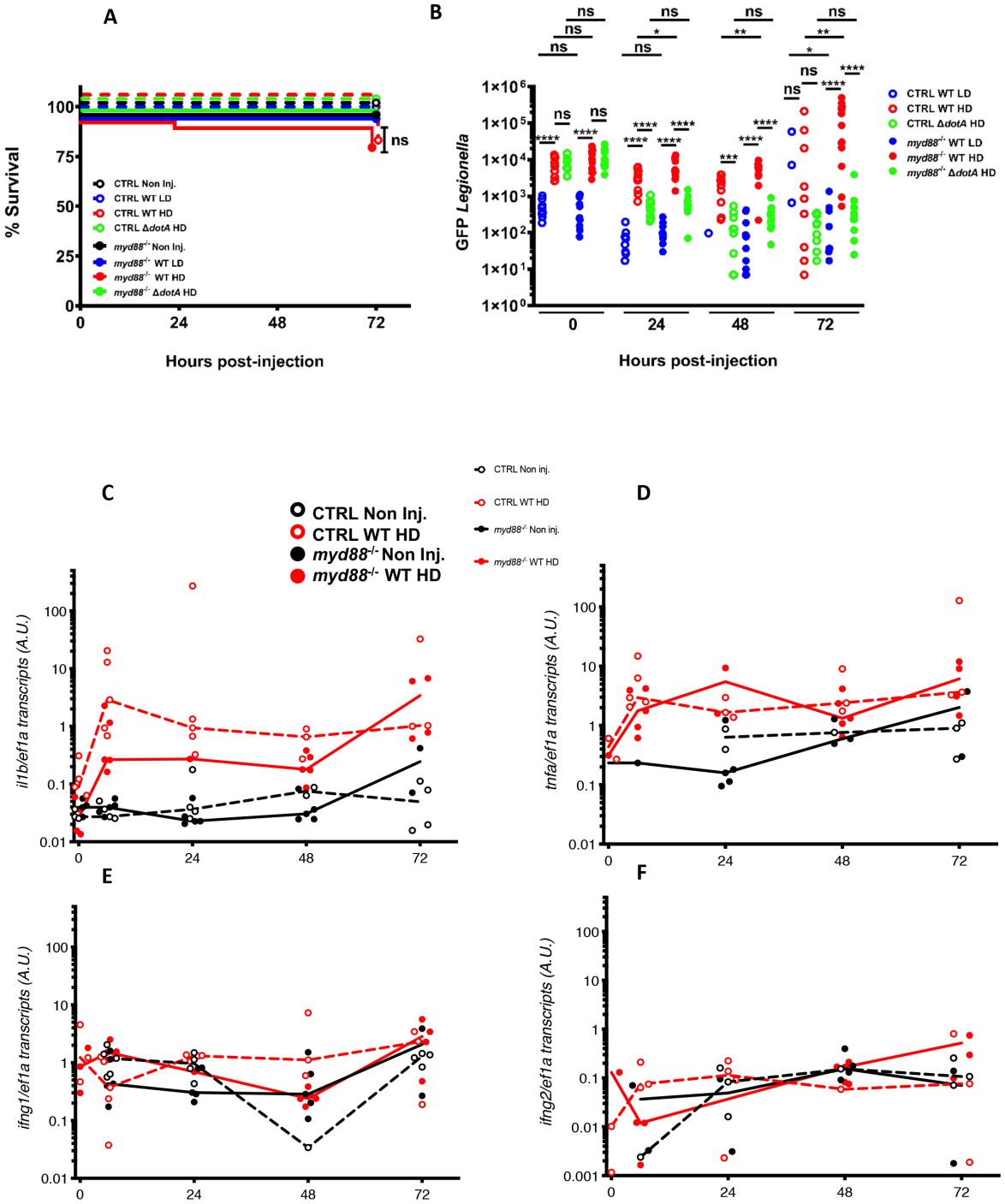
A
% Survival
Hours post-injection
CTRL Non Inj.
CTRL WT LD
CTRL WT HD
CTRL ΔdotA HD
myd88-/- Non Inj.
myd88-/- WT LD
myd88-/- WT HD
myd88-/- ΔdotA HD
ns
B
GFP Legionella
Hours post-injection
C
il1b/ef1a transcripts (A.U.)
D
tnfa/ef1a transcripts (A.U.)
E
ifng1/ef1a transcripts (A.U.)
F
ifng2/ef1a transcripts (A.U.)

Figure 7

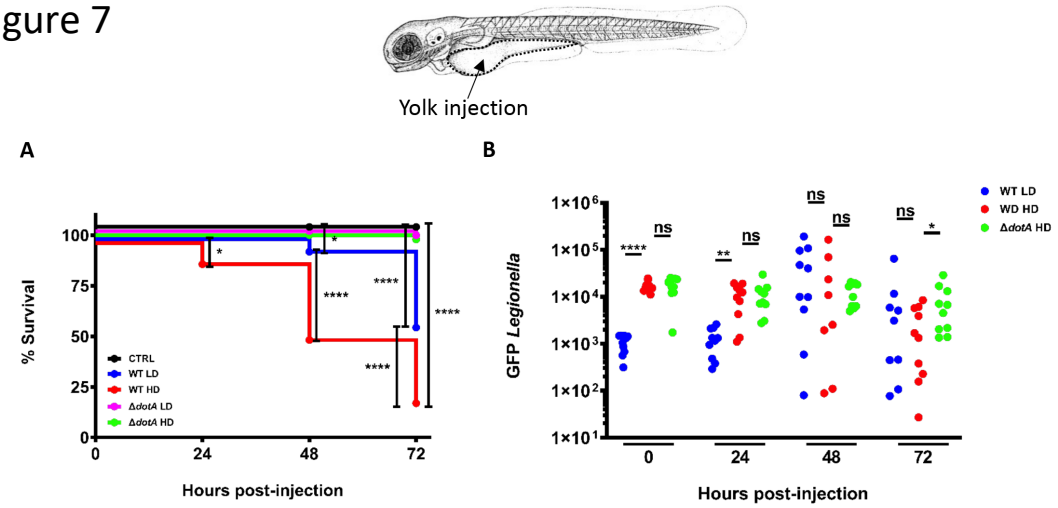
Yolk injection
A
B
% Survival
Hours post-injection
CTRL
WT LD
WT HD
ΔdotA LD
ΔdotA HD
GFP Legionella
WT LD
WD HD
ΔdotA HD
ns
C
CTRL
WT LD
ΔdotA LD
4hpi
24hpi
48hpi
72hpi
Neutrophil Lpp
D
CTRL
WT HD
ΔdotA HD
4hpi
24hpi
48hpi
72hpi
Neutrophil Lpp

List of abbreviations

AROS	Active regulator of SIRT1
BCYE	Buffered charcoal yeast extract agar
BEC	bronchial epithelial cells
C3b	Complement component 3b
CD93	Cluster of differentiation 93
CDC	Center for Disease Control and Prevention
CR1	Complement receptor 1
CSE1L	Chromosome segregation 1 like
DNA	Deoxyribonucleic acid
DNMT	DNA methyltransferase
Dot/Icm	Defective organelle trafficking/Intra cellular multiplication
ECDC	European Centre for Disease Prevention and Control
EEA	European Economic Area
ELDSNet	European Legionnaires' disease Surveillance Network
ELISA	enzyme-linked immunosorbent assay
ER	Endoplasmic reticulum
ESCMID	European Society of Clinical Microbiology and Infectious Diseases
ESGLI	ESCMID Study Group for Legionella Infections
EU	European Union
FACT	Facilitates chromatin transactions
GAP	GTPase-activating protein
GEF	Guanine nucleotide exchange factor
GTP	Guanosine-5'-triphosphate
HAD	haloacid dehalogenase
HCV	Hepatitis C virus
HDAC	Histone deacetylase
HMG	High mobility group protein

HP1	Heterochromatin protein 1
HULC	Highly Up-regulated in Liver Cancer
IκB	Inhibtor of NF-κB
IKK	IκB kinase
LCV	*Legionella*-containing vacuole
LLO	Listeriolysin O
lncRNA	Long non-coding RNA
MAPK	Mitogen-activated protein kinases
MeCP2	Methyl CpG binding protein 2
NCP	nucleosome core particles
NF-κB	nuclear factor kappa-light-chain-enhancer of activated B cells
NLRC4	Nod-like receptor Family caspase activation and recruitment Domain Containing 4
NODAL	Nodal Growth Differentiation Factor
NRL	nucleosome repeat length
PCR	Polymerase chain reaction
RNA	Ribonucleic acid
RNA-seq	RNA sequencing
RT-qPCR	Reverse transcription quantitative real-time PCR
SET	su[var]3-9, enhancer-of-zeste and trithorax
SIRT	Sirtuin
SNARE	Soluble N-ethylmaleimide-sensitive factor attachment protein receptors
snRNP	small nuclear ribonucleoprotein
SPL	Sphingosine-1 phosphate lyase
SUMO	Small Ubiquitin-like Modifier
T4SS	Type IV secretion system
TSA	Trichostatin A
Xist	X-inactive specific transcript

List of figures

Rôle fonctionnel d'une histone désacétylase codée par *Legionella pneumophila*

RÉSUMÉ

Legionella pneumophila est une bactérie intracellulaire qui sécrète plus de 300 protéines dans la cellule hôte via un système de sécrétion spécialisé de type 4. L'un de ces effecteurs sécrétés, RomA, s'est avéré modifier directement la chromatine de l'hôte en méthylant la lysine 14 de l'Histone H3 (H3K14), un résidu généralement acétylé. Cela a conduit à la question de savoir comment la désacétylation de cette marque pourrait se produire pendant l'infection. Une recherche bioinformatique approfondie du genome de *L. pneumophila* a conduit à l'identification d'une protéine qui devrait coder pour une histone désacétylase (HDAC), nommée LphD. Au cours de ma thèse, j'ai montré que LphD est sécrétée dans la cellule hôte lors de l'infection et cible spécifiquement le noyau, où elle présente une activité désacétylase avec une efficacité élevée pour H3K14. En effet, j'ai montré que LphD désacétyle H3K14 également pendant l'infection, et que l'activité de LphD influence directement les niveaux de méthylation de H3K14 dans les cellules infectées, mettant en évidence une synergie entre LphD et RomA. J'ai également pu montrer que LphD et RomA ciblent un complexe de liaison à la chromatine endogène, nommé HBO1, qui contient l'histone acétyltransférase KAT7, contrôlant l'état d'acétylation de H3K14. Des RNAseq de cellules infectées soit par des bactéries de type sauvage, soit par le knock-out LphD et RomA, ont mis en évidence l'influence de ces effecteurs bactériens sur le paysage transcriptionnel de l'hôte, en particulier sur les gènes liés à la réponse immunitaire. Le modèle que je propose est que les deux effecteurs sécrétés, LphD et RomA, travaillent ensemble pour détourner la machinerie épigénétique de l'hôte afin de faciliter la subversion de la réponse immunitaire et favoriser la réplication intracellulaire de *L. pneumophila.*

Mots clés: *Legionella pneumophila*, Histone désacétylases, nucleomodulines, épigénétique

Functional role of a histone deacetylase encoded by *Legionella pneumophila*

SUMMARY

Legionella pneumophila is an intracellular bacterium that secretes over 300 proteins in the host cell through a specialized type 4 secretion system. One of these secreted *L. pneumophila* effectors, RomA, was shown to directly modify the host chromatin by methylating lysine 14 of Histone H3 (H3K14), a usually acetylated residue. This led to the question how deacetylation of this mark might happen during infection. An in-depth bioinformatics search led to the identification of a protein predicted to code for a histone deacetylase (HDAC), named LphD. During my PhD, I showed that LphD is secreted into the host cell during infection and specifically targets the host cell nucleus, where it exhibits deacetylase activity with high efficiency for H3K14. Indeed, I showed that LphD deacetylates the H3K14 residue also during infection, and that the activity of LphD directly influences the levels of H3K14 methylation in infected cells, highlighting the synergy between LphD and RomA. I also could show that LphD and RomA target an endogenous chromatin binding complex, named HBO1, that contains the histone acetyltransferase KAT7, controlling the acetylation status of H3K14. RNAseq of cells infected with either wild type bacteria or the LphD and RomA knockout assessed the influence of these bacterial effectors on the host's transcriptional landscape, in particular on genes related to immune response. The model I propose is that the two secreted effectors, LphD and RomA, work together to hijack the host's epigenetic machinery in order to facilitate the subversion of the host immune response and promotes the intracellular replication of *L. pneumophila*.

Key words: *Legionella pneumophila*, Histone deacetylases, nucleomodulins, epigenetics